IMPROVED RECOMBINANT ADENOVIRAL VECTOR WITH ENHANCED TRANSDUCTION EFFICIENCY AND REDUCED VIRAL TOXICITY: CHARACTERISATION OF THE ANTI-ADENOVIRAL IMMUNE RESPONSES IN THE CENTRAL NERVOUS SYSTEM.

A thesis submitted to the University of Manchester for the degree of Doctor of Philosophy in the Faculty of Medicine, Dentistry, Nursing & Pharmacy.

2001

Christian Antonio Gerdes

School of Medicine

ProQuest LLC.
789 East Eisenhower Parkway
P.O. Box 1346
Ann Arbor, MI 48106 – 1346

CONTENTS

Chapter 2: Material and Methods

LIST OF FIGURES

Chapter 4

Chapter 5

LIST OF TABLES

Chapter 4

Abstract

Using the major immediate early murine Cytomegalovirus (mCMV) promoter to drive expression of ß-galactosidase, we have demonstrated that, following adenoviral-mediated transduction of brain cells *in vivo*, a **single** viral infectious unit is capable of producing detectable levels of transgene expression. Gene transfer into the brain is close to 100% efficient, showing for the first time the unparallel efficiency of transduction that can be achieved with adenoviral vectors *in vivo*. The amount of virus required to transduce large numbers of brain cells can be now reduced 1000 fold when using the mCMVp in comparison with the hCMVp, completely eliminating the cellular inflammation and viral cytotoxicity associated with the delivery of adenoviral vectors into the brain. Even though RAd 36 doses of 10^6 iu can avoid the innate immune response, we found that RAd doses as low as 10^3 iu can be recognised by an activated adaptive immune response. This suggests that, even in the absence of early brain inflammation after RAd striatal injection, peripheral adenoviral infection may eventually occur, terminating transgene expression in the brain when using 1^{st} generation adenovirus. Vectors such as the new helper dependant adenovirus, devoid of any adenoviral gene expression and therefore, capable of evading transgene elimination by an activated immune response, together with the mCMV promoter, which enables maximal adenoviral transduction efficiency without triggering an early cellular inflammation and direct viral cytotoxicity, will be needed to ensure long-term transgene expression even in the presence of a systemic immunisation against adenoviruses.

Declaration

No part of the work referred to in this thesis has been submitted in support of an application for another degree or qualification of this or any other university or institute of learning.

The work done in section 5.2.7 was done by our collaborators (Ignacio Anegon group, Institut national de la sante et de la recherche medicale, U437, Nantes, France).

Copyright

1. Copyright in text of this thesis rests with the author. Copies (by any process) either in full, or of extracts, may be made only in accordance with instructions given by the author and lodged in the John Rylands University Library of Manchester. Details may be obtained from the librarian. This page must form part of any such copies made. Further copies (by any process) of copies made in accordance with such instructions may not be made without the permission (in writing) of the author.

2. The ownership of any intellectual property rights which may be described in this thesis is vested in the University of Manchester, subject to any prior agreement to the contrary, and may not be made available for use by third parties without the written permission of the University, which will prescribe the terms and conditions of any such agreement.

Further information on the conditions under which disclosures and exploitation may take place is available from the head of the School of Medicine

Dedication

This thesis is dedicated to my grandmother Ena Kraus, my mother Rosemary Kaufman, to the memory of my father John Gerdes, to my wife Valeria Gonzalez Nicolini who was a big support for me to achieve my degree, and my two little sweet hearts Thomas Antonio Gerdes and Sophie Maria Gerdes.

Acknowledgments

First of all, I would like to thank my supervisors Maria Castro (Pluma Blanca- White Feather) and Pedro Lowenstein (Toro Sentado- Seating Bull) for all their efforts to give me the possibility of doing my Ph.D, in this fascinating field, in one of the top gene therapy labs in the world, which I am proud, not only to have been part of, but also to have acted as one of the pieces that enabled its rising to the high position it currently has.

I would like to thank all of the present and past members of the Molecular Medicine and Gene Therapy Unit, which had the pleasure of tolerating me, and became part of my nice memories during these years, this will include: Dominique Bataille (Dom), with our programmed strategic discussions about Diplomacy; Anne (Nanou) David; Adam (Toromba) Zermansky; Alireza Bigliari (Ali) and his unforgettable life sayings; Mark (Twain) Ackroyd; Penny (Lane) Edwards; Jennifer (Capriatti) Podesta; Tom (el gato) Southgate; Wei Dong Sung (Tun shi nie number 1), without discussion the kindest person I ever met; Xiang Peng Yuang (Tun shi nie number 2); Emma (Thomson) Jones, known as well by the name of "Heidi"; Jerard Ross (William Wallace) who truly believes that one day he will liberate Scotland; Peter (the Geordie) Stanley, who definitely will not let that happen; Daniel (Piedra) Stone; Clare Thomas (Clarita); Thomas (el gordo Makis) Verakis, what would be of the culinary world without him? Maximiliano (Pelopicho) Jimenez (no comments), and Judith Williams (Ms Williams) also the first to kindly correct the messy English of one of the chapters of my thesis.

I have to thank all the friendly people of the BSU, for their constant help and everlasting, contagious happiness, especially Mike Jackson, Brian Landamom, Christopher (Chris) Tomlin, Sally Bolton, Elaine Breeze and Graham (Chucky) Morrisey.

I should thank also my dear friend Tony, from the computing and imaging department, who always got ready in record time, any image, slide or poster that I took to him, with no more than ~3 minutes before the deadline.
I am Truly grateful to Ignacio Anegon for sending me so fast his *in vivo* results with the virus I have generated (RAd m40), for letting me add them in the fifth chapter of my thesis and for patiently cleared the questions I had about the results he obtained.

I would like to give super extra especial thanks to the lovely ladies, who truly believed I was dying from starvation, and didn't let that happen: Evelin Abordo Adesida (Evelina) and Ana (Aninha) Grande Perez, with her Spanish specialitys "Calamar en su tinta and Crema Catalana " who not only delight me with her "alta cocina" but also corrected the second chapter of my thesis.

A separate thank must go to Sumia Ali (Meri jaan) also known as the great stubborn, who not only was my great scientific, fun and ice-cream friend throughout these last two years of PhD, but also she corrected the difficult fourth chapter of my thesis and introduced me to her home made spicy Asian dishes (actually I think the pasta was a bit overcooked...) honestly what would I have done without her.

Finally I cannot forget to thank my HLA (Latin American Brotherhood) comrades: Pablito (Carepi) Umana, Andres (Tico) Hurtado, and Federico (HLAa2-Bolognesa) Bolognani, all co-founders of the glorious and never ending HLA, which were a great support, scientifically, intellectually and sportily, granting always an unconditional friendship.

Abbreviations

Ad - Adenovirus

AAV - Adeno-associated virus

ACTH - Adreno-corticotrophic hormone

ADA - Adenosine deaminase

APC - Antigen presenting cell

APES - 3-aminopropyl-triethoxysilane

ATP - Adenosine triphosphate

AtT20 - Murine ACTH secreting pituitary cell line

BBB - Blood brain barrier

bp - Base pairs

BSA - Bovine serum albumin

$CaCl_2$ - Calcium chloride

CAR - coxsackie and adenovirus receptor

cDNA - Copy DNA

CHO - Chinese hamster ovary cell line

CIAP - Calf intestinal alkaline phosphatase

CMV - Cytomeglaovirus

CNS - Central nervous system

CNS 1 - Rat glioblastoma cell line

Cos7 - African green monkey kidney cell line

CTL - Cytotoxic T lymphocyte

DAPI - 6-Diamidino-2-phenylindole

DC - Dendritic cell

dH_2O - Distilled water

DIG - Digoxigenin

DMEM - Dulbecco's modified eagle medium

DMSO - Dimethylsulphoxide

DNA - Deoxyribonucleic acid

dNTP - (dATP, dTTP, dGTP, dCTP mix)

EBV - Epstein-Barr virus

E.coli - Escherichia coli

EDTA - Ethylenediaminetetraacetic acid

FCS - Fetal calf serum

GH3 - Rat prolactin secreting pituitary cell line

HCl - Hydrogen chloride

hCMV - Human major immediate early cytomegalovirus

hCMVp - Human major immediate early cytomegalovirus promoter

HEK 293- Human embryonic kidney 293 cell line

Hela - Human cervical epitheloid carcinoma cell line

hPrl - Human prolactin promoter

HSV-1 - Herpes simplex virus type-1

IL-1 - interleukin-1

IL-2 - interleukin-2

IL-4 - interleukin-4

IL-10 - interleukin-10

ITR - Inverted terminal repeat

iu - Infectious units

KCl - Potassium chloride

kbp - Kilobase pairs

KH_2PO_4 - Potassium hydrogen orthophosphate

LPS - Lipopolysaccharide

mCMV - Murine major immediate early cytomegalovirus

mCMVp - Murine major immediate early cytomegalovirus promoter

MEM - Minimal essential medium

$MgCl_2$ - Magnesium chloride

$MgSO_4$ - Magnesium sulphate

MHC I - major histocompatability complex class I

MHC II - major histocompatability complex class II

ml - mililitre

mm - milimetre

MMQ - Rat prolactin secreting pituitary cell line

mu - Map units

$MnCl_2$ - Manganese chloride

MOI - Multiplicity of infection

NaCl - Sodium chloride

NaOH - Sodium hydroxide

Na_2HPO_4 - diSodium hydrogen orthophosphate

NK - Natural killer

nm - Nanometres

N2A - Murine neuroblastoma cell line

OD - Optical density

PBS - Phosphate buffered saline

pg - picogram

RAd - Recombinant adenovirus

RAd h40 - Recombinant adenovirus with CD40lg as transgene under the control of the hCMV promoter

RAd m40 - Recombinant adenovirus with CD40lg as transgene under the control of the mCMV promoter

RAd PLZ - Recombinant adenovirus with β-galactosidase as transgene under the control of the hPrl promoter

RAd 0 - Recombinant adenovirus with no transgene

RAd 35 - Recombinant adenovirus with β-galactosidase as transgene under the control of the hCMV promoter

RAd 36 - Recombinant adenovirus with β-galactosidase as transgene under the control of the hCMV promoter

RCA - Replication competent adenovirus

RNA - Ribonucleic acid

rpm - Revolutions per minute

SCID - Severe combined immunodeficiency

SDS - Sodium dodecyl sulphate

SV40 - simian virus 40

TBS - Tris buffered saline

TH1 - CD4 T helper type 1 immune response

TH2 - CD4 T helper type 2 immune response

TNF - Tumour necrosis factor

UV - Ultraviolet

X-Gal - 5-bromo-4-chloro-3-indolyl-β-D-galactoside

µg - microgram

µl - microlitre

µm - micrometre

Chapter 1: General Introduction

1.1 Gene Therapy

Gene therapy can be defined as the transfer of nucleic acids into cells in order to express a transgene of interest, for the purpose of altering a given condition or disease. After unprecedented advances in the field of molecular biology have allowed the understanding, at a molecular level, of an enormity of biological conditions and diseases, gene therapy has come onto the scene as the new promise in medical strategies, possibly the future of applied medicine. As a developing field the problems for successful gene therapy treatment are vast. Major steps need to be taken in order to improve gene transfer and the efficacy of gene therapy for therapeutic intent.

The first time that gene delivery was successfully accomplished in human patients, bone marrow harvested from children with acute myeloid leukaemia was transduced *ex vivo* with a retoviral vector carrying the neomycin resistance transgene. These cells were then re-implanted into the patients (Brenner et al, 1993). Transgene was detected in patients 18 month after re-infusion, demonstrating not only transgene transduction but also long-term transgene expression.

Later in 1990 the first gene therapy trial carried out to change the course of a disease was done with *ex vivo* transduction of bone marrow using retroviral vectors (Blaese et al,1995). This time, a therapeutic transgene, adenosine deaminase, was

used to treat patients suffering from adenosine deaminase deficiency, which produces severe immunodeficiency (Blaese et al, 1995). The clinical experimental data was evident to the fact that a significant improvement in the patients condition had been achieved. The sole benefit of gene therapy, however, could not be accurately assessed as throughout the trial pharmaceutical intervention of the disease with ADA was sustained.

Unfortunately in 1999, a gene therapy clinical trial led by James Wilson, University of Pennsylvania, went terribly wrong when an eighteen year old boy, Jesse Gelsinger, died during treatment. The aim was to treat ornithine transcarbamylase deficiency with a first generation adenoviral vector encoding the defective enzyme. The disease is untreatable and, therefore, a good target for gene therapy. Although the adverse effects underlying the fatality were not entirely elucidated, pre-clinical trials governed by the same research group, found the viral concentration used to treat Jesse Gelsinger to be toxic in non-human primates. The fact that this data had been acquired before the clinical trial generated heavy criticism. Gene therapy clinical trials were not stopped but regulations and guidelines have being rigorously revised.

Last year the first successful gene therapy clinical trial was done, conducted by Fischer and colleagues in Paris, where they successfully treated 3 babies suffering from fatal severe combined immunodeficiency-x1 syndrome (SCID-X1). SCID-X1 is an X-linked inherited disorder characterized by an early block in T and natural killer (NK) lymphocyte differentiation. This block is caused by mutations of the gene encoding the gammac cytokine receptor subunit of interleukin-2, -4, -7, -9, and -15 receptors, which participates in the delivery of growth, survival, and differentiation

signals to early lymphoid progenitors. Haematopoietic stem cells (CD34+) from the patients were transduced *ex vivo* with a retroviral vector encoding for the normal γ-c receptor subunit and then re-administered to the patients. Normal number of T cells and Natural Killer cells were found, expressing the γ-c receptor subunit, 10 month after re-administration, appearing to have no symptoms of disease (Cavazzana-Calvo et al, 2000).

1.2 Vehicles for gene transfer

Gene therapy is based on the successful delivery of therapeutic nucleic acids into target cells. Cellular uptake and expression of naked DNA is extremely inefficient so gene transfer vectors are being developed in order to improve the transduction efficiency. The vector, in which the nucleic acids are to be incorporated, can be viral or non-viral; the therapeutic potential of each approach depends on the nature of the disease.

1.2.1 Non-viral vectors

Cationic groups are bound to the DNA molecule, changing the polarity of the DNA. The change in polarity facilitates binding of the DNA to the negatively charged cell membrane, increasing transduction efficiency as the DNA is more likely to be internalised.

Cationic DNA complexes are relatively simple to prepare, with no limit on the size of the transgene and a low risk of generating infectious forms or tumours due to the low integration frequency (Kay et al. 1997a). Cationic-DNA complexes show good transfection activity *in vitro* (Caplen et al. 1995) but there is no evidence to suggest that efficient gene transfer is possible *in vivo*. Gene expression tends to be transient *in vivo*, decreasing to less than 1% of the peak level by day 4, an aspect thought to be caused by transgene degradation (Song et al. 1997). The main limiting step for efficient transduction is the transfer of the DNA from the endosome into a suitable environment for DNA replication and protein synthesis. Once the DNA has been released from the endosome it is degraded in the cytoplasm, unless it is delivered into the nucleus where it would have to remain to allow sustained expression of the transgene. Until improvements are made to non-viral vectors, their use in gene therapy will be limited to *in vitro* work.

1.2.2 Viral Vectors

Throughout evolution, viruses have continuously refined their mechanisms of infection, providing an ideal system to exploit when delivering and expressing DNA in host cells. Construction of the viral vector requires deletion of genes that causes pathology, at the same time providing room for therapeutic gene insertion. This must be achieved without altering the viruses ability to deliver DNA.

There are several criteria to be taken into consideration when choosing an appropriate vector model. If the viral vector is immunogenic, as with first generation

adenoviral vectors, the immune response will impede long-term expression of the transgene and subsequent re-administration. Recombination could lead to generation of the infectious form of pathogenic virus. If the DNA delivered integrates with the hosts genome as with retroviral vectors, there is a risk of inducing tumorigenic mutations. The size of the transgene influences the choice of vector due to differing insert-carrying capabilities. Adeno-associated viruses (AAV), for example, could only be used when transferring relatively short sequences of DNA, up to 5 kb. The target cells are also a determinant. Certain vectors, such as retroviral vectors, cannot transduce non-dividing cells, so would not be of consideration when transducing neuronal cell types. Finally, the transduction efficiency of the chosen vector has to be considered. If the transduction efficiency is low, undesirably high doses of virus will be required to achieve the necessary levels of transgene expression.

There are several viral vectors in development. Those used in current clinical trials or advanced pre-clinical development are the ones that will be discussed in more detail in this thesis. This includes: retroviral vectors, lentiviral vectors (a type of retroviral vector), adeno asociated virus (AAV) vectors, and finally adenoviral vectors. There are several other viral vectors under development, which includes herpes viruses (Kay, 2001), α-viruses (Hewson, 2000), hepatitis virus (Chaisomchit, 1997), SV-40 (Strayer, 1999), RNA viruses like influenza (Palese, 1996) and Epstein-Barr virus (Sclimenti et al, 1998), among others.

1.2.2.1 Retroviruses

These vectors are lipid enveloped particles comprising a linear single-stranded RNA genome of 7-11 Kb. Following infection of the target cell, the RNA genome is retro-transcribed into a linear double-stranded DNA and integrates into the cell chromosome. Most of the viral genes are removed, making them relatively safe and capable of inserting and expressing up to 8 kb of exogenous DNA instead of the viral genes (Miller, 2000).

Retroviral vectors efficiently integrate into the chromatin of the target cell, fact that don't guarantee expression but will ensure maintenance of the genetic information in a renewing dividing tissue. Also the integration is random so it may produce undesirable tumourigenic effects. The main disadvantage of these vectors is that they need the nuclear membrane to be disrupted to gain access to the chromatin (Roe *et al*, 1993) so is strictly dependant on target cell mitosis shortly after entrance for integration and transgene expression (Miller et al, 1990), making these vectors of limited use for transgene delivery. Another disadvantage is the low concentration of virus that can be produced up to 10^7 iu/ml.

Recently it has been shown that a retroviral vector, a lentiviral vector, can transduce non-dividing cells (Mitani et al, 1995) relying on active transport of the preintegration complex through the nucleopore by the nuclear import machinery of the target cell (Bukrinsky et al, 1999). Nevertheless lentiviral vectors requires further studies, and the viral production yield has continued to be relatively low.

The obligatory RNA step in the retroviral lifecycle greatly limits its exploitation for gene transfer purposes. The transgene must be of limited size without introns and polyadenylation signals. These characteristics together with the random integration of the delivered nucleic acids in maybe not so active regions of the chromatine, make a combination of factors that limit the expression of the transduced genes.

1.2.2.2 Adeno-associated virus

These are parvoviruses that rely on a helper virus, like adenovirus, to mediate successful replication. From the six known human viral serotypes to date, AAV-2 and AAV-5 are the most commonly used adeno-asociated viruses. The viral genome consists of two genes, rep (viral replication) and cap (for structural proteins) flanked by ITRs. AAV vectors can be produced lacking all viral coding sequences, adding separate plasmids containing the ITRs flanking the transgene cassette, the rep/cap genes and helper adenoviral genes (Matsushita et al, 1998, Xiao et al, 1998). The total packaging capacity is about 5 kb, which severely limits the applications of this vector.

Wild type AAV have the ability to integrate their DNA into a specific region on chromosome 19, but this property is lost in AAV vectors due to the absence of the rep gene. It has been shown (Samulski, 2001) that viral capsids interfere with the expression of cellular DNA replication genes, leaving more than 90% of the transduced viral DNA in an episomal state, decreasing transgene long term expression in dividing cells (Duan et al, 1999; Miao et al, 1998).

Each particle contains a single positive or a single negative DNA strand. Both single strands are needed in the same cell to produce an effective transduction (Samulski, 2001) hence multiple infectious hits are needed in each cell, which may explain the extremely low transduction efficiency found in vivo (less than 5% of the detected infected cells) (Samulski, 2001).

1.2.2.3 Adenovirus

This vector is the most efficient delivery system among viral vectors so far, transducing a wide variety of cell types (including dividing and non-dividing cells) (Gerdes et al, 2000) and can accept large DNA inserts up to 30Kbp (Parks et al 1996). RAds genomes, rarely integrate into the cell chromosome existing as a stable episome in the nucleus. Unless using the latest technology of HdAd vectors, first generation RAds are very immunogenic limiting long term transgene expression.

Adenoviral virions are icosahedral particles (87% protein and 13% DNA) that are 70 to 100 nm in diameter, consisting of a protein shell of a regular icosahedron (20 equilateral triangular surfaces) surrounding a DNA core. The capsid is composed of 252 subunits, of which 240 are hexons and 12 are pentons (fig.1). Each penton capsomere comprises a penton base and a fiber. The penton base is surrounded by 5 hexons while each hexon is surrounded by 6 hexons. The viral genome consists of a single linear double-stranded DNA molecule of about 36 kb. The genome contains two inverted terminal repeats (ITR) situated at each end, carrying origins of replication, and one cis acting packaging sequence per genome to direct the

interaction of the viral DNA and the encapsidating proteins. The viral chromosome carries five early transcription units (E1A, E1B, E2, E3, and E4) two delayed early units (IX and IVa2) and one late unit (major late) which is processed to generate five families of late mRNAs (L1 to L5) all transcribed by RNA polymerase II (Shenk, 1996).

1.2.2.3.1 Adenoviral infection-cycle and replication

Initially the knob region on the fibre protein of the adenoviral particle binds to the coxsackie and adenovirus receptor (CAR) (Bergelson et al, 1997 & 1998; Roelvink et al 1998 & 1999). After this initial encounter, the penton base interacts with $\alpha_v\beta_3$ or $\alpha_v\beta_5$ integrins on the cell membrane and triggers the viral particle internalisation by clathrin-coated vesicles ending in cellular endosomes (Wickham et al, 1993).

Acidification of the endosomes which falls to a pH of 5.5, produces a conformational change in the virion proteins which in turn disrupts the endosome (endosomolysis) and the viral particle is released into the cell cytoplasm (Stewart et al, 1995).
The capsid is transported through the cytoplasm by a microtubule-dependant process and finally encounters and binds to the nuclear membrane (Wisnivesky et al, 1999).

The adenoviral genome is actively translocated into the nucleus via an ATP dependent process leaving the capsid in the cytoplasm. The DNA remains as a stable episome in the nucleus.

Figure 1.

A.

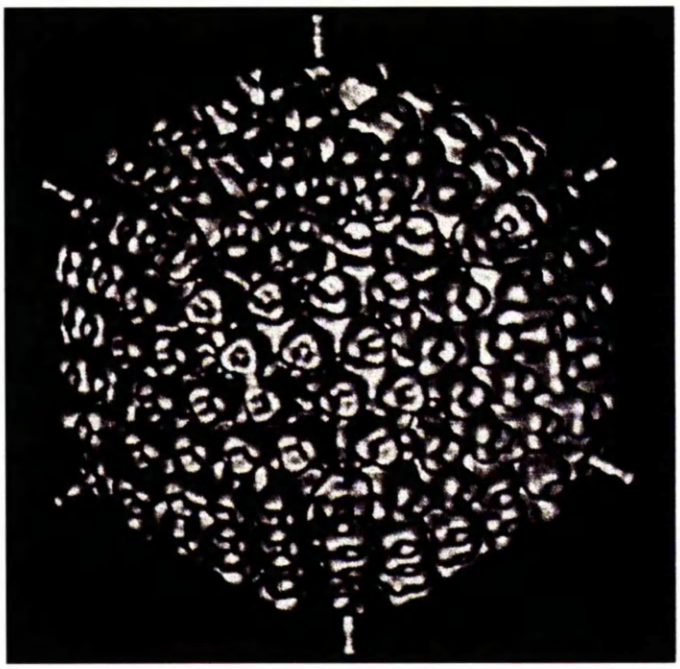

B.

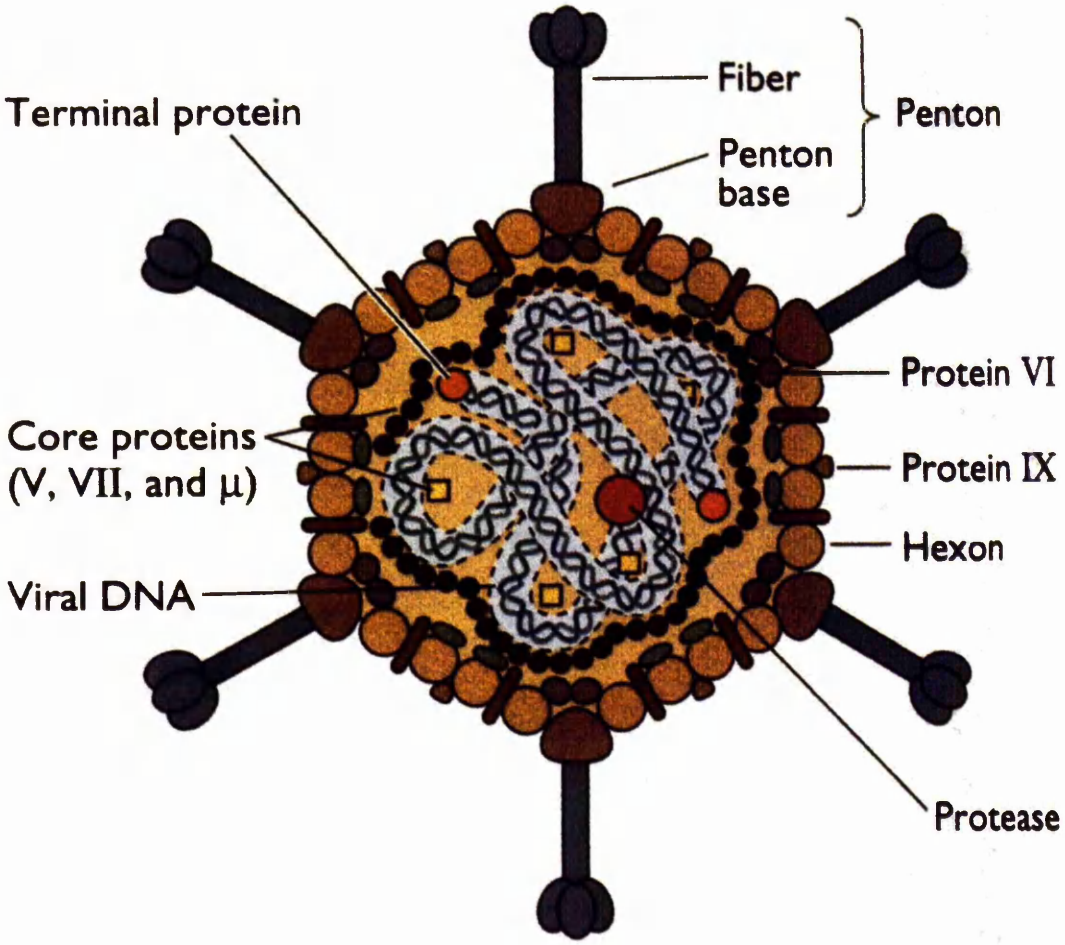
Fiber
Penton
Terminal protein
Penton base
Protein VI
Core proteins (V, VII, and μ)
Protein IX
Hexon
Viral DNA
Protease

Figure 1. Adenovirus virion.

a. Three dimensional image of the intact adenovirus particle viewed along an icosahedral three-fold axis.

b. Schematic representation of an adenovirus particle based on the current understanding of its polypeptide constituents and genome. Modified from (Flint et al., 2000).

Figure 2

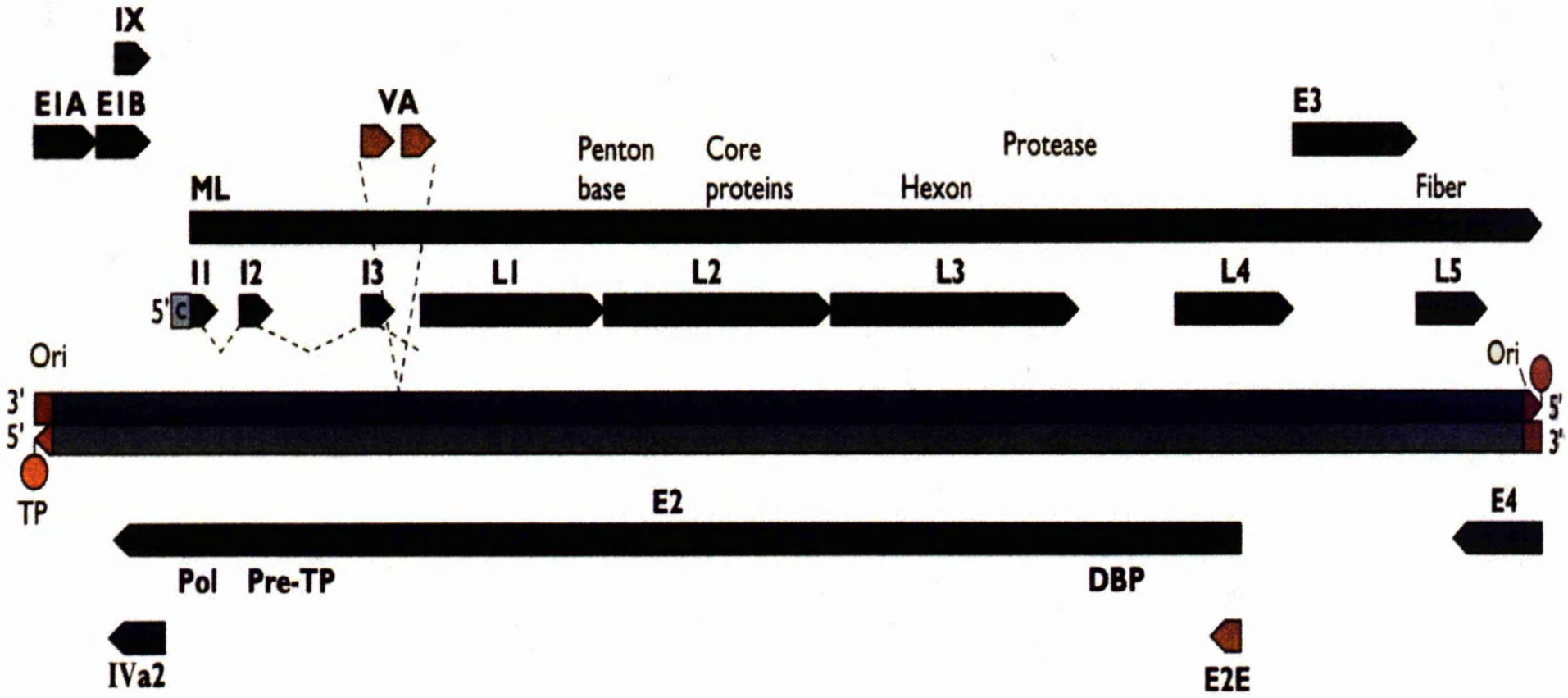
IX
E1A E1B
VA
E3
Penton base
Core proteins
Protease
ML
Hexon
Fiber
I1 I2 I3 L1 L2 L3 L4 L5
5'
C
Ori
Ori
3'
5'
5'
3'
TP
E2
E4
Pol Pre-TP
DBP
IVa2
E2E

Figure 2. Adenoviral genome and transcription map. The genome by convention is arbitrarily divided into 100 map units (mu) each map unit consisting of 360 bp. Early primary mRNA transcripts are designated in bold. Certain polypeptides are identified by conventional numbering system (roman numerals). Modified from (Flint et al., 2000).

Once in the nucleus, transcription of the E1A transactivator is initiated from the constitutive E1 promoter. The transactivator instigates transcription of the remaining viral genes, enabling viral DNA replication. Protein products from the E1 region induce cell cycle arrest in the S phase, inhibit apoptosis by E1B-19K, and inhibits tumour suppressor factors p53 by E1B-55K and pRb by E1A, providing an optimal environment for viral DNA replication.

An anti-immune response is triggered to protect the infected cell from an immune attack and safely allowed viral replication. E1A proteins protect the infected cell from α and β interferon responses. E3 proteins also play an important role in evading the immune response by: downregulating MHC class I by E3-gp19K, impeding viral antigen presentation; inhibiting tumour necrosis factor alpha (TNFα) induced cell death by E3 14.7K and down regulating Apo (receptor of Fas ligand) by E3 14.5K/10.4K complex, protecting the cell from Fas ligand induced apoptosis.

After transcription of the delayed early genes, the major late promoter becomes active, enabling transcription of the late genes, which produce the viral capsid proteins. Once the capsid proteins are imported into the nucleus from the cytoplasm, viral assembly starts, packaging suitable adenoviral genomes (which have to be of the right size for encapsidation and need to possess the packaging signal). Finally late adenoviral proteins induce cytoskeleton disruption, resulting in cell lysis (Chen et al, 1993) and an average 10000 viral particles per cell are released, terminating the adenoviral replication cycle.

1.2.2.3.2 Adenovirus as viral vectors

1.2.2.3.2.1 E1/E3 deleted first generation and second generation adenoviral vectors

Graham and colleagues developed an adenovirus type 5 vector system with deletions in the E1 and E3 regions (Bett et al, 1994), rendering the virus non-replicative and creating enough free space to insert therapeutic DNA without altering its capacity to be encapsidated. The vector must be propagated in cell lines that complement the necessary E1 region for replication, like HEK 293 cells (Graham et al, 1977).

E1a region proteins induce infected cells to move from G1 to S phase providing an optimal environment for viral replication. In addition they activate the expression of other adenoviral transcription units. E1B binds to the p53 protein, inhibiting p53 induction of programmed cell dead (apoptosis). E3 is a non-essential gene for viral replication, that protects the cell from apoptosis triggered by TNF-α and down-regulates the presentation of viral antigens via MHC class I to T-cells. E1/E3 deleted viral vectors have enhanced safety features, impeding viral replication and cellular transformation, with the additional benefit of increasing the potential size of transgene that can be accommodated within the viral genome.

The Graham system is based on two plasmids. The first plasmid, the shuttle vector, contains a portion of the left end of the viral genome (from map units 0 to 1.1) including the inverted repeat sequence, the packaging signal and viral sequences from map units 10 to 16 (figure 3). The transgene is inserted into the shuttle vector. The other plasmid is the circularised version of the complete adenoviral genome with deletions within the E3 region and of its packaging signal. Genes coding for ampicillin resistance and an *E.coli* origin of replication are inserted on the E1 region. The two plasmids are subsequently co-transfected into HEK 293 cells, which trans-complement the E1 deficient viral region, leading to the formation of adenoviral particles with the transgene placed replacing the deleted E1 region by homologous recombination.

The development of second generation recombinant adenoviruses have additional deletions of other essential regions of the adenoviral genome, providing them *in trans* within a complementing cell line for vector amplification. These vectors show increased cloning capacity, reduced viral protein expression, and a reduced incidence of replication competent adenovirus (RCA) formation, due to the increased number of individual recombinations that are needed to generate a replication competent genome. For the generation of the different second generation recombinant adenoviral vectors different cell lines have been generated to trans-complement the deleted genes. These cell lines express E1/E4 (Krougliak *et al.* 1995), E1/E2A (Gorziglia *et al.* 1996), E1/E2B precursor terminal protein (Schaack *et al.* 1996), E1/E2B adenovirus polymerase (Amalfitano *et al.* 1996) and E1/ E2B precursor terminal protein and adenovirus polymerase (Amalfitano & Chamberlain 1997).

The main disadvantage of these vectors is that even though the E1 gene is deleted in the vector, the other adenoviral genes are still being transcribed in small amounts. This happens because of the basal level of transcription from viral promoters which is independent of transactivation from E1. Adenoviral protein levels from these genes are not enough to produce viral replication but they are high enough for the immune response to recognise the infected cell and eliminate transgene expression. The viral capsid itself induce a blocking humoral immune response, which impedes repeated re-administrations. Taken together the immune responses elicited against the adenoviral vector hamper its use for long-term gene therapy treatments and repeated re-administrations.

Figure 3

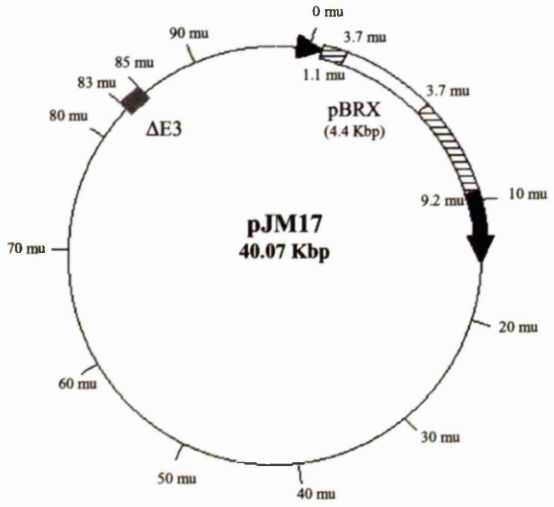
0 mu
3.7 mu
1.1 mu
3.7 mu
90 mu
85 mu
83 mu
80 mu
ΔE3
pBRX
(4.4 Kbp)
9.2 mu
10 mu
pJM17
40.07 Kbp
70 mu
20 mu
60 mu
30 mu
50 mu
40 mu

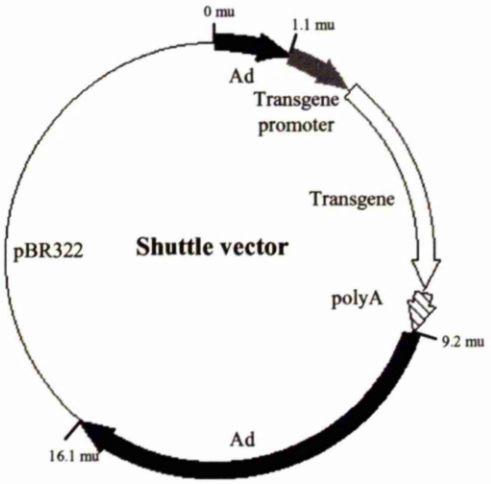
0 mu
1.1 mu
Ad
Transgene
promoter
Transgene
pBR322
Shuttle vector
polyA
9.2 mu
Ad
16.1 mu

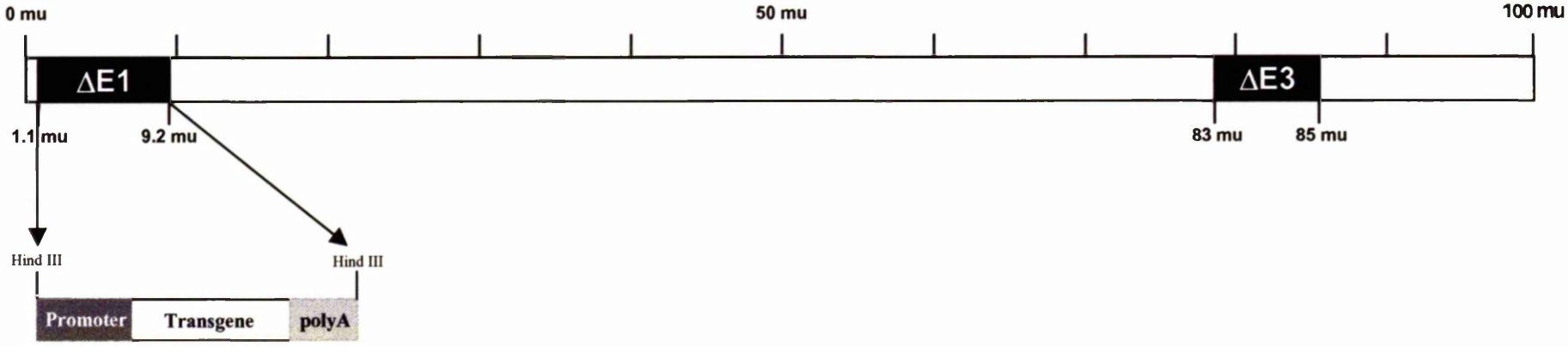
0 mu
50 mu
100 mu
ΔE1
ΔE3
1.1 mu
9.2 mu
83 mu
85 mu
Hind III
Hind III
Promoter
Transgene
polyA

Figure 3. Generation of E1/E3 first generation adenoviral vectors. For the generation of RAds the shuttle vector containing an expression cassette flanked by adenoviral sequences 0mu - 1.1 mu on one side and 9.2mu - 16.2 mu on the other one is co-transfected into HEK 293 cells (providing the E1A region) with pJM17 which contains the whole adenoviral genome with the plasmid pBRX inserted in the E1 region at map unit 3.7 and a deletion in E3 from 83 mu to 85 mu. After cotransfection of both plasmids into HEK 293 cells, recombination eventually occurs between the homologous regions (black regions of pJM17 and the shuttle vector) of both plasmids, resulting in the replacement of the pBRX and the E1 region of the pJM17 by the expression cassette of the shuttle vector. The recombinant plasmid now posses the encapsidation signal and the right size to be packed into viral capsides (unlike pJM17 which is too large to be encapsidated because of the pBRX insertion) producing the RAds. RAds can be subsequently scaled up infecting HEK 293 cells which will provide the missing E1A region for viral replication.

1.2.2.3.2.2 High capacity, helper dependant adenoviral vector

First and second generation adenoviral vectors produce deleterious effects and limited transgene expression mainly due to residual expression of viral genes present in the vector, which leads to acquired immune responses and direct toxicity to infected cells (Yang et al, 1994; Dewey et al, 1999; Brand et al, 1999) reducing long term expression of the transgene of interest. These problems have been overcome by developing a helper-dependent adenoviral vectors (HdAd), devoid of all viral coding sequences (Mitani et al, 1995; Kochanek et al, 1996; Parks et al, 1996; Hardy et al, 1997) (figure 4). HdAd vectors are associated with very low toxicity, have a large cloning capacity of up to 30 kb, mediate long-term transgene expression (Chen et al, 1997; Schiedner et al, 1998; Morsy et al, 1998; Morral et al, 1998; Morral et al, 1999; Thomas et al 2000; Sandig et al, 2000) and are able to transfer and direct expression of therapeutic genes *in vivo* with unsurpassed efficiency among gene therapy vectors (Maione et al, 2000).

HdAd vectors are produced by co-infection of producer cells with a helper first generation adenovirus that provides *in trans* all necessary functions for virus replication and packaging. Currently, the most widely used system for HdAd vector production avoids significant contamination with helper virus by applying selection against helper DNA packaging (Parks et al, 1996). This is achieved by using producer cells stably expressing a nuclear-targeted *Cre* recombinase and an engineered first generation helper virus with parallel loxP sites flanking its packaging signal. A majority of helper virus-DNA molecules are thus rendered unpackagable

by *Cre* recombinase-mediated excision of their packaging signal, a process that does not interfere with viral DNA replication or with the packaging of HdAd vector.

The HdAd virus is initially generated by transfection of producer cells with HdAd vector DNA, followed by infection with helper virus. The resulting HdAd virus is subsequently amplified in a series of helper-plus- HdAd virus co-infection passages in *Cre* recombinase-expressing cells. The levels of helper virus remaining in the final HdAd vector preparation are normally around 0.1% (Maione et al, 2000; Park et al, 1996; Sandig et al, 2000). However, these low levels of contamination are achieved only after a final density-based separation of helper and HdAd viruses using ultracentrifugation, an operation that seriously hinders large-scale production of HdAd vectors.

The efficiency of *Cre* recombinase-catalyzed excision of helper virus-packaging signals is likely to be an important factor determining the levels of helper contamination. In the original description of this HdAd vector production system (Parks et al, 1996) it was noted that a few hours after infection of *Cre*-expressing cells, the fraction of helper virus DNA molecules with an excised packaging sequence reached a maximum of approximately 80%, and did not increase at later times. This level is consistent with the findings of previous studies on the maximum fraction of excised molecules for the *Cre*–catalyzed, reversible excision reaction (Ringrose et al, 1998).

A new system has been developed which uses instead of the *Cre recombinase* the yeast *Flp* recombinase (Umana et al, 2001). Although *Flp* has a significantly lower

specific activity than *Cre*, it mediates maximum levels of excision close to 100% (Ringrose et al, 1998). This is apparently due to a much faster dissociation rate of the excised DNA-enzyme complex in the case of *Flp*, which favors the excision relative to the reverse integration reaction rate (Ringrose et al, 1998). As the wild type *Flp* enzyme is not very active at 37°C, an *Flp* mutant (*Flpe*) that was recently developed by *in vitro* evolution for applications at this temperature (Abremski et al, 1984) was used. It was found that *Flpe*-based production of HD vectors results in levels of helper contamination lower than 0.1% prior to any density-based separation by ultracentrifugation, thus enabling a scalable production process. This new scalable system (Umana et al, 2001) together with the high transduction efficiency that can be achieved by RAds (Gerdes et al, 2000) and the discovery that HdAd successfully avoids recognition by a primed immune response (Thomas et al, 2000) puts adenoviral vectors in a very strong position, when a viral vector has to be chosen.

Figure 4

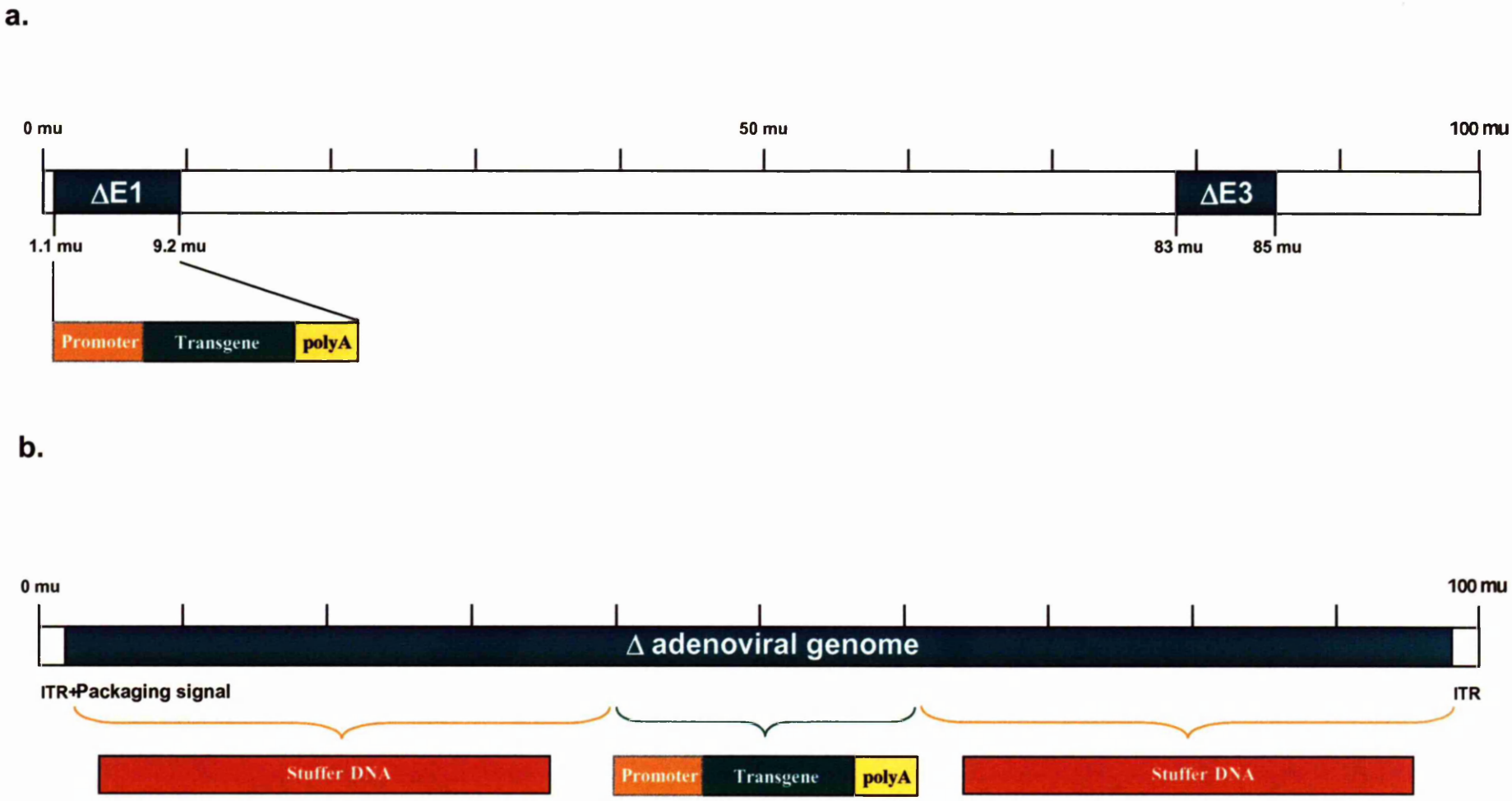
a.
0 mu
50 mu
100 mu
ΔE1
ΔE3
1.1 mu
9.2 mu
83 mu
85 mu
Promoter
Transgene
polyA
b.
0 mu
100 mu
Δ adenoviral genome
ITR+Packaging signal
ITR
Stuffer DNA
Promoter
Transgene
polyA
Stuffer DNA

Fig 4. Schematic representation of adenoviral vector genomes comprising first generation (used in the construction of the Rads generated for this thesis), and helper dependent adenoviral vectors.

a. E1/E3 First generation adenoviral vector genome constructed using pAL 119 or pAL 120 and pJM17 in HEK 293 cells. Expression cassettes comprising the transgene, promoter and poly A, were inserted in the ΔE1 region in all RAds generated for this thesis. Position of adenoviral map units are shown, including the exact position of genome deletions.

b. Helper dependant adenoviral vector genome only has the ITR and packaging sequences from wild type adenovirus. The rest of the genome is composed by the expression cassette and enough stuffer DNA to alow genome encapsidation.

1.3 Immune responses to RAds

RAds stimulates two inter-related immune responses. The early stage, involves the innate immune response, occurring within 24 hours post infection. This response is characterised by macrophage and neutrophil infiltration with antigen non-specificity, independent of the delivered transgene. The later stage, which is responsible for the complete elimination of the RAd and its transgene, is the adaptive immune response. This response is characterised, contrary to the innate immune response, by its specificity against the infectious agent. Antigen-presenting cells (APC), such as dendritic cells (DC), T cells and B cells, comprising the humoral (neutralising antibodies) and cytotoxic (cytotoxic T cells) immune responses form part of this stage.

1.3.1 T cell activation

Both humoral and cytotoxic immune responses to RAds depend on T cell activation. In order for T cell activation to occur, viral antigen must be up-taken by immature DC (see fig.5). The antigens are processed and presented via major histocompatibility complex (MHC) molecules on mature DC to naive T cells in the lymph nodes. The MHC-antigen complexes are recognised by specific naive T cells with specific T cell receptors (TCR) (which differentiate T cell clones from one another, and gives the specificity of the immune response). This action triggers the first step of T cell

activation, upregulating the expression of IL-2 high affinity receptor, Fas, and CD40L on the T cell surface membrane (Grewal et al, 1996).

Via the upregulated CD40L the T cell binds to the DC constitutively expressed CD40. This binding evokes a second activation signal, but this time is the T cell, which gives the signal to the DC. The B7 family of receptors are then up-regulated within the DC (Inabe et al, 1994), which in turn gives the final activation signal to the T cell, by CD28-B7 interaction. The CD28-B7 binding signal triggers the activation of the T cell, triggering the secretion of IL-2, that in an autocrine and paracrine way induces the T cell to rest in S phase, enabling its clonal expansion. Bcl-xL is also induced preventing the Fas induced programmed cell death (Boise et al, 1995).

If no further co-stimulation occurs after the first step of activation (no second step activation), the T cell becomes in a dormant status called anergy. Anergic cells are unable of further activation (Boussiotis et al, 1997), and are most probably deleted lately, as they expressed Fas and they are not protected from apoptosis (Boise et al, 1995). This mechanism is very important in the prevention of autoimmune diseases, deleting autoreactive T cells, which were not destroyed in the thymus during maturation (Kruisbeek et al, 1996).

Figure 5

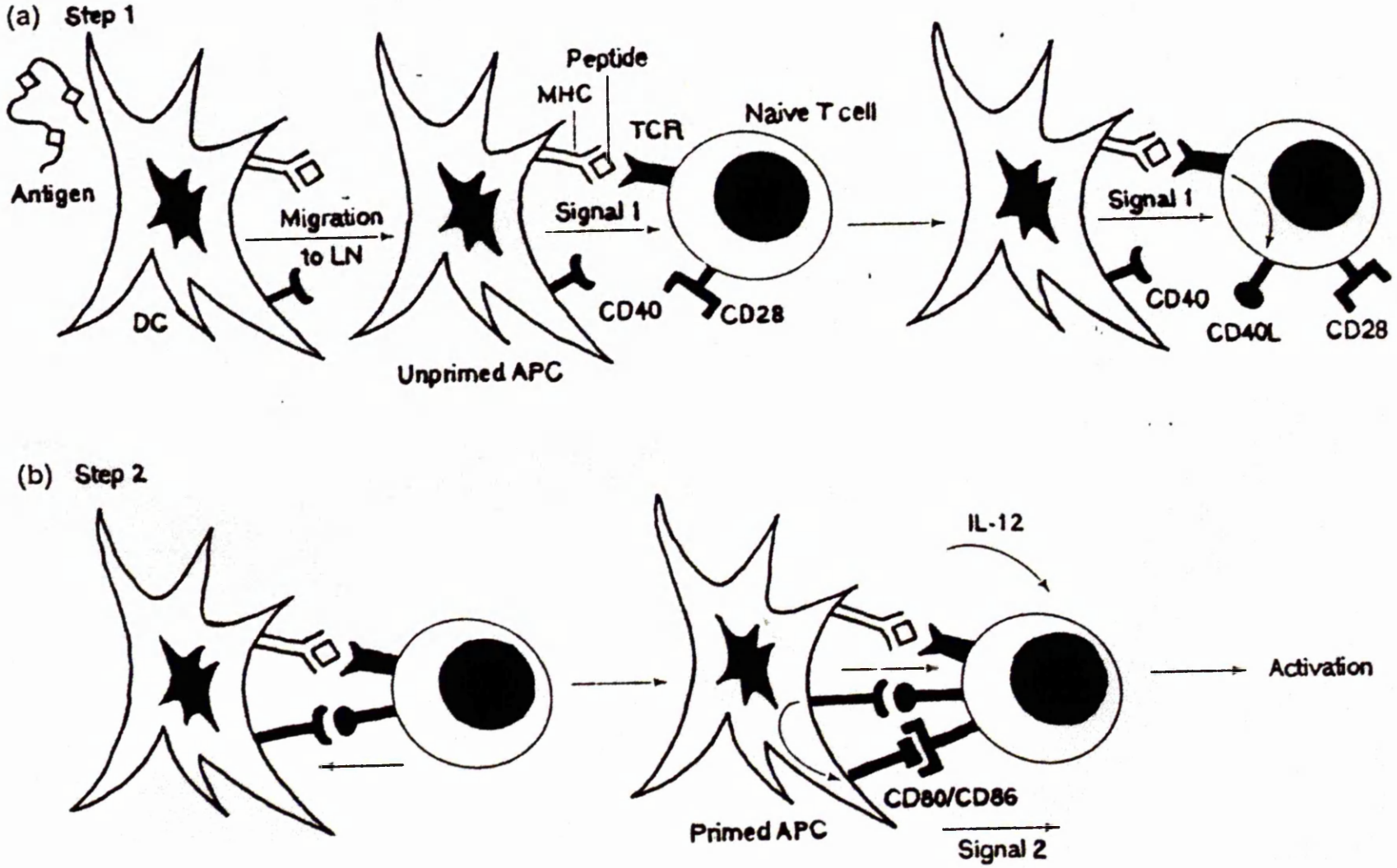
(a) Step 1
Antigen
DC
Migration
to LN
Unprimed APC
Peptide
MHC
TCR
Naive T cell
Signal 1
CD40
CD28
Signal 1
CD40
CD40L
CD28
(b) Step 2
IL-12
Primed APC
CD80/CD86
Signal 2
Activation

Fig.5. T cell activation: a) Step 1: induction of CD40L on T cells. Antigens are taken up by immature DCs, and these DCs migrate to the lymph node, where they present the processed antigen to naïve T cells in the form of MHC-peptide complexes, which gives the antigenic signal (signal 1) binding to the TCR of naïve T cells. As a result T cells upregulate CD40L on their surface. b) Step 2: induction of co-stimulatory activity on DCs via the CD40-CD40L interaction. This primed APC now expressing co-stimulatory molecules sends a second co-stimulatory signal to T cells along with signal 1 for full activation of T cells to produce cytokines and perform effector functions.

1.3.2 TH1 and TH2 immune responses

The T cells are either CD8 T cells (mostly cytotoxic) or CD4 T cells (generally acting as helper cells). Antigen presentation is very important because it determines whether the acquired immune response is activated in favour of a TH1 or a TH2 response. The immune responses to antigens is often distinguished by two distinct patterns of cytokines produced by CD4 T cells.

During TH1 immune responses CD4 T cells secreting the appropriate cytokines (IL-2, Interferon γ) help the activated cytotoxic CD8 T cells (CTLs) (Mosmann et al, 1989). The CTLs are activated, but the antigen is presented in the context of a MHC class I molecule (Kelly et al,1992). MHC class I molecules present mainly endogenous antigens i.e. antigens up taken from inside the cell, which are processed and presented on the cell membrane through the MHC class I. Once activated, the CTLs recognise infected cells by viral antigen presentation through MHC class I on the cell membrane, and eliminates them. The CTLs can destroy the infected cells by Fas ligand signalling (triggering apoptosis of the infected cell), or by releasing perforins, damaging the infected cell membrane inducing its death (Zychlinsky et al, 1991; Podack et al, 1988).

The TH2 immune response involves CD4 T cells, acting as helpers, for B cell activation. The CD4 T cell is activated by an antigen presentation through an MHC class II molecule. MHC class II molecules present exogenous antigens, usually soluble proteins outside the cells, which are internalised, processed and presented in

the cell membrane via MHC class II molecules. CD4 TH2 cell, secretes a different kind of cytokines such as IL-4 and IL 10 (Mosmann et al, 1989).

The primed CD4 T cell will activate B cells (via CD40-CD40L interaction) and will trigger a humoral immune response. This response, causes the release of antibodies against the recognised viral antigens, neutralising the RAd and rendering the virus incapable of infecting (Toogood et al, 1992). The antibodies that bind to the viral antigens expressed on the infected cell membrane trigger a complement cascade which damages the infected cell membrane leading to cell dead (Hirsh, 1982).

1.3.3 B cell activation

The humoral immune response against RAds depends on CD4 T cell activation, stimulated by the recognition of antigen presented by MHC class II molecules on APCs. Once activated, the T cells in the lymph nodes subsequently activate specific B cell clones, which produce antibodies specifically against the presented antigen (Janeway et al, 1997). The specific B cell uptakes the viral antigen by membrane bound antibodies. The antigen is processed and presented on the B cell surface activating CD4 T cells via class II molecules in association with specific CD4 T cell receptors.

The CD4 T cell then produces an activation signal to the B cell by the CD40L T cell receptor binding to the CD40 B cell receptor. This CD40L-CD40 binding activation signal triggers B cell clonal expansion, with apoptotic protection, enabling IgG

antibody class switching (Armitage et al 1993) and germinal centre production (Ma et al, 1995).

Before the B cell is properly primed, it express only IgM antibodies (Yang et al, 1996), which have a short half-life, significantly increased by the IgG switching. The germinal centres produce mutated B cell clones (originated from the activated B cell clone) which produce antibodies with increased affinity for the viral antigen that triggered the activation (Janeway et al, 1997).

1.3.4 Role of CD40-CD40L interaction in the immune response to RAds

One of the objectives of this thesis will be to inhibit the acquired immune response with a RAd carrying a soluble form of CD40, the CD40 Ig, by CD40-CD40L interaction blockade.

CD40L genetic deficiency in mice and humans illustrates the multiple defects in B cell activation, including failure to form germinal centres, activate memory B cells and IgG class switching (Ma et al, 1995). Experiments in knockout mice have implicated CD40L in the antigen-specific priming of T cells, and enhanced susceptibility of CD40L-deficient mice to Leishmania infection is consistent with an important role of this molecule in TH1 immune responses (Grewal et al, 1996;Soog et al, 1996; Campbell et al, 1996). Similar results were obtained by blocking the CD40-CD40L interaction by anti CD40L antibodies, preventing Experimental Alergic

Encephalomielitis by hampering a TH1 T cell differentiation (Samoilova et al, 1997; Carayaniotis et al, 1997; Gerritse et al, 1996).

It has been shown that TH1 inhibition is due to a TH2 immune deviation, produced by the blockade of the CD40-CD40L interaction (Tang et al, 1997). CD40L when bound to DC CD40, has been shown to strongly induce the secretion of IL-12 by the DC (Koch et al, 1996). IL-12 is a strong inducer of TH1 responses and Interferon γ production of CD4 T cells (Heufler et al, 1996). By blocking the CD40-CD40L interaction, the production of IL-12 is hampered. This impedes a TH1 response enabling TH2 differentiation of the primed CD4 T cells, decreasing or inhibiting CTL effector functions by TH2 cytokines secretion.

Infection with E1/E3 deleted RAds, containing the LacZ as transgene, into mice (by tail vein administration), led to transgene expression in 93% of hepatocytes in the liver, harvested after 3 days, diminishing to undetectable levels at day 24 (Yang et al, 1996). This is due to the immune response, demonstrating the important role of the acquired immune response in RAd clearance. Analysis of the CD4 T cells *in vitro* demonstrated activation against viral antigens of both TH1 (interferon γ and IL 2 detection) and TH2 (IL 10 and IL 4 detection) CD4 T cells subsets. The presence of CTLs against viral-infected cells were detected 10 days after gene transfer and germinal centres were found producing neutralising antibodies against the RAd (Yang et al, 1996).

Similar studies performed in CD40L deficient mice demonstrate the requirement of CD40-CD40L interactions for cellular and humoral immune responses to RAds. In

these mice, transgene expression was stable for 24 days and CTLs against viral infected cells were significantly reduced. CD4 T cells harvested 10 days after gene transfer, were unable to respond to viral antigens. No germinal centres were detected, and no IgG neutralising antibodies were produced. IgM antibodies were found (Yang et al, 1996). Consistent with this information, if the CD40-CD40L interaction is blocked at the time of RAd infection, the humoral and/or the cytotoxic immune responses against the RAd and its transgene could be inhibited or at least decreased. This would enable longer transgene expression and repeated readministrations of the RAd, as it was recently shown by anti CD40L antibody (MR1) (Scaria et al, 1997).

1.3.5 Immunoprivilege status of the brain parenchyma

Contrary to the results obtained within the CNS periphery E1/E3 RAds can promote sustained transgene expression within the brain (Byrnes et al, 1997; Thomas et al, 2000; Thomas et al, 2001). There is still controversy with regard to the reasons underlying the prolonged transgene expression in the brain, but certainly it has to be related to the fact that an immune response can not be elicited when injecting RAds into the brain parenchyma. Numerous studies (Byrnes et al, 1996; Thomas et al, 2000; Gerdes et al, 2001) have shown that peripheral priming of the immune response (by intradermal injection of RAds), after RAd injection in the brain, eliminates transgene expression. These results indicate that the acquired immune response is able to recognize antigens within the brain, but it has to be previously activated in the periphery of the CNS in order to eliminate transgene expression.

After peripheral immunisation occurs, activated T cells can cross the blood brain barrier (BBB) and enter the CNS (Wekerle et al, 1986), encounter the target infected cell and eliminate transgene expression, whereas circulating naive T cells cannot readily cross the BBB (Fabry et al, 1994).

These observations suggest that the brain does not possess the necessary requirements for antigen presentation in a co-stimulatory way via DC, and is therefore incapable of priming an immune response. The brain becomes then an immuno-privileged organ, not because the adaptive immune response can not act but because it can not be triggered.

An explanation as to why DCs can not prime immune responses within the brain is open to debate. Lowenstein (2001) sustains that during the evolution of the immune response, DCs were unable to colonise the brain. This theory concludes that antigen presentation does not occur because there are no resident DCs in the brain to uptake and present the antigens. Another possibility might be that there are DC, also capable of brain antigen uptake, but the cytokine background of the brain prevents DCs maturation and professional antigen presentation. Very recently it has been shown (Ali et al, 2001) that after Flt3-L (a cytokine which recruits immature DC) adenoviral transduction into rat brain striata, OX62 positive cells (DC marker) were found within the site of injection. The recruitment of this cell population was not seen when applying the same dose of a control RAd harboring no transgene, indicating that the infiltrating OX62 positive cells were induced by the Flt3-L expression and not by the RAd injection. If those cells can be identified as DC, the results will indicate that effectively DC can be present in the brain when the appropriate cytokine

environment is created. The appearance of this cell population, inexistent before RAd Flt3-L injection, could be due to differentiation of resident cells or by infiltration from the CNS periphery. Very recently Fischer et al demonstrated functional DC differentiation from resting microglia after *in vitro* exposure to GM-CSF and CD40 ligation. Nevertheless future experiments are necessary in order to confirm the origin and class of the infiltrating cells found by Ali et al, and even if shown to be DCs, to prove that they can mature and present antigens in order to stimulate an adaptive immune response.

1.4 Objectives of the thesis

1. Generate an E1/E3 deleted first generation adenoviral vector carrying β-galactosidase as transgene under the control of the mCMV promoter (RAd 36) to characterised the promoter strength.

2. Compare the ability of RAd 36 to express β-galactosidase with the expression achieved by RAd 35 (an E1/E3 deleted first generation adenoviral vector carrying β-galactosidase as transgene under the control of the hCMV promoter) to determine the stronger promoter.

3. Analyse and describe the transduction efficiency of E1/E3 deleted first generation adenoviral vectors in the brain.

4. Lower the viral vector dose in the brain, in order to find a threshold of virus that can avoid the immune response, hence prolonging transgene expression.

5. Describe the innate and adaptive immune responses against first generation adenoviral vectors in the brain.

6. Generate E1/E3 deleted first generation adenoviral vectors carrying therapeutic transgenes under the control of the mCMV promoter i.e. RAd M40 containing CD40lg as a transgene in order to block activation of the adaptive immune response.

Chapter 2: Materials and Methods

2.1 Molecular Biology

2.1.1 Bacterial cultures

Molecular biology procedures requiring bacteria, were all carried out in DH5α E.coli carrying the ampicillin resistance gene. Bacterial suspension cultures were grown at 37°C on a shaker overnight in LB broth containing ampicillin at a final concentration of 100 μg/ml. Bacteria were also grown in LB-agar plates with ampicillin (100 μg/ml) at 37°C.

2.1.2 Preparation of competent bacteria (Hanahan's method)

To enable DH5α Ecoi to be transformed with foreign DNA, bacteria cultures were treated as follows:

1. DH5α bacteria were grown in 10 ml of sterile PsiB overnight.
2. Then 1 ml of the culture was added to 100 ml of sterile PsiB, and grown to OD_{500}= 0,8-1.0.
3. Incubated on ice for 15 minutes
4. Centrifuged at 3000 rpm for 15 minutes and resuspended in 40 ml of cold TfbI.

5. Incubated for 15 minutes on ice, centrifuged 15 minutes at 3000 rpm (4°C) resuspended in 4 ml of TfbII
6. Incubated for 15 minutes on ice, and aliquoted in eppendorf tubes pre chilled in 70% ethanol at -70°C and stored immediately at -70°C.

2.1.3 Transformation of competent bacteria

This procedure was done in order to obtain bacterial clones that will carry particular constructions of plasmidic DNA, so that this DNA of interest can be easily obtained and scaled up.

1. 50 μl of competent DH5α bacteria were added to 10 μl of ligation mix containing 100ng of DNA
2. Incubated for 30 minutes on ice, then 2 minutes at 42°C and 2 minutes on ice to finish the transformation.
3. Then 1ml of LB media was added and incubated at 37°C for 1 hour.
4. Finally it was spread in LB agar plates with ampicillin and left it overnight.

2.1.4 DNA digestions by restriction enzymes

DNA was needed to be cut in order to isolate and use specific DNA fragments, to generate the desired DNA constructs and produced RAds

carrying the transgene of interest. To cut the DNA different restriction enzymes were used, all of them commercially obtained from Promega, UK. It was used approximately 2 U of enzyme per μg of DNA. The appropriate provided buffer was used for each enzyme to achieve maximal enzimatic activity. The enzyme amount added to the digestion solution was never more than 10% the final volume, in order to avoid glycerol interference with DNA cutting. The water used was sterile and DNAse free. Digestions were run for 2 hours-overnight.

2.1.5 Agarose Gel Electrophoresis

The results of restriction enzyme digest were analysed by agarose gel electrophoresis, staining the DNA with ethidium bromide, and visualised by ultraviolet irradiation of the gel. The gel was prepared with TAE buffer and agarose (NBL, Gene Sciences, UK) to a final concentration of 0.8%. 1 μl of a 10 mg /ml of ethidium bromide was added for visualisation.

2.1.6 DNA gel extraction

This procedure was done to recover particular DNA fragments after cutting with the appropriate restriction enzymes and running an agarose gel electrophoresis:

1. The DNA was run on 0.8% agarose gel, and after good separation, the appropriate band was excised from the gel with clean sharp scalpel.
2. The gel slice was weighed and the DNA was purified with a QIAquick Gel extraction Kit, (from QIAGEN, Germany).

2.1.7 DNA dephosphorylation

Linear DNA, which will be used for ligations with a specific insert, was dephosphorylated to prevent religation of the backbone without DNA insert. To Fifty µl of linearised DNA, it was added:

1. 2 µl of Calf Intestinal Alcaline Phosphatase (CIAP)
2. 6 µl of CIAP buffer
5. 2 µl of dH_2O (to a final volume of 60µl)

The solution was incubated for 2 hours at 37°C, 2 µl of CIAP was added and further incubated at 37°C for another 2 hours. Reaction was stopped with 0.2 M EDTA.

2.1.8 DNA ligations

DNA was digested to generate compatible ends for cloning. To ensure that the right fragment is obtained, the DNA was purified by agarose gel electrophoresis. After obtaining the appropriate DNA fragments (vector and insert) the correct DNA amounts were calculated for ligation:

ng of Vector x size in bp of Insert / size in bp of Vector= ng of Insert

Ligation was carried out always in a final volume of 20 µl overnight at 10-15°C, following the Promegas protocols and applications guide (third edition).

2.1.9 5' protrudance blunt end ligation

When the DNA fragments didn't contain compatible ends with the vector, blunt end terminus were generated in order to enable ligation.

1. To blunt end the insert and the vector a mix was prepared containing: 40 µM of dNTP, 0.1 mg/ml of BSA, 1u/µg of DNA of Klenow enzyme (Promega, UK), Klenow buffer, and 10 µg of the respective DNA.
2. This was incubated at room temperature for 30 minutes, and the reaction was stop with 0.5 M EDTA.
3. A phenol chloroform extraction was carried out adding equal volume of a solution of phenol:chloroform:isoamyl alcohol (25:24:1) vortex and centrifuge 2' at 12000 rpm.
4. To the supernatant it was added ½ volume of NH_4OAc 7.5 M, one volume of ethanol (100%) and incubated at -20°C for 2 hours. Then pellet and resuspended in DNAse free water. The vector was also dephosphorilated as described in the Promegas protocols and applications guide (third edition).

5. Ones the DNA fragments (Insert and vector) were ready; they were ligated overnight as described previously

2.1.10 Southern blot

Presence of the transgene DNA in each generated RAd was positively identified by digestion with Hind III and subsequent southern blotting. The DNA probe to detect the transgene was labelled by random priming with dioxigenin-dUTP (Boehringer Mannheim, Bell Lane, East Sussex, UK). The viral DNA was digested with Hind III and run on a 0.8% agarose gel.

1. DNA on the gel was denature by soaking the gel 20 minutes in 0.4M NaOH with constant shaking.
2. The gel was placed on wrapped Whatman 3 MM paper soaked in 0.4 M NaOH and placed in a special container for blotting with 400 ml of 0,4 M NaOH.
3. Then a nylon filter of the same size was carefully placed on top of the gel (Nytran, Schleicher & Schuell, NH, USA) and covered with two additional pieces of Whatmann 3 MM paper. After that 2 inches of towel paper and finally 0,5 kg weight was placed on top to assure DNA transfer by capillarity to the nylon membrane after more than 6 hours.
4. Pre-hybridisation: The nylon membrane was collected, soaked briefly in 5x SSC, and transfer to a plastic bag. Then added pre-hybridisation

solution and seal the bag removing air bubbles. This was left 2 hours at 68 °C.

5. Hybridisation: after pre-hybridisation, the bag was open and the probe (previously denatured for 10 minutes in boiling water, and chilled immediately on ice) was added. The bag was resealed and left it overnight at 68°C. Then washed with 2x SSC and 0.1% SDS solution twice for 5 minutes, and finally washed in 0.1x SSC, 0.1% SDS solution for 30 minutes at 65°C.

Immunodetection: The filter was washed in buffer 1 for 1 minute, incubate for 30 minutes in buffer 2, and re-washed in buffer 1. Then the membrane was incubated for half an hour with an antibody against dioxigenin conjugated to peroxidase (Boehringer Mannheim, Bell Lane, East Sussex, UK) diluted 150mU/ml with buffer 1. After this, the membrane was equilibrated in buffer 3 for 2 minutes, and the colour substrate was added. After the bands appeared the membrane was washed in buffer 4 for 5 minutes and dried at room temperature.

2.1.11 Small-scale plasmid DNA preparations (minipreps).

It was done in order to obtain small amounts of DNA (<5 μg) from bacterial cultures, eg. for DNA identification of bacterial clones.

1. Transfer a single bacterial colony into 2 ml of LB medium containing the appropriate antibiotic in a 15 ml tube. Incubate the culture O/N at 37°C with vigorous shaking.
2. Transfer 1.5 ml of the culture into an eppendorf tube (keeping the rest at 4°C). Centrifuge at 12000g for 30 seconds at 4°C.
3. Remove medium and leave the bacterial pellet as dry as possible.
4. Resuspend the pellet in ice-cold 100 ul solution I by vortexing.
5. Add 200 μl of solution II, and vortex.
6. Add 150 μl ice-cold solution III.
7. Centrifuge at 12000 g for 5 minutes at 4°C and transfer the supernatant to a fresh tube.
8. Optional: add equal volume of phenol:chloroform and mix by vortex. After centrifuge at 12000g for 2 minutes at 4°C. Transfer the supernatant to a fresh tube.
9. Precipitate the double-stranded DNA with 2 volumes of ethanol at room temperature. Vortex, and leave for 2 minutes.
10. Centrifuge at 12000g for 5 minutes at 4°C.
11. Remove supernatant, removing any fluid drops of the wall of the tube.
12. Rinse the pellet with 1 ml of 70% ethanol at 4°C and remove supernatant as in 11.

13. Redissolve nucleic acids in 50 ul of TE (pH 8.0) containing RNAse (20 ug/ml). Store at -20°C.

Notes

This protocol was modified to accommodate up to 10 ml of bacterial culture as follows when more DNA was needed:

a. Centrifuge 10 ml of bacterial culture at 4000 rpm for 10 minutes at 4°C.

b. Step 1, resuspend in 200 µl Solution I.

c. Step 2, add 400 µl solution II.

d. Step 3, add 300 µl solution III.

e. Step 5, transfer 600 µl of supernatant to a fresh tube.

f. Step 6, precipitate DNA with 600 µl isopropanol.

2.1.12 Large scale plasmid DNA preparation by QIAGEN protocol.

When high amounts of DNA were required (eg. to obtain DNA for the generation of RAd) the following protocol was used:

1. Grow O/N 500 ml of bacteria in LB with appropriate antibiotics.
2. Spin down cells at 3500 rpm for 20-30 minutes at 4°C.
3. Drain off the supernatant, and resuspend pellet in 10 ml buffer P1.
4. Add 10 ml buffer P2 mix gently and incubate for 5 minutes.

5. Add 10 ml of chilled buffer P3, mix gently and incubate for 20 minutes on ice.

6. Centrifuge at 20000 g for 30 minutes at 4°C and recover supernatant.

7. Equilibrate QIAGEN column with 10 ml buffer QBT.

8. Apply supernatant of step 6 to the column and allow gravity flow.

9. Wash column with 30 ml of buffer QC.

10. Elute DNA from column with 15 ml buffer QF.

11. Precipitate DNA with 10.5 ml (0.7 volumes) isopropanol, mix and centrifuge at 15000g for 30 minutes at 4°C.

12. Wash DNA pellet with 5 ml of 70 % ethanol and centrifuge at 15000 g for 10 minutes.

13. Discard supernatant, air-dry pellet and re-dissolve in TE (pH 8.0).

2.1.13 Phenol: chloroform extraction

Performed to denaturate and remove proteins from a given solution.

1. Add equal volume of phenol:chloroform:isoamylalcohol (25:24:1) and mix thoroughly

2. Centrifuge at 13000 rpm (in a microcentrifuge) 2 minutes

3. Rescue the top colourless layer (from the 3 visible layers) containing the DNA.

2.1.14 Ethanol precipitation

To precipitate and separate DNA from a given solution.

1. Add to the DNA (to be precipitated) 1/10th volume of 3M sodium acetate (pH 5.2)
2. Add 2 volumes of chilled 100% ethanol
3. Incubate at –70 C for 1-2 hours
4. Pellet by centrifuging at 13000 rpm for 10 minutes
5. Wash with 70% ethanol (to remove salts)
6. Centrifuge 2 minutes at 13000 rpm and discard the supernatant
7. Resuspend in sterile dH_2O

2.2 Cell culture

2.2.1 Cell lines

Human embryonic kidney cells, HEK 293, 293 cells are transformed cells derived from human embryonal kidney cells, which encodes for the E1 region of the human adenovirus type 5 (Ad5). Being sensitive to adenoviral infection and transcomplement replicative deficient Ad5. They were obtained from Microbix, Biosystems Inc., Toronto, Ontario, Canada. The glioblastoma cell line (CNS-1), was kindly provided by Dr. William F Hickey (Pathology Dept.. Darmouth Medical School, NH, USA). The murine neuroblastoma cell line (Neuro2A), the SV40 transformed African green monkey kidney cell line (COS7), the human cervical epitheloid carcinoma cell line (Hela), and the Chinese hamster ovary cell line (CHO) were purchased from the European Collection of Animal Cell Cultures (Porton Down, Salisbury, UK).

2.2.2 Growth of cell lines

Cells stored in cryo-vials in liquid nitrogen were quickly thawed at 37°C, and inoculated after washing the cryo-preservation media, into 25 cm3 flasks containing 6 ml of growing media, being incubated at 37°C with 5% carbon dioxide. When they reach 80-90% confluency, cells were split in 1:4.

HEK 293 cells were growm in Minimum essential medium (from Gibco BRL) supplemented with 10% (v/v) fetal calf serum (FCS) (Gibco BRL), 1% (v/v) 1X MEM non-essential amino acids (Gibco BRL), 2mM L-glutamine (Gibco BRL), 100 units/ml Penicillin (Gibco BRL) and 1mg/ml Streptomycin (Gibco BRL). All other cell lines were grown in Grow all medium: DMEM with 10% (v/v) horse serum (Gibco BRL), 5% (v/v) fetal calf serum (Gibco BRL), 1X MEM non-essential amino acids (Gibco BRL) 2mM L-glutamine (Gibco BRL), 1mM sodium pyruvate (Gibco BRL).

2.2.3 Splitting of cells

To split and scale up, a given cell line.

1. When a cell line grown in flasks, reached 80-90% confluency, they were rinse with 5 ml Dulbecco's PBS (Gibco BRL),
2. Then Detached by I ml of trypsine-EDTA 1x solution (Gibco BRL) and suspended by flask hand striking.
3. Six ml of appropriate growing medium was added, and after carefully disaggregated the cells by pipetting, 1 ml was added to each of 4 flasks containing 5,5 ml of media and incubated at 37°C with 5% carbon dioxide.

2.2.4 Cell freezing

For long term storing cell stocks.

1. 80-90% confluent cell flasks were trypsinised, added 9 ml of fresh 293 media and desegregated the cells by gently pipetting.
2. Then placed into 15 ml tubes (Falcon, New Jersey, USA) and centrifuge at 1100 rpm for 10 minutes.
3. The supernatant was discarded and the cells were resuspended in 1 ml of freezing media and aliquoted in a cryo-vial, placed overnight at -70°C, and stored after in liquid nitrogen.

2.3 Recombinant Adenovirus (RAds)

2.3.1 Recombinant adenoviral generation

RAds were generated by co-transfection of 293 cells, using the calcium chloride precipitation method, with recombinant shuttle vectors and the pJM17. pJM17 is a bacterial plasmid containing a circular and unpackageable form of Ad5 genome, with deletions in E1 and E3 (Microbix Biosystems Inc., Toronto, Ontario, Canada) Rads were generated by homologous recombination of these plasmids.

2.3.2 Calcium chloride precipitation method for co-transfection.

1. 5 μg of shuttle vector and 5 μg of pJM17 were added to sterile15 ml tube containing sterile low TE buffer, to a final volume of 210 μl.
2. Then 30 μl of sterile 2 M calcium chloride was added dropwise with gently vortexing.
3. This solution was added dropwise to a 15 ml tube containing sterile 2x HBS while vortexing gently, and left it 30 minutes at room temperature.
4. During this time, 293 flasks splited the day before, and grown to 40-50% confluency, were fed with fresh 293 media, and after the 30 minutes of DNA precipitation, the mixture was added to the 293 flasks

and left 16 hours. Then washed first with 5 ml of Dulbecco's PBS, and 5 ml of 293 media.

5. Then 6 ml of fresh 293 media was added and changed every 3 days. Plaques were visible after 5-7 days, the virus was allowed to spread, and it was harvested collecting the cells and resuspending them in 1 ml of PBS.
6. Then freeze in liquid nitrogen and thaw 3 times to brake the cells, and centrifuge to pellet the debris. It was stored at -20°C. All the collected viruses were inspected to detect the positives ones by southern blot.

2.3.3 Small scale preparation of RAd stocks

This was done when small amounts, of a particular virus, was needed, as for viral DNA extraction, or viral scaling up.

1. 293 cells were grown in 25 cm3 flasks to 50% confluence.
2. The flasks were then inoculated with 10 µl of the viral stock obtained after co-transfection.
3. After 2-3 days was observed and the cells were collected in 15 ml tubes and centrifuged for 5 minutes at 1000 rpm.
4. The supernatant was discarded the cells resuspended in 1 ml of Dulbecco's PBS and placed in screw cap eppendorfs. Then freeze thawed 3 times and stored at –70°C.

2.3.4 Viral DNA extraction

To check identity of a particular virus, DNA was extracted in order to study the digestion pettern and detecting specific genes by southernblot.

1. 293 cells were infected with 10 µl of the stock virus, and harvested after cytopathic effect was observed (2-3 days).
2. Centrifuged and the pellet resuspended in 360 µl of TE pH 8.0.
3. Then 25 µl of 10% SDS was added, 8 µl of EDTA 0.5M and 4 µl of proteinase K (20 mg/ml) and Incubate 2 hours at 37°C.
4. Then 100 µl of NaCl 5M was added keeping on ice for 3 hours and centrifuge for 1 hour at 4°C.
5. The supernatant was extracted with phenol:chloroform:isoamyl alcohol (25:24:1) and precipitated the DNA with 2 volumes of ethanol.
6. Centrifuge for 15 minutes, washed with 70% ethanol and dried in the hood resuspending in 50 µl of dH_2O with 0.1 mg/ml RNAse.

2.3.5 Serial dilution viral purification.

During RAd generation is possible to obtain, not only the desired virus, but also at the same time, it can be produced undesirable RAd constructs or even replication competent adenovirus. This products would contaminate the RAd stocks, reducing safety and/or viral dose therapeutic effect. To fight this

possibility, generated RAds, were purified by serial dilution in order to obtain viral stocks originated by a single infectious viral particle.

1. A 96 well plate was seeded with 7000-9000 293 cells per well and incubated overnight.
2. Serial dilutions of RAds, from 10^{-2} to 10^{-11}, were prepared in 293 medium. Medium from the plate was removed and 100 µl was added to 3 wells for each viral dilution.
3. After an overnight incubation, another 100 µl of 293 medium was added to each well.
4. After 8 days, the endpoint well (the last serial dilution well with plaque formation) was determined, and harvested by freeze thawing 3 times. The plaque purification process was repeated two further times using the harvested virus from the previous plaque purification, ensuring that the final virus stock is derived from a single infectious particle.

2.3.6 Purification of RADs by Caesium Chloride gradient centrifugation.

As a final purification step, to completely eliminate proteins, cellular DNA and most defective RAd particles, that will contaminate the final viral stock also increasing the chances to triggered undesirable immune responses.

1. Grow 20 175cm^2 flasks of 293 cells to 70% confluence in 293 medium.

Aspirate the medium and inoculate each flask with 25ml fresh 293 medium with the viral stock at an MOI of 3.

2. 24 hours later add an additional 25ml of fresh pre-warmed 293 medium to each flask.
3. When complete CPE can be observed throughout the monolayer, recover the detached cells in sterile 50 ml centrifuge tubes (2 flasks per tube) and spin down the cells at 300*g* for 15 minutes at 4°C.
4. Discard supernatant of each tube and resuspend the cell pellet in 0.5m sterile PBS cm^2.
5. Pool the cell suspension from all the tubes in one sterile 15ml tube and add an equal volume of Arklone P™ to lyse the cells.
6. Mix and centrifuge at 500*g* for 20 minutes at 4°C.
7. Harvest the top aqueous layer, and store it in a 15 ml centrifuge tube at – 70°C, (can be stored for several years), or proceed to purification by caesium chloride gradient centrifugation.
8. Layer 1.5ml of caesium chloride at a density of 1.45g/ml and 2.5ml of caesium chloride at a density of 1.33 g/ml in a Beckman 14ml centrifuge tube using a 5ml syringe and 18G wide bore needle. Densities are calculated by determination of the refractive index. Caesium chloride is dissolved in CsCl buffer, (8.31g of CsCl was added to 11ml of CsCl buffer to form the 1.45g/ml solution and 8.31g of CsCl to 16ml of CsCl buffer to form the 1.33 g/ml solution, both solutions were freshly prepared). Place the least dense layer at the bottom of the tube first using a syringe and then float this layer on top of the more dense layer by placing the wide bore needle at the bottom of the tube and injecting very slowly

9. Carefully layer up to 8ml of the Arklone P™ purified virus onto the gradient.
10. Layer mineral oil on top of the viral layer until 1-2mm from the top of the tube. Weigh the tube and set up balance tube to an identical weight before placing the tubes in the centrifuge buckets.
11. Centrifuge for 2 hours at 90,000*g* at 4°C in a Beckman ultracentrifuge in the Beckman swing-bucket SW40 rotor, using maximum acceleration and minimum deceleration (1 & 7 respectively)
12. Carefully remove the tubes from the buckets in class 2 laminar flow cabinet and recover the banded virus by side puncturing the wall of the tube approximately 1cm below the level of the band with a syringe and needle. The viral band will be the lowest of the 3 bands that are visible
13. Dilute the virus fraction with half a volume of sterile TE; pH7.8.
14. Prepare a second caesium chloride gradient prepared as in step 1 using 1ml of 1.45 g/ml and 1.5ml of 1.33 g/ml. Carefully layer the diluted virus band on the gradient and layer mineral oil on top of the virus solution as before.
15. Balance the tube weigh and centrifuge in the SW40 rotor for 18 hours at 100,000*g* at 4°C.
16. Remove the viral band as in step 12.
17. Dialyse the banded virus twice against buffer A for 1 hour and once against buffer B for 2 hours at room temperature.
18. Aliquot the dialysed virus in 5-10µl aliquots and store at -70°C.

2.3.7 Adenovirus Titration

To quantify the amount of infectious viral particles of a given preparation.

1. Inoculate 69 wells of a 96 well plate with $8x10^4$ 293 cells per well in (100 µl).
2. After 24 hours replace medium with 100 µl of serially diluted virus in fresh media, by triplicate for each dilution from 10^{-2} to 7.63×10^{-12}.
3. Add 100 µl to each well of fresh media 24 hours later
4. After 8 days find the end point dilution where all of the three wells of the given dilution shows cytophatic effect.
5. Read off the end point and consult table for iu/ml

Dilution (Total of 22 dilutions)

10 µl of stock virus in 990 µl media 10^{-2} fold

100 µl of 10^{-2} in 900 µl media 10^3 fold

100 µl of 10^{-3} in 900 µl media 10^4 fold

100 µl of 10^{-4} in 900 µl media 10^5 fold

100 µl of 10^{-5} in 900 µl media 10^6 fold

500 µl of 10^{-6} in 500 µl media $5x10^7$ fold

500 µl of $5x10^{-7}$ in 500 µl media $2.5x10^7$ fold

Repeat for further 15 times until $7.63x10^{-12}$

Well	1	2	3	4	5	6
Dilution	10^{-2}	10^{-3}	10^{-4}	10^{-5}	10^{-6}	$5.0x10^{-7}$
i.u./ml	$1.0x10^{3}$	$1.0x10^{4}$	$1.0x10^{5}$	$1.0x10^{6}$	$1.0x10^{7}$	$2.0x10^{7}$
Well	7	8	9	10	11	12
Dilution	$2.5x10^{-7}$	$1.25x10^{-7}$	$6.25x10^{-8}$	$3.12x10^{-8}$	$1.56x10^{-8}$	$7.81x10^{-9}$
i.u./ml	$4.0x10^{7}$	$8.0x10^{7}$	$1.6x10^{8}$	$3.2x10^{8}$	$6.4x10^{8}$	$1.28x10^{9}$
Well	13	14	15	16	17	18
Dilution	$3.91x10^{-9}$	$1.95x10^{-9}$	$9.77x10^{-10}$	$4.88x10^{-10}$	$2.44x10^{-10}$	$1.22x10^{-10}$
i.u./ml	$2.56x10^{9}$	$5.12x10^{9}$	$1.02x10^{10}$	$2.05x10^{10}$	$4.10x10^{10}$	$8.19x10^{10}$
Well	19	20	21	22	23	24
Dilution	$6.10x10^{-11}$	$3.05x10^{-11}$	$1.53x10^{-11}$	$7.63x10^{-12}$	control	control
i.u./ml	$1.64x10^{11}$	$3.28x10^{11}$	$6.55x10^{11}$	$1.32x10^{12}$	control	control

2.4 Support protocols

2.4.1 Adenoviral delivery into the brain striatum

Adult male Sprague-Dawley rats of 200g-250g in weight were anaesthetised with 4% halothane gas vaporised with an oxygen: nitrous oxide mix (1.5l/ minute of oxygen: 0.6l/ minute nitrous oxide). The heads were then shaved and the rats placed in a stereotaxic frame (model 51603, Stoelting) and the halothane level was reduced to 1.6%. The scalp was exposed and a small hole drilled (to allow needle passage and adenoviral injection) 0.6mm forward and +3.4mm and/or –3.4mm lateral from the bregma. Animals were injected using a 26 gauge Hamilton syringe 5.0mm vertical from the dura. Different RAd doses diluted in PBS (pH 7.4) in a total volume of 3µl, were injected in the striatum. An interval of 1 minute was left between each microlitre injected. After the final microlitre was delivered the needle was left in position for a further 3 minutes before withdrawal.

2.4.2 Perfusion-fixation of Brains

At the endpoint of the *in vivo* experiments, animals were terminally anaesthetised with an intra-peritoneal overdose of pentobarbitone (Animal Care limited) (~0.7 ml). Once the animal was unconscious the heart was exposed, pierced with a wide needle (connected by tubing to Tyrode solution),

in the left ventricle and pushed until the ascendant aorta. The procedure was done with constant flow of tyrode solution through the piercing needle. The needle then was clamped (to remain in position throughout the perfusion), and the right atrium was cut to allow flow of tyrode through out the vascular system. To avoid coagulation of the blood and blockage of the vascular system 0.8 ml of heparine was added to every litre of tyrode solution. After circulating 150 ml of tyrode, the solution was changed to 4% (w/v) paraformaldehyde for tissue fixation. At this moment the descending aorta was clamped to restrict paraformaldehyde circulation to the upper part of the body. When tissue fixation was evident the procedure was stopped, and the brain carefully removed from the scalp. Brains were post-fixed overnight in a 50 ml falcon tube with 10 ml of 4% (w/v) paraformaldehyde, and then washed and kept until used in PBS containing 0.1% (w/v) Sodium Azide.

2.4.3 Vibratome sectioning of brains

Paraformaldehyde fixed brains, were serially sectioned on a Leica VT 1000S vibratome in sections 50 μm thick. Sections were stored in 6 well plates in PBS containing 0.1% Sodium Azide. Successive brain sections were distributed in alternate wells of a 6 well plate, to obtain 6 representative sets of the whole brain, each set containing brain serial sections at intervals of 300 μm.

2.4.4 Staining of tissue sections using glucose oxidase

To detect different cell markers (CD8, ED1) or transgene expression (β-galactosidase) directly on brain sections, the following protocol was used:

1. Wash tissue in TBS+0.5% triton, at least 5 minutes.
2. Incubate 15 minutes with 0.3% hydrogen peroxide in PBS.
3. Wash 5 minutes in TBS+0.5% triton.
4. Incubate 60 minutes with 10% horse normal serum (HNS) in TBS+0.5% triton.
5. Incubate with 1st antibody over night at room temperature (diluted as appropriate with 1% HNS in TBS+0.5% triton).
6. Wash at least twice with TBS+0.5% triton.
7. Incubate with 2nd antibody (1/200) for 3-4 hrs.
8. Wash at least twice with TBS+0.5% triton.
9. Incubate with Avidin/Biotin complex for 3 hrs to overnight (prepared at least 1 hr before use to allow complex formation. Use 100 ul Avidin+10 ml PBS+ 100 ul Biotin).
10. Wash twice with PBS.
11. Wash in freshly prepared 0.1M Sodium acetate (pH 6)
12. Develop carefully with a mixture of 1:1 A:(B+C) (B+C must be prepared before used).

2.4.5 RNA extraction from brain tissue

1. Brains were recovered without perfusion of the animals, divided in 5 parts (cerebellum, and 4 size equivalent parts: frontal right, frontal left, medium right and medium left) and quickly frozen in liquid nitrogen in different label tubes.
2. The frontal left part (which contains the injection site) was ground in a mortar containing liquid nitrogen, and the resulting brain powder was stored at -80 in 3 different aliquots.

2.4.6 X-Gal assay (with glutaraldehyde)

To detect expression of β-galactosidase gene from RAd35 or RAd 36 after transduction in different cell lines.

1. Seed day before $8x10^4$ 293 cells/well of 24 well plate
2. Infect with appropriate viral dilution, in triplicate
3. Centrifuge for 90 minutes at 2300 rpm
4. Incubate for 20 hrs
5. Wash once with PBS
6. Replace with 0.5% glutaraldehyde
7. Incubate 5 minutes at 37 C
8. Wash with PBS
9. Add x-gal (1mg/ml) in 5mM K_4 Fe $(CN)_6$, 5mM K_3 Fe $(CN)_6$, 2mM Mg Cl_2
10. Incubate 4 hrs-o/n
11. Count bfu.

2.4.7 X-Gal staining (with paraformaldehyde)

This is an alternative protocol to the glutaraldehyde x-gal staining.

1. Rinse with PBS
2. Fix 4% paraformaldehyde 15 minutes
3. Permeabilise 5 minutes in PBS+ 0.1% triron X-100
4. Wash with PBS
5. stain with X-gal staining solution (in 20 ml PBS add: 42 mg potassium Ferrocyanide, 32 mg Potassium Ferricyanide, 8 mg magnesium chloride and 20 mg X-gal in ½ ml DMSO)
6. wash with PBS
7. air dry

2.4.8 β-Galactosidase activity assay

This was done to measure β-Galactosidase activity, as a way to quantify promoter strength.

1. Enzymatic activity was tested by infecting a. human Hela cell line; b. hamster ovary cell line (CHO); c. mouse neuronal cell line (N2A); d. rat glial cell line (CNS1); e. monkey kidney cell line (Cos7) (figure 5); f & g. rat pituitary cell lines (GH3 and MMQ), h. murine pituitary cell line (AtT20); at increasing MOIs (0, 10, 30, 100, and 300) with RAd35, RAd36, or RAd-Prl/lacZ.

2. Cells were plated in 24-well plates at a density of 20000 cells/ well 1 day prior infection. On day of infection 2 wells/ plate were counted and infected with appropriate MOIs values for each virus.

3. The cells were incubated for two days and then harvested in lysis buffer [25mM Tris-HCL (pH7.8), 6.7% (v/v) glycerol, 10mM $MgCl_2$, 0.01% (v/v) Triton X-100, 1mM EDTA (pH8)].

4. The lysates were incubated with the O-nitrophenol-β-D-galactopyranoside (ONPG) (4mg/ml) substrate solution at 37°C for appropriate time intervals until colour developed within the linear range of the standard curve.

5. The reactions were stopped by the addition of 510μl Na_2CO_3 and samples were read on a spectrophotometer (Pharmacia Biotech, St Albans, UK) at 420nm. The enzyme activity was expressed as units of β-galactosidase produced per μg of total protein detected. Each experimental condition was done in triplicate and each experiment was repeated three times.

2.4.9 BCA Pierce protein assay

1. Mix reagents A and B (Pierce) at a ratio 50:1 and add 250 μl to each sample
2. Incubate at 60 C for 30 minutes

3. Make a standard curve using bovine serum albumin (BSA) as the sample diluting 50, 25, 12.5, 5, 2.5, 1, 0.5, and 0 μg of BSA in 50 μl of dH_2O.

4. Read the optical absorbance at 562 nm in duplicate of each sample, and the average was used to calculate the protein concentration, using the standard curve generated with the BSA values at 562 nm.

2.4.10 Neutralising antibody assay

This procedure was carried out to analyse the presence of neutralising antibodies against adenoviral vectors in blood serum of animals.

1. Heat-inactivate serum samples by incubating at 56°C for 30 minutes

2. Serially dilute 100 μl of serum sample, two-fold in medium (without FCS), in duplicate as follows: ½, ¼, 1/8, 1/16, 1/32, 1/64, 1/128, 1/256, 1/512, 1/1024, 1/2048, 1/4096

3. Add 10 μl of RAd 35 (10^6 iu) to each dilution

4. Incubate at 37°C for 90 minutes

5. Add 50 μl of each dilution to 80 % confluent 293 cells in a 96 well flat bottom plate ($4x10^4$ cells/ well) and incubate for one hour at 37°C

6. Add 50 ml of DMEM with 10% FCS to each well and culture for 12 hours at 37°C

7. X-gal stain

8. neutralising antibody are reported as the dilution which results in a 50 % decrease in transduction compared to the negative control.

2.4.11 LPS assay

The E. coli used to scale up the plasmids to produce RAds posses in their cell walls lipopolysacharids (LPS). Hence it could contaminate adenovirus preparations (Cotten *et al.* 1994). LPS are known to elicit inflammatory responses in the brain, so all preparations were tested for the presence of LPS. Detection of LPS within caesium chloride purified adenovirus was carried out using the BioWhittaker, limulus amebocyte lysate PYROGENT® test (cat no: N184) following the manufacturers instructions. All virus preparations had LPS levels of less than 2 milli-endotoxin units (mEU)/µl.

2.4.12 Preparation of dialysis tubing for CsCl RAd purification

To dialyse CsCl purified viruses, dialysis tubes were prepared.

1. Dialysis tubes 10-20cm long were boiled for 10 minutes in 2% (w/v) Sodium bicarbonate, 1mM EDTA.
2. Then washed in dH_2O, and boiled for 10 minutes in 1mM EDTA
3. Then stored at 4°C maintaining them submersed to prevent drying of the tubes. Before use they were washed in sterile dH_2O.

2.4.13 Gelatin coated slides

To fix brain sections on to glass slides, they were coated with gelatin.

Slides were placed in gelatin solution for 10 minutes and then dried at 37°C in the oven for 2 hours. Alternatively they were dried at 56°C for 1 hour. This procedure was repeated 3 times.

2.4.14 Dehydration and cover slip of brain sections

Brain sections mounted on gelatin coated slides needed to be dehydrated and cover with glass cover slips to allow proper visualization of cells in the microscope.

Sections already mounted on slides were dehydrated by serially washing for 5 minutes in 70% ethanol, 5 minutes in 90% ethanol, 5 minutes in 96% ethanol 5 minutes in 100% ethanol and finally 5 minutes in xylene. Immediately after the xylene, slides were taken out one by one adding DPX mountant for microscopy all over the sections of each slide and finally covered with glass cover slips.

2.4.15 Brain Transduced area quantification.

To determine the extent of transduced cells expressing ß-galactosidase, ED1 or CD8, a Leica Quantimet 600 Image Analysis System (Leica Cambridge

Ltd., UK) was used. The system is controlled by QWin software and a Leica RMDB microscope was used to capture the images. The equipment was calibrated using standard micrometer slides for each lens, and then used to measure the area of transduced cells.

2.4.16 Statistical test used

To generate the statistical P values, the Student T test was used.

2.5 Buffers and Media

LB medium (500 ml):

LB powder	10 g
dH_20	500ml

Sterilised by autoclave, and allowed to cool down before adding respective antibiotic.

LB Agar for plates (500 ml)

Same as above, adding 7,5 g of agar. Sterilised by autoclave and cool down before adding antibiotic. Pour into plates from the flask (~20 ml per plate) and used after solidification.

PsiB medium (500ml)

Bacto-yeast extract	2.5 g
Bacto-tryptone	10,0 g
$MgSO_4$	2.5 g

Sterilise by autoclave

293 grouth medium (~500 ml)

on 500 ml of minimum essential medium Eagle's (Gibco BRL)	
Bovine foetal serum (Gibco BRL)	50 ml
Penicillin/ Streptomycin (5000 U/ml) (Gibco BRL)	6 ml
L-Glutamine (Gibco BRL)	6 ml
MEM non-essential amino acids (Gibco BRL)	6 ml

Freezing medium

Dilbecco's modified Eagle's medium (Gibco BRL)	50%
Dimethyl sulphoxide (DMSO) (Sigma)	10%
Foetal calf serum (Gibco BRL)	40%

2.6 Solutions

Ampicillin

Ampicillin was diluted in dH_2O (100mg/ ml), filter sterilised through a 0.2 μm filter and stored at –20°C until used.

Cell lysis buffer

1.25 ml 1M Tris-HCl (pH 7.8)

100 μl 0.5 M EDTA (pH 8)

15% (v/v) glycerol

10 mM $MgCl_2$

1% (v/v) triton X-100

made up to 50 ml dH_2O

EDTA 0.5 M (pH 8.0)

186.1 g of disodium ethylene diamine tetraacetate 2 H_2O to 800 ml H_2O, mix and adjust pH with NaOH (aprox. 20 g of NaOH), and take to 1 litre. Sterilised by autoclave.

Tris 1 M

121.1 g tris in 800 ml H_2O. adjust pH with HCl and take to 1 litre. Sterilised by autoclave

Ammonium Acetate 5 M

385 g of ammonium acetate in 800 ml H_2O. Complete to 1 litre. Sterilised by filtration.

NaOH 10 M

400 g NaOH pastilles in 800 ml H_2O. Complete to 1 litre. Sterilised by filtration

SDS 10%

100 g of electrophoresis-grade SDS in 900 ml H_2O. Heat to 68°C for dilution. Adjust pH to 7.2 with HCl. Complete to 1 litre.

PBS 10x

1.37 M NaCl, 26.8 mM KCl, 43 mM NaH_2PO_4 and 14.7 mM KH_2PO_4, pH 7.4

LB broth

10 g of Lennox L broth base (Gibco BRL) were dissolved in 500ml of dH_2O and sterilised in autoclave.

TE (pH 8.0)

10 mM Tris HCl (pH 8.0)

1 mM EDTA (pH 8.0)

Sterilised by autoclave

TAE 50x

Tris base 242 g, glacial acetic acid 57.1 ml, 0.5 M EDTA (pH 8.0) 100 ml, complete to 1 litre with dH_2O. The working solution is 1x.

Ethidium bromide (10 mg/ml)

1 g of ethidium bromide to 100 ml H_2O. Stir for several hours. Protect from light, and store at 4°C.

Gel loading buffer (6x)

.25% bromophenol blue, 0.25% xylene cyanol, 40% sucrose in H_2O. Store at 4°C.

Dialysis buffer A

10 mM Tris-base, 1mM $MgCl_2$ and 135 mM NaCl., pH to 7.5 and sterilased by autoclave.

Dialysis buffer B

Dialysis buffer A plus 10% (v/v) glycerol. Sterilised in autoclave.

Gelatin solution

3g of gelatin dissolved in 1 l of dH_2O, heated at 60°C and left to cool down. Sterilised through Whatmann paper and stored at 4°C.

Southern blot solutions

20X SSC

175.3 g of NaCl and 88.2 g of sodium citrate was dissolved in 800 ml of dH2O. pH was adjusted to 7.0 (with NaOH 4M) and taken to 1 litre. Sterilised by filtration.

Pre-hybriditation solution

5x SSC, 1% (w/v) blocking reagent (DIG DNA labelling and detection kit of Boehringer Manheim), 0.1% (w/v) N-lauroylsarcosine and 0.02 % (w/v) SDS, heated to 65 C for 30 minutes to dissolve blocking reagent

Buffer 1 (500 ml)

50 ml Tris-HCl 1M (pH 7.5)

15 ml NaCl 5M

235 ml dH_2O

adjusted pH to 7.5 and complete to 500 ml

Buffer 2 (blocking solution)

0.5 g of blocking reagent (Boehringer Mannheim, UK)

50 ml of buffer 1

Dissolving must be at ~70°C

Buffer 3

10 ml Tris-HCl 1 M pH 8.0

2 ml NaCl 5 M

5 ml $MgCl_2$ 1 M

33 ml dH_2O

Adjust pH to 9.5 and completed to 100 ml with dH_2O

Buffer 4

1 ml Tris-HCl 1 M pH 8.0

200 µl EDTA o.5 M pH 8.0

48.8 ml dH_2O

Adjust pH to 8.0 and completed to 100 ml

Competent bacteria solutions

TbfI

50 mM KAc, KCl 100 mM, 10 mM $CaCl_2$, $MnCl_2$ $4H_2O$ 50 mM, glycerol 15%. Adjust pH to 5.8 with 0.2 M HAc. Sterilised by filtration.

TbfII

MOPS (PIPES) 10 mM, CaCl2 75 mM, KCl 10 mM, glycerol 15%. Adjust pH to 6.5 with KOH. Sterilised by filtration.

Co-transfection solutions

Low TE buffer

Dilute 1:10 TE (pH 8.0) final volume 100 ml. Sterilised by filtration.

2x Hepes Buffered Saline (HBS)

5.6 ml NaCl 5M, 50 mM Hepes, 0.75 ml Na_2HPO_4 0.2M. Adjust pH to 7.12, and complete to 100 ml with dH_2O. Sterilised by filtration.`

$CaCl_2$ 2M

29.4 g of $CaCL_2$ in 100 ml dH_2O. Sterilised by filtration.

Tissue sections staining solutions.

Solution A

7.25 g Ammonium nickel sulphate

150 ml freshly made 0.2 Sodium acetate (pH 6)

600 mg Glucose

120 mg Ammonium chloride

Solution B

150 mg DAB

150 ml dH2O

Solution C

8 mg Glucose oxidase

Small-scale plasmid DNA preparations solutions

Solution I

50 mM Glucose

25 mM Tris Cl (pH 8.0)

10 mM EDTA (pH 8.0)

Solution II

0.2 N NaOH

1% SDS

Solution III

60 ml of 5 M potassium acetate

11.5 ml glacial acetic acid

28.5 ml H2O

Perfusion solutions

yrode (2.5 l)

19.25g	NaCl (132mM)
0.65g	$CaCl_2$ 2. H_2O (1.8 mM)
0.11g	NaH_2PO_4. H_2O (0.32 mM)
2.5g	Glucose (5.56 mM)
2.5g	$NaHCO_3$ (11.6 mM)
0.5g	KCl (2.68 mM)

Na_2HPO_4 (0.2 M)

28.4g / litre

NaH_2PO_4 (0.2 M)

15.6 g / 500 ml

Phosphate buffer (2 l)

1 l	Na_2HPO_4 (0.2 M)
228.8 ml	NaH_2PO_4 (0.2 M)
770 ml	dH_2O
3.8 g	EGTA
0.8 g	$MgCl_2$. 6 H_2O

Fix

600 ml	dH_2O (prewarmed at 60^0C)
80 g	paraformaldehyde
3 pellets	NaOH
1.4 l	phosphate buffer

Chapter 3: Strong promoters are the key to highly efficient, non-inflammatory and non-cytotoxic adenoviral mediated transduction into the brain.

3.1 Introduction

In spite of their importance to the potential clinical success of gene therapy, neither the efficiency of viral vector mediated gene transfer *in vivo*, nor the number of viral infectious particles (iu) needed to transduce a single cell *in vivo*, have been previously determined. Although viral vector mediated gene transfer *in vitro* is thought to be very efficient (Mittereder et al, 1996), *in vivo* gene transfer normally requires the use of high numbers of viral infectious units to achieve anatomically detectable and physiologically relevant levels of transgene expression. Similar data have been reported with the different types of viral vectors utilised to date (Blomer et al, 1997).

In addition to the apparently low efficiency of transgene expression *in vivo*, it has been demonstrated important side effects of E1/E3 deleted first generation adenoviral vectors used to transfer genes to the CNS. Direct cytotoxicity, and strong persistent brain inflammation were observed following the injection into the brain of functionally effective doses of first generation adenoviral vectors (Wood et al, 1996; Dewey et al, 1999; Thomas et al 2001). Titres of 10^7 iu were found to produce acute inflammation (macrophage/microglial, and CD8+ lymphocyte/NK cell infiltration)

while doses of 10^8 iu and above caused also direct cytotoxicity (astrocyte and neuronal cell death) when injected into the adult rat brain (Gerdes et al, 2000; Thomas et al 2001). Using an adenoviral vector expressing ß-galactosidase from the very strong major immediately early murine cytomegalovirus (mCMV) promoter (Addison et al, 1997; Sallanave et al, 1998; Marr et al 1998) we now demonstrate the extremely high gene transfer efficiency and expression in the adult rat brain that can be achieved with adenoviral vectors. At very low doses of this vector (10^1-10^3 infectious units per injection site), the number of detectable transduced brain cells is equal or very close to the number of viral infectious units injected, demonstrating for the first time that a **single** infectious adenoviral particle is capable of transducing a brain cell *in vivo* producing sufficient transgene expression to be reliably detected by immunocytochemistry.

This vector allows transgene expression throughout relatively large areas of the brain at high levels, in the complete absence of any cellular inflammation or cytotoxicity. This was achieved because of the high transduction efficiency of this novel vector, which allowed a decrease of the viral dose to levels below 10^6 iu. With these doses of virus, even though we detected very high levels of transgene expression, we were able to completely avoid the deleterious effects associated with RAd doses above 10^7 iu in the brain.

3.2 Results

3.2.1 Construction of pAL 120

In order to produce a shuttle vector for future generation of E1/E3 deleted first generation adenoviral vector (section 1.2.2.3.2) carrying the mCMV as the transgene promoter, pAL 120 was constructed (figure 6). The shuttle plasmid contains a 1.4 kb version of the mCMV promoter (provided by Dr. Martin Messerle, Max von Pettenkofer Institute, Munich, Germany).

A Hind III fragment from the pUC19-mCMVp containing a ~1.4 kb major immediately early murine cytomegalovirus (mCMV) promoter and an ~0.15Kb SV40 polyadenylation signal, was subcloned into a Hind III digested pAL119 backbone (with the major immediately early human cytomegalovirus (hCMV) promoter and the SV40 polyadenylation signal deleted, by the hind III digestion) (figure 6). Identification of the right clone carrying the pAL120 after ligation was verified by Sac I and Hind III digestion (gel picture in figure 6). The plasmid pAL119 is a shuttle vector which contains the left ITR, the packaging signal and viral sequences from adenoviral map units 10 to 16. It is used to generate, by Grahams method (section 1.2.2.3.2), E1/E3 deleted first generation recombinant adenoviral vectors by co-transfection in HEK 293 cells with pJM17. pJM17 carries the complete version of the adenoviral genome, with the packaging signal deleted, a deletion in E3 and an insertion in E1.

Figure 6

Generation of pAL120

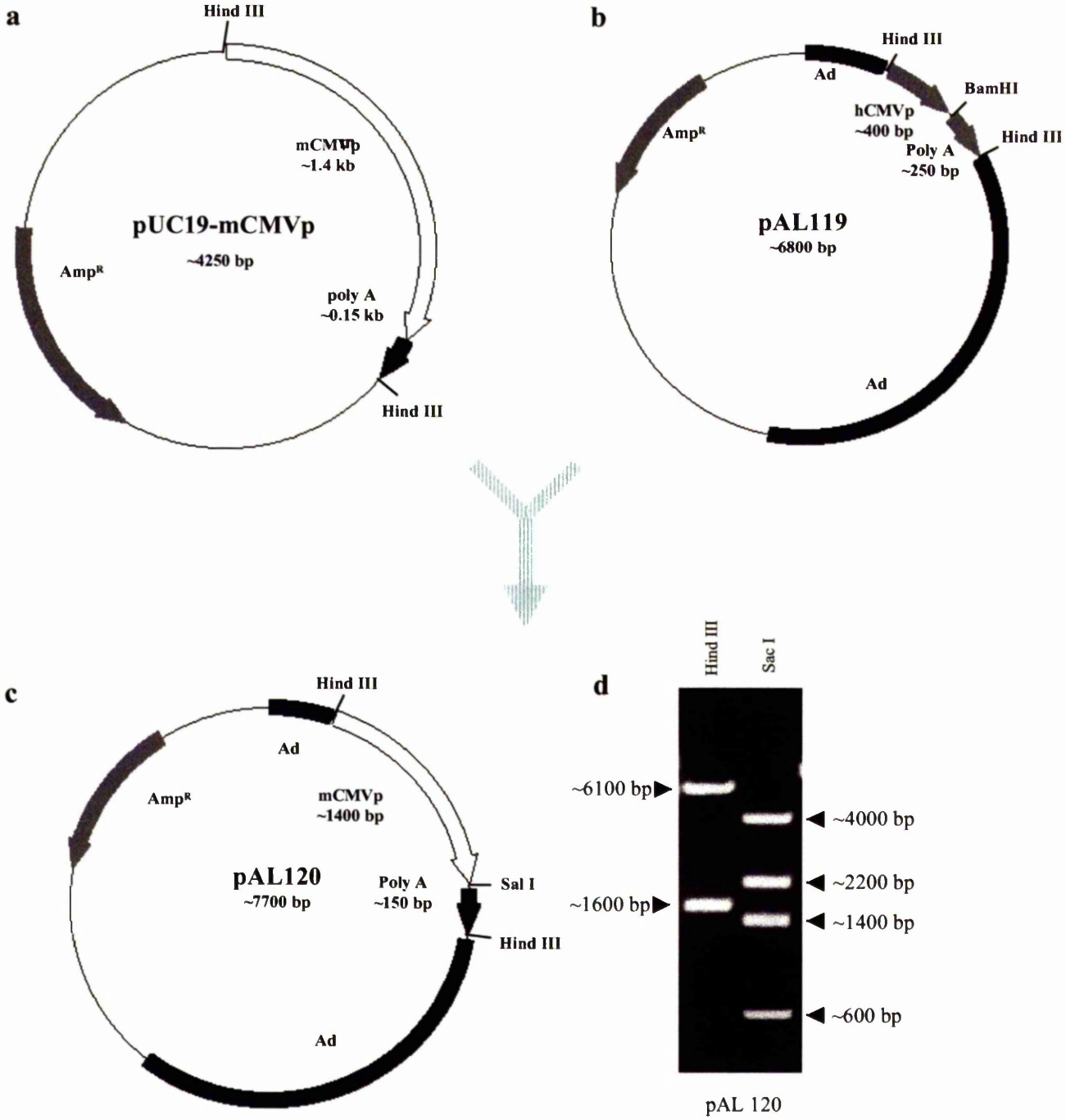

Figure 6.

a. Plasmid pUC19-mCMVp. From this plasmid, sent by Dr. Martin Messerle, Max von Pettenkofer Institute, Munich, Germany , the mCMVp plus a SV40 poly A was isolated by Hind III digestion.

b. Representation of the plasmid pAL 119, shuttle vector for the construction of an E1/E3 deleted first generation adenoviral vector, lacking transgene (which can be inserted in the cloning site Bam HI) having the hCMV promoter and a SV40 poly A one on each side of the cloning site. This shuttle plasmid was used to generate the RAd 0, a recombinant adenovirus carrying no transgene (section 3.2.3)

c. After ligation between a Hind III fragment containing mCMVp plus a SV40 poly A and the Hind III digested backbone of pAL119 (without the hCMVp+polyA cassette) it was generated pAL 120. This plasmid is a shuttle vector used for the construction of an E1/E3 deleted first generation adenoviral vector, lacking transgene (which can be inserted in the cloning site Sal I) having the mCMV promoter and a SV40 poly A one on each side of the cloning site. In this plasmid the Lac Z gene was cloned in the Sal I site by blunt end ligation generating the shuttle plasmid to produce RAd 36, a recombinant adenovirus carrying Lac Z as transgene under the control of the mCMV promoter (section 3.2.2).

d. Restriction enzyme analysis, to verify identity of pAL 120. Plasmidic DNA of pAL 120 was digested with Hind III, which should release the mCMVp-PolyA cassette, giving two bands: ~1600 bp (the cassette) and ~6000 bp (plasmid backone). The plasmid was also digested with Sac I to check the right orientation of the insertion, which should give 4 bands: ~4000 bp, ~2200 bp, ~1400 bp (mCMVp) and ~600 bp (which includes the polyA).

Successful subcloning of the mCMV-polyA promoter in the pAL119 (hCMV-polyA deleted) was checked by the release with Hind III of the 1.6 Kb fragment. The right orientation was verified by digestion with Sac I, which released 4 bands: ~1.4 Kb, ~0.5 Kb, ~2.1 Kb and ~4.0 kb. Incorrect orientation would release the same bands but a ~0.3 Kb instead of the ~0.5 Kb band shown in the right orientation.

The final plasmid contained adenoviral sequences from map units 10 to 16 including the ITR and the packaging signal and a cloning site to insert the transgene of interest, between the mCMV promoter and a SV40 polyadenilation sequence.

3.2.2 Generation pAL120-LACZ

Blunt end ligation was used to subclone a Sal I/ Xba I fragment containing the Lac Z gene (extracted from pGEM 9ZF-Lac Z), into Sal I digested, and blunt-ended pAL 120. The ligation occurred between the mCMVp and the poly A and the resulting plasmid called pAL120-LacZ (figure 7).

3.2.3 Generation of RAd 36

In order to test the efficiency of β-galactosidase expression driven by the mCMV promoter and to compare it with RAd 35 (an E1/E3 deleted first generation adenoviral vector with Lac Z as the transgene under the control of the hCMV promoter), an E1/E3 first generation adenoviral vector was generated carrying

Figure 7

Generation of pAL120-LacZ

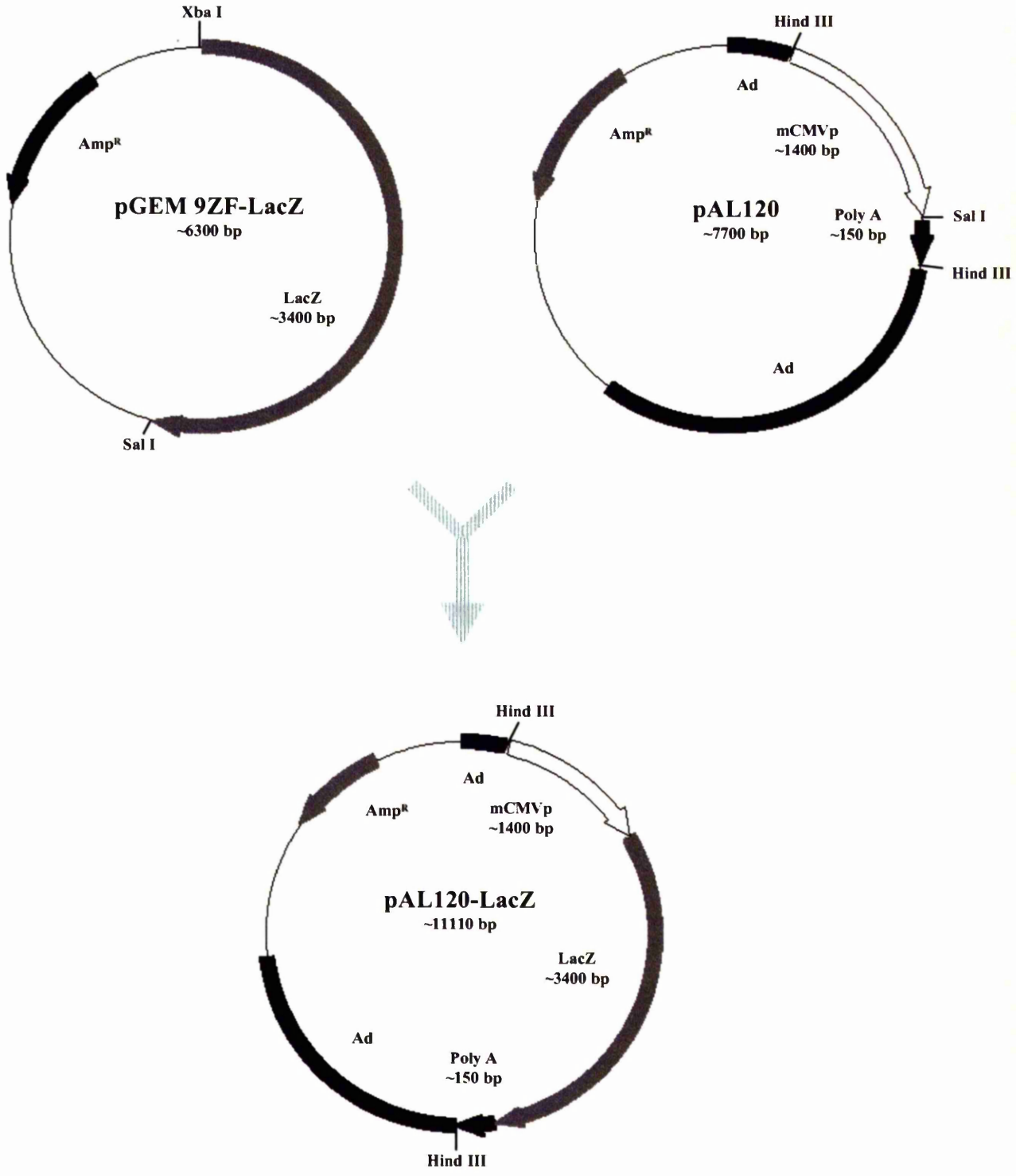

Figure 7. Generation of pAL120-LacZ. A Sal I/ Xba I fragment from pGEM 9ZF-Lac Z plasmid (containing the Lac Z gene) was blunt ended and subcloned into a Sal I digested and blunt-ended pAL 120 by blunt end ligation. The resulting plasmid pAL120-LacZ has the LacZ gene between the mCMVp and the poly A.

Lac Z as transgene under the control of the mCMV promoter (RAd 36) (figure 8a).

pAL 120-LacZ (section 3.2.2) was co-transfected with pJM17 into 293 cells by quadruplicate. Cytopathic effect was seen in the 4 flasks after 3 days post-cotransfection, and after 8 days (ensuring complete cytophathic effect) the virus was harvested and identified by restriction enzyme and Southern blot analysis of the viral DNA (figure 8b).

3.2.4 Generation of RAd 0

As a control virus for experiments of this thesis, a RAd containing no transgene (RAd 0) was constructed. 293 cells were cotransfected with pJM17 and pAL119. After complete cytophatic effect, the generated virus was harvested and identified by viral DNA analysis (figure 9).

Figure 8

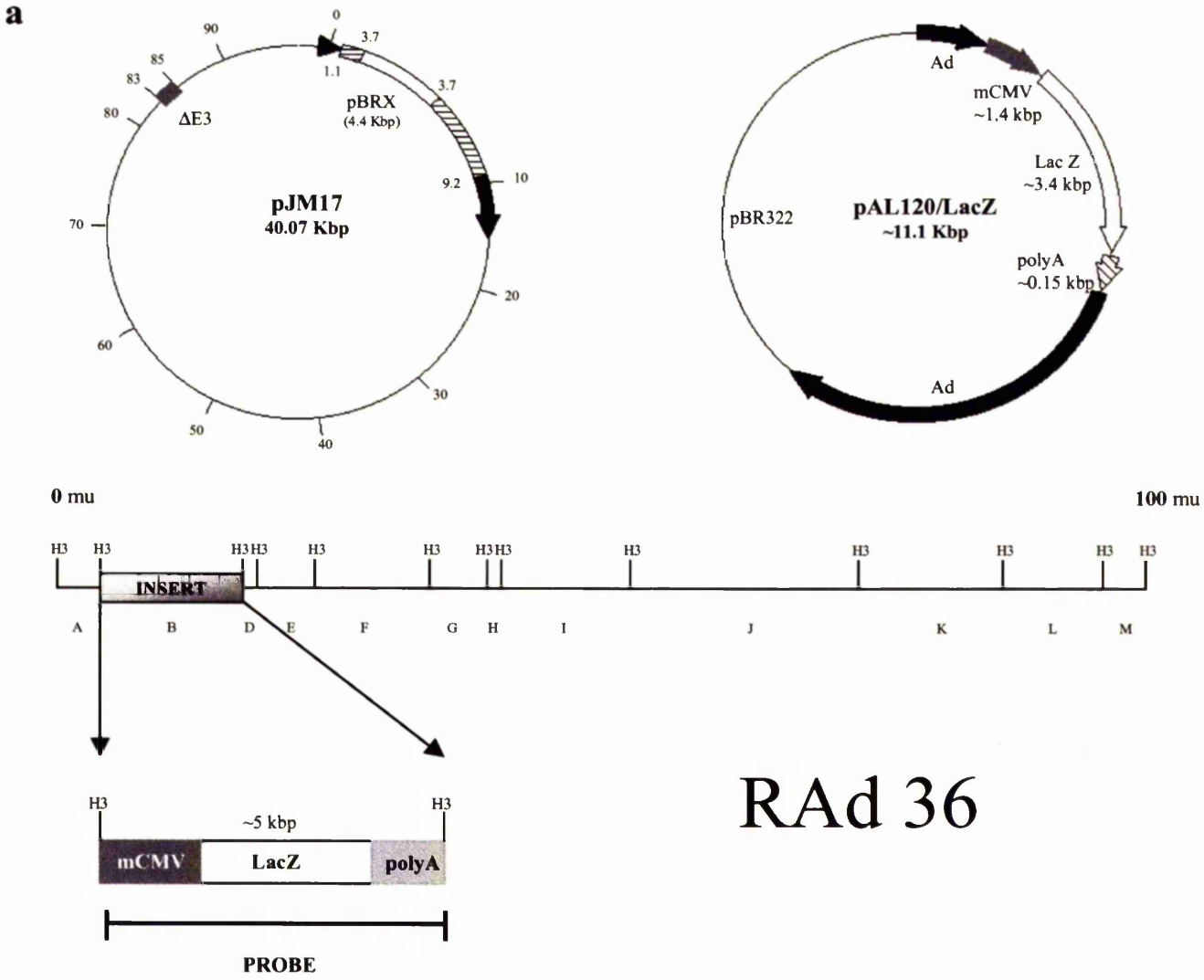

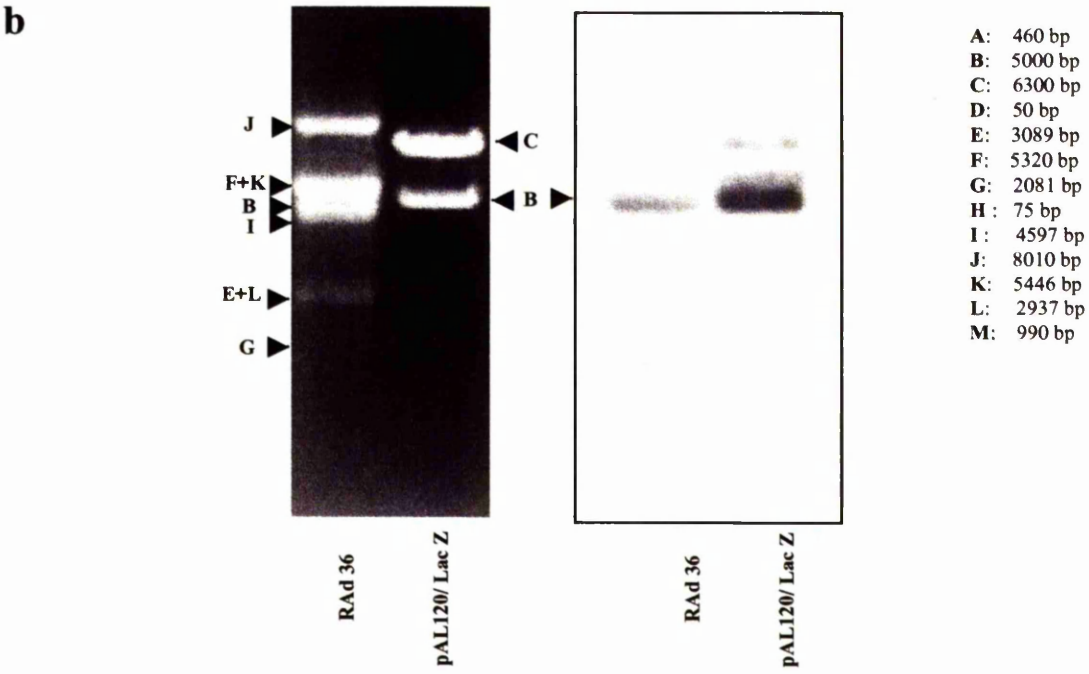

A: 460 bp
B: 5000 bp
C: 6300 bp
D: 50 bp
E: 3089 bp
F: 5320 bp
G: 2081 bp
H: 75 bp
I: 4597 bp
J: 8010 bp
K: 5446 bp
L: 2937 bp
M: 990 bp

Figure 8.

a. Cotransfection in 293 cells, of shuttle vector pAL 120-Lac Z with pJM17 resulted in the generation of an E1/E3 deleted first generation adenoviral vector, carrying Lac Z as a transgene under the control of the mCMV promoter (RAd 36).

b. To verify the identity of the obtained RAd, a Southernblot was performed with extracted viral DNA. The Southernblot probe was done using a Hind III fragment of pAL 120-Lac Z containing the mCMV promoter-Lac Z-Poly A.

3.2.5 Verification of RAd 36 β-galactosidase expression.

50 µl of the crude RAd 36 obtained after cotransfection, without purification or titration was used to infect Hela cells. After 36 hrs, cells were stained with X-gal. 90% of the infected cells were β-galactosidase positive compared to the non infected Hela cells. This proved that the virus was expressing β-galactosidase.

3.2.6 In vitro β-galactosidase expression, comparing hCMV and mCMV promoters.

To test the strength of the mCMV promoter, the constructed RAd 36 (mCMV-LacZ) was compared to RAd 35 (hCMV-LacZ) in different cell lines, at several MOIs ranging from 10 to 300.

The aim was to test the promoter in a wide variety of cell lines from different species to asses not only the promoter strength but also its promiscuity. For this reason β-galactosidase expression was verified using X-gal and β-galactosidase assays in the following cell lines:

Figure 9

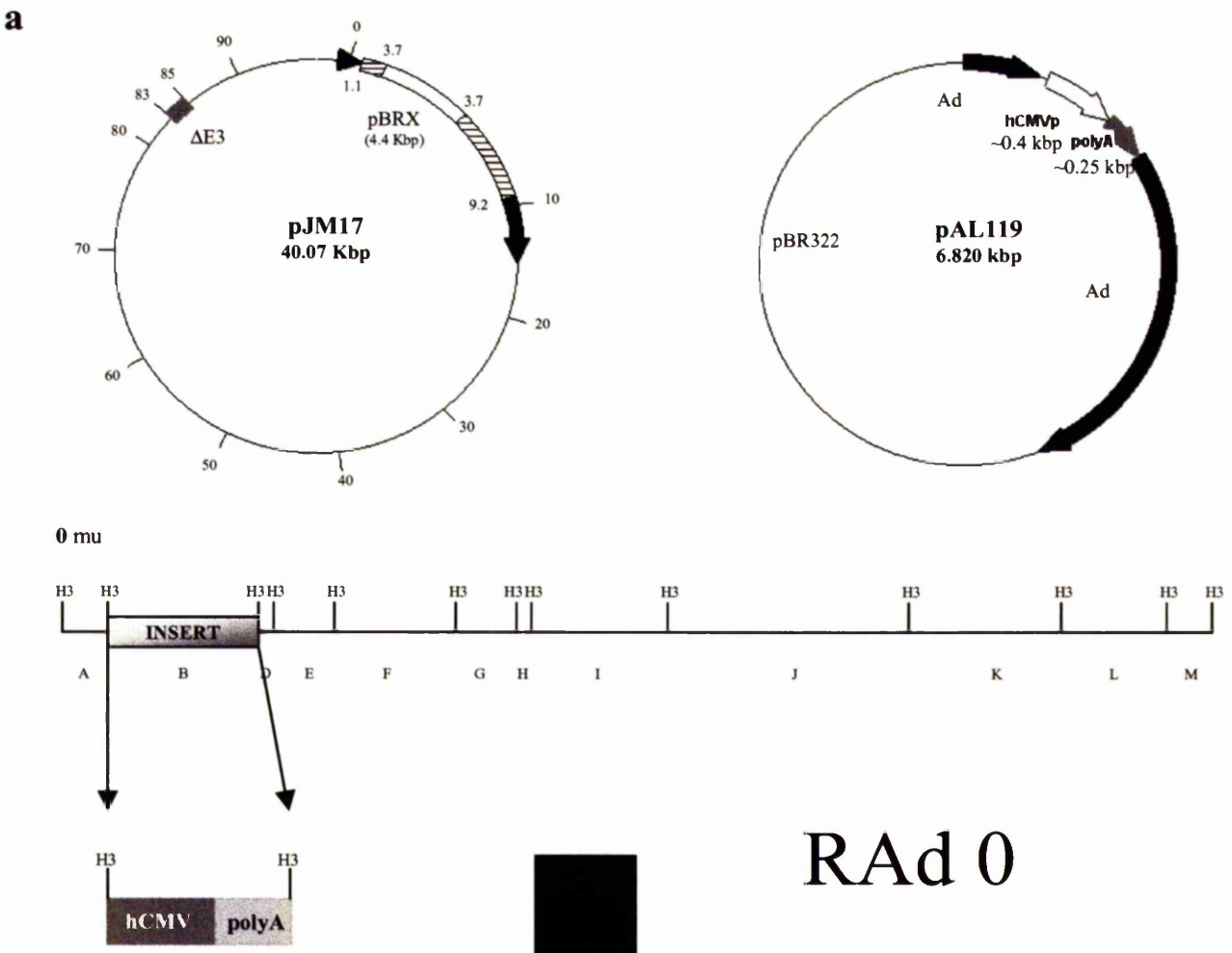

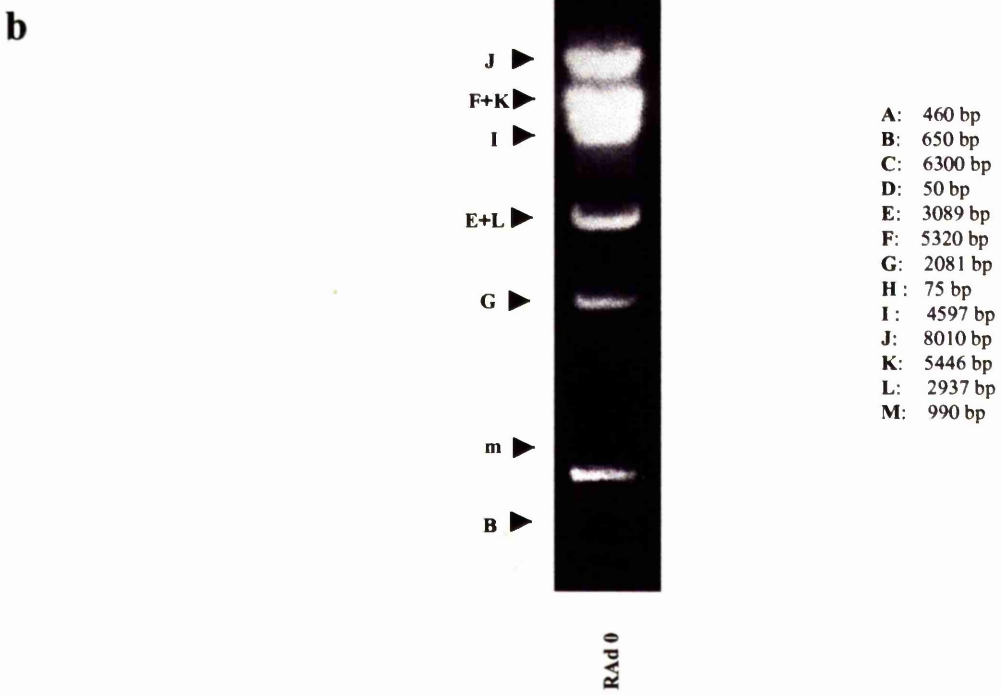

A: 460 bp
B: 650 bp
C: 6300 bp
D: 50 bp
E: 3089 bp
F: 5320 bp
G: 2081 bp
H: 75 bp
I: 4597 bp
J: 8010 bp
K: 5446 bp
L: 2937 bp
M: 990 bp

Figure 9.

a. Co-transfection in 293 cells, of shuttle vector pAL 119 Z with pJM17 in HEK 293 cells, resulted by recombination in 293 cells, in the generation of an E1/E3 deleted first generation adenoviral vector, carrying no transgene (RAd 0).

b. To verify the identity of the obtained RAd 0, extracted viral DNA was Hind III digested and pattern compared to the theoretical version.

human Hela cell line (figure 10); hamster ovary cell line (CHO) (figure 11); mouse neuronal cell line (N2A) (figure 12); rat glial cell line (CNS1) (figure 13); monkey kidney cell line (Cos7) (figure 14).

In all cell lines the activity levels of β-galactosidase activity driven by the mCMV promoter was significantly higher than the β-galactosidase activity detected when driven by the hCMVp (RAd35) (in agreement with Addison et al, 1997; Marr et al 1998; Sallonave et al, 1998; Southgate et al 2000). The difference of expression varied from ~9 fold in human Hela cells to ~500 fold in rat CNS-1 cells at MOI of 10. This result is highly relevant as the mCMV promoter (derived from a murine virus) was not only stronger than the hCMVp (derived from a human virus) in rodent cell lines but also in non human primate and human cell lines.

Figure 10

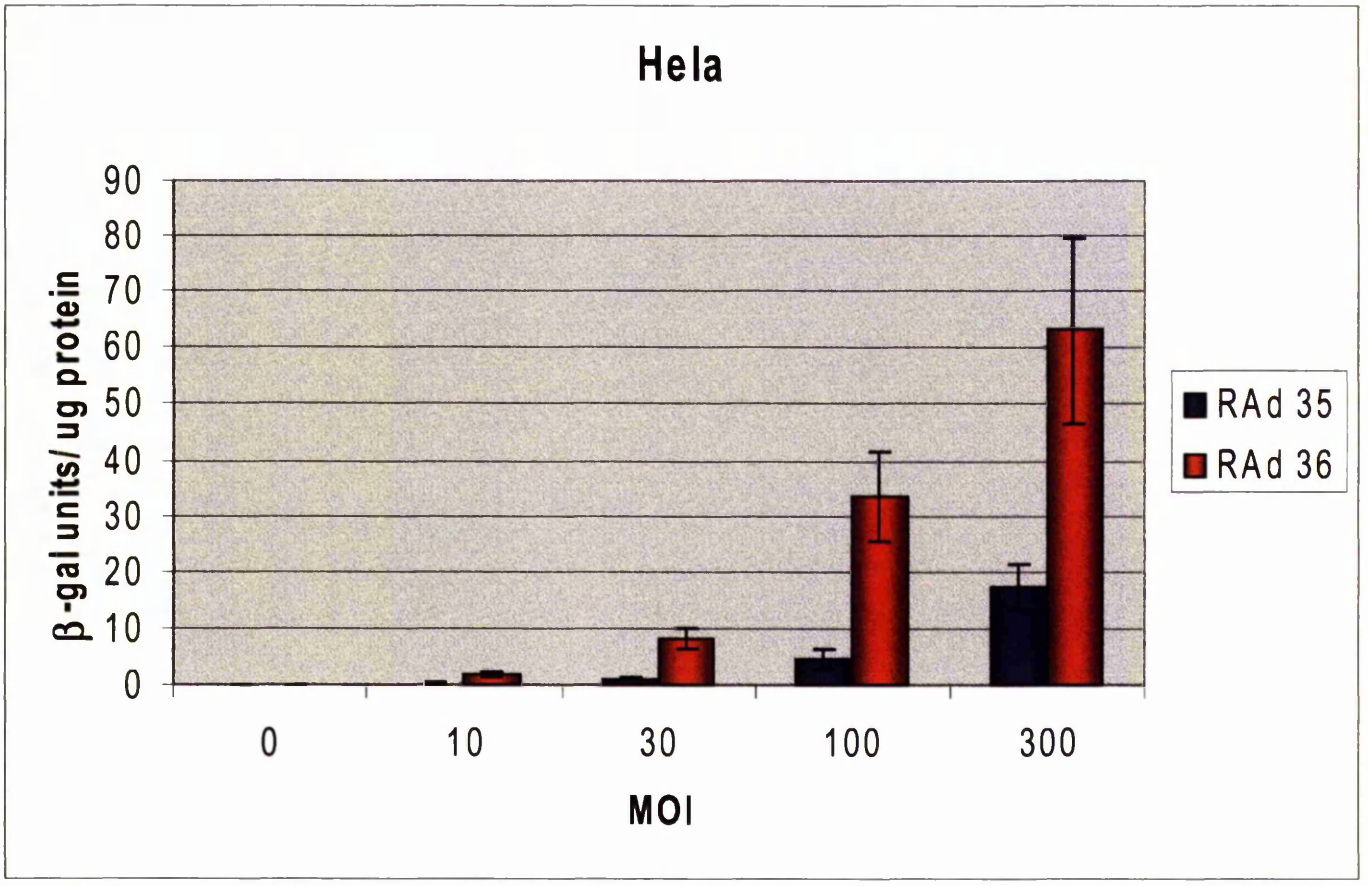

MOI	Fold increase of activity RAd 36/ RAd 35
10	+9.10 (p<0.001)
30	+8.51 (p<0.001)
100	+7.62 (p<0.001)
300	+3.68 (p<0.001)

Figure 10. *In vitro* β-galactosidase expression of RAd 36 and RAd 35 quantified by β–galactosidase assay. In human Hela cells with doses ranging from MOI of 10 to 300. Difference of expression between RAd 35 and RAd 36 is given specifying the MOI used. RAd 36 β-galactosidase expression driven by the mCMV promoter, which evolved for murine expression, is significantly higher than RAd 35 β-galactosidase expression (driven by the hCMV from the human CMV) even in human (Hela) cells. The difference at lower MOIs is much higher because of the multiple infectious hit requirement of the RAd 35 to achieve β-galactosidase expression. The experiment was repeated 3 separate times in triplicate, with new aliquots of virus and cells each time.

Figure 11

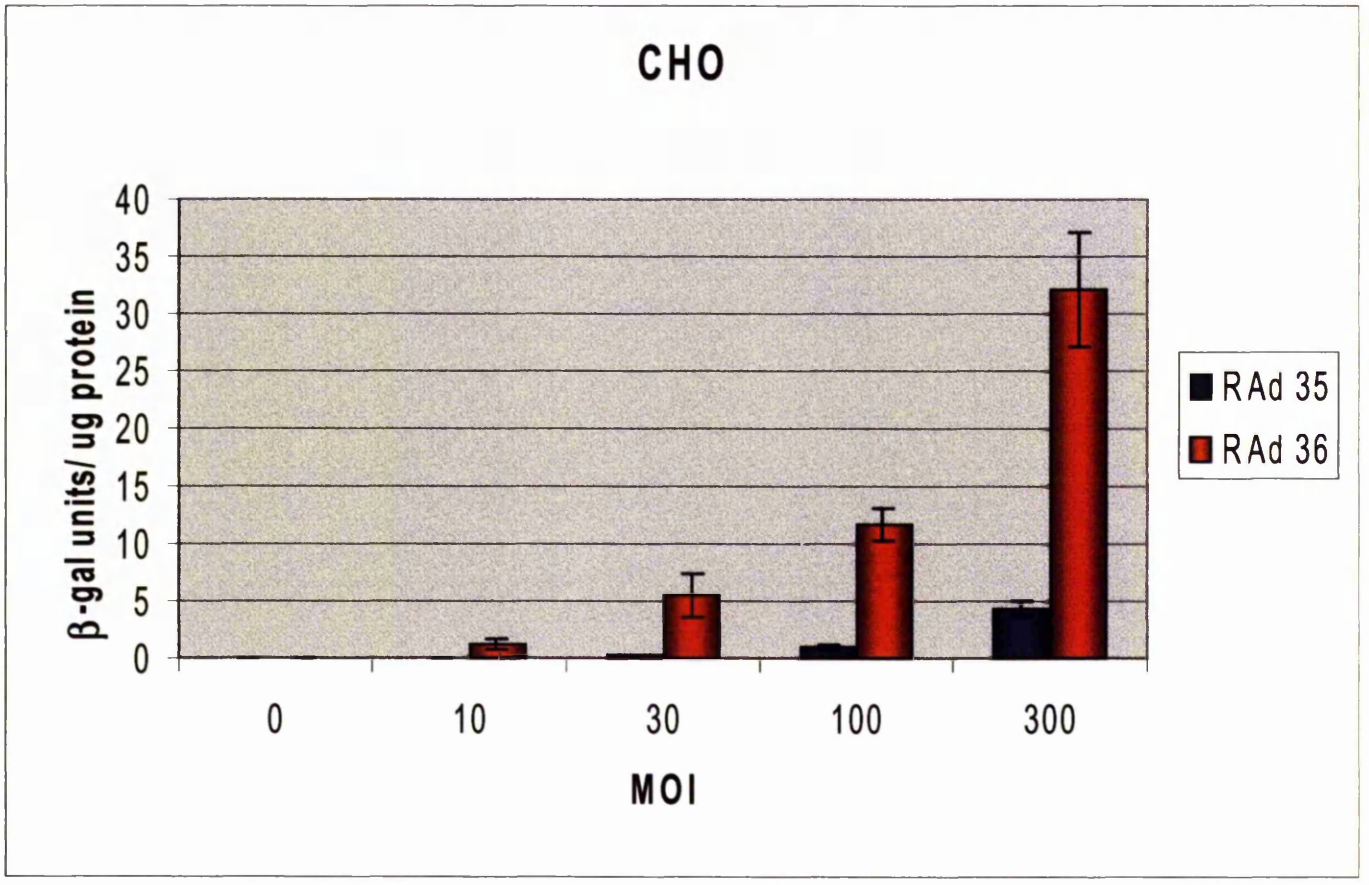

MOI	Fold increase of activity RAd 36/ RAd 35
10	+∞
30	+27.00 (p<0.001)
100	+13.06 (p<0.001)
300	+7.40 (p<0.001)

Figure 11. *in vitro* β-galactosidase expression of RAd 36 and RAd 35 quantified by β–galactosidase assay, in CHO cells (hamster ovary cell line) with doses ranging from MOI of 10 to 300. Difference of expression between RAd 35 and RAd 36 is given specifying the MOI used. RAd 36 β-galactosidase expression, driven by the mCMV promoter, is significantly higher than RAd 35 β-galactosidase expression (driven by the hCMV). The difference at lower MOIs between both promoters is much higher because of the multiple infectious hit requirement of the RAd 35 to achieve β-galactosidase expression. The experiment was repeated 3 separate times in triplicate, with new aliquots of virus and cells each time.

Figure 12

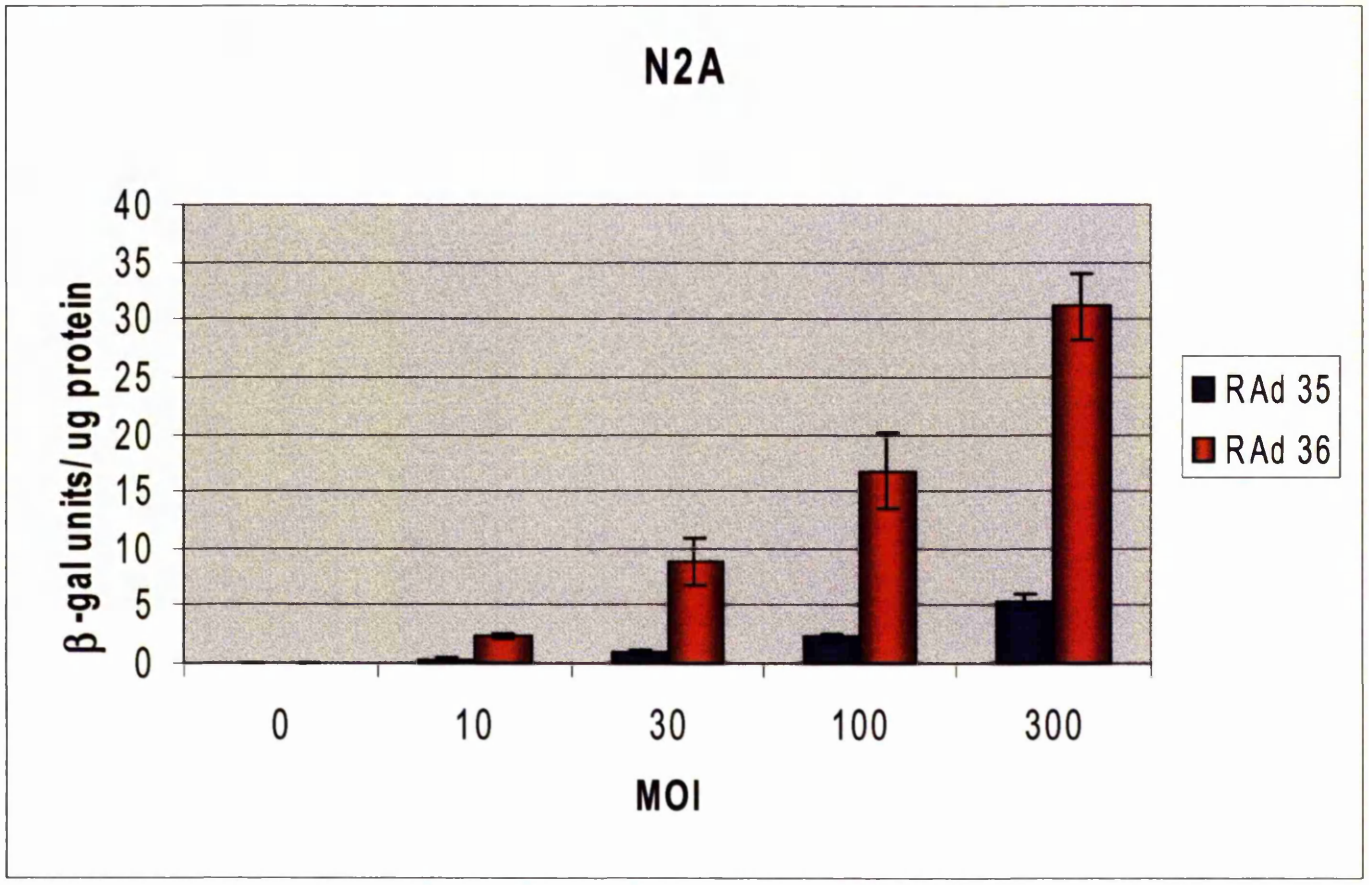

MOI	Fold increase of activity RAd 36/ RAd 35
10	+7.67 (p<0.001)
30	+9.21 (p<0.001)
100	+7.59 (p<0.001)
300	+5.87 (p<0.001)

Figure 12. *in vitro* β-galactosidase expression of RAd 36 and RAd 35 quantified by β–galactosidase assay, in N2A cells (mouse neuronal cell line) with doses ranging from MOI of 10 to 300. Difference of expression between RAd 35 and RAd 36 is given specifying the MOI used. RAd 36 β-galactosidase expression, driven by the mCMV promoter, is significantly higher than RAd 35 β-galactosidase expression (driven by the hCMV). The difference at lower MOIs between both promoters is much higher because of the multiple infectious hit requirement of the RAd 35 to achieve β-galactosidase expression. The experiment was repeated 3 separate times in triplicate, with new aliquots of virus and cells each time.

Figure 13

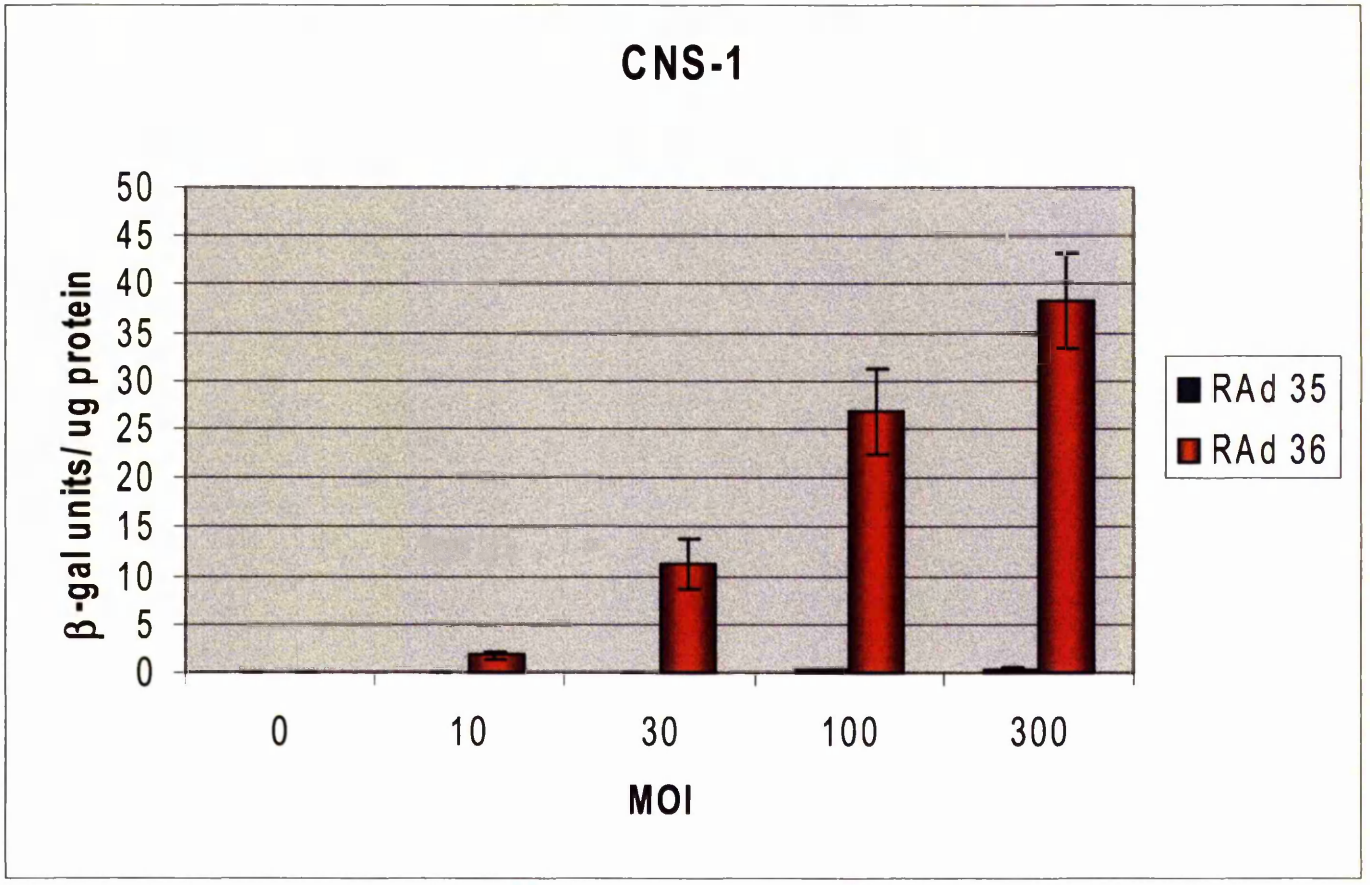

MOI	Fold increase of activity RAd 36/ RAd 35
10	+508.57 (p<0.001)
30	+321.86 (p<0.001)
100	+168.38 (p<0.001)
300	+107.96 (p<0.001)

Figure 13. *in vitro* β-galactosidase expression of RAd 36 and RAd 35 quantified by β–galactosidase assay, in CNS1 cells (rat glioma cell line) with doses ranging from MOI of 10 to 300. Difference of expression between RAd 35 and RAd 36 is given specifying the MOI used. RAd 36 β-galactosidase expression, driven by the mCMV promoter, is significantly higher than RAd 35 β-galactosidase expression (driven by the hCMV). The difference at lower MOIs between both promoters is much higher because of the multiple infectious hit requirement of the RAd 35 to achieve β-galactosidase expression. The experiment was repeated 3 separate times in triplicate, with new aliquots of virus and cells each time.

Figure 14

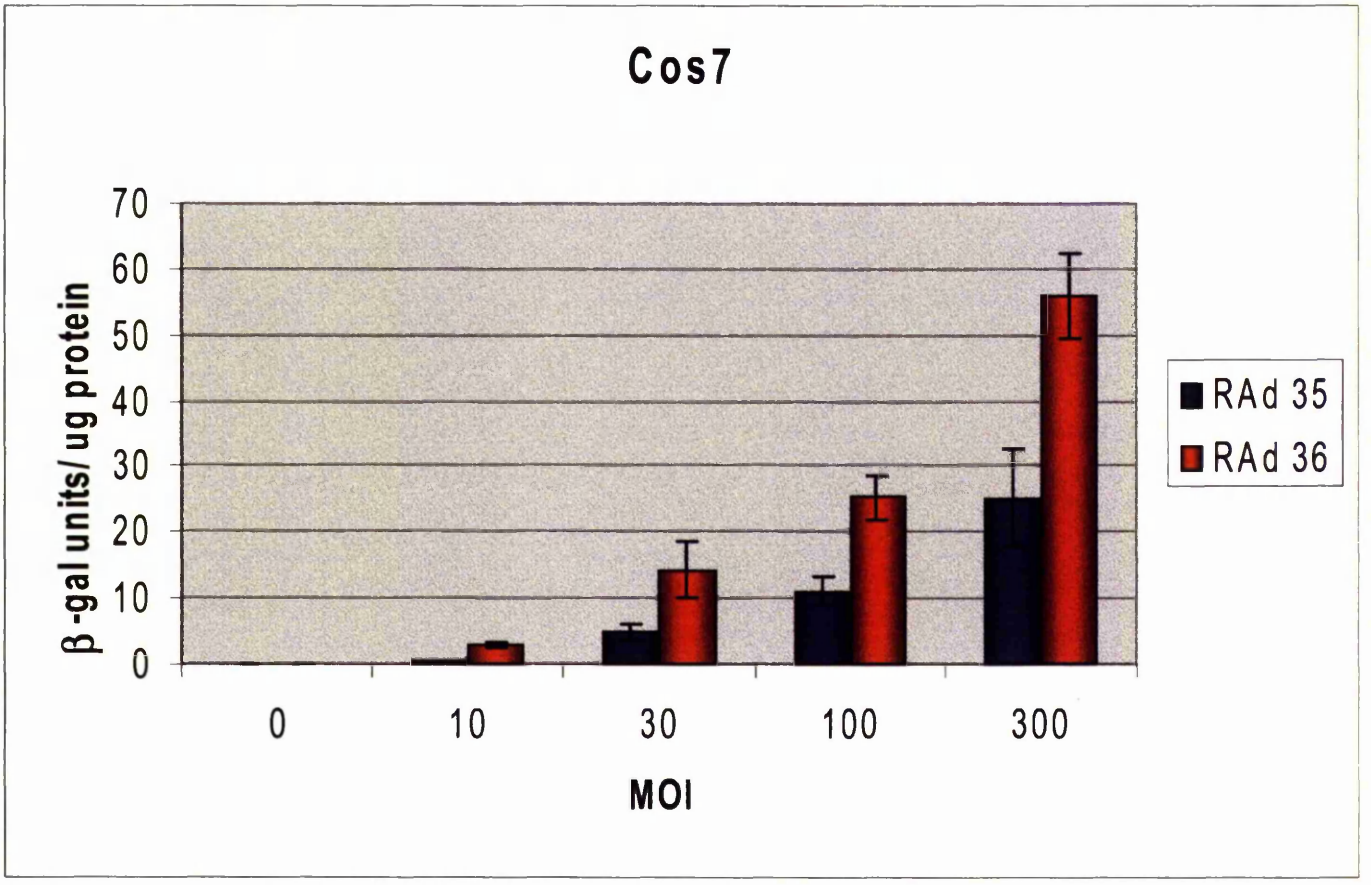

MOI	Fold increase of activity RAd 36/ RAd 35
10	+8.43 (p<0.001)
30	+2.83 (p<0.001)
100	+2.28 (p<0.001)
300	+2.23 (p<0.001)

Figure 14. *in vitro* β-galactosidase expression of RAd 36 and RAd 35 quantified by β–galactosidase assay, in Cos7 cells (monkey kidney cell line) with doses ranging from MOI of 10 to 300. Difference of expression between RAd 35 and RAd 36 is given specifying the MOI used. RAd 36 β-galactosidase expression, driven by the mCMV promoter, is significantly higher than RAd 35 β-galactosidase expression (driven by the hCMV). The difference at lower MOIs between both promoters is much higher because of the multiple infectious hit requirement of the RAd 35 to achieve β-galactosidase expression. The experiment was repeated 3 separate times in triplicate, with new aliquots of virus and cells each time.

3.2.7 In vitro β-galactosidase expression, comparing the viral hCMV and mCMV promoters to the human prolactin promoter, a mammalian cell type specific promoter.

To further illustrate the strength of the mCMV promoter in-vitro, β-galactosidase expression driven by the mCMV promoter (using RAd 36) was compared to the levels β-galactosidase obtainable with the hCMV promoter (using RAd 35), and the tissue specific human prolactin promoter (hPrl) (using RAd-PLZ) in pituitary derived cell lines. The hPrl, is a cell type specific promoter, of mammalian origin, which is only active in lactotrophic and mamosomatotrophic cells.

The comparison between viral promoters and a cell type specific promoter is of great value, as many gene therapy strategies are based on selective transgene expression in cells targeted by a cell type specific promoter. Promoter specificity restricts transduction to those cells that are permissive, therefore limiting transgene expression to a selected cell type. This is an ideal tactic to be employed when using a transgene that could be toxic if ubiquitously expressed.

Promoter strengths were evaluated by infecting different pituitary cell lines at several MOIs, and detecting β-galactosidase expression 48 hours after infection. The different cell lines used were: the rat prolactin secreting pituitary cell line GH3 (figure 15); the rat prolactin secreting pituitary cell line MMQ (figure 16); the murine ACTH secreting pituitary cell line (AtT20) (figure 17).

Figure 15

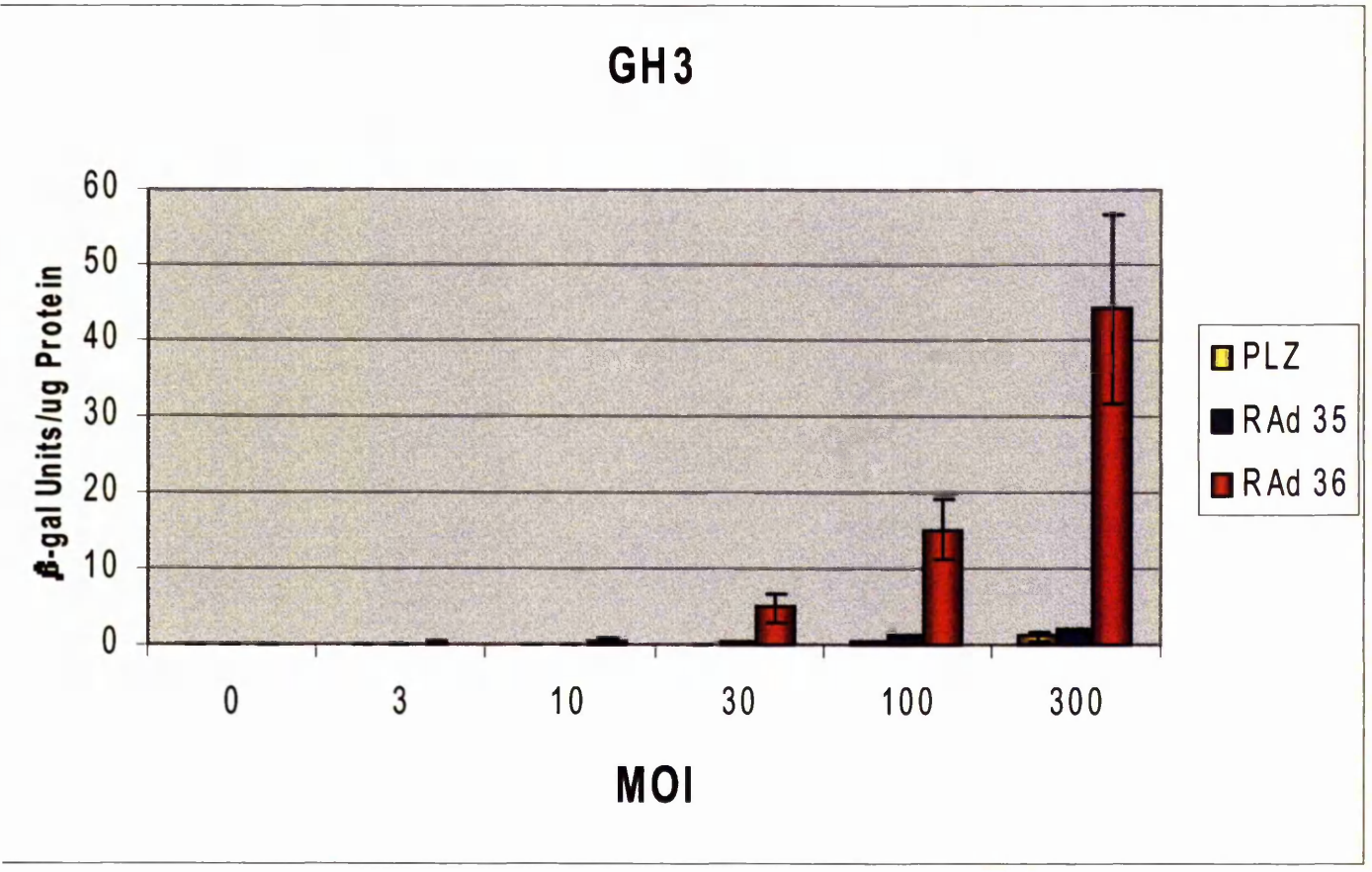

MOI	Fold increase of activity RAd 36/ RAd 35	Fold increase of ativity RAd 36/ PLZ
3	+80.26 (p<0.001)	+80.26 (p<0.001)
10	+12.62 (p<0.001)	+14.20 (p<0.001)
30	+13.30 (p<0.001)	+37.43 (p<0.001)
100	+13.04 (p<0.001)	+43.77 (p<0.001)
300	+22.39 (p<0.001)	+40.65 (p<0.001)

Figure 15. Quantitative analysis of β-galactosidase enzymatic activity, in rat pituitary tumour GH3 cell line. Cells were infected with increasing MOIs of RAd-35, RAd-36, or RAd-hPrl/lacZ (the human prolactin promoter is a cell type specific promoter for lactotrophic and mamosomatotrophic cells). Two days later, cells were harvested and tested for β-galactosidase activity. As expected, the RAd 36 β-galactosidase expression is higher than the one detected with RAd 35 or RAd-hPrl/lacZ. The experiment was repeated 3 separate times in triplicate, with new aliquots of virus and cells each time.

Figure 16

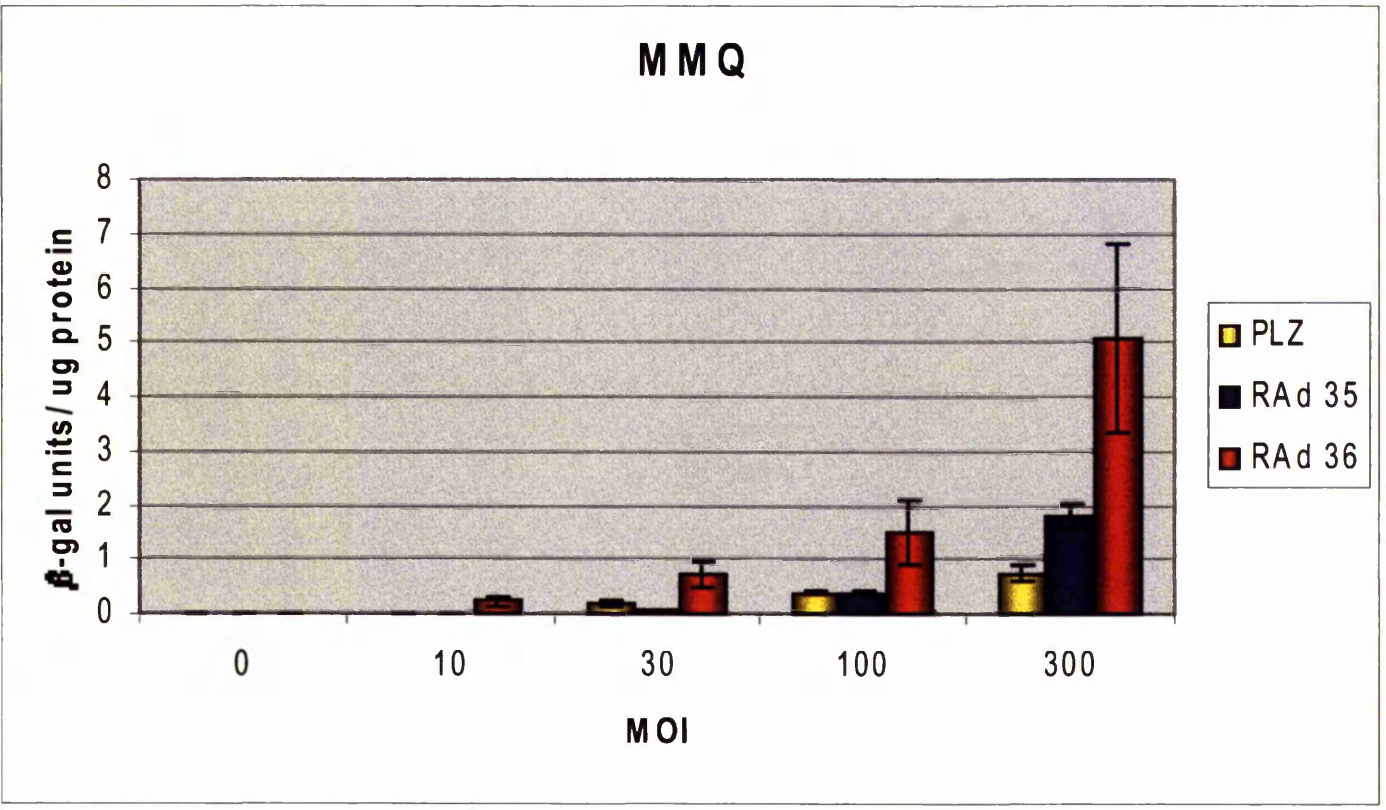

MOI	Fold increase of activity RAd 36/ RAd 35	Fold increase of ativity RAd 36/ PLZ
10	+30.67 (p<0.001)	+30.67 (p<0.001)
30	+13.90 (p<0.001)	+4.87 (p<0.001)
100	+4.11 (p<0.001)	+4.11 (p<0.001)
300	+2.85 (p<0.001)	+6.90 (p<0.001)

Figure 16. Quantitative analysis of β-galactosidase enzyme activity in rat pituitary tumour MMQ cell line. Cells were infected with increasing MOIs of RAd-35, RAd-36, or RAd-hPrl/lacZ (the human prolactin promoter is a cell type specific promoter for lactotrophic and mamosomatotrophic cells). Two days later, cells were harvested and tested for β-galactosidase activity. As expected, the RAd 36 β-galactosidase expression is higher than the one detected with RAd 35 or RAd-hPrl/lacZ. The experiment was repeated 3 separate times in triplicate, with new aliquots of virus and cells each time.

Figure 17

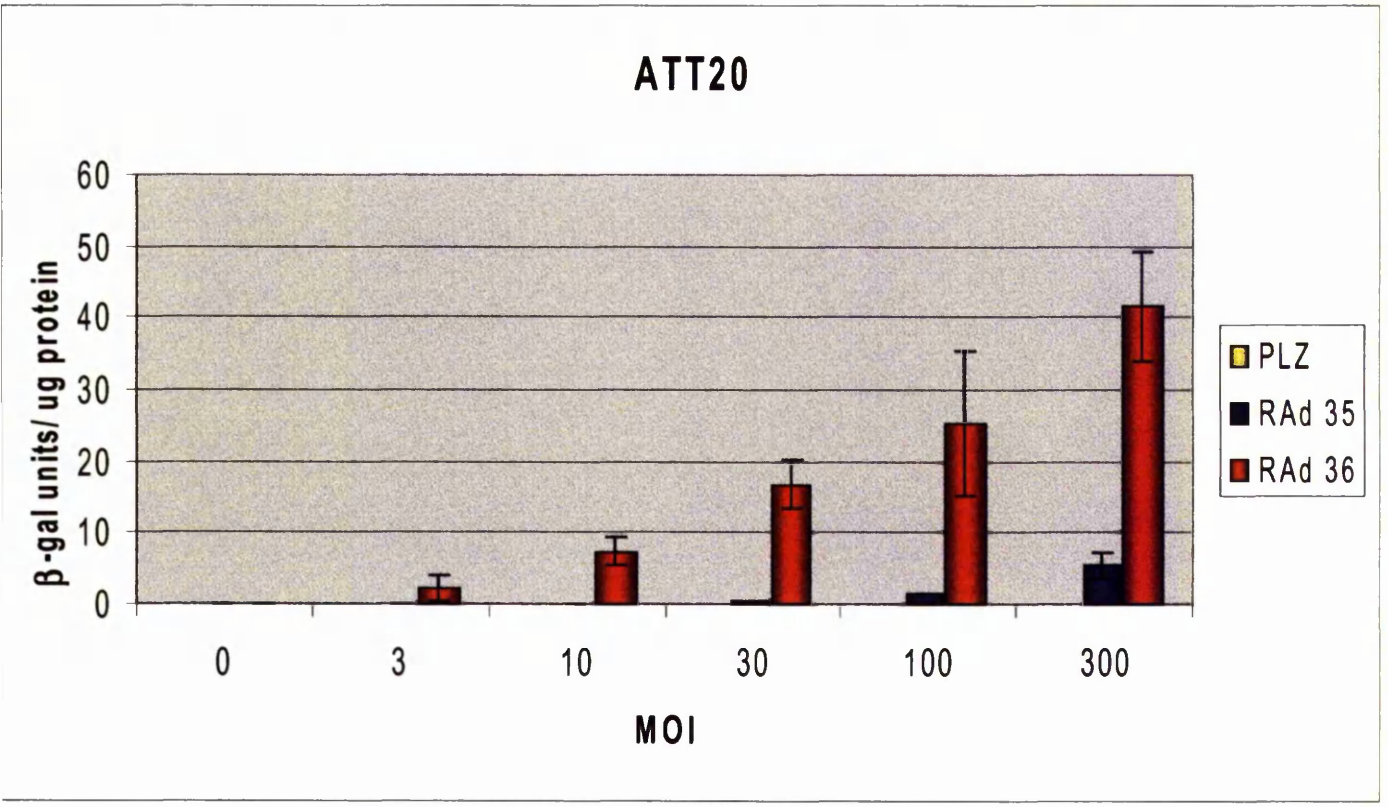

MOI	Fold increase of activity RAd 36/ RAd 35
3	+66.21 (p<0.001)
10	+60.39 (p<0.001)
30	+40.36 (p<0.001)
100	+18.76 (p<0.001)
300	+7.86 (p<0.001)

Figure 17. Quantitative analysis of β-galactosidase enzyme activity in murine the pituitary tumour ATT20 cell line. Cells were infected with increasing MOIs of RAd-35, RAd-36, or RAd-hPrl/lacZ (the human prolactin promoter is a cell type specific promoter for lactotrophic and mamosomatotrophic cells). Two days later, cells were harvested and tested for β-galactosidase activity. The RAd 36 β-galactosidase expression is higher than the one detected with RAd 35. As expected, there was not detected β-galactosidase expression in cells infected with RAd-hPrl/lacZ, as the human prolactin promoter is not active in this cell line. The experiment was repeated 3 separate times in triplicate, with new aliquots of virus and cells each time.

In all cell lines the viral mCMV promoter was more powerful than both the viral hCMV promoter and the human prolactin promoter. As expected, there was no detectable β-galactosidase expression with the RAd-PLZ in AtT20 as the prolactin promoter is inactive in this cell line as it is not a lactotrophic nor a mamosomatotrophic cell line.

3.2.8 Highly efficient transgene expression in the brain in vivo.

In vivo, viral doses from 10^4 to 10^8 infectious units of RAd 35 and RAd 36 were injected into adult rat striata. Five days later, the brains were sectioned and the presence of immunoreactive ß-galactosidase enzyme was assessed by immunohistochemistry. At all doses used, the levels of immunoreactive ß-galactosidase expressed from RAd36 were higher than those detected following injection of RAd35 (Figure 18).

A low dose of 10^4 infectious units of RAd 36 allowed transduction of a relatively large area of the rat striatum (Figure 18c), comparable to the area transduced by 10^7 iu of RAd 35 (Figure 18j; Figure 19). A dose of 10^4 iu of RAd35, however, produced only very few immunoreactive cells (Figure 18d).

Figure 18

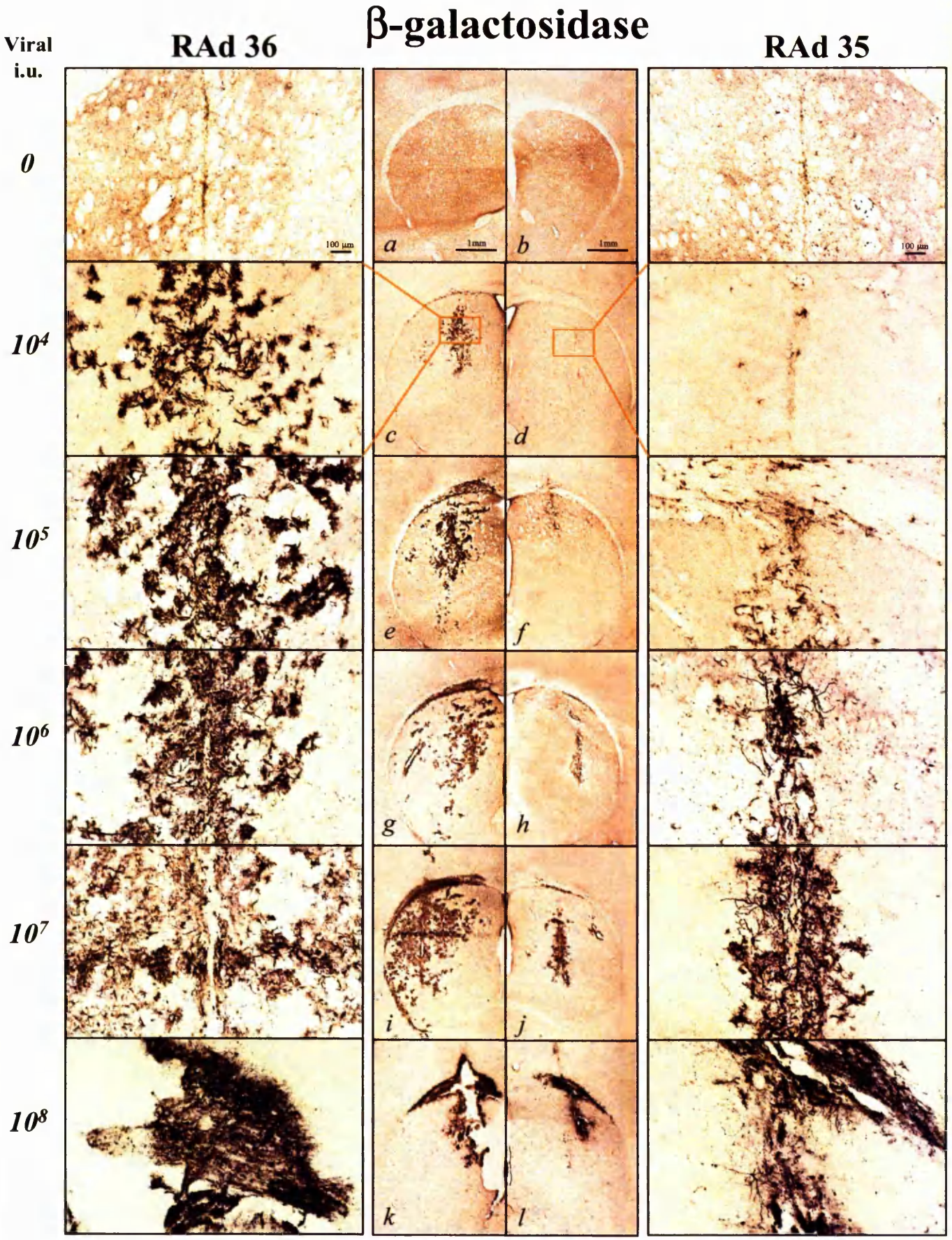
β-galactosidase
RAd 36
RAd 35
Viral i.u.
0
10⁴
10⁵
10⁶
10⁷
10⁸
100 µm
a
1mm
b
1mm
100 µm
c
d
e
f
g
h
i
j
k
l

Figure 18. Expression of β-galactosidase in rat brain striata after RAd 35 or RAd 36 injection. Increasing doses of vectors were injected into the striatum of adult rats. Three µl containing the appropriate dose of either RAd36 or RAd35 were injected into the brain, and animals were perfusion-fixed five days later (n numbers of animals for each viral dose of RAd 36 was: $1x10^4$-$1x10^5$ i.u., n=3; $1x10^6$-$1x10^8$ i.u., n=6; RAd35, $1x10^4$-$1x10^5$ i.u., n=3; $1x10^6$-$1x10^8$ i.u., n=6; saline injection, n=6). Brains were processed as described in (Thomas et al, 2001b). Note that already at 10^4 iu substantial transduction can be seen with RAd36, while expression is barely detectable in the site injected with RAd35. The area of striatum encompassing transduced cells is always larger in those sites injected with RAd36, compared to those injected with RAd35. The central panels show low magnification views of the centres of each injection site; the lateral panels at either side of the central panels show higher magnification of boxes, as indicated in **c** and **d**. Scale bars for the central panels are shown in **a** and **b**, while scale bars for the lateral panels are shown in the top left and top right images. Viral iu = 0 represents the injection of saline.

Figure 19

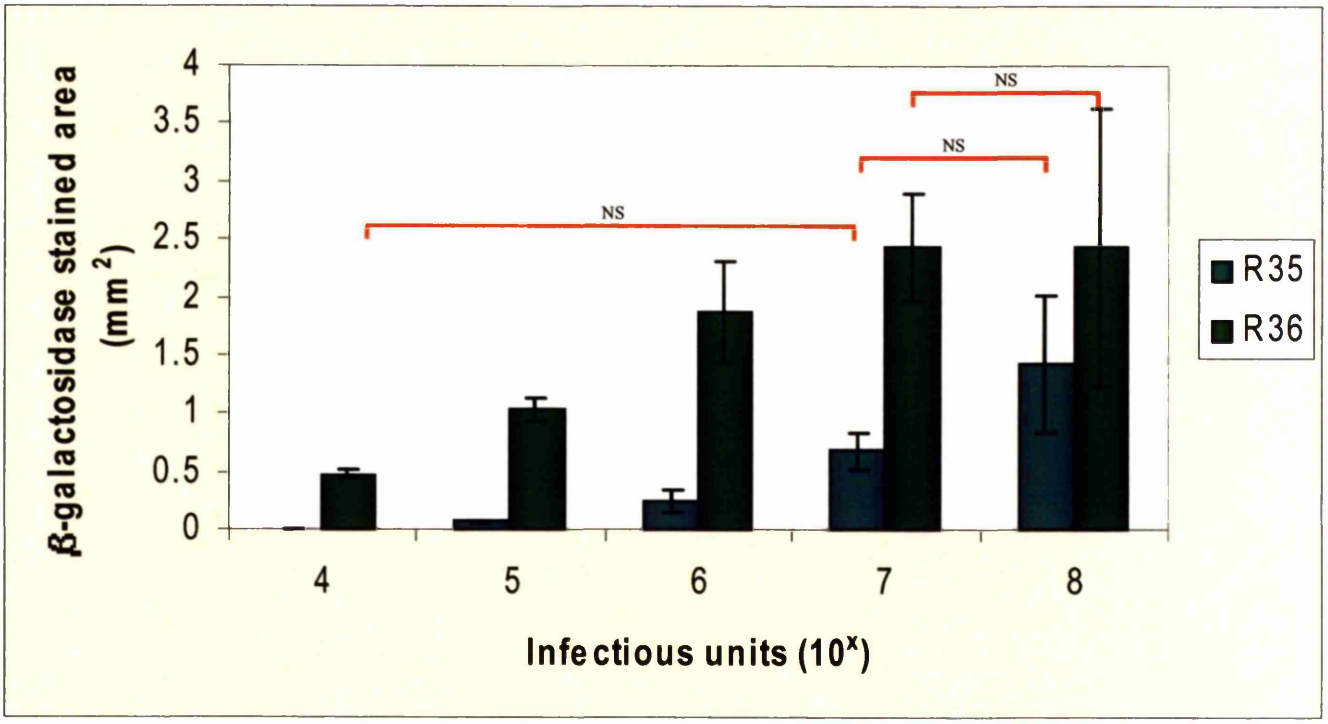
β-galactosidase stained area (mm²)
4
3.5
3
2.5
2
1.5
1
0.5
0
NS
NS
NS
4
5
6
7
8
Infectious units (10^x)
R35
R36

Figure 19. ß-galactosidase immunoreactive cells brain area quantification, using a semi-automatic Quantimet imaging system. Expression of ß-galactosidase following injection of RAd36 (green bars) was always significantly higher than expression from RAd35 (blue bars) at all doses ($p<0.001$), except at 10^8 iu, at which the difference was not statistically significant. The area of ß-galactosidase immunoreactivity after injecting 10^4 iu of RAd36 was not statistically different from that obtained following infection of RAd35 at 10^7 iu. This shows the expression from RAd36 to be approximately 1,000 fold more effective than expression from RAd35. The difference in expression from RAd36 did not differ between 10^7 and 10^8 iu, demonstrating that with RAd36 maximal transgene expression is achieved at 10^7 iu. The difference in expression between 10^7 and 10^8 iu of RAd35 was not statistically significant, probably due to the increased toxicity at 10^8 iu, which can eliminate transduced cells.

For each brain, a section representing the midline of the needle track was analysed and the total area of ß-galactosidase immunoreactivity quantified. The results demonstrated that the area transduced by RAd36 is significantly larger than the one transduced by RAd35 following the injection of vector doses of 10^4-10^7 (Figure 19; and see Figure 18 *c-j*). At 10^8, the difference in transduction between both vectors was not significant due to the neurotoxicity associated with the high dose of vector and high levels of transgene expression.

Maximal transduction for RAd36 and RAd35 was achieved at 10^7 iu. At 10^8 iu there was significant toxicity associated with both vectors (Figure 18 *k*, *l*; Figure 19; Figure 20 *k*, *l*; Figure 21 *k*, *l*). Following infection with 10^8 iu of RAd35, ß-galactosidase expression appeared to be higher than at 10^7 iu, but not statistically different due to a high variability in ß-galactosidase levels in animals injected with 10^8 iu. This was possibly a result of direct vector cytotoxicity observed following the injection of high vector dose (Figure 18 *j*, *l*; Figure 19) (Thomas et al, 2001).

Further, when comparing the efficiency of expression, statistical analysis demonstrated that a dose of 10^4 infectious units of RAd36 expresses ß-galactosidase throughout an area equivalent to that achieved by 10^7 infectious units of RAd35 (Figure 19). This indicates that RAd36 is approximately 1,000 times more effective than RAd35 in expressing ß-galactosidase in the brain *in vivo*.

3.2.9 Absence of virus induced brain cytotoxicity and inflammation at viral doses achieving high level transgene expression.

Inflammatory cell infiltration in response to viral vector injection was studied in serial brain sections from animals injected with either RAd35 or RAd36, and stained for the presence of CD8+ NK and T-cells (Figure 22), or ED1+ macrophages/microglia (Figure 20), by immunohistochemistry.

The inflammatory response to injection of either viral vector was greater than that observed following the injection of saline, only at doses of 10^7 iu and above. The inflammation detected was only dependent on the viral dose and independent of the transgene expression. When comparing the cellular inflammation within the same viral dose between RAd 35 or RAd 36, no significant differences were found (figure 20; figure 21 and figure 22). This means that the cellular inflammation was independent of the amount of transgene expression and only dependent on the viral dose.

Figure 20

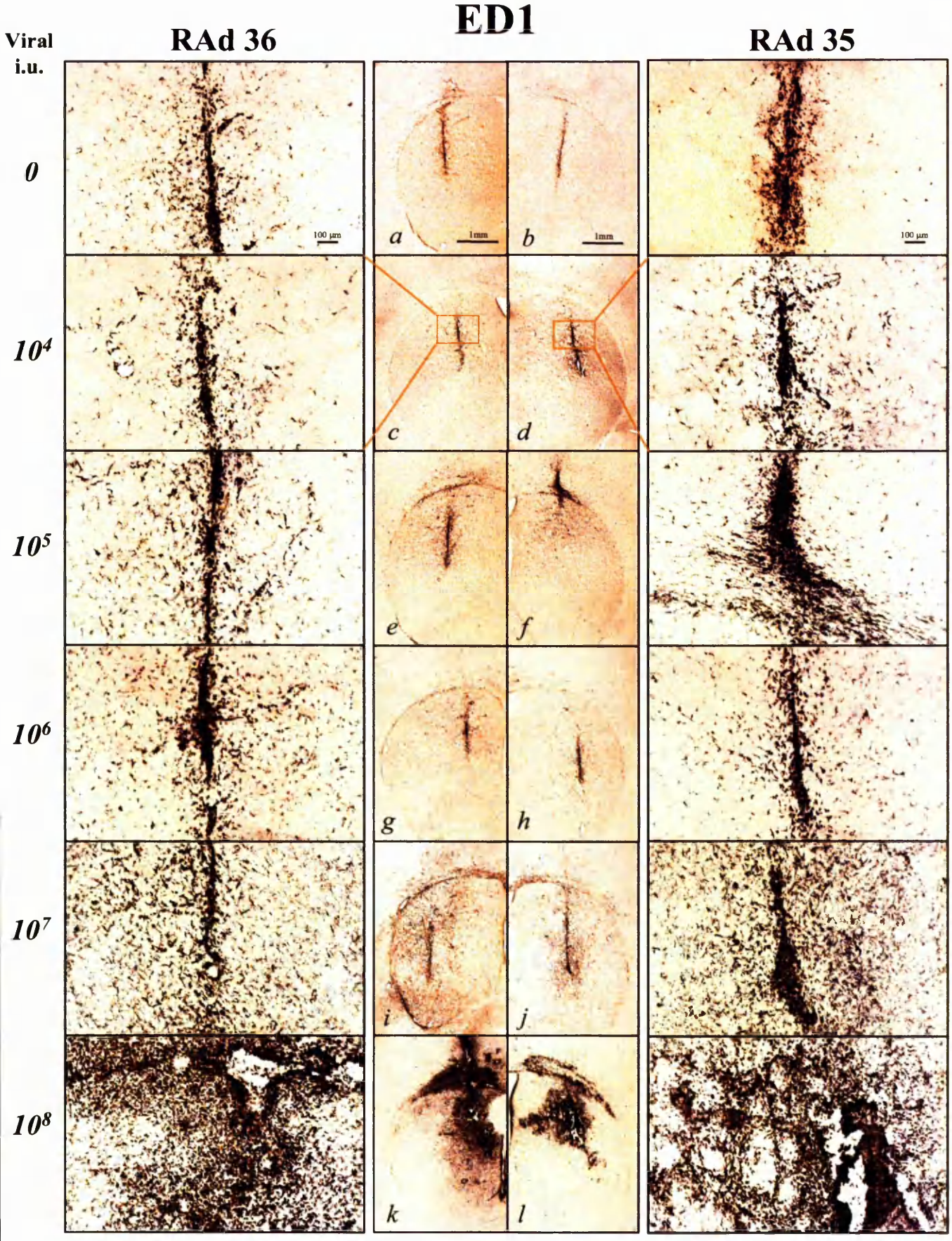
ED1
RAd 36
RAd 35
Viral i.u.
0
10^4
10^5
10^6
10^7
10^8
100 µm
1mm
a
b
c
d
e
f
g
h
i
j
k
l

Figure 20. Increasing doses of vectors were injected into the striatum of adult rats, and serial sections of the ones illustrated in Figure 18 were analysed for the presence of ED1+ activated macrophages/microglial cells, and are shown in this figure (n numbers of animals for each viral dose of RAd 36 were: $1x10^4$-$1x10^5$ i.u., n=3; $1x10^6$-$1x10^8$ i.u., n=6; for RAd35: $1x10^4$-$1x10^5$ i.u., n=3; $1x10^6$-$1x10^8$ i.u., n=6; saline injection, n=6). Increased influx of ED1+ cells is only seen at 10^7 and 10^8 iu of both RAd36 and RAd35. The central panels show low magnification views of the centres of each injection site; the lateral panels at either side of the central panels show higher magnification of boxes, as indicated in **c** and **d**. Scale bars for the central panels are shown in **a** and **b**, while scale bars for the lateral panels are shown in the top left and top right images. Viral iu = 0 represents the injection of saline.

Figure 21

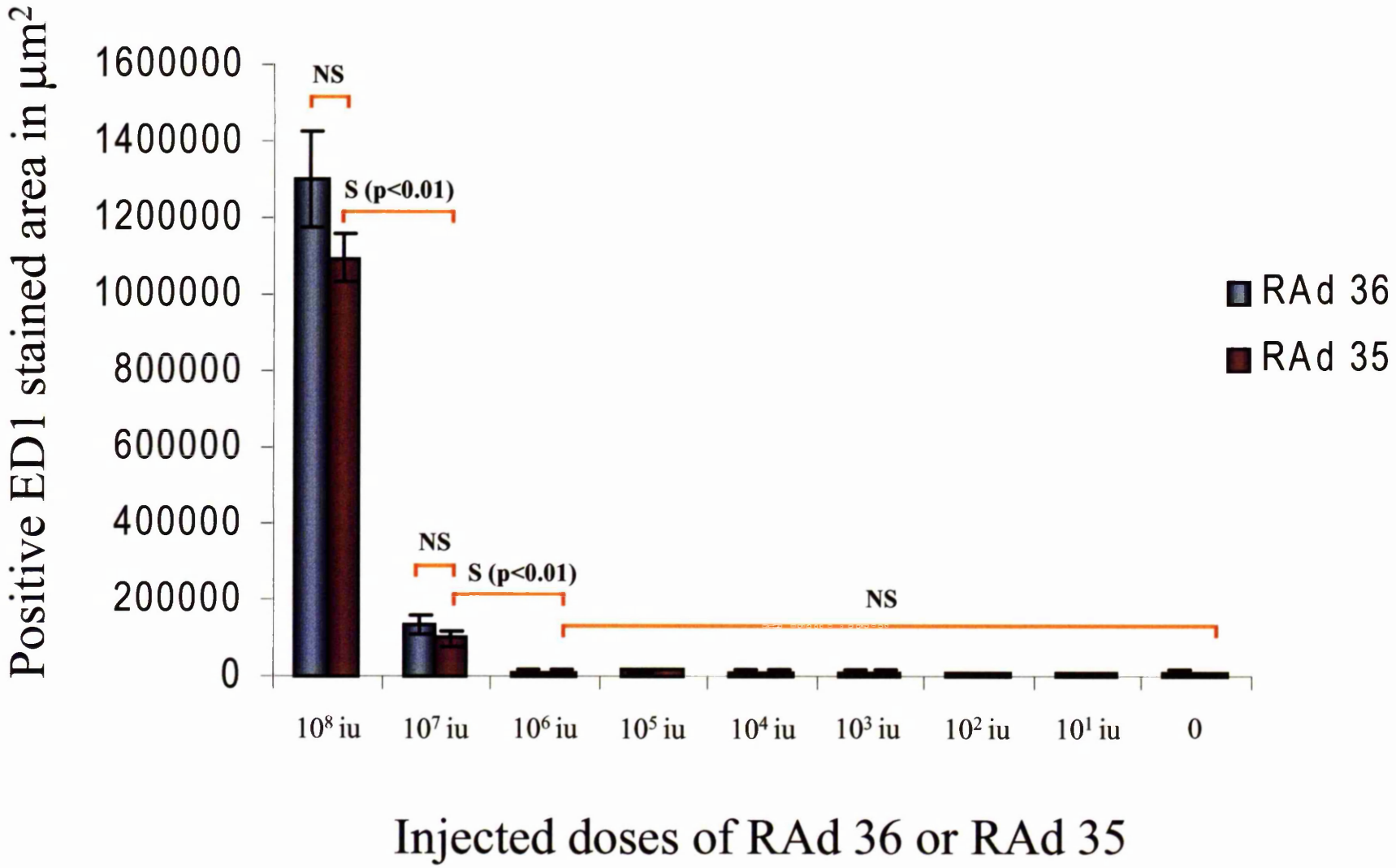
Positive ED1 stained area in µm2
1600000
1400000
1200000
1000000
800000
600000
400000
200000
0
NS
S (p<0.01)
NS
S (p<0.01)
NS
RAd 36
RAd 35
10^8 iu
10^7 iu
10^6 iu
10^5 iu
10^4 iu
10^3 iu
10^2 iu
10^1 iu
0
Injected doses of RAd 36 or RAd 35

Figure 21. ED1 immunoreactive cells brain area quantification, using a semi-automatic Quantimet imaging system. There is a significant difference of ED1 infiltration compared to the saline injected control only at viral doses of both RAd 35 and RAd 36 of 10^7 iu or higher. When lower doses of virus were injected no significant difference was seen when compared to the saline control with either, RAd35 or RAd 36.

Figure 22

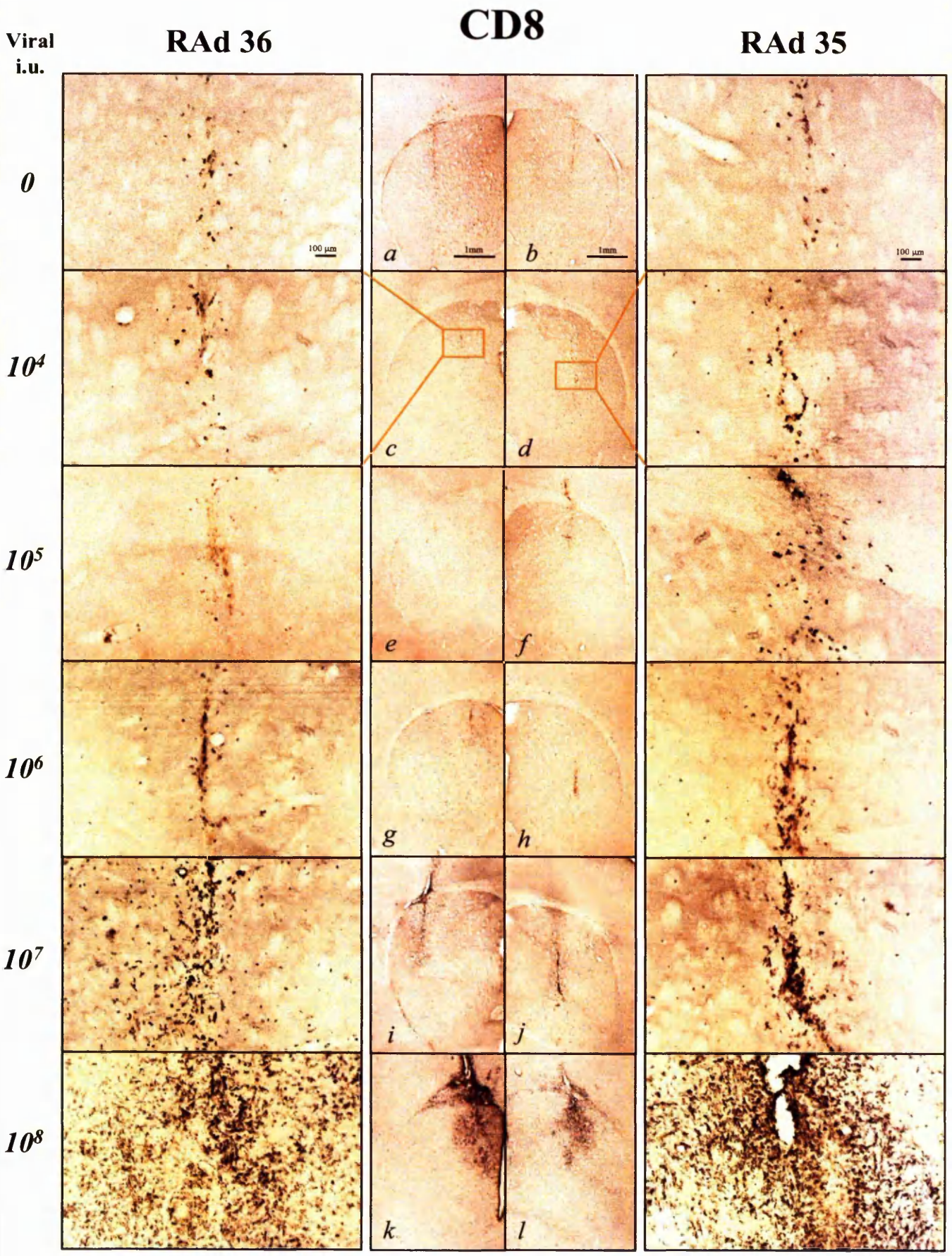
CD8
RAd 36
RAd 35
Viral i.u.
0
10^4
10^5
10^6
10^7
10^8
100 µm
a
1mm
b
1mm
100 µm
c
d
e
f
g
h
i
j
k
l

Figure 22. Increasing doses of vectors were injected into the striatum of adult rats, and serial sections to those illustrated in Figure 18 were analysed for the presence of CD8+ (inflammatory NK and T cells), and are shown in this figure (n numbers of animals for each viral dose of RAd 36 were: $1x10^4$-$1x10^5$ i.u., n=3; $1x10^6$-$1x10^8$ i.u., n=6; RAd35, $1x10^4$-$1x10^5$ i.u., n=3; $1x10^6$-$1x10^8$ i.u., n=6; saline injection, n=6). Increased influx of CD8+ cells is only seen at 10^7 and 10^8 iu of RAd36, and 10^8 iu of RAd35. The central panels show low magnification views of the centres of each injection site; the lateral panels at either side of the central panels show higher magnification of boxes, as indicated in ***c*** and ***d***. Scale bars for the central panels are shown in **a** and **b**, while scale bars for the lateral panels are shown in the top left and top right images. Viral iu = 0 represents the injection of saline.

3.2.10 One infectious event is enough to allow transgene detection in the brain in vivo.

To determine the lower limit of detection of transgene expression from RAd36 in the brain *in vivo*, viral doses ranging from 10-1,000 total infectious units were injected into the brain. Serial brain sections taken throughout the injection sites were immunohistochemically stained for ß-galactosidase and positive cells were counted throughout the injection sites.

Initially in animals injected with 10 infectious units (n=4), 8±3 ß-galactosidase immunoreactive cells were detected, in animals injected with 100 infectious units (n=4) 127±12 ß-galactosidase immunoreactive cells, and in animals injected with 1,000 infectious units (n=4), 1,298±29 immunostained cells were detected. The number of immunoreactive cells found for each viral dose injected was unexpected. Surprisingly, the number ß-galactosidase immunoreactive cells counted were higher than the number of infectious units injected. The first hypothetical explanation was that the titre determined for the virus, may have been underestimated. Alternatively, the number of immunoreactive positive cells detected was being overestimated because of the detection method used. According to the thickness of the brain sections and the size of the positive cells, there is a possibility that a single cell may be present in more than one section, which means that the same cell will probably be counted more than once. Abercrombie et al (1946) described a mathematical correction to address the probability of overestimating the number of immunoreactive positive cells during quantification. This correction was applied by us to rectify the

quantification of total number of positive transduced counted cells, after the final number of positive cells was obtained:

$$(\Sigma x)\ f\ st/\ (st+cd) = \text{corrected number of positive cells}$$

Where **Σx** is the total number of positive cells counted which was 8±3 ß-galactosidase immunoreactive cells when 10 iu were injected, 127±12 ß-galactosidase immunoreactive cells with 100 iu, and 1,298±29 transduced cells whith 1000 iu injected.

f is the frequency of sections sampled. In our model the brains were serially sectioned in 6 well plates and sections of wells 1 and 4 were immuno-stained and positive cells counted. This factor was already taken into account to calculate the total number of cells in **Σx,** where the number of positive cells obtained were multiplied by 3, to extrapolate the number of positive cells that will be present in wells 2, 3, 5 and 6, which were not counted as they were used to detect inflammatory cell infiltration. So for the formula ***f*** it will be equal to 1 as it was already included.

st is the section thickness, which was 50 μm.

cd is the estimated cell body diameter. To calculate the cell body diameter, the diameters of 100 positive transduced cells were messured, not taking into account their cell processes. In this way when only positive cell processes were detected they were not considered positive for cell counting purposes. The average cell diameter experimentally found was 12 μm. Ones the Abercrombie correction was

made, applying the explained formula to the counted positive cells, the final number of corrected transduced cells were as follows:

Infectious units striatally injected	Average of transduced cell counted	Average of transduced cells after Abercrombie correction
10	8	7
100	127	102
1000	1298	1046

The numbers of transduced cells obtained after the Abercrombie correction were now very close to the viral dose injected (figure 23). This shows that effectively the initial number of ß-galactosidase immunoreactive cells counted were overestimated.

Figure 23

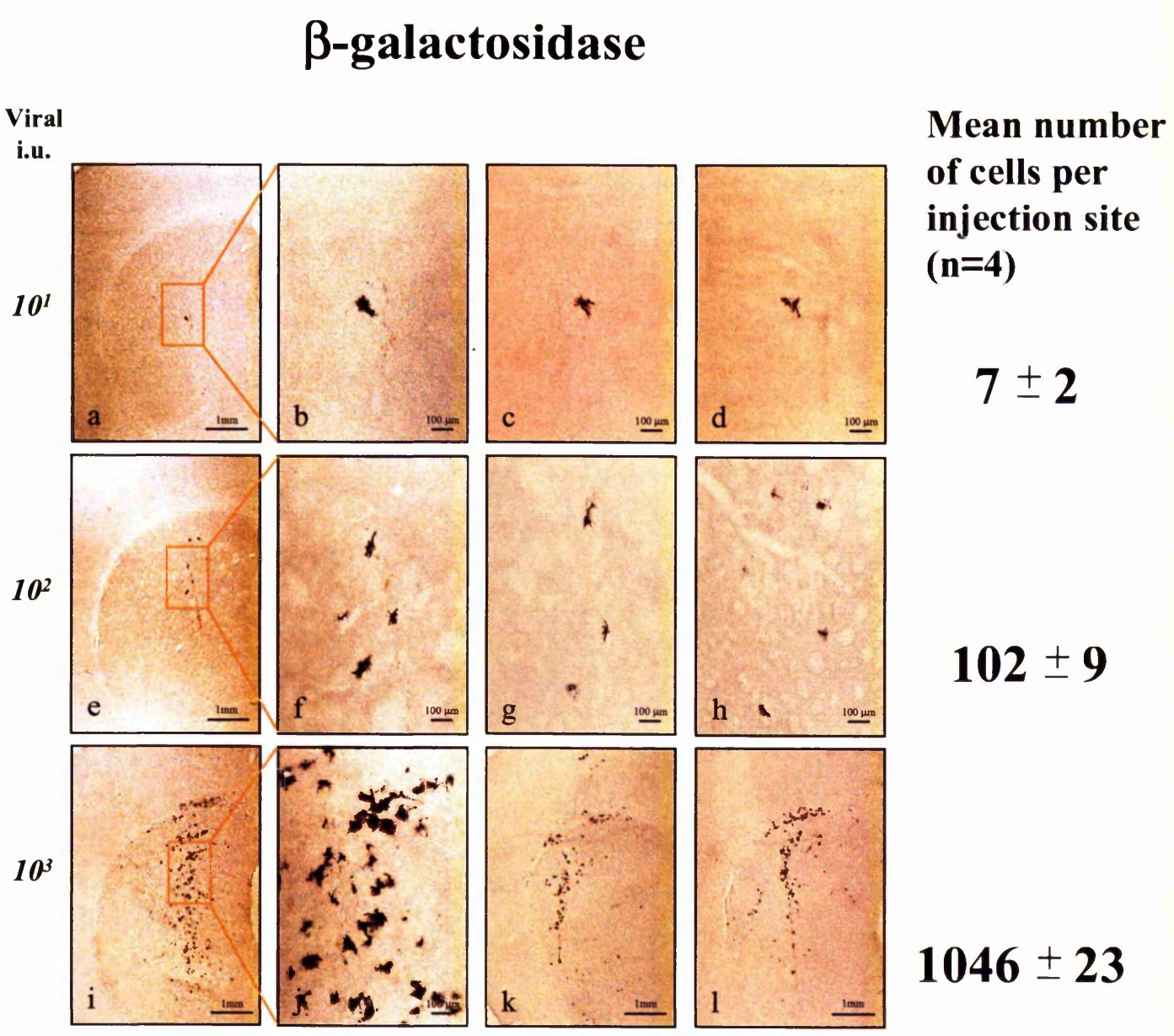
β-galactosidase
Viral i.u.
10¹
10²
10³
a
b
c
d
e
f
g
h
i
j
k
l
1mm
100 µm
Mean number of cells per injection site (n=4)
7 ± 2
102 ± 9
1046 ± 23

Figure 23. Low doses of RAd36 were injected into the adult rat striatum, 10^1, 10^2, and 10^3 iu (the n number for each viral dose of RAd 36 was: $1x10^1$-$1x10^3$ iu, n=4). **a**, **e**, and **i** show a low power view through the middle of an injection site at either dose. **b**, **f**, and **j**, show an enlarged view of the injection site, as outlined in the boxes in **a**, **e**, and **i**. **c**, **d**, **g**, **h**, **k**, and **l** each show further examples of different injection sites. In **c**, **d**, **g**, **h**, higher power views are shown to illustrate the morphology of transduced cells; while **k**, and **l** are shown at the lower power to demonstrate the full extent of distribution of RAd36 transduced cells at this viral vector dose. Scale bars and their magnification are shown for each panel. The mean number of cells per injection site (n=4) is shown on the right hand of the figure. All transduced cells detected at these low doses displayed characteristic astrocyte-like morphology.

The correlated linear increase in the number of positive cells with increasing dose of RAd36 (in the 10^1-10^3 iu range) with or without the Abercrombie correction, shows that *in vivo* infection by a single infectious unit of RAd36 is sufficient to express enough ß-galactosidase to detect transgene expression in an infected cell by immunohistochemistry. Such a linear relationship is predicted by the mathematical Poisson's distribution, if and only if, a single infectious viral unit directs the expression of sufficient transgene to be reliably detected (Mittereder et al, 1996; Luria et al, 1978). This means that each positive cell observed in figure 23, is the product of a successful infection of only **one** adenoviral particle, uncovering for the first time the extremely high transduction efficiency of recombinant adenoviral vectors when used in the CNS.

3.2.11 Method of titre determination does not affect the high transduction efficiency.

The calculated "efficiency" of transgene expression obtained in our experiments depends on the infectious titre assigned to the viral stock used. The standard method accepted (Nyberg-Hoffman et al, 1999), for determining adenovirus titres, gives a titre which is calculated from the highest dilution of virus capable of producing cell infection and complete cytopathic effect within infected wells.

Due to the importance of an accurate and reproducible titre, especially when injecting very low amounts of infectious units, any mistake in the titre determination could drastically affect the results. To find the best method for titre determination, different methods were assessed and the traditional technique (serial dilution

titration, section 2.3.7) (Nyberg-Hoffman et al, 1999), was modified to maximise accuracy and reproducibility.

As shown in detail in the material and methods section (2.3.7), in the traditional viral titration method the virus is serially diluted in final volumes of 1ml, sampling 300 µl of each dilution in 3 separate wells (of a 96 well plate) each one with 100 µl of viral solution, plated the day before onto replication permissive 293 cells. The last sampled dilution found to have all three wells with viral cytopathic effect (CPE) after 8 days of viral addition is considered to have at least 1 infectious viral particle in each well. This means that there is at least 3 infectious viral particles in the 300 µl sampled. Extrapolating this result, in the total volume of the given dilution, which is 1 ml, it will be at least 10 infectious particles. With this fact established and by correcting with the dilution factor (table in section 2.3.7 of material and methods), we can extrapolate the original titre of the undiluted stock.

This titre determination is mathematically correct, but unfortunately in the practice there are several physical variables that may alter the result from one titration to the other. In order for a viral plaque to form the infectious viral particle has to infect a cell and begin the amplification process. When the viral dilution is added to each well, the viral particles themselves may be some distance away from the HEK 293 cells to infect. The time taken for the virus to infect the HEK 293 cells via natural tropism may be longer than the half life of the virus itself. It is possible therefore, that infectious viral particles in the sample do not succeed in infecting cells and are not accounted for, resulting in the underestimation of the viral titre. To minimize this problem the plates are centrifuged for 90 minutes at 1000 g. This centrifugation will

force the viral particles to the bottom of the wells, increasing the likelihood of infecting the monolayer of HEK 293 cells. In this way we assure that all possible infectious particles are close to the permissive cells in a very short time (90 minutes) maximising the chance of a successful infectious event.

Another variable to be taken into account during viral titration, is the number of permissive cells seeded in each well which the infectious viral particle will have to find and infect. Excess cells will lead to premature death of the monolayer of HEK 293 cells, preventing the occurrence of plaque formation. On the contrary if too few cells are seeded, the viral particles will have less chance to produce an infectious hit event, giving an underestimation of the viral titre. Experimentally, it was found that 6000-8000 cells per well in 96 well plates, provides maximum titres. This cell number allows plaque formation and detection without cell death due to overpopulation even after 14-20 days post-infection. The growing media for the HEK 293 cells in the titration plates was not renewed to minimise disturbance in the infectious process.

The final variable to be taken into consideration, is the fact that viral particles might not be homogenously distributed within a viral dilution. When sampling a viral dilution more than one, or alternatively no viral particles, may be added to each well simply by mathematical probabilities. In the traditional titration method the viral titre is considered to be the last dilution producing CPE in all 3 sampled wells. It is supposed that, for CPE to occur, there should be at least one viral particle in each of those wells. In practice, however, 2 or more infectious viral particles could be responsible for plaque formation in a single well. The calculated titre is therefore an underestimation of the actual titre. To reduce the risk of miscalculating the viral titre,

4 wells representing each dilution (400 µl) instead of the standard 3 (300 µl) were infected (increasing the net volume sampled for each viral dilution) and all wells conferring CPE taken into account. In order to calculate the titre, dilutions resulting in CPE in 50% (2 wells) and 25% (1 well) were also taken into consideration together with the dilution that gave 100% CPE (all 4 wells) (figure 24). It was assumed that dilutions producing CPE in 50 % of the sampled wells contained 5 viral particles/ ml (as opposed to 10 iu/ ml in dilutions producing 100% CPE) and when only one well conferred CPE it was presumed that the sampled dilution contained at least one infectious viral particle/ ml. The final titre was taken to be the highest obtained after titre calculation with the 3 CPE considerations (see figure 24). This is thought to be a more accurate and reproducible method of titre determination.

Recently, Nyberg-Hoffmann et al. (1999), have proposed a theoretical correction to apply after biological method of viral titration. Concern arose when viral titres obtained by serial dilution of the virus by detection of CPE, were compared with the number of actual viral particles physically detected by spectrophotometry. The titres obtained by spectrophotometry were always much higher than the ones obtained by biological methods. This variation can be explained by the fact that spectrophotometry provides a total viral particle count (including the defective ones) whereas serial dilution is a measurement of viable viral particles. On the contrary Nyberg-Hoffmann et al. concluded that the disparity is due to the physical probability of an infectious unit to encounter and infect a cell. There is also a possibility that more than one particle infects the same cell. Nyberg-Hoffmann et al, devised a mathematical correction which compensates for the deviations in titre values. They

conclude that their correction gives a more accurate and reliable titre as the final titre obtained is closer to the amount of viral particles detected by spectrophotometry.

Even though this may be in part true, as explained previously, several different measures were taken to the titre determination method to maximise infectious viral particle detection. What it has not been studied, is the actual number of defective particles present in the different preparations, which may explain the difference in the number of detected particles with both the physical and biological methods. Using the standard method of titration, a titre for RAd36 of $8.2x10^{10}$ iu/ml was obtained (with a particle:iu ratio of 17), and an efficiency of gene transfer of 100% (Figure 11).

Applying the theoretical corrections to the titre, according to Equation 6 of Nyberg-Hoffman et al. (Nyberg-Hoffman, 1999), the obtained titre was $2.3x10^{11}$ iu/ml (with a particle:iu ratio of 6) and a corresponding efficiency of 33%. Whether the standard titre or the corrected titre is used for the calculations, the calculated efficiency of RAd36-mediated gene transfer to the brain remains very high. In this work, vector titres are refer as the calculated from the standard method of titration.

Importantly, regardless of the titration method considered (with or without Nyberg-Hoffman correction) to calculate the viral titre, the linear increase in the number of ß-galactosidase expressing cells obtained at increasing viral doses from 10^1-10^3 proves that each stained cell is infected by a single viral particle, demonstrating that one infecting physical particle is enough to produce detectable levels of ß-galactosidase in a cell *in vivo* (Mittereder et al, 1996; Luria et al, 1978).

Figure 24

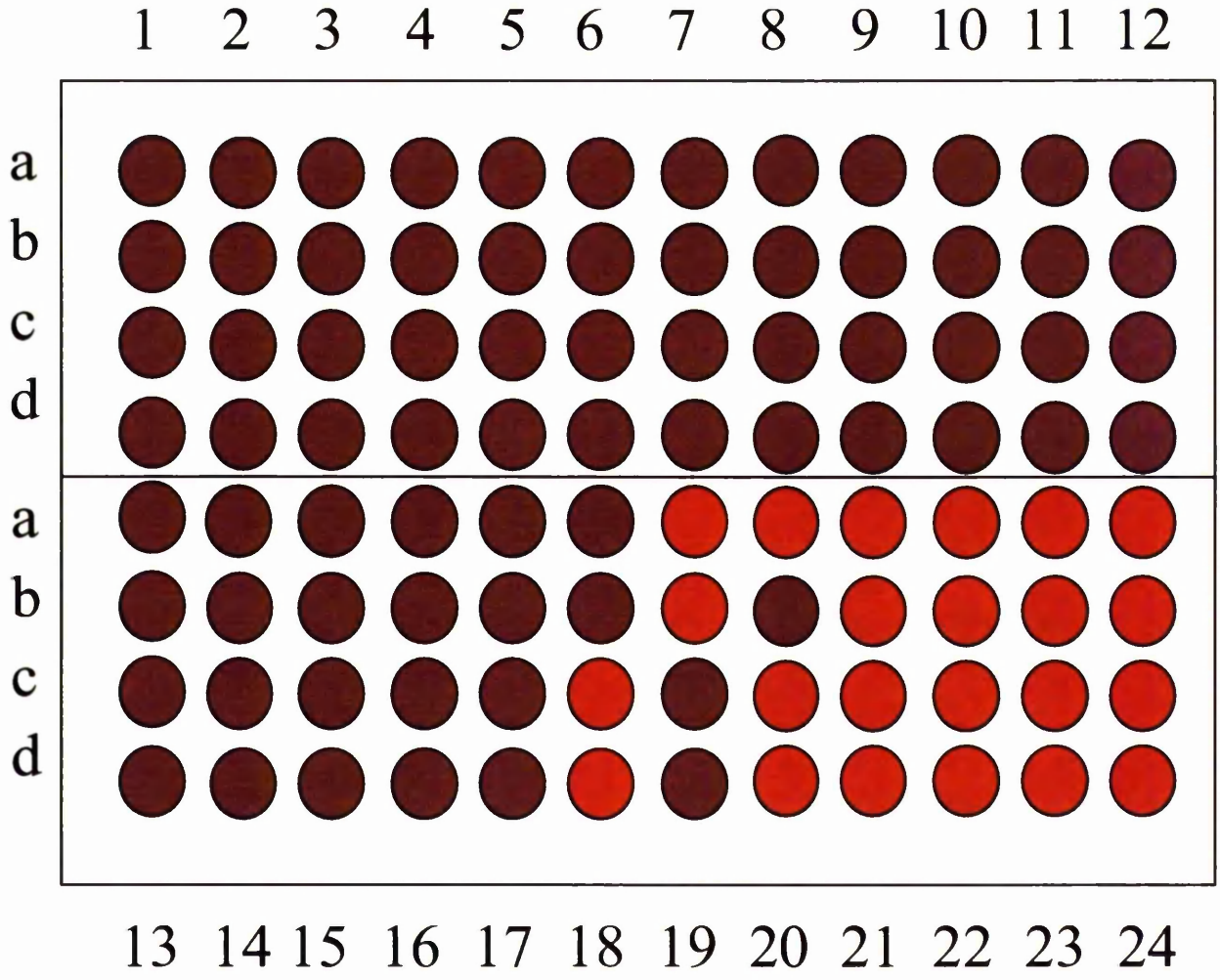

Well with cythopatic effect

Well with normal 293 cell monolayer

Figure 24. Reading exemplification of the improved titration method. The virus was serially diluted (section 2.3.7), and 400 µl of each dilution was sampled on a 96 well plate in 4 separate wells with 100 µl each. The last dilution to have complete CPE was found to be 17. According to the table described in material and methods for titer determination, the titer obtained considering to have 10 particles in the 17 dilution will be 4.1×10^{10} iu. We also considered well 18, which is the last dilution to have 50% of detected CPE, estimating then to have 5 total infectious viral particles in this dilution. Using again the titration table it will give a titer of 4.1×10^{10} iu which is the same one obtained before. Finally we make the titer calculation considering dilution 20, which is the last dilution in which we detected only one sampled well with CPE. This will mean that in this dilution (number 20) we have at least one infectious viral particle. Making the calculation using the titration table considering that we have 1 particle in the dilution 20, the resulting titer will be then 3.28×10^{10} iu. The final titer obtained for the undiluted viral stock will be considered to be of 4.1×10^{10} iu, which is the highest one calculated with the 3 independent values.

3.3 Discussion

Efficiency of gene delivery and expression is likely to depend on a number of factors. Possessing the appropriate viral receptors at high density, the processes of viral internalisation and delivery of the vector genome from endosomes to the nucleus of infected cells, and transcription-translation efficiency of the transgene will all play a role. *In vivo*, one has to further consider the role played by the diffusion of virus throughout brain tissue, and the effects of inflammatory and immune cells.

Single viral particles are very efficient in infecting their preferred target cells *in vitro* during the determination of viral titres (Mittereder et al, 1996). However, *in vivo* gene transfer, as assessed by the number of detectable transduced cells, appears to be inefficient. This has led to the use of high titres of vectors to transduce the brain *in vivo*, to obtain either anatomically detectable cells, or a therapeutic effect in animal models of disease (Blomer et al, 1997; Dewey et al, 1999).

When using adenoviral vectors encoding marker transgenes under the transcriptional control of very powerful promoters (i.e. an adenovirus vector encoding ß-galactosidase under the transcriptional control of a powerful short hCMV promoter) no transgene expression is seen if fewer than 10^4 infectious units are injected into the target brain area. Similar data have been reported by many other laboratories, but the reasons for the apparently inefficient gene transfer and expression *in vivo* have never been properly explored. In most papers doses of 10^4-10^{10} total infectious units have been injected into the brain of rodents. All studies available so far report that at least 10^6-10^8 total infectious units need to be injected into the brain in order to

detect anatomically, or physiologically relevant transgene expression. Significantly, similar titres (10^6-10^8 infectious units) have been used when transducing the brain with either AAV, lentiviral, or herpes simplex virus type 1 vectors (Blomer et al, 1997).

It has been demonstrated in a previous paper (Shering et al, 1997) that, while RAd35 was able to infect neocortical neurons in primary cultures, transgene expression was not seen until cells were superinfected with other viruses, an experimental paradigm which was found to activate the hCMV promoter sequence in RAd35. This was taken to indicate that, although neurons in primary culture were infected with RAd35, the hCMV promoter remained silent.

The current work demonstrates that *in vivo* gene expression from viral vectors depends on the promoter element employed. Using very low doses of a viral vector expressing a transgene from a very strong promoter we have demonstrated for the first time that a single viral infectious unit is sufficient to transduce a single glial cell *in vivo*. This in turn allowed us to determine that the efficiency of Ad-mediated gene transfer into the rat brain *in vivo*, in our experimental conditions, is 100%. The reason for the generally low efficiency of gene transfer and expression observed *in vivo* appears thus to be due to the low activity of promoters used previously.

Viral vector diffusion throughout brain tissue has so far been regarded as very poor, but has not been evaluated experimentally. Results with RAd36 demonstrate that adenoviral vectors can diffuse relatively large distances in the brain, even in the absence of special physical delivery methods such as high-pressure injections into

the brain (Bobo et al, 1994). Our data show that RAd36 at each viral vector dose transduces an area of the striatum, which is much larger than the area transduced by the same dose of RAd35. This might be due to the fact that a single viral particle of RAd36 leads to detectable ß-galactosidase expression, while co-infection with a high number of particles of RAd35 is necessary to achieve detectable levels of transgene expression in the brain with this vector. RAd35 transgene expression can only be detected at 10^4 iu. Since experiments with RAd36 show that virus does indeed enter brain cells after delivery of lower doses, multiple hits must be necessary for detectable transgene expression following infection with RAd35.

Much work has been devoted to the development of cell type specific promoters, inducible promoter elements, or even combined cell type specific and inducible transcriptional regulatory systems. Such cell type specific promoters are at least 10^3-10^4 fold weaker *in vivo* than the mCMV promoter that has been used in these experiments (Smith-Arica, 2001; Southgate et al 2000), and thus at least 10^3-10^4 fold more virus would be required to detect equivalent numbers of transgene expression in the brain.

Investigators have so far been forced to choose between accepting a high degree of inflammation and cytotoxicity accompanying administration of higher doses of vector, which will in turn curtail the duration of transgene expression, or using lower doses and achieving a more limited transduction (Thomas et al 2001, Thomas et al, 2000). Now, however, it is demonstrated for the first time that high-level expression in the brain can be obtained in the complete absence of cellular inflammation or viral cytotoxicity, and using very low doses of adenoviral vectors.

The activity of cell type specific or inducible promoters will have to be improved substantially, in order to achieve efficient and safe gene therapy approaches for the treatment of human neurological diseases.

Further optimisation of viral vectors (Umana et al 2001), including the basic knowledge necessary for successful retargeting of viral vectors (Douglas et al, 1999; Roelvink et al, 1999) will maximise transgene expression and eliminate direct cytotoxicity and inflammation. In conclusion, these data demonstrate that gene transduction using adenoviruses *in vivo* can be extremely efficient, and devoid of any direct cytotoxicity or acute brain inflammation.

Chapter 4: Innate vs. adaptive immune responses to first generation adenoviral vectors.

4.1 Introduction

The intrinsic high efficiency of adenoviral vectors for transgene delivery and expression in the brain was revealed when using the very strong mCMV promoter to drive the expression of the marker transgene β-galactosidase in an E1/E3 deleted first generation adenoviral vector (RAd 36). Using this vector it has been possible to achieve very good transduction of the brain in the absence of viral cytotoxicity or early cellular inflammation, when using viral doses of 10^6 iu and below (Gerdes et al, 2000). Hence it is possible that if doses up to 10^6 iu avoid detection by an early inflammatory response in the brain, we postulate that similar doses of virus might be used to evade the adaptive immune response to achieve long-term transgene expression.

The brain, due to its immuno-privileged status, is unable to trigger an adaptive immune response unless the adaptive arm of the immune system is primed by injection of antigen outside of the CNS, e.g. skin. Thus, the CNS provides a perfect environment to compare the adenoviral dose that can avoid recognition by the innate or adaptive immune responses independently.

To determine the RAd dose thresholds, which avoid detection by the innate or the adaptive immune responses in the brain, the experimental design described by Byrnes et al was used (Byrnes et al, 1997; Thomas et al, 2000) (figure 25). Increasing doses of RAd 36 (10^1 iu to 10^7 iu) were injected into the brain and after one month, the immune response was primed by an intra-dermal rechallenge with 10^8 iu of a RAd harbouring no transgene (RAd 0). Sixty days later, brains were recovered and analysed. This experimental model can be used to test the hypothesis that with RAd 36 doses of 10^6 iu and below, there will be no diminishment of transgene expression in the brain after intra-dermal adenoviral immunisation. We expect that at these viral doses the acquired immune response will not be able to recognise and eliminate transgene expression, taking into consideration the results obtained in chapter 3, where doses of 10^6 iu and below of RAd 35 or RAd 36 avoided the early cellular infiltration characteristic of the innate immune response.

Animals injected with RAd 36 in the brain but without intra-dermal adenoviral immunisation were used as controls for these experiments. The levels of transgene expression in the brain from these controls was also used to compare to the levels obtained in previous experiments, when transgene detection was carried out only 5 days post RAd 36 brain injection (section 3). This new information is of great relevance as it will complement the results obtained in chapter 3 about adenoviral transduction efficiency and innate immune response effector functions 90 days after adenoviral delivery into the brain.

The dose of adenoviral intra-dermal immunisation, required to clear RAd transgene expression in the brain was taken from previous reported experiments (Thomas et al,

2000). The lower limit of adenoviral dose necessary to achieve peripheral priming and subsequent immune response activation with transgene expression elimination in the brain has never been studied before. To asses this issue, an experimental design similar to the above was employed. This time the doses of intra-dermaly injected RAd 0 were varied (10^1 iu to 10^7 iu), whereas the dose of brain injected RAd 36 was maintained at 10^7 iu (figure 35).

The results obtained from these experiments indicate that, while doses above 10^6 iu injected into the brain are needed to stimulate innate immune responses, even as little as 10^3 iu can be recognised in the brain by elements of the adaptive immune response, following intra-dermal immunisation with a first generation adenoviral vector (10^8 iu of RAd 0).

This suggests that, even in the absence of early brain inflammation after RAd striatal injection, peripheral adenoviral infection may eventually occur, terminating transgene expression in the brain when using 1st generation adenoviral vectors to deliver the desired transgene. Vectors such as the new helper dependant adenovirus (see section 1 of this thesis), devoid of any adenoviral gene expression, therefore capable of evading transgene elimination by an activated immune response (Thomas et al, 2000), will need to be used to ensure long-term transgene expression in the presence of a systemic immunisation against adenoviruses.

4.2 Results

4.2.1 Only very low doses of RAds in the brain can avoid detection by the adaptive immune response after immune priming in the CNS periphery.

Viral doses from 10^1 to 10^7 infectious units of RAd 36 were injected into adult rat striata (n=3). Thirty days later, animals were peripherally immunised, injecting 10^8 iu of RAd 0 (RAd with no transgene) intra-dermaly. 60 days later brains were sectioned and the presence of immunoreactive ß-galactosidase enzyme was assessed by immunohistochemistry (RAd 36 transduced cells). Brain inflammation was characterised by immunohistochemistry by CD8 (T cells and natural killer cells) and ED1 (macrophages) cell markers detection. (Figure 25)

Only doses of 10^1 iu and 10^2 iu of RAd 36 injected in the brain avoided detection by the primed adaptive immune response, achieving unaltered long term expression (figures 26, 30). At these doses the number of ß-galactosidase positive cells detected with or without immunisation in the periphery were identical.

Transgene expression from doses of RAd 36 from 10^3 iu to 10^6 iu injected into the brain decreased significantly after intra-dermal immunisation. Even though there is a reduction in transgene expression at these doses, RAd 36 ß-galactosidase expression is still macroscopically detectable after immune response priming. Interestingly, the phenotype of some of the transduced brain cells, found in the brain of these animals, were different from normal. A great number of these brain cells,

appeared to be damaged (figure 34). The transgene expression detected 90 days after RAd 36 injection with doses of 10^4 iu, by cell counting after peripheral immunisation, was 10.5 % of that observed in the same time period without immune response priming (3447±844 cells without priming and 328± 107 with peripheral immunisation) (figure 30). On the contrary, when brains injected with a dose of 10^7 iu of RAd 36 and peripherally immunised with RAd 0 were analysed, not a single ß-galactosidase positive cell was detected.

To show that peripheral priming of the immune response by intra-dermal injection with RAd 0 was successful in each case, adenoviral neutralising antibodies were measured by demonstrating the ability of animal serum to inhibit adenoviral infection in HEK 293 cells. Adenoviral neutralising antibodies were found in all RAd 0 intra-dermally injected animals, indicating that an anti-adenoviral immune response was primed (table 1).

Characterisation of the brain inflammation shows strong cellular infiltration in the injection site of all immune primed animals, injected with RAd 36 doses above 10^4 iu into the brain (figures 28, 29 & 33). Nevertheless the infiltration was not independent of the viral dose. Higher infiltration was correlated with higher dose of virus injected into the CNS. The cellular inflammation in animals injected with 10^3 iu of RAd 36 or below was not different from saline controls with or without immune priming.

Figure 25

What dose of first generation Adv can sustain transgene expression in the CNS in the presence of an anti-adenoviral immune response elicited through intra-dermal infection with adenovirus?

Experimental Design:

Day 0:
RAd36 (mCMVp-βgal),
at doses from 10^1-10^7 iu,
injected into the striatum
of adult rats.

Day 30:
RAd0 (no transgene), 10^8 iu,
injected into the skin.

Day 90:
Brains analysed for evidence
of transgene expression (β–gal)
and cellular inflammation (ED1 & CD8).

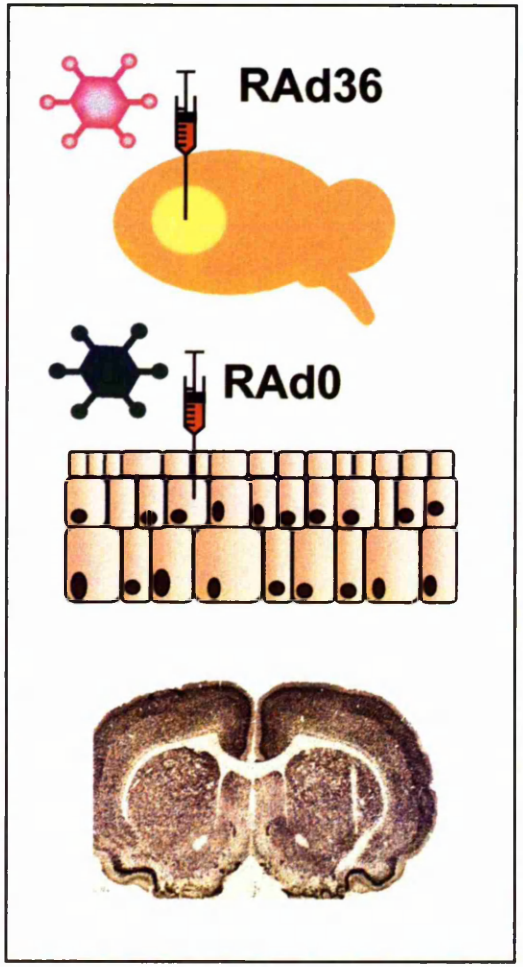

Figure 25. Experimental model designed to answer the question: what dose of first generation adenovirus (RAd 36) can sustain transgene expression in the CNS in the presence of an anti-adenoviral immune response elicited through intra-dermal infection with a recombinant adenovirus carrying no transgene (RAD 0). For each dose of RAd 36 analyse 3 animals were used (n=3), all intra-dermally injected with the same dose of 10^8 iu of RAd 0 to generate an anti-adenoviral immune response.

Table 1

RAd 36 striatal injection with peripheral immunisation with 10^8 iu of RAd 0 (IU)	Animal 1	Animal 2	Animal 3
10^7	1/512	1/32	1/64
10^6	1/32	1/16	1/128
10^5	1/16	1/32	1/64
10^4	1/64	1/16	1/64
10^3	1/64	1/64	1/32
10^2	1/32	1/8	1/64
10^1	1/32	1/64	1/32
Saline+ priming with 10^8 RAd 0	1/32	1/32	1/32
Saline+no priming	-	-	-

Table 1. Neutralising antibody assay. Detection of neutralising antibodies against adenovirus, from the serum of animals injected with different doses of RAd 36 in the brain striatum and intra-dermally immunised with 10^8 iu of RAd 0. In all the peripherally immunised animals, positive detection of neutralising antibodies against adenoviral vectors were detected, indicating immune response activation. Neutralising antibody are reported as the dilution which results in a 50 % decrease in transgene transduction in HEK 293 cells with 10^6 iu of RAd 35 pre-incubated with animals serum when compared to the expression achieved with a non-blocked RAd 35 control.

4.2.2 Long term unaffected transgene expression in the brain at doses, which avoided early cellular inflammation.

As a control experiment for section 4.2.1 (carried out in parallel), viral doses from 10^1 to 10^7 infectious units of RAd 36 were injected into adult rat striata (n=3 for each dose) without intra-dermal adenoviral exposure to prevent anti-adenoviral immune response activation. Ninety days later, the animals were perfused and the brains were sectioned. The presence of immunoreactive ß-galactosidase enzyme (cells transduced by RAd 36), CD8 (for T cells and Natural Killer cells) and ED1 (macrophages) cell markers were assessed by immunohistochemistry.

At all RAd 36 doses used in this experiment, except 10^7 iu, the levels of immunoreactive ß-galactosidase 90 days after brain injection were similar to those detected in the previous experiments where ß-galactosidase detection was done 5 days after RAd 36 brain injection (Figures 18, 19, 26, 27).

The immune response markers analysed (ED1 and CD8) showed that no detectable difference of cellular inflammation was found with doses between 10^1 iu and 10^6 iu of RAd 36 90 days after brain injection, when compared to the saline control or the inflammation observed 5 days after RAd infection with same viral doses (Gerdes et al 2000) (Figures 21 vs 33).

When animals injected in the brain with doses of 10^7 iu of RAd 36 were analysed 90 days post injection, a low decrease of ß-galactosidase expression was observed,

with a significant difference of cellular infiltration compared to the rest of the doses (10^1 iu to 10^6 iu) (figure 33).

Interestingly the linear relationship between the number of positive immunoreactive cells counted and the viral dose administered seen previously (section 3.2.8), when low doses of RAd 36 were injected into the brain (10^1-10^3 iu) (Gerdes et al, 2000), was strictly maintained (Figures 23 and 30). This means that each cell positively detected for ß-galactosidase at these doses (figure 30) was transduced by one single infectious viral particle as predicted by the Poisson distribution (Mittereder et al, 1996).

The number of positive cells counted, using a test dose of 10^4 iu of RAd 36 showed a discontinuation in the linear relationship observed at lower doses, confirming the previous suggestion (Gerdes et al, 2000) that at this dose of adenoviral vector multiple infectious hits begin to occur.

Figure 26

β-galactosidase detection

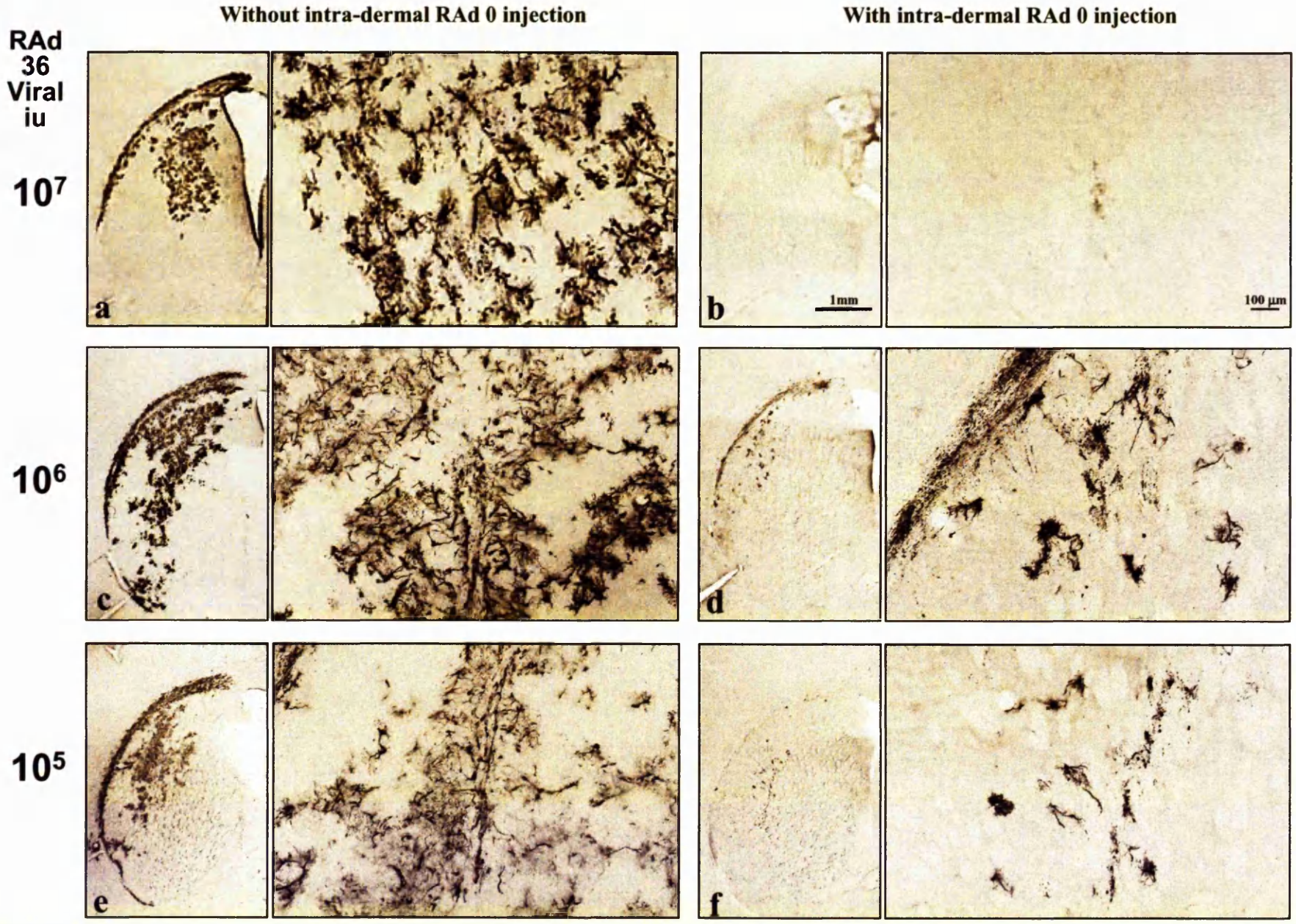

Fig 26. β-galactosidase staining of brains injected with doses from 10^5-10^7 iu of RAd 36 into the striatum, as stated in the experimental model shown in figure 25. Panels **b**, **d** and **f** show animals injected with RAd 36 and were immunise intra-dermally with 10^8 iu of RAd 0. Panels **a**, **c** and e show RAd 36 injected brains without intra-dermal immunisation with RAd 0. Magnifications of each picture are shown to appreciate cell transduction. Note the dramatic decrease of transgene expression in the animals intra-dermally immunise with RAd 0.

Figure 27

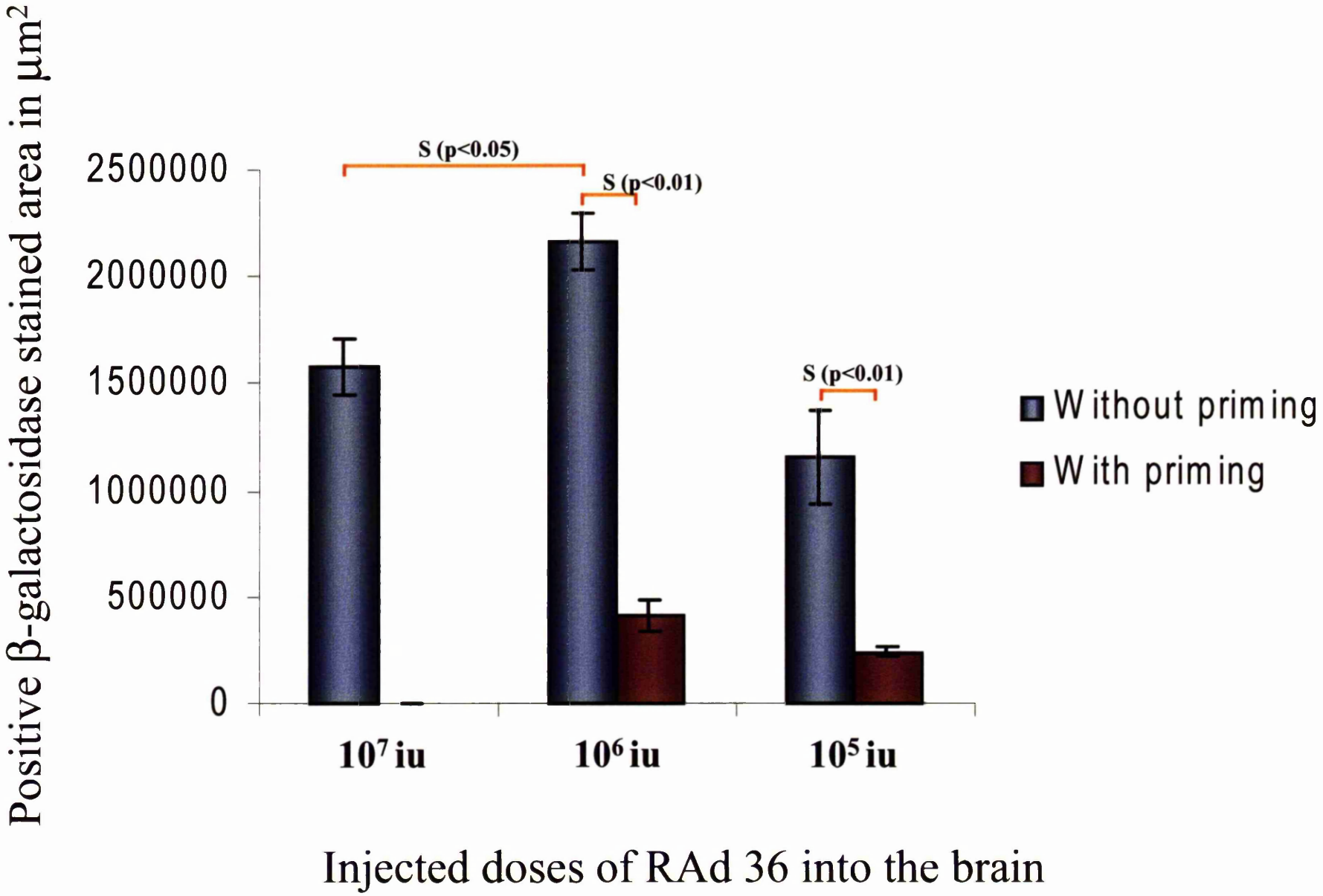
Positive β-galactosidase stained area in μm2
2500000
2000000
1500000
1000000
500000
0
S (p<0.05)
S (p<0.01)
S (p<0.01)
10^7 iu
10^6 iu
10^5 iu
Without priming
With priming
Injected doses of RAd 36 into the brain

Figure 27. Quantification of the β-galactosidase stained area of brains injected with doses of 10^5 iu, 10^6 iu and 10^7 iu of RAd 36 (90 days after injection), with or without intra-dermal immunisation with 10^8 iu of RAd 0, using a semi-automatic Quantimet imaging system. β-galactosidase expression in animals injected with doses of 10^6 iu and 10^5 iu of RAd 36 into the brain, without intra-dermal immunisation, have comparable staining to the one detected at same doses but 5 days after brain injection (figure 19 in section 3). At the dose of 10^7 iu there is a significant decrease in transgene expression when comparing the expression detected 5 or 90 days after brain injection, maybe due to viral dose toxicity. When intra-dermal immunisation was done, a significant decrease in transgene expression was seen at all these doses, being completely eliminated at the dose of 10^7 iu of RAd 36.

Figure 28

ED1 cell infiltration

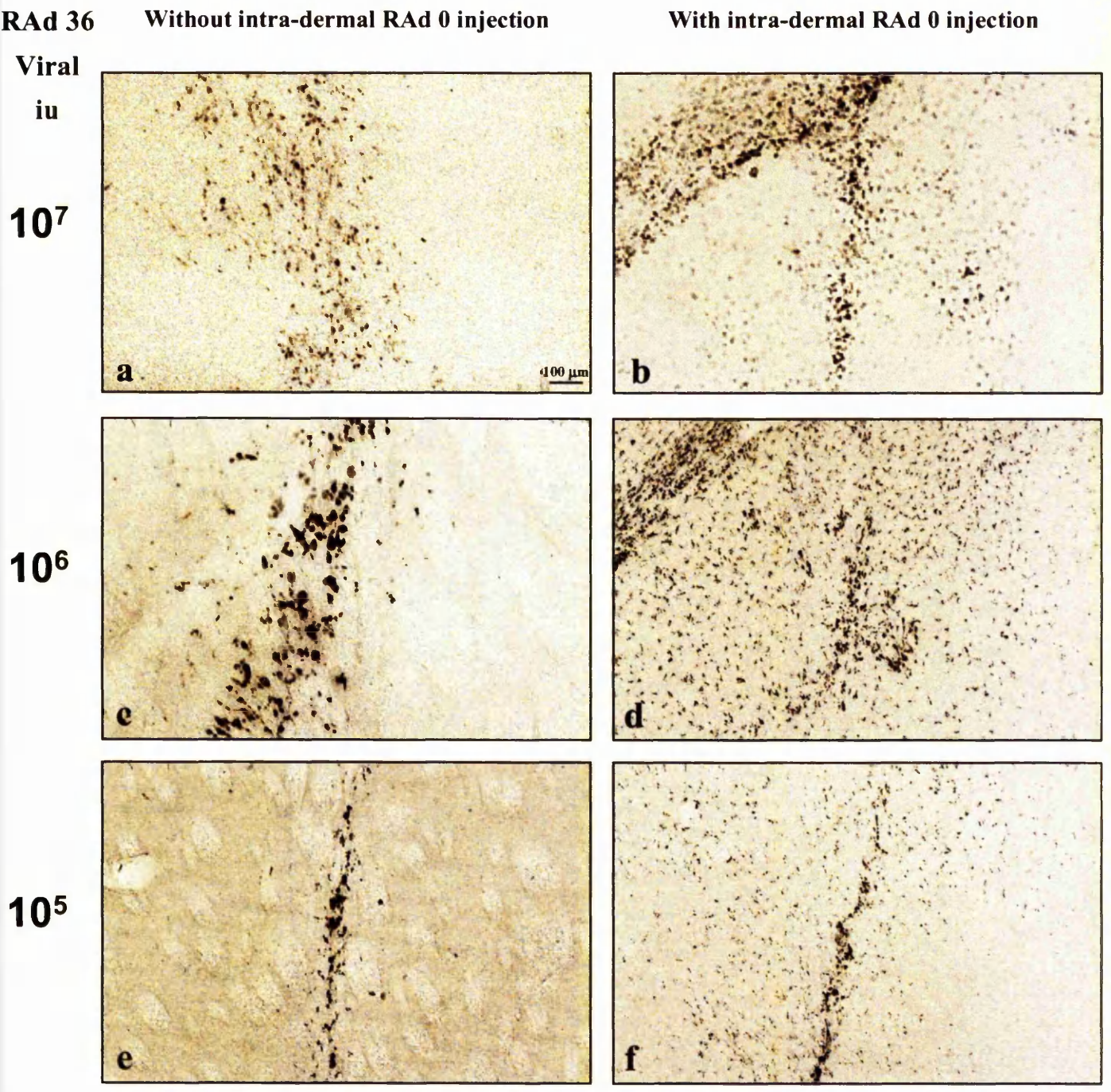

Figure 28. ED1 staining of serial sections from the brains shown in figure 26, injected with doses from 10^5-10^7 iu of RAd 36 into the striatum, using the experimental model shown in figure 25. Panels **b**, **d** and **f** show animals injected with RAd 36 and were immunise intra-dermaly with 10^8 iu of RAd 0. Panels **a**, **c** and **e** show RAd 36 injected brains without intra-dermal immunisation with RAd 0. Note the higher infiltration of ED1 positive cells in the animals intra-dermally immunise with RAd 0. Also note the significant ED1 infiltration in **a**, even though it was not intra-dermally immunised compared to **c** and **e**.

Figure 29

CD8 cell infiltration

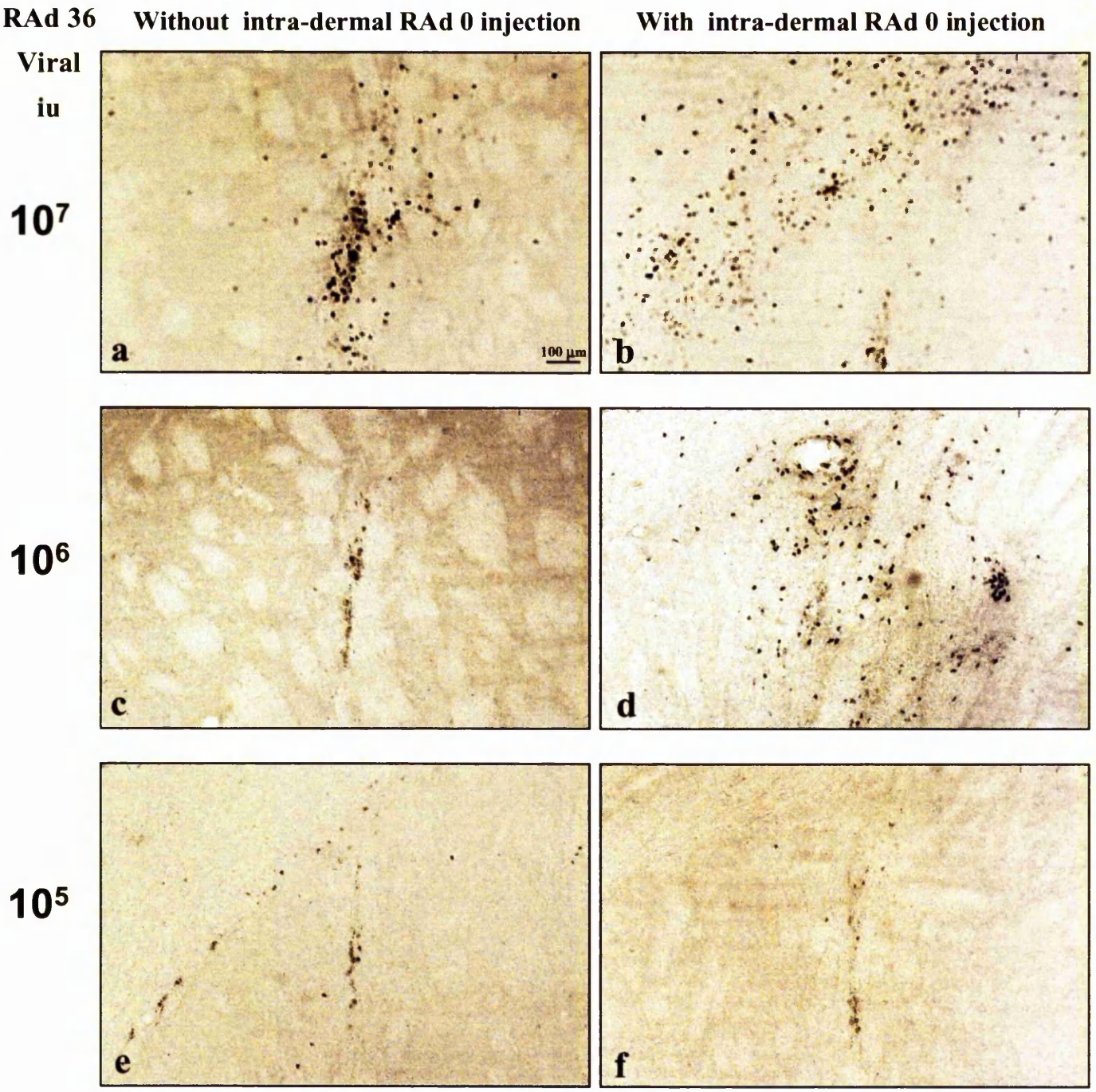

Figure 29. CD8 staining of serial sections from the brains shown in figure 26, injected with doses from 10^5-10^7 iu of RAd 36 into the striatum, using the experimental model shown in figure 25. Panels **b**, **d** and **f** show animals injected with RAd 36 and were immunise intra-dermally with 10^8 iu of RAd 0. Panels **a**, **c** and **e** show RAd 36 injected brains without intra-dermal immunisation with RAd 0. Note the higher infiltration of CD8 positive cells in the animals intra-dermally immunise with RAd 0 at the doses of 10^7 iu and 10^6 iu of RAd 36 (**b** and **d**). Also note the significant CD8 infiltration in **a**, even though it was not intra-dermally immunised compared to **c** and **e**.

Figure 30

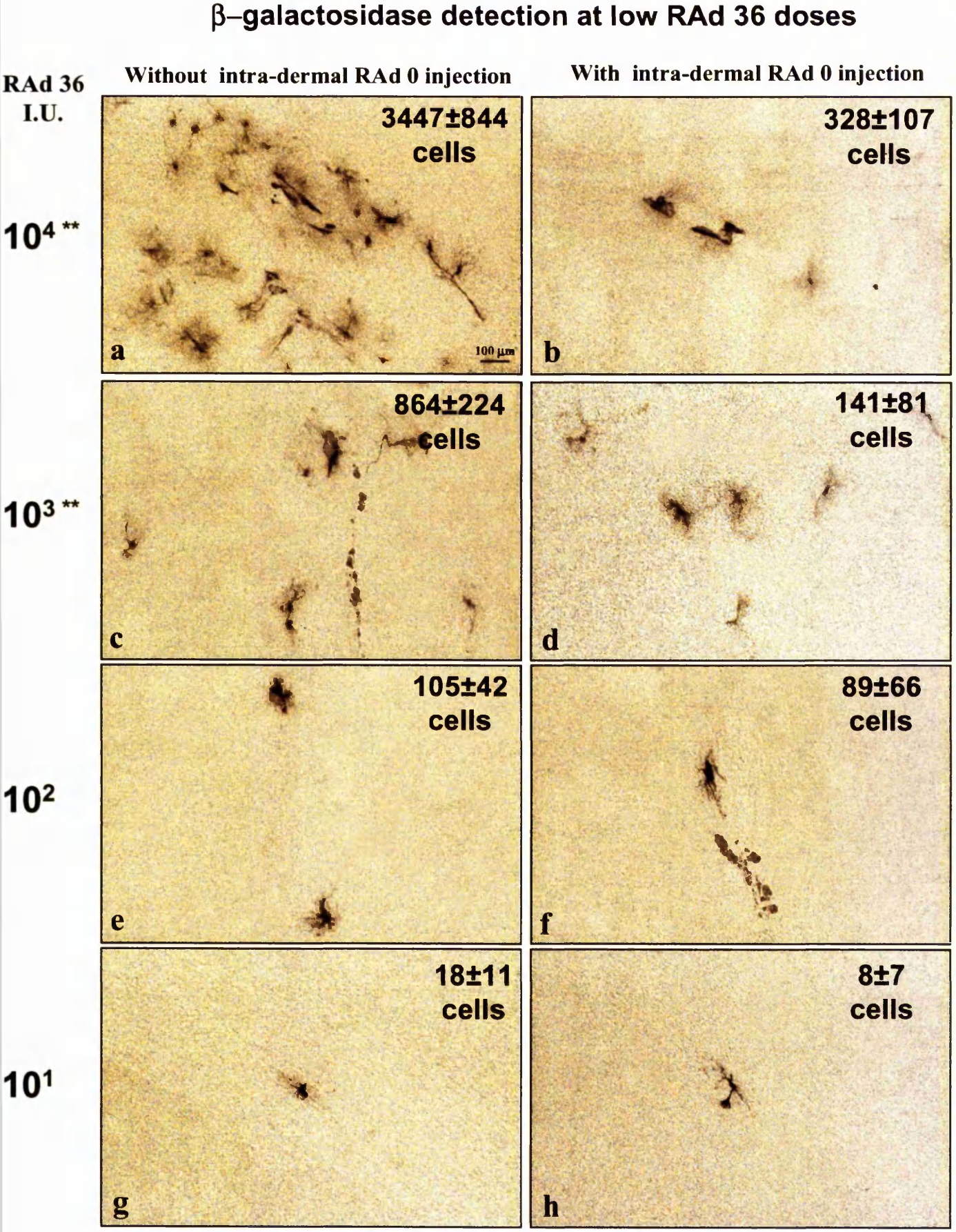
β–galactosidase detection at low RAd 36 doses
RAd 36 I.U.
Without intra-dermal RAd 0 injection
With intra-dermal RAd 0 injection
10⁴ **
10³ **
10²
10¹
3447±844 cells
328±107 cells
864±224 cells
141±81 cells
105±42 cells
89±66 cells
18±11 cells
8±7 cells
a
b
c
d
e
f
g
h
100 µm

Figure 30. β-galactosidase staining of brain sections where doses from 10^1-10^4 iu of RAd 36 were injected, with or without intra-dermal immunisation against RAds. The number of positive cells detected are shown on the top right corner of each picture. Significant difference, between the numbers of cells detected at each dose with or without immune priming is marked with a two stars. ** Significant difference ($p< 0.01$). Note that at doses of 10^2 iu of RAd 36 and below there is no significance in the number of positive cells.

Figure 31

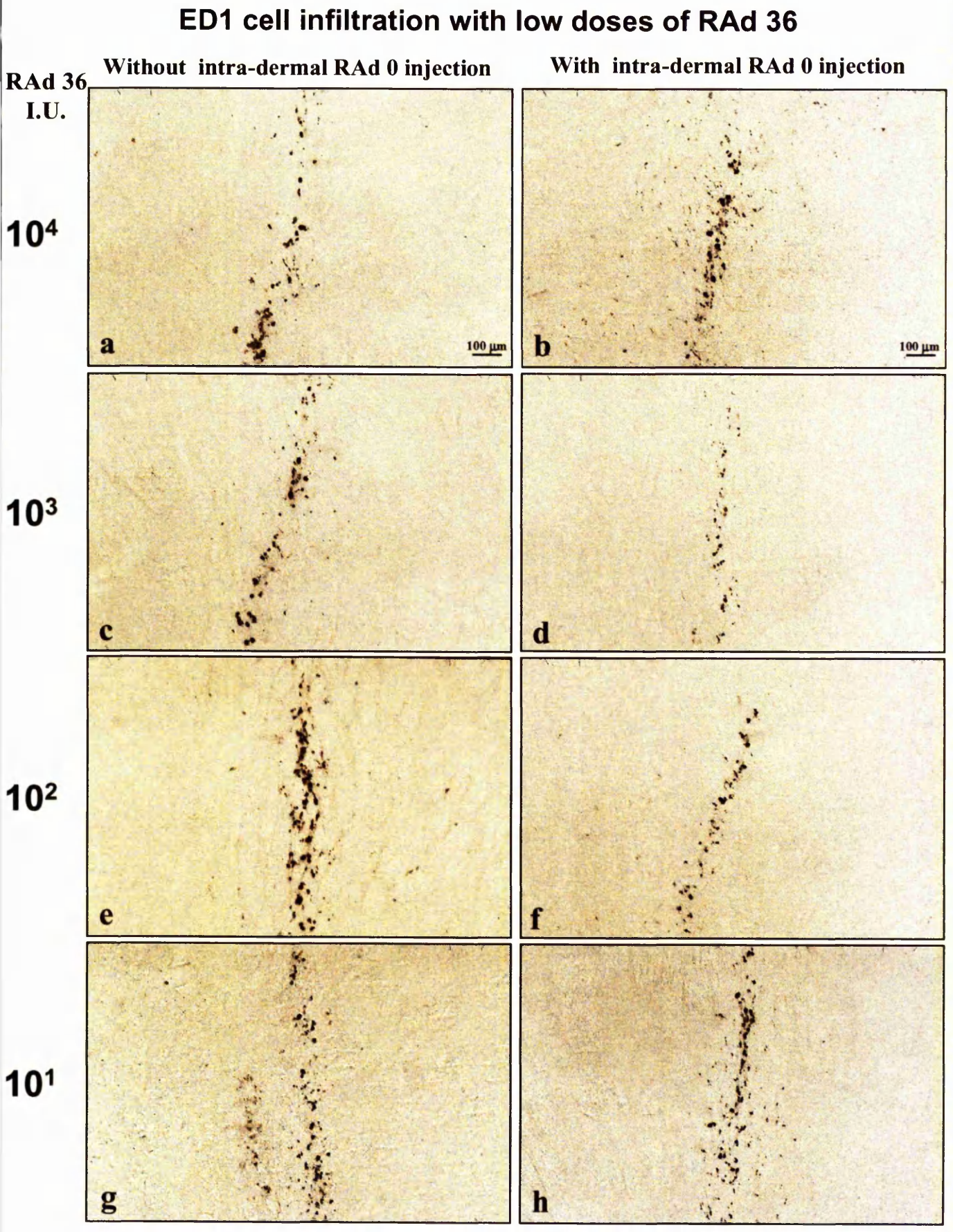
ED1 cell infiltration with low doses of RAd 36
Without intra-dermal RAd 0 injection
With intra-dermal RAd 0 injection
RAd 36 I.U.
10⁴
10³
10²
10¹
a
b
c
d
e
f
g
h
100 µm
100 µm

Figure 31. ED1 staining of the brain sections shown in figure 30, where doses from 10^1-10^4 iu of RAd 36 were injected, with or without intra-dermal immunisation against RAds. Note that there is not a significant difference of ED1 infiltration between the different viral dose groups without peripheral priming.

Figure 32

CD8 cell infiltration with low RAd 36 doses

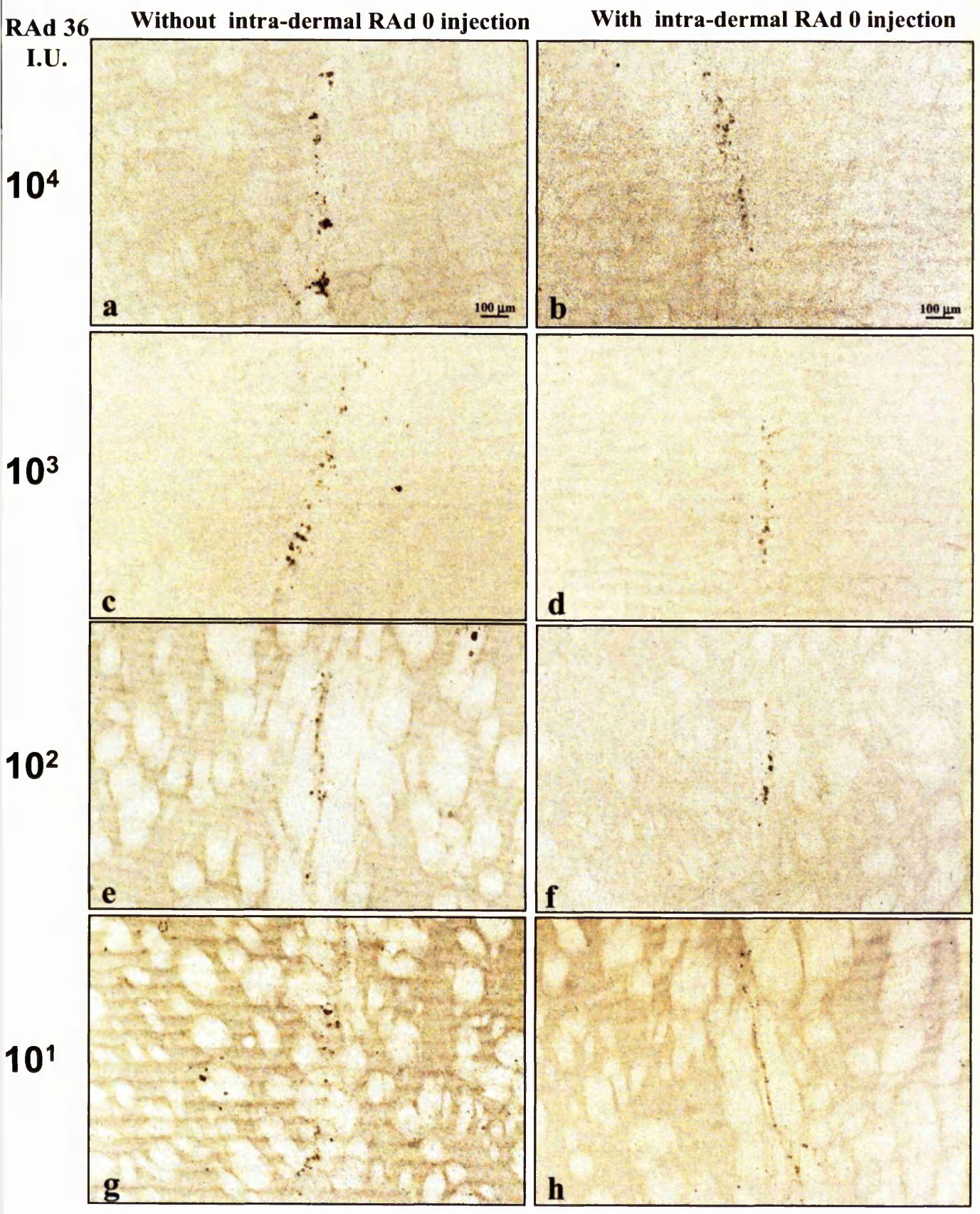

Figure 32. CD8 staining of the brain sections shown in figure 30, where doses from 10^1-10^4 iu of RAd 36 were injected, with or without intra-dermal immunisation against RAds. Note that there is not a significant difference of CD8 infiltration between the different adenoviral dose groups.

Figure 33

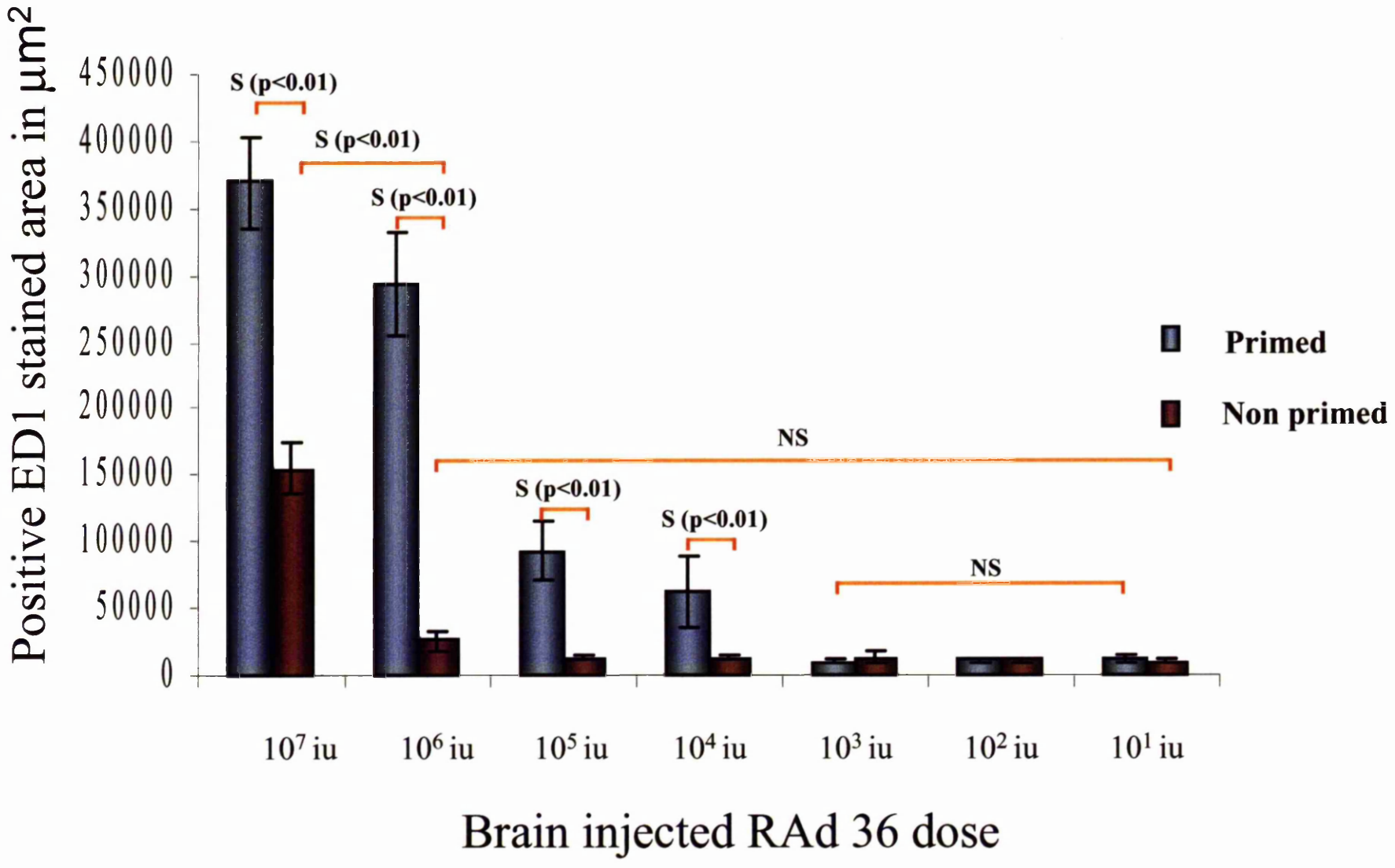
Positive ED1 stained area in µm2
450000
400000
350000
300000
250000
200000
150000
100000
50000
0
S (p<0.01)
S (p<0.01)
S (p<0.01)
NS
S (p<0.01)
S (p<0.01)
NS
Primed
Non primed
10^7 iu
10^6 iu
10^5 iu
10^4 iu
10^3 iu
10^2 iu
10^1 iu
Brain injected RAd 36 dose

Figure 33. Quantification of the stained area of the brain, detected by ED1 immunoreactive cells using a semi-automatic Quantimet imaging system. ED1 positive infiltration at the dose of 10^7 iu of RAd 36 without peripheral priming of the immune response was significantly higher than the rest of the doses. Doses below 10^6 iu of RAd 36 in the same paradigm had non significant differences. When priming in the periphery was done (blue bars), non-significant difference in the amount of ED1 positive cells infiltration was seen with doses of 10^3 iu and below of RAd 36 in the brain, and this levels of infiltration are the same ones detected without priming.

Figure 34

Phenotype of β-galactosidase immunoreactive cells seen after RAd 36 striatal injection, in animals with intra-dermal immunisation

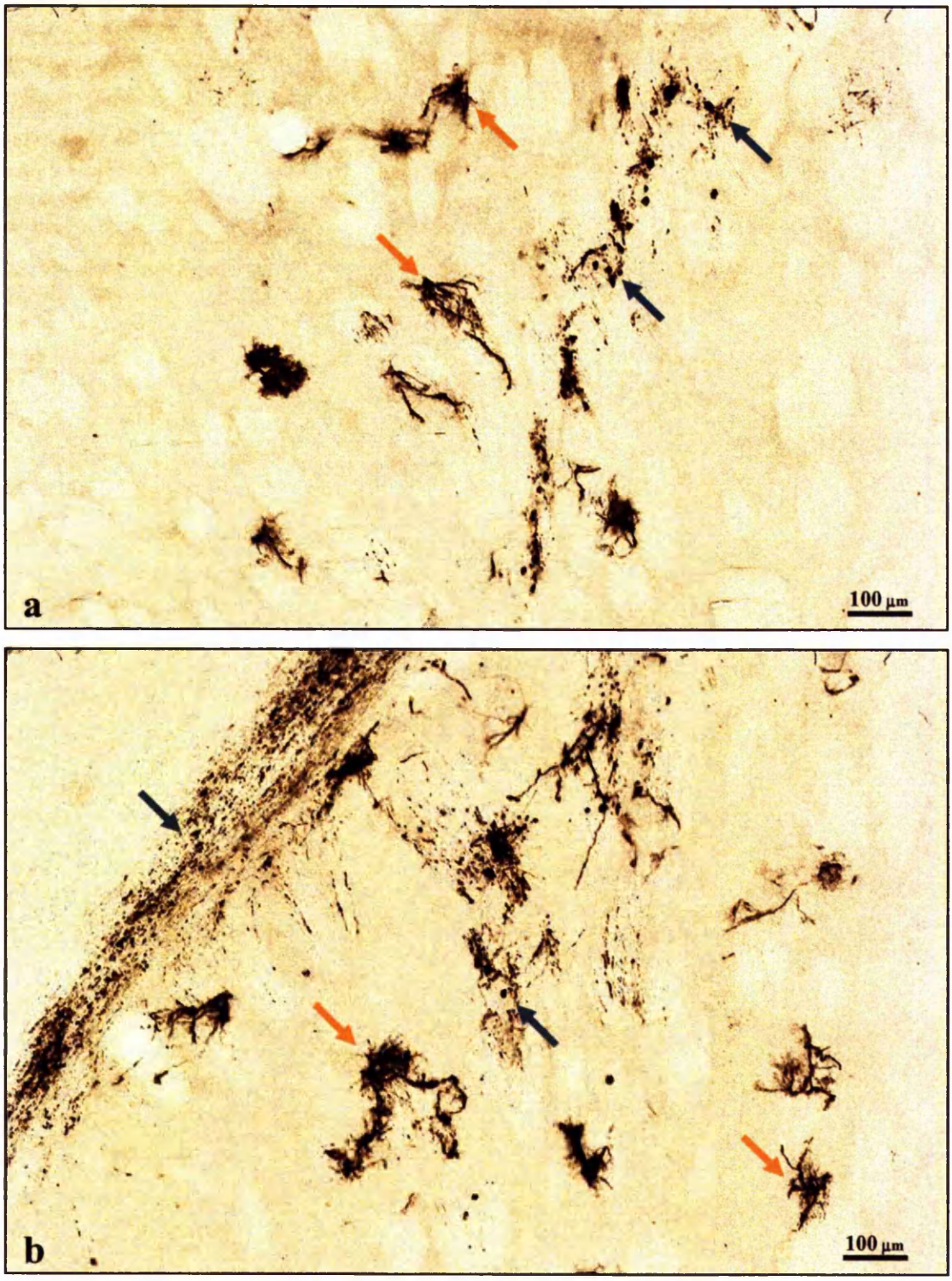

Figure 34. High magnifications of β-galactosidase stained brain sections, striataly injected with 10^5 iu (a) or 10^6 iu (b) of RAd 36. Animals were intra-dermally immunised 30 days after RAd 36 injection with RAd 0. Sixty days later animals were perfused, brains recovered and sectioned, and immuno-reactive β-galactosidase positive cells detected.

Note the unusual transduced brain cell phenotypes found (orange arrows) compared to the normal transduced glial cells (blue arrows).

4.2.3 Adenoviral dose thresholds for the activation of an adaptive immune response.

Doses of 10^7 infectious units of RAd 36 were injected into adult rat striata. Thirty days later, animals were rechallenged by injecting viral doses from 10^1 to 10^7 iu of RAd 0 (RAd with no transgene) intradermaly. One month later, brains were sectioned and the presence of immunoreactive ß-galactosidase enzyme (transduced cells), and ED1 cell markers (to measure innate immune response infiltration, i.e. macrophages) were assessed by immunohistochemistry (figure35).

The aim was to analyse the threshold of adenoviral dose required to activate an immune response. Activation of the immune response by intra-dermal immunisation should lead, as already seen (section 4.2.1), to a reduction of transgene expression in RAd 36 injected brains. Doses of 10^7 iu of RAd 36 were chosen to be injected in the rat striatum before priming, as that was the viral dose, used in previous experiments, that had complete elimination of the transgene expression, when the immune response was activated (figure 26b).

Priming doses of 10^7 iu and above of RAd 0 completely eliminated transgene expression of brains injected with RAd 36. These brains showed strong inflammation widespread throughout the entire ipsilateral striatum (Figure 36).

An intra-dermal injection of 10^6 iu of RAd 0 eliminated transgene expression from the brain in 66% of the animals (n=3) and 33% of them had unaltered transgene expression when compared to animals injected with same dose of RAd 36 in the

brain but without immune priming (Figure 36). This result may be due to the fact that the viral threshold for priming the adaptive specific immune response lies around 10^6 iu of RAd 0.

With an intra-dermal injection of 10^5 iu of RAd 0 or below, no transgene elimination from RAd 36 injected brains was seen (Figure 36), except in one animal that was primed with 10^2 iu of RAd 0. This animal had complete transgene elimination and, even though high levels of cellular infiltration was detected in the injected striatum and neutralising antibodies were found in the animal serum (table 2), the immune response activation was most probably triggered not by the intra-dermal immunisation but because of RAd 36 leaking from the brain striatum to non immuno-privilege areas.

The cellular infiltration detected in the brains injected with RAd 36 and intra-dermally immunised with RAd 0 doses below 10^5 iu, was confined to the needle track, with some extending to the corpus callosum (white matter), except in the one animal intra-dermally injected with 10^2 iu of RAd 0, that showed complete elimination of transgene expression, and strong cellular infiltration widespread throughout the ipsilateral striatum as in figure 36c, f and i.

When the existence of adenoviral neutralising antibodies was assessed in the animals that were primed with the different doses of RAd 0, a direct correlation was found between transgene expression elimination and the presence of adenoviral neutralising antibodies (Table 2). This result shows that when transgene expression is eliminated, an immune response against adenoviral vectors is triggered. No

neutralising antibodies were detected in animals that had normal transgene expression (table 2).

What dose of Adv injected intradermally is necessary to induce an anti-adenoviral immune response capable of eliminating Adv-mediated transgene expression in the brain?

Experimental Design:

Day 0:
RAd36 (mCMVp-βgal) at the Dose of 10^7 iu, injected into the striatum of adult rats.

Day 30:
RAd0 (no transgene), at doses from 10^1-10^8 iu, injected into the skin

Day 60:
Brains analysed for evidence of transgene expression (β–gal) and cellular inflammation (ED1 & CD8).

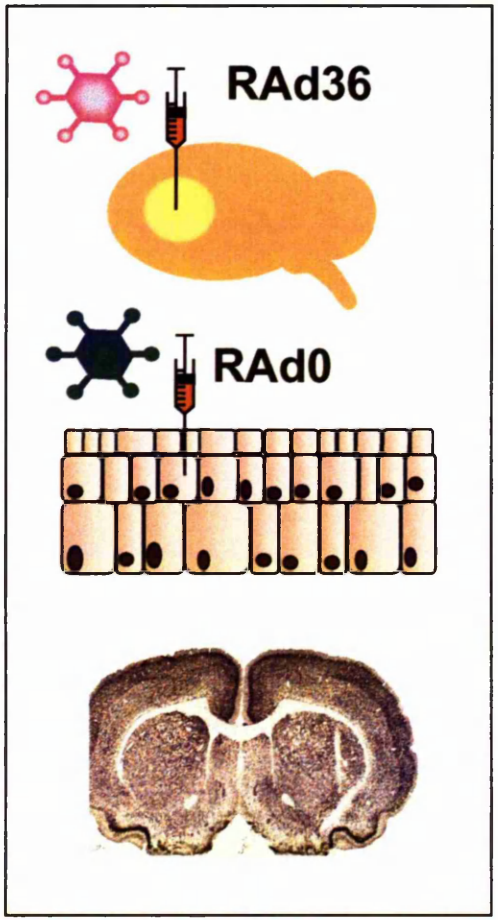

Figure 35. Experimental model designed to answer: What dose of adenovirus injected intra-dermally (RAd 0) is necessary to induce an anti-adenoviral immune response capable of eliminating adenoviral-mediated transgene expression (RAd 36) in the brain. For each RAd 0 dose tested (from 10^1 iu to 10^7 iu) an n=3 was used. All the animals were previously injected into the brain with the same dose of 10^7 iu of RAd 36, which was the dose of RAd 36 found to have complete elimination of the transgene when an anti-adenovirus immune response is triggered (section 4.2.1, figure 26).

Figure 36

Activation threshold of the immune response

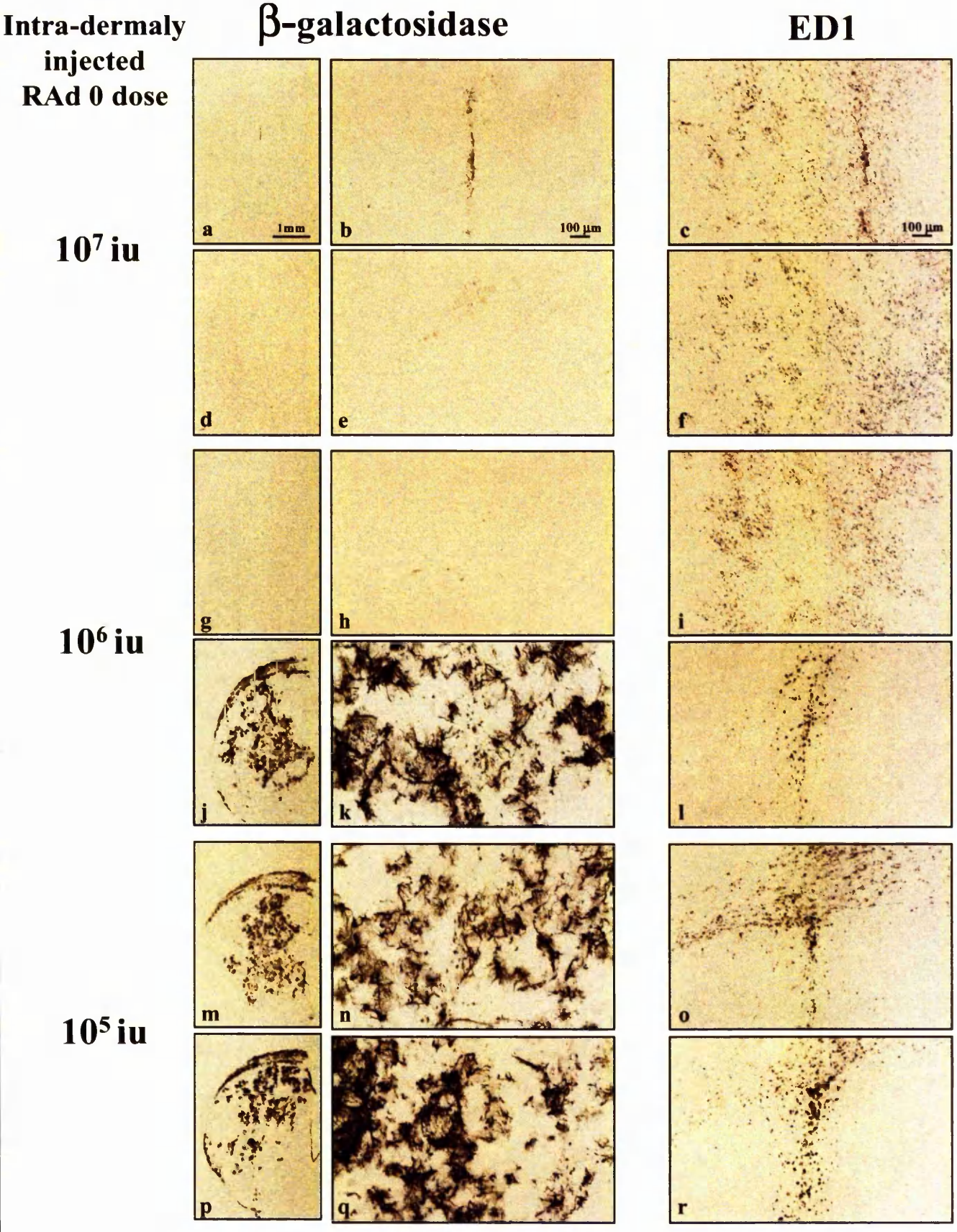

Figure 36. β-galactosidase and ED1 staining of the experiment in which rat brains were injected with 10^7 iu of RAd 36 with peripheral intra-dermal injection of RAd 0 doses, ranging from 10^8 iu to 10^1 iu. Only doses between 10^5 iu to 10^7 iu were illustrated. The figure shows the viral dose range threshold for the activation of an immune response, which is capable of eliminating β-galactosidase expression in the brain. In animals where transgene expression is eliminated there is a strong infiltration of ED1 positive cells within the injected brain parenchyma. When 10^5 iu of RAd 0 or lower where used for intra-dermal priming, the transgene expression remains unaltered and is quantitatively comparable to transgene expression observed in animals injected with 10^7 iu of RAd 36, without priming. At the RAd 0 dose of 10^6 iu 66% of the animals had normal β-galactosidase expression while 33% of them had immune response priming and transgene elimination. These results suggest that the intra-dermal viral dose threshold to prime an adaptive immune response lies around 10^6 iu of RAd 0.

Table 2

RAd 0 intra-dermal injection (IU)	Animal 1	Animal 2	Animal 3
10^7	1/64	1/32	1/64
10^6	1/32	-	-1/2
10^5	-	-	-
10^4	-	-	-
10^3	-	-	-
10^2	-	1/128	-
10^1	-	-	-
Saline+ priming with 10^8 RAd 0	1/32	1/32	1/64
Saline+no priming	-	-	-

Table 2. Table illustrating the detection of neutralising antibodies against adenovirus, from the serum of animals injected with different doses of RAd 0 intra-dermally. Only animals intra-dermally injected with RAd 0 doses of 10^7 iu and above and some animals injected with the dose of 10^6 iu, generated neutralising antibodies, in accordance with the elimination of β-galactosidase expression (figure 36). In all the animals where transgene expression was detected, the presence of adenoviral neutralising antibodies was inexistent, meaning that at this doses of virus it was not possible to trigger an adaptive immune response hence enabling long term β-galactosidase expression. Empty boxes represent non-detectable neutralisation. Neutralising antibody are reported as the dilution which results in a 50 % decrease in transgene transduction in HEK 293 cells with 10^6 iu of RAd 35 pre-incubated with animals serum when compared to the expression achieved with a non-blocked RAd 35 control.

4.3 Discussion

The adenoviral dose thresholds to elicit innate or adaptive immune responses and its effect in the long-term expression of delivered transgenes into the brain have never been elucidated before.

The brain, due to its immuno-privileged status, is unable to trigger an adaptive immune response unless the adaptive arm of the immune system is primed by injection of antigen outside of the CNS. Thus, the CNS provides a perfect environment to compare both arms of the immune response independently.

The new data obtained confirms the previous result that one single infectious viral particle is enough to direct the expression of sufficient transgene which is detected at 5 days post injection (figure 11), but which also persists for up to 3 month (figure 26 and 30). This demonstrates the unparalleled high efficiency of RAds when used in the brain.

When the innate immune response was studied, the early cellular inflammation detected five days after RAd injection into the brain in previous experiments is comparable to the cellular infiltration produced by RAd 36 detected 90 days after brain injection.

Doses of RAd 36 injected in the brain which avoided early inflammation (doses between 10^1 iu and 10^6 iu), achieved unaltered long-term expression (90 days after injection), when no immune response priming is triggered. This is true until doses of

10^7 iu of RAd 36, where the early inflammation was distinguishably higher comparing to lower viral doses (figures 20, 21, 28 & 33).

When a dose of 10^7 iu of RAd 36 is injected into the brain, a decrease in transgene expression is observed with time between 5 and 90 days post intra-striatal injection. As reported by Thomas et al 2001, this decrease of transgene expression between days 5 and 90 may be due to excessive viral dose. This viral overload produces direct cell cytotoxicity leading to reduced expression as the cells die. The strong early inflammation seen at this dose may be the result of cell death produced by the viral overload.

Following peripheral intra-dermal priming of the immune response, complete elimination of the transgene expression is only detected in the brain when 10^7 iu of RAd36 are injected (figures 26 and 30). With lower viral doses, complete transgene elimination was not seen. At these doses there was still transgene expression, but the levels of expression were reduced.

Another interesting observation was the peculiar phenotype seen in the brain cells infected with RAd 36 after priming in the periphery. Contrary to what normal brain cells looks like after infection with RAd 36, when an activated immune response is present, the cells appear to be damaged. This phenotype is most probably due to the attack of the immune response, which is damaging the infected cells maybe via perforin release. This destruction mainly appears to occur at the cell process level, because transgene expression within the cell processes is fragmented. This immune attack, seems not to kill the cell but produce the damaged phenotype.

Interestingly in a different set of experiments (Thomas et al, unpublished results) it was also shown, in brains injected with doses above 10^7 iu of RAds expressing β-galactosidase, that after intra-dermal immunisation with 10^8 iu of RAd 0, transgene expression was eliminated. Surprisingly, when the presence of transgene DNA was assessed by PCR, even though transgene expression was completely eliminated the transgene DNA was still present. This result might be used to support the hypothesis that in the brain, the transgene elimination does not occur due to cell killing by the immune response but because of the cytokine microenvironment triggered which results in the shut down of the transgene promoters. The promoters used for these experiments are of viral origin, and are therefore very sensitive to cytokine shutdown. The controversy of the mechanism involved in the decrease of transgene expression may be elucidated if the transgene to be detected is driven not by a viral promoter but by an endogenous promoter, which will not be shut down by cytokines. The challenge will then be to find a strong enough endogenous promoter to allow transgene detection. The most probable scenario might be that the transgene expression is eliminated by a combination of both cell killing and promoter shut down, the latter having a more relevant role.

An interesting result from this experiment and others, when using high doses of RAd 36 (10^7 iu) in the brain, was the potential triggering of an adaptive immune response in some animals, without peripheral immunisation. In these animals no transgene expression was detected, and analysis of the animals serum revealed presence of neutralising antibodies against adenovirus. One possible explanation for the priming of the immune response would be the damage of brain blood vessels during viral

injection and subsequent leakage of virus to the CNS periphery where the adaptive immune response can be triggered.

When the brain of these animals are analysed it can be seen that there is no leakage of virus into the contralateral ventricle (no β-galactosidase expression detected), and the injection site without a doubt is in the striatum, as demonstrated by the infiltration of ED1 and CD8 positive inflammatory cells along the needle track.

When different doses of RAd 0 were injected into the CNS periphery it was found that between viral doses of 10^5 to 10^7 iu, there is a viral threshold that can activate the adaptive immune response (Figure 36). When the immune response was activated (verified by the presence of adenoviral neutralising antibodies-table 2) there was complete elimination of transgene expression in animals injected with 10^7 iu of RAd 36 as expected. These animals showed strong cellular infiltration. The threshold for activation of an adaptive immune response lies around 10^6 iu of RAd 0, which is comparable to the dose of virus required to trigger an innate immune response in the brain (figure 20). This suggests, that the innate immune response may need to be triggered to generate an adaptive one. Nevertheless doses as little as 10^3 iu can be recognised in the brain by an activated immune response (figure 30) showing a highly sensitive threshold of recognition, but only after the adaptive immune response is already triggered.

The presence of neutralising antibodies to adenoviral vectors in the serum of immunised animals clearly correlates with diminished transgene expression in the brain. This is to be expected. Nevertheless Kajiwara et al. (2000) found after RAd

parenchymal injection, that even in the absence of peripheral priming against adenoviruses, antibodies were generated against the viral vector (not neutralising antibodies) and the transgene. In these cases the transgene expression is unaffected by the presence of the antibodies. This suggests that the immune response can identify the foreign antigens within the brain parenchyma but is unable to elicit a fully activated response, strong enough to eliminate transgene expression. Kajiwara et al identified a high influx of B cells into the RAd injection site in the brain. Some of the B cells might be up-taking the antigens within the brain and initially activating specific B cell clones. Hypothetically, antigens loaded into the brain parenchyma can not be presented by professional APC, because of the inexistence of normal DC within this area that can mature and present antigens in a co-stimulatory way. If this is true B cells already primed by its first activation event, because of the encounter with their specific antigens, will not have the second activation signal (which ultimately needs antigen presentation via mature DC) which is needed to enable B cell clonal expansion, IgG antibody class switching and germinal centre production (see section 1.3). This would explain why antibodies against RAds are found but without the high avidity required to effectively block adenoviral infection.

This data taken together suggests that, even in the absence of early brain inflammation after RAd parenchymal injection, peripheral activation of the immune response may occur, leading to the elimination of transgene expression. Vectors such as the new helper dependant adenovirus which were shown to evade an activated adaptive immune response (Thomas et al, 2000) will need to be used in

long-term neurological gene therapy in order to assure long-term transgene expression even in the presence of a systemic immunisation against adenoviruses.

Chapter 5: Permanent acceptance of rat cardiac allografts after first generation adenovirus-mediated gene transfer of CD40 Ig under the control of the mCMV promoter.

5.1 Introduction

As discussed earlier, it has been previously demonstrated (section 1.3) that CD40-CD40L interaction is the main B cell activation signal. This was clearly demonstrated in CD40L knockout mice, which failed to form germinal centres, B cell clonal expansion and IgG class switching (Dissanto et al, 1993). The blockade of the CD40-CD40L interaction, not only impedes B cell priming, but also prevents the B7 family upregulation on APC (Inaba et al, 1994). If the B7 family of receptors are not upregulated on the APC, this will affect the CD28-B7 T cell activation signal, leading also to an inhibition or decrease of the cytotoxic immune response (Lu et al, 1997).
In addition, it has been shown that the blockade of the CD40-CD40L interaction inhibits the induction of IL-12, decreasing the TH1 response, by hampering the IL-2 and interferon γ secretion, leading to a TH2 response deviation (Tang et al, 1997).

Consistent with this information, if blockade of the CD40-CD40L interaction can be efficiently achieved by the CD40Ig RAd, a TH2 immune deviation could be obtained, decreasing the cytotoxic immune response. But at the same time B cells activation will be inhibited, by impeding the B cell co-stimulation signal with the same CD40-CD40L interaction blockade, leading to a humoral response inhibition.

In conclusion, blocking the CD40-CD40L interaction by a soluble form of CD40, CD40Ig could lead to an inhibition or decrease of both the humoral and cytotoxic responses of the acquired immune response.

To test this hypothesis RAds encoding for CD40 Ig were generated under the control of the hCMV (RAd h40) or the mCMV (RAd m40) promoters. The RAd m40 was sent to be tested in a rat heart transplant model by collaborators (Ignacio Anegon group, Institut National de la Sante et de la Recherche Medicale, U437, Nantes, France). Using RAd m40, they tried to achieve long term allograph transplantation by blockade of the immune response. In the same model, an antibody specific for CD40L was used to block the CD40-CD40L interaction. The results were compared with those obtained from the RAd m40 experiments in order to test our hypothesis that RAd m40 works more efficiently than the anti-CD40L antibody. We expect that to happen, as the RAd m40 infected cells, contrary to the antibody applications, will continue to release CD40Ig in a local and sustained manner. In this chapter we described the generation of the viruses encoding for CD40 Ig, and very briefly, in order to show the efficacy of the generated RAds, we show Anegon's group results.

5.2 Results

5.2.1 Construction of an intermediate vector containing the CD40Ig in the pSP72 intermediate plasmid.

In order to test the hypothesis of immune response inhibition by blockade of the CD40-CD40L interaction, recombinant adenoviral vectors carrying a gene that expresses a soluble form of CD40, the chimeric protein CD40 Ig, were constructed under two different promoters, the hCMV promoter (RAd h40) and the mCMV promoter (RAd m40).

To generate the CD40 Ig recombinant adenoviruses, a ~2.1 Kpn I-BamHI fragment containing the extracytoplasmic domain of the CD40 receptor cDNA chimeric with the IgG1 Fc domain cDNA of a human antibody (provided by Dr Peter Lane, Basel Institute for Immunology, Basel, Switzerland), was cloned into a Kpn I-BamHI digested pSP72 (intermediate vector) to generate pSP72-CD40Ig. This was in order to incorporate Bgl II sites on either side of the CD40Ig fragment. This restriction enzyme site adaption was needed for the next step of the CD40 Ig RAds constructions (section 5.2.2 & 5.2.3)

Successful cloning was determined by the release of the insert with BamHI-KpnI digestion, resulting in 2 bands: ~2.1 kb (CD40Ig) and ~2.5 kb (pSP72). Further verification was accomplished by Bgl II-Hind III digestion, which released the three

Figure 37

Generation of pSP72-CD40Ig

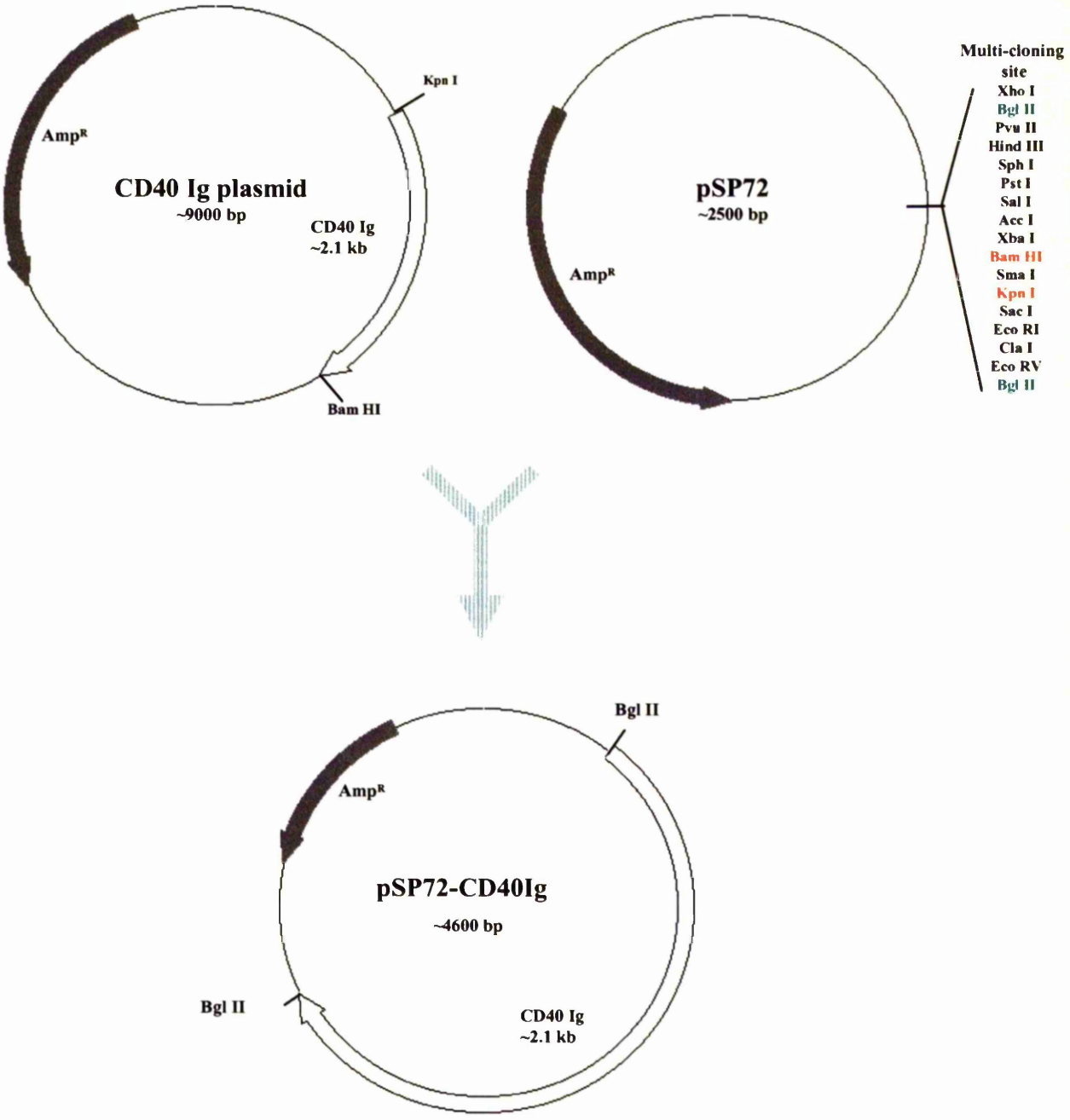

Figure 37. Generation of pSP72-CD40Ig. In order to add Bgl II sites at both ends of the CD40Ig gene, a Kpn I-Bam HI fragment including the complete CD40Ig (~2.1 kb) was cloned into a Kpn I-Bam HI digested pSP72, generating the pSP72-CD40Ig. From the resulting plasmid, CD40Ig can be cut out now with Bgl II.

bands expected: ~2.5 Kb (the pSP72 backbone), ~1.6 Kb (the Ig fragment), and ~0.7 Kb (the CD40). No special orientation was needed.

5.2.2 Construction of a shuttle vector containing the CD40Ig under the control of the hCMV promoter (pAL119-CD40Ig)

In order to produce an E1/E3 deleted first generation adenoviral vector (section 1.2.2.3.2), with CD40Ig as the transgene and hCMVp as its promoter, CD40Ig was cloned in the shuttle vector pAL119 (section 3.2.1, figure 4a).

The ~2.1 Kb CD40Ig was excised from the pSP72 with Bgl II, and this fragment was cloned into a BamHI digested pAL119 (compatible enzymes). Insertion and right orientation was checked with Xba I digestion which released the correct 3 bands: ~2.6 Kb (the hCMVp and the CD40Ig), ~0.25 Kb (the poly A), and ~6.15 Kb (the plasmid backbone); and EcoRI digestion, which would give 3 bands: ~0.86 Kb (hCMV plus part of the plasmid), ~0.15 Kb (part of the CD40) and ~7.95 Kb (pAL119 backbone+polyA+Ig +part of the CD40).

Figure 38

Generation of pAL119-CD40Ig

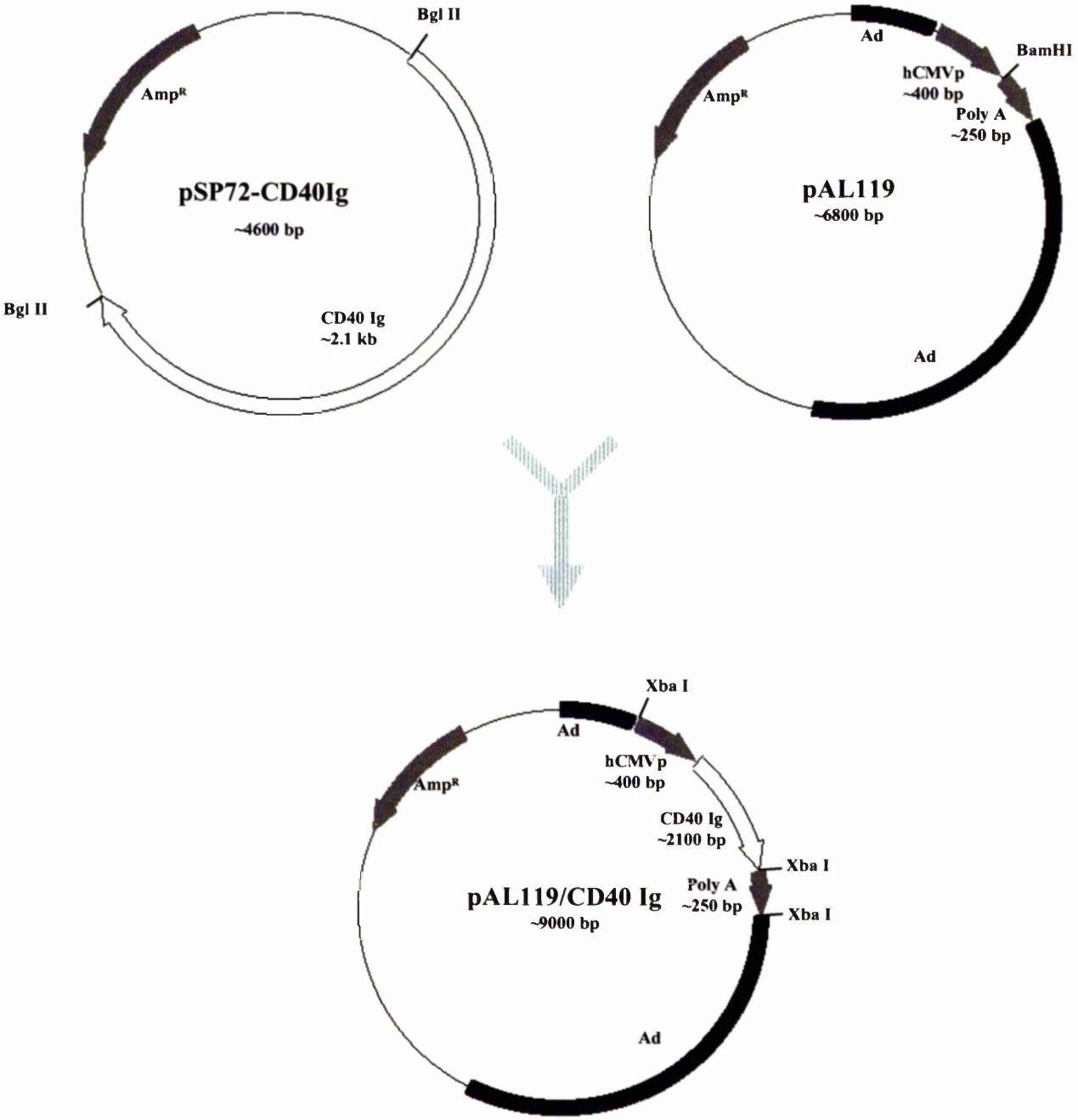

Figure 38. Generation of pAL119-CD40Ig. In order to produce a shuttle vector to construct a RAd encoding for CD40Ig under the control of the hCMV promoter, a Bgl II fragment of pSP72-CD40Ig containing the CD40Ig was cloned into a Bam HI digested pAL119 (Bgl II and Bam HI are compatible enzymes for ligation). The resulting plasmid, pAL119-CD40Ig will be used to generate RAd h40.

5.2.3 Construction of a shuttle vector containing the CD40Ig under the control of the mCMV promoter (pAL120-CD40Ig).

In order to produce an E1/E3 deleted first generation adenoviral vector (section 1.2.2.3.2), with CD40Ig as the transgene and mCMVp as its promoter, CD40Ig was cloned into the shuttle vector pAL120 (section 3.2.1, figure 4b).

An EcoR V-Sal I CD40Ig fragment was excised from the pSP72-CD40Ig plasmid, blunt ended and cloned into a pAL120 Sal I digested and blunt ended. Right orientation was verified by: 1) EcoRI which would give 4 bands: ~8.0 Kb (pAL120 backbone+CD40Ig+polyA), ~0,20 Kb (part of the CD40), ~1.4 Kb (mCMV promoter), ~0.5 Kb (part of the pAL120).2) Xba I, which should give 4 bands: ~6.45 Kb (pAL120 backbone), ~1.4 Kb (mCMVp), ~2.1 Kb (CD40Ig) and ~0.15 Kb (polyA).

5.2.4 Construction of a recombinant adenoviral vector (RAd) containing the CD40Ig under the control of the hCMV promoter (RAd h40)

The pAL119-CD40Ig shuttle vector was cotransfected into HEK 293 cells with pJM17. After viral cytopathic effect was confirmed, viral DNA was extracted and checked by restriction enzyme digestion with Hind III and Southernblot (hybridised with a Hind III-Xba I CD40Ig probe) for successful recombination. Hind III should release the Ig fragment (~1.4 Kb), and the CD40+hCMVp (~1.1 Kb) (this band overlaps with a virus band of ~1.1 Kb increasing the band intensity). The DNA probe hybridised as expected with the ~1.4 band of the gel.

Figure 39

Generation of pAL120-CD40Ig

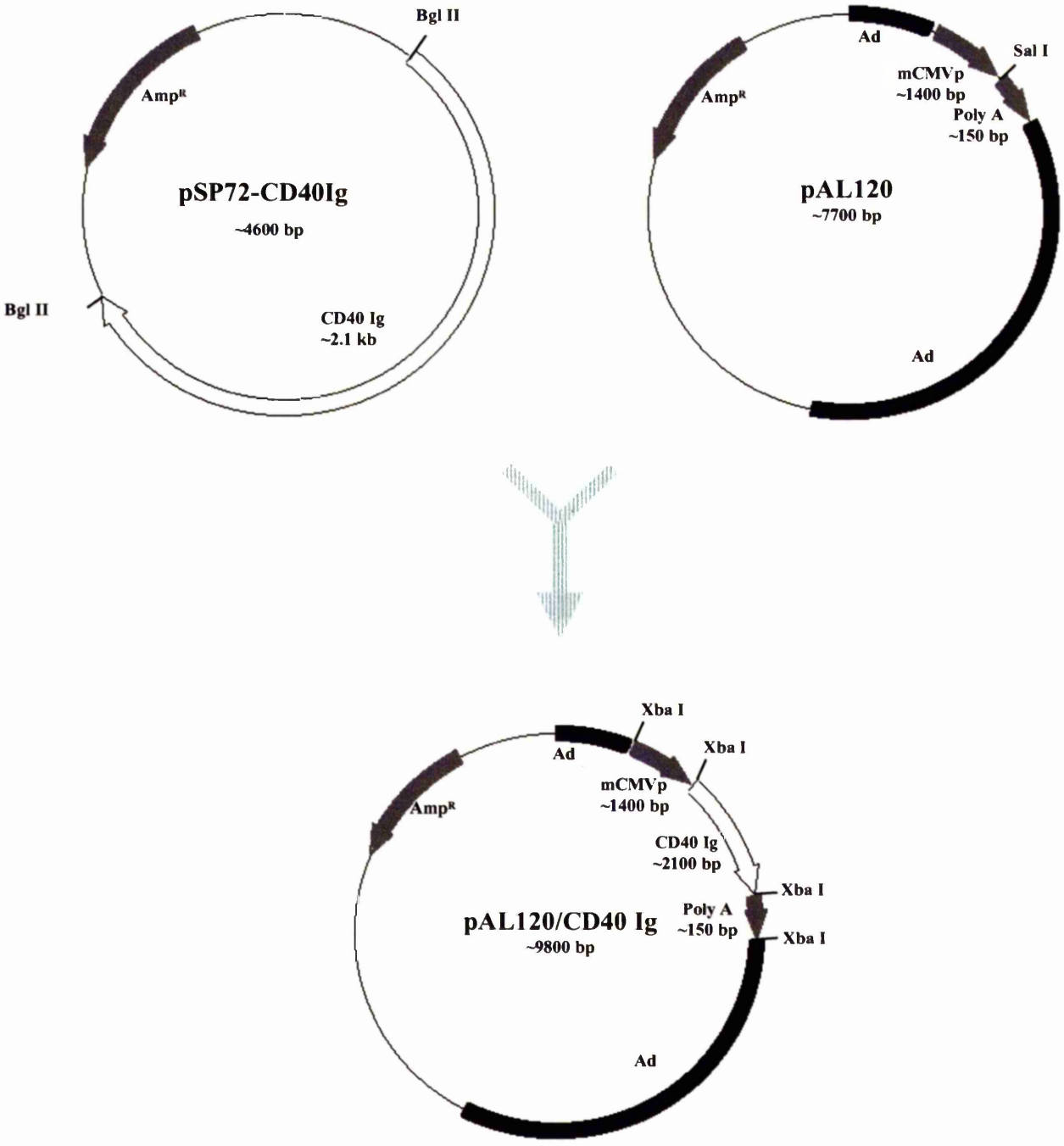

Figure 39. Generation of pAL120-CD40Ig. In order to produce a shuttle vector to construct a RAd encoding for CD40Ig under the control of the mCMV promoter, a Bgl II fragment of pSP72-CD40Ig containing the CD40Ig was blunt ended and cloned into a Sal I digested and blunt ended pAL120. The resulting plasmid, pAL120-CD40Ig will be used to generate RAd m40.

Following viral confirmation, the virus was purified by 3 rounds of plaque purification, and RAd h40 identity reconfirmed by viral DNA digestion and Southern blot hybridisation (figure 40).

5.2.5 Construction of a RAd containing the CD40lg under the control of an mCMV promoter (RAd m40)

The pAL120-CD40lg (section 5.2.3) shuttle vector was cotransfected with the pJM17 into HEK 293 cells. Viral cytopathic effect was confirmed, and viral DNA extracted.

The viral DNA was digested with Hind III, and identified by southern blot, with the same probe used for the hCMV-CD40lg RAd. The Hind III digestion confirmed the released of a ~1.6 Kb band (The Ig fragment plus the poly A) and a ~2.1 Kb band (containing the CD40 plus the mCMVp) overlapped with a viral band of ~2.1 Kb (given an increased intensity of the band). The DNA probe hybridised with the ~1.6 Kb band as expected.

Following viral confirmation, the virus was purified by 3 rounds of plaque purification, and RAd m40 identity reconfirmed by viral DNA digestion and Southern blot hybridisation.(figure 41).

5.2.6 RAd h40 & RAd m40 transgene expression in vitro

Hela cells were infected at MOI of 50, with both RAd h40 and RAd m40. Fourty eight hours after infection, positive CD40 Ig expression was detected by immunocytochemistry of the infected cells with FITC conjugated antibody against the human Ig domain. Both viruses positively stained for CD40Ig expression within the cells. Interestingly it was found positive staining within the endoplasmic reticulum, suggesting that the CD40 Ig as expected is being exported outside the cell. (Figures 40c & 41c).

5.2.7 Blocking of CD40-CD40L interactions by adenovirus mediated expression of CD40 Ig results in permanent allograft acceptance in rats.

The results of the following experiments were done by our collaborators (Ignacio Anegon group, Institut national de la sante et de la recherche medicale, U437, Nantes, France) and are briefly described here. They were carried out to test the therapeutic efficacy, in rats, of our constructed RAd m40 in an allograft transplantation model (Mathieu et al, 2001a; Mathieu et al, 2001b).

The experiments were added to this thesis in order to show the first successful therapeutic approach with an animal model, using our virus, RAd m40, to test our hypothesis of immune response tolerance (section 5.1) with a therapeutic transgene (CD40 Ig) under the control of the mCMV promoter.

The ability of RAd h40 (section 5.2.4) to induce CD40-CD40L blockade was not tested, because of the results described in section 3. *In vitro* and *in vivo* analysis showed the high difference of the transgene expression driven by the mCMVp when compared to the hCMVp (section 3). As the aim of the RAd encoding for CD40Ig is to block the CD40-CD40L interaction by its secretion and binding competition to the membrane bound CD40, higher doses of secreted CD40Ig should have a better chance of achieving the desired effect. Therefore the RAd encoding for CD40Ig under the control of the stronger mCMVp was chosen.

Lewis 1W [$RT1^u$] rats were used as heart donors and Lewis1A [$RT1^a$] as recipients. RAd m40 coding for the extra-cellular portion of mouse CD40 fused to Fc portion of a human IgG, was delivered at a dose of $5x10^{10}$ iu at the time of transplantation either into rat donor hearts by intra-myocardial or intra-portal injection. As control, a non-coding recombinant adenovirus (RAd I324) was used. Another group was intra-peritoneally injected at days 0, 3 and 6 from transplantation with 12 mg/ kg of an antibody anti-CD40L.

CD40Ig gene transfer into the myocardium allowed indefinite graft survival (> 100 days) in 83 % of cases (n=6). Intra-portal injection of RAd m40 allowed indefinite allograft survival (n=3). Hearts non-transduced or transduced with RAd I324 were rejected in 11±0.6 (n=11) and 8.5±0.7 (n=9) days, respectively. Animals treated with antibodies against CD40L had similar heart rejection to that observed in the control animals without any significant survival improvement (figure 42).

Figure 40

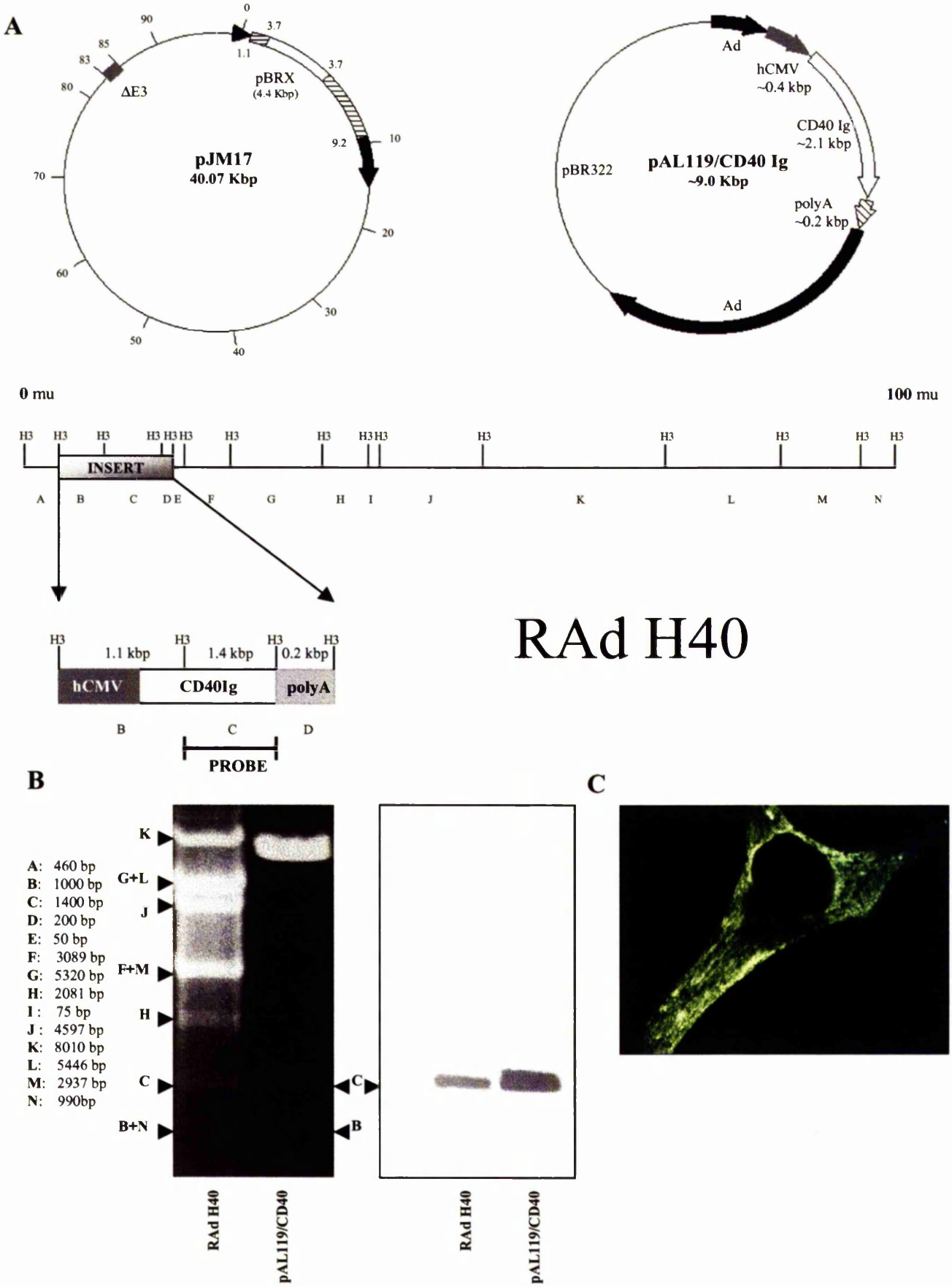
A
pJM17
40.07 Kbp
pBRX
(4.4 Kbp)
ΔE3
pAL119/CD40 Ig
~9.0 Kbp
pBR322
Ad
hCMV
~0.4 kbp
CD40 Ig
~2.1 kbp
polyA
~0.2 kbp
0 mu
100 mu
INSERT
RAd H40
1.1 kbp
1.4 kbp
0.2 kbp
hCMV
CD40Ig
polyA
PROBE
B
A: 460 bp
B: 1000 bp
C: 1400 bp
D: 200 bp
E: 50 bp
F: 3089 bp
G: 5320 bp
H: 2081 bp
I: 75 bp
J: 4597 bp
K: 8010 bp
L: 5446 bp
M: 2937 bp
N: 990bp
K
G+L
J
F+M
H
C
B+N
RAd H40
pAL119/CD40
C
RAd H40
pAL119/CD40

Figure 40.

a. Generation of RAd H40 was carried out by cotransfection of pJM17 and pAL119/ CD40 in 293 cells.

b. Identification of RAd H40 was checked by restriction enzyme digestion of viral extracted DNA and posterior southernblot analysis using a Hind III fragment of the CD40 Ig as the DNA probe.

c. Verification of transgene expression of RAd H40 (CD40Ig) was checked by immunocytochemestry. Hela cells were infected with RAd H40 and expression of CD40Ig detected with FITC conjugated antibodys against human IgG. Positive detection was seen as strong fluorescent green Hela cells.

Figure 41

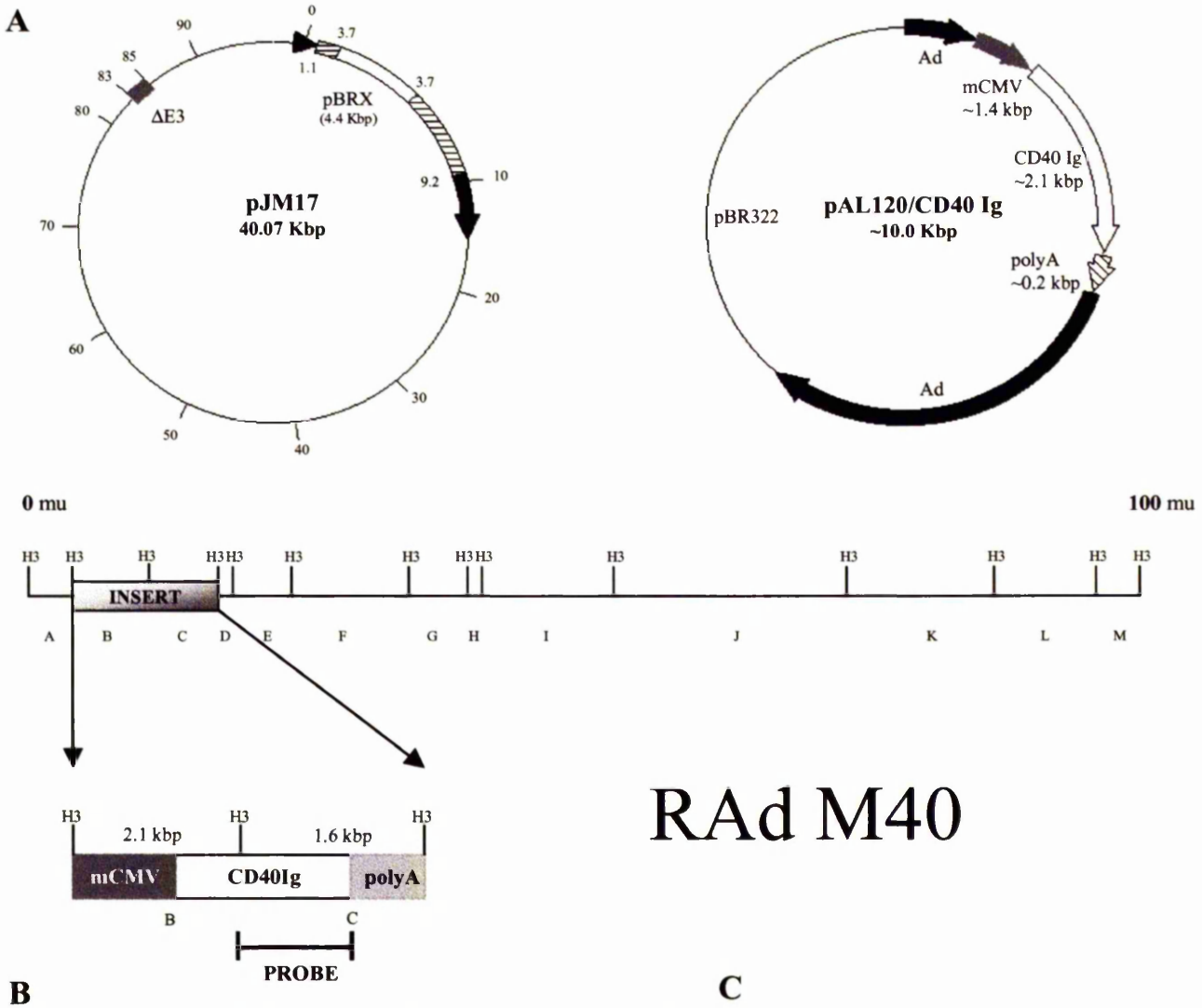
A
pJM17
40.07 Kbp
ΔE3
pBRX
(4.4 Kbp)
pAL120/CD40 Ig
~10.0 Kbp
pBR322
Ad
mCMV
~1.4 kbp
CD40 Ig
~2.1 kbp
polyA
~0.2 kbp
0 mu
100 mu
INSERT
2.1 kbp
1.6 kbp
mCMV
CD40Ig
polyA
PROBE
RAd M40

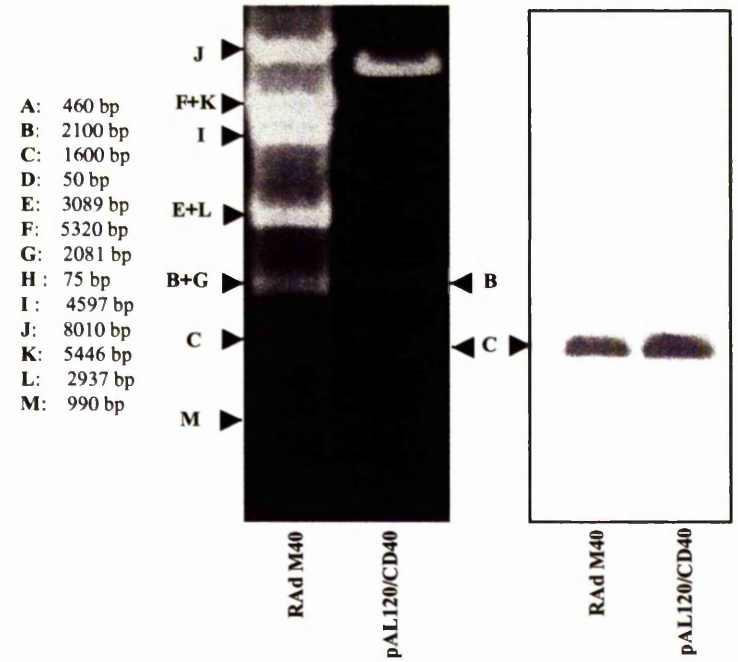
B
A: 460 bp
B: 2100 bp
C: 1600 bp
D: 50 bp
E: 3089 bp
F: 5320 bp
G: 2081 bp
H: 75 bp
I: 4597 bp
J: 8010 bp
K: 5446 bp
L: 2937 bp
M: 990 bp
J
F+K
I
E+L
B+G
C
M
B
C
RAd M40
pAL120/CD40
RAd M40
pAL120/CD40

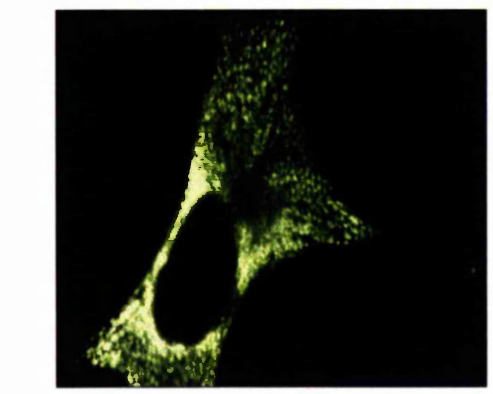
C

Figure 41. a. Generation of RAd M40 was carried out by cotransfection of pJM17 and pAL120/ CD40 in 293 cells.

b. Identification of RAd M40 was checked by restriction enzyme digestion of viral extracted DNA and posterior southernblot analysis using a Hind III fragment of the CD40 Ig as the DNA probe.

c. Verification of transgene expression of RAd M40 (CD40Ig) was checked by immunocytochemestry. Hela cells were infected with RAd M40 and expression of CD40Ig detected with FITC conjugated antibodys against human IgG. Positive detection was seen as strong fluorescent green Hela cells.

CD40Ig was detected in serum of RAd m40 treated animals by an ELISA using two different anti-human IgG antibodies. CD40Ig levels in the serum were between 147 and 229 μg/ml at day 5 after gene transfer into the graft. Levels declined thereafter but CD40Ig levels were still detected between 8 and 12 μg/ml 6 months after gene transfer.

Immunohistologic analysis was performed on day 5 after transplantation. Immunostaining for CD40Ig was intense in the graft, spleen and liver and barely detectable in lymph nodes. Total leukocytes, leukocyte subpopulations and expression of activation markers (MHC class II, CD25, IFNγ) within the grafts were comparable in RAd m40 and RAd l324-treated grafts.

Five days after gene transfer, MLR responses of total splenocytes from rats treated with RAd m40 against donor dendritic cells were inhibited in 6 out of 6 recipients (86.3±21.6 % of inhibition, $p<0.05$) compared to those of RAd l324-treated controls. Inhibition of proliferation in these splenocytes MLRs was not reversed by the addition of IL-2. Proliferation of T cells isolated from splenocytes against donor dendritic cells was partially inhibited (24 and 26 %) in 2 out of 5 cases.

Serum levels of IgM and IgG alloantibodies were analyzed by cytofluorimetry on donor splenocytes at day 10 and 17, respectively. IgM alloantibody levels were reduced, whereas IgG alloantibodies were absent in recipients of RAd m40-treated hearts.

Recipients were immunized with SRBC at transplantation and anti-SRBC antibodies were analyzed at day 17. Recipients of long-term surviving grafts (> day 80) were immunized into the footpad with KLH and anti-KLH antibodies were evaluated 10 days later. Statistical significance was evaluated using a one-way analysis of variance test and Kaplan-Meier analysis of graft survival.

Immune responses against cognate antigens did not show a major inhibition in recipients of RAd m40-treated grafts since levels of anti-SRBC antibodies were moderately reduced (50%) and those anti-KLH were identical compared to those of controls at day 17 and 100 after gene transfer, respectively. Recipients with long-term surviving cardiac grafts accepted donor-matched second heart grafts (> 150 days, n=2) and rejected third-party hearts (rejection at day 11 and 12, n=2).

In recipients of accepted grafts, MLR responses of total splenocytes against donor dendritic cells were inhibited in all cases (91.3±12 % of inhibition, n=7, $p<0.05$) and against third-party cells in 6 out of 7 cases (56.3±14 % of inhibition, $p<0.05$) compared to those of controls. Proliferation of T cells purified from these splenocytes against donor or third party dendritic cells was inhibited in all cases (36.3±14 % of inhibition, n=7, and 26.1±12 % of inhibition, n=7, respectively, $p<0.05$).

Long-term surviving grafts (> 100 days) showed clear signs of chronic allograft rejection since over 50 % of medium-size arteries displayed from moderate to severe intimal thickening.

Figure 42

Heart allograft survival after adenovirus-mediated expression of CD40Ig

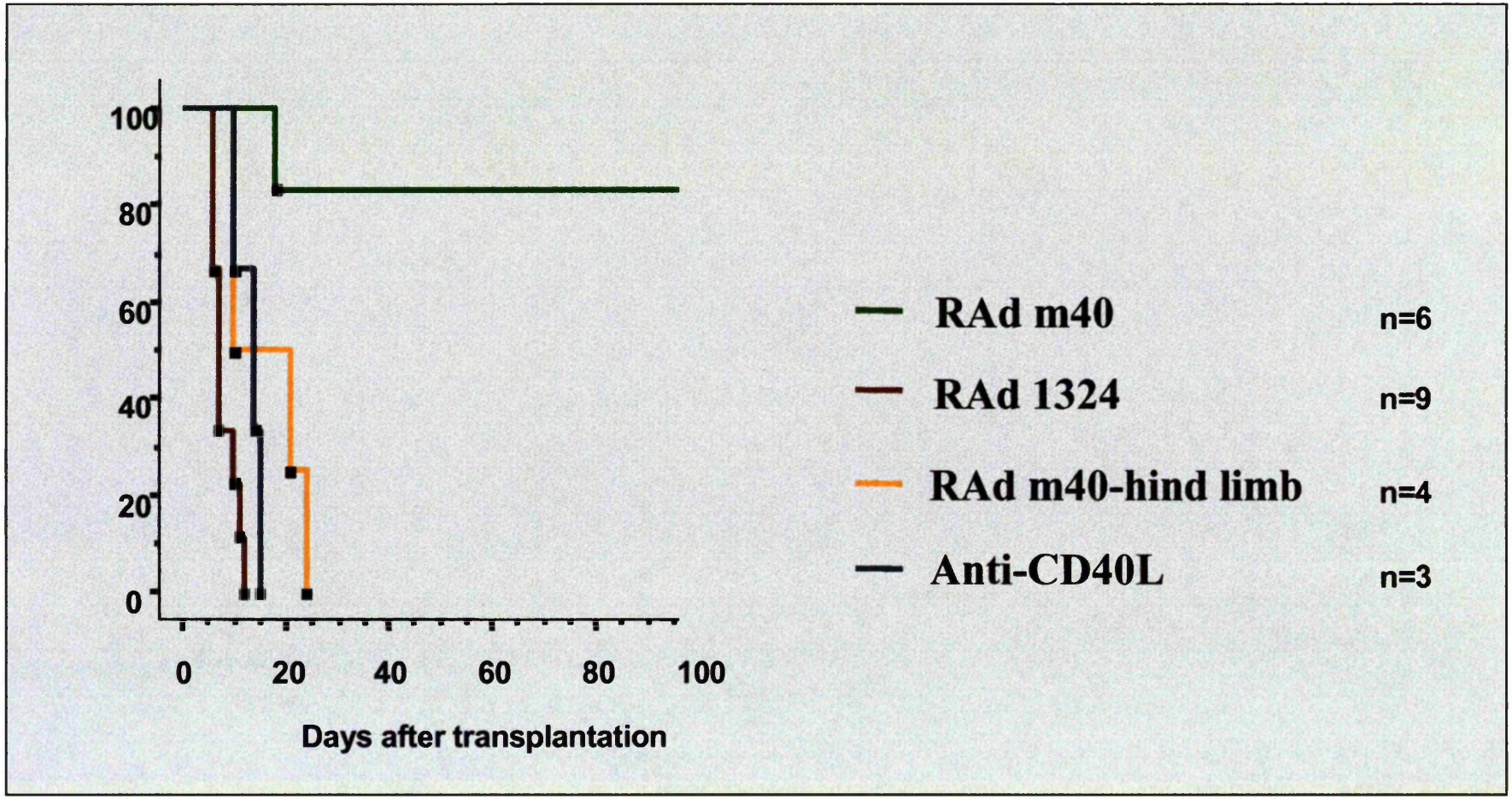

Figure 42. Graphic representation of hearts allograft survival. Lewis 1W [$RT1^u$] rats were used as heart donors and Lewis1A [$RT1^a$] as recipients. For different treatments groups of transplanted animals are represented: 1. animals treated with RAd m40 coding for the extra-cellular portion of mouse CD40 fused to Fc portion of a human IgG, delivered at a dose of $5x10^{10}$ iu at the time of transplantation into rat donor hearts by intra-myocardial injection; 2. animals treated with RAd 1324 (Rad with no transgene) at a dose of $5x10^{10}$ iu at the time of transplantation into rat donor hearts by intra-myocardial injection; 3. animals treated with RAd m40, delivered at a dose of $5x10^{10}$ iu at the time of transplantation into the left hind-limb; 4. animals injected at days 0, 3 and 6 from transplantation with 12 mg/ kg of an antibody anti-CD40L. Number of animals for each group are shown.

5.3 *Discussion*

Expression of CD40Ig from RAd m40 *in vivo* was high and long lasting after adenovirus-mediated gene transfer as detected in the serum of RAd m40 treated animals. In animals treated with RAd m40 inhibition of alloantibody production and of helper responses in vitro (MLRs) was observed, contrary to the results obtained in transplanted animals treated with RAd 1324. This suggests that expression of CD40Ig is impairing the immune response against the allograft, generating donor-specific tolerance mechanisms as seen by the acceptance of donor-derived and rejection of third-party-derived second cardiac grafts.

Complete IgG antibody absence in RAd m40 treated animals, supports the theory that secretion of CD40Ig is blocking CD40-CD40L interaction therefore inhibiting IgG isotype switching. Immune responses observed against cognate antigens (SRBC & KLH) were not substantially inhibited by CD40Ig expression even though protection from allograft rejection was achieved. This suggests that expression of CD40Ig from a RAd inhibits immune responses in a local manner, sparing non-local immune activation.

An important result is the observation of insufficient CD40-CD40L blockade when using an antibody against CD40L, resulting in allograft rejection within the same time frame than in non-treated and RAd 1324 treated animals. This shows that CD40 Ig being released in a localized continuous manner is more efficient than anti-CD40L antibody applications to effectively block co-stimulation and achieve immune

tolerance to the desired alloantigens. Importantly, this result greatly reinforces gene therapy strategies.

Nevertheless, not all alloantigenic immune responses were efficiently inhibited since early graft leukocyte infiltration was not modified and chronic rejection developed in long surviving grafts. This may be due to the fact that, even though a CD40-CD40L blockade exists (inhibiting formation of germinal centres, B cell clonal expansion and IgG class switching), IgM antibody generation will be unaffected. CD40-CD40L blockade will also affect CD4 T cells helper function, although direct cytotoxicity mediated by CD8 T cells may still be present. The immune response not affected by the CD40-CD40L blockade is not strong enough to produce acute allograft rejection, but still produces a chronic damage.

Chapter 6: The Next Step

After showing the high transduction efficiency, achieved with adenoviral vectors in the rat brain together with the unparallel strength of the mCMV promoters especially in glial cells (see figure 13), the next step will be to treat a rat glioma tumour model, which seems to be the perfect target for our improved adenoviral vector .

The strategy will be to generate first generation adenoviral vectors, and gutless vectors, encoding for antiangiogenic factors, angiostatin and endostatin, under the control of the mCMV promoter to treat a CNS 1 rat glioma model.

Solid tumors rely on angiogenesis (neo-vascularisation) for growth and survival beyond a certain size (~2 mm^3). If these vessels are unable to emerge, tumour growth will be inhibited. Antiangiogenic factors such as angiostatin (O'Reilly et al, 1996) and endostatin (O'Reilly et al, 1997) potently inhibit the growth of primary carcinomas in mice, completely inhibiting tumour growth, achieving regression without detectable toxicity or resistance. The carcinomas regress to microscopic dormant foci in which tumour cell proliferation was balanced by apoptosis in the presence of blocked angiogenesis. The great advantage of this cancer treatment is its lack of specificity, attacking any tumour that requires angiogenesis for survival. This means that it will attack not only the primary tumour but also tumour metastasis, which no single therapy, to date, has been able to deal with, without generalised cytotoxicity. Another advantage is that the target vessels that are inhibited by these antiangiogenic factors are specific for tumour vascularisation, without affecting any other physiologically normal neo-vascularisation, which occurs during processes such as wound healing or the female oestrus cycle.

The successful antiangiogenic treatments, so far, were achieved by direct injection of the purified proteins in high concentrations. Purification of angiostatin and endostatin are cost-ineffective for clinical application at the high concentrations needed. Gene therapy enables antiangiogenic genes to be delivered directly to the host cells where the therapeutic protein is going to be produced. It will then be a question of achieving the high levels of expression necessary to have the desired therapeutic effect. So far several laboratories have tried to exploit this strategy, mainly using first generation adenoviral vectors. The best result obtained though was tumour inhibition without regression even with microscopic tumors (Kuo et al 2001). We found that the strategy used by these labs had several main drawbacks, which we think we can solve:

1) Transgene expression was transient, as the first generation adenoviral vector used was systemically delivered, being rapidly cleared by the immune response in the short term. We aim to treat tumours in the brain, where it can be expected longer transgene expression because of its immuno-privilege status. Also we are aiming to use the new generation of gutless adenoviral vectors (Umana et al, 2001) to deliver the antiangiogenic transgenes. It has been demonstrated that gutless adenoviral vectors avoid recognition by an activated immune response (Thomas et al 2000);

2) The stronger promoter used in all previous experiments was the hCMVp. Now we will use the mCMVp, which we showed to be between 2 to 3 logs stronger than the hCMV promoter in rat glial cells (Gerdes et al, 2000), which will be the target cells of our future therapy;

3) Finally the angiostatin and endostatin used in previous experiments are human in origin. The codified proteins we will deliver, are rat in origin. In theory, we expect that these proteins will have better activity in a rat model than the human ones.

So far, in collaboration with Pablo Umana, we have generated a first generation recombinant adenoviral vector encoding rat angiostatin under the control of the mCMVp. This virus is currently in the process of being scaled up. We have also rescued various candidates for recombinant adenovirus encoding rat endostatin under the control of the mCMVp, after cotransfection in 293 cells. These potential RAds are presently in the process of identification. Shuttle vectors for the future generation of RAds encoding for human angiostatin and endostatin under the control of the mCMVp have also been constructed.

The ultimate aim, will be to use the antiangiogenic RAd therapy in human patients. We have, therefore, started to produce in parallel RAds with the human versions of angiostatin and endostatin. The gutless viruses, however, will be constructed after the initial results from the first generation recombinant adenoviruses have been obtained. We are in the process of testing the strength of the mCMV promoter (with RAd 36) *in vivo* in monkeys in order to compare it to the hCMV promoter (RAd 35). We expect that the mCMVp will be stronger than the hCMVp reflecting our *in vitro* results with monkey Cos 7 cells (figure 14).

Chapter 7: References

Abercrombie M (1946). Estimation of nuclear populations from microtome sections. *Anat. Rec.* 94:23-29.

Abremski K and Hoess R (1984). Bacteriophage P1 site-specific recombination. Purification and properties of the Cre recombinase protein. *J.Biol. Chem.* 259: 1509-1514.

Addison CL, Hitt M, Kunsken D &. Graham FL (1997). Comparison of the human versus murine cytomegalovirus immediate early gene promoters for transgene expression by adenoviral vectors. *J Gen Virol.* 78:1653-1658.

Ali S, Castro MG and Lowenstein PR (2001). Combined cytotoxic and immune stimulatory adenovlral mediated gene transfer in prolonging the survival of animals in experimental model of glioma. *Mol Ther.* 3:S76.

Amalfitano A, Begy CR & Chamberlain JS (1996). Improved adenovirus packaging cell lines support the growth of replication defective gene delivery vectors. *Proc Natl Acad Sci U S A.* 93: 3352-3356.

Amalfitano A & Chamberlain JS (1996). Isolation and characterisation of packaging cell lines that co-express the adenovirus E1, DNA polymerase and preterminal proteins: implications for gene therapy. *Gene Ther.* 4: 258-263.

Armitage RJ, Macduff BM, Spriggs MK and Fanslow WC (1993). Human B cell proliferation and Ig secretion induced by recombinant CD40 ligand are modulated by soluble cytokines. *J Immunol.* 150:3671-3680.

Bergelson JM, Cunningham JA, Droguett G, Kurt-Jones EA, Krithivas A, Hong JS, Horwitz MS, Crowell RL, and Finberg RW (1997). Isolation of a common receptor for Coxsackie B viruses and adenoviruses 2 and 5. *Science* 275 :1320-1323.

Bergelson JM, Krithiyas A, Celi L, Droguett G, Horwitz MS, Wickham T, Crowell RL, and Finberg RW (1998). The murine CAR homolog is a receptor for coxsackie B viruses and adenoviruses. *J Virol.* 72:415-419.

Bett AJ, Haddara W, Prevec L and Graham FL (1994). An efficient and flexible system for construction of adenovirus vectors with insertions or deletions in Early regions 1 and 3. *Proc.Natl,Acad.Sci.USA* 91:8802-8806.

Blaese RM, Culver KW, Miller AD, Carter CS, Fleisher T, Clerici M, Shearer G, Chang L, Chiang Y, Tolstoshev P, Greenblatt JJ, Rosenberg SA, Klein H, Berger M, Mullen CA, Ramsay WJ, Muul L, Morgan RA & Anderson WF (1995). T-lymphocyte directed gene therapy for ADA-SCID: Initial trial results after 4 years. *Science* 270: 470-475.

Blomer U, Naldini L, Kafri T, Trono D, Verma IM & Gage FH (1997). Highly efficient and sustained gene transfer in adult neurons with a lentivirus vector. *J Virol.* 71:6641-6649.

Bobo RH, Laske DW, Akbasak A, Morrison PF, Dedrick RL & Oldfield EH (1994). Convection-enhanced delivery of macromolecules in the brain. *Proc. Natl. Acad. Sci. USA* 91:2076-2080.

Boise LH, Minn AJ, Noel PJ, June CH, Accavitti MA, Lindsten T, Thomson CB. (1995). CD28 costimulation can promote T cell survival by enhancing the expression of Bcl-Xl. *Immunity* 3:87-98.

Boussiotis VA, Freeman GJ, Berezovskaya A, Barber DL, Nadler LM (1997). Maintenance of human T cell anergy: blocking of IL-2 gene transcription by activated Rap 1. *Science* 278:124-127

Brand K, Klocke R, Possling A, Paul D and Strauss M. 1999. Induction of apoptosis and G2/M arrest by infection with replication-deficient adenovirus at high multiplicity of infection. *Gene Ther.* 6:1054-63.

Brenner MK, Rill DR, Moen RC, Krance RA, Mirro J, Anderson WF & Ihle JN (1993). Gene-marking to trace origin of relapse after autologous bone-marrow transplantation. *Lancet* 341:85-86.

Bukrinsky MI & Haffar OK (1999). HIV-1 nuclear import: in search of a leader. *Front. Biosci.* 4:772–781.

Byrnes AP, MacLaren RE & Charlton HM (1996). Immunological instability of persistent adenovirus vectors in the brain: peripheral exposure to vector leads to renewed inflammation, reduced gene expression, and demyelination. *J. Neurosci.* 16:3045-3055.

Cavazzana-Calvo M, Hacein-Bey S, de Saint Basile G, Gross F, Yvon E, Nusbaum P, Selz F, Hue C, Certain S, Casanova JL, Bousso P, Le Deist F & Fischer A (2000). Gene therapy of human severe combined immunodeficiency (SCID)-X1 disease. *Science* 288: 669-672.

Campbell KA, Ovendale PJ, Kennedy MK, Fanslow WC, Reed SG, Maliszewski CR (1996). CD40 ligand is required for protective cell-mediated immunity to Leishmania major. *Immunity* 4:283-289.

Carayanniotis G, Masters SR, Noelle RJ (1997). Supression of murine thyroiditis via blockade of CD40-CD40L interaction. *Immunology* 90:421-426.

Caplen NJ, Kinrade E, Sorgi F, Gao X, Geddes D, Coutelle C, Huang L, Alton EW, Williamson R (1995). *In vitro* liposome mediated DNA transfection of epithelial cell lines using a cationic liposome DC-CHOL/Dope. *Gene ther.* 2:603-613.

Chaisomchit S, Tyrrell DL & Chang LJ (1997). Development of replicative and non-replicative hepatitis B virus vectors. *Gene Ther.* 4:1330–1340.

Chen HH, Mack LM, Kelly R, Ontell M, Kochanek S and Clemens PR (1997) persistance in muscle of adenoviral vector that lacks all viral genes. *Proc. Natl. Acad. Sci. USA* 94:1645-1650.

Chen PH, Ornelles DA & Shenk T (1993) The adenovirus L3 23-kilodalton proteinase cleaves the amino-terminal head domain from cytokeratin 18 and disrupts the cytokeratin network of HeLa cells. *J Virol.* 67: 3507-3514.

Cotten M, Baker A, Saltik M, Wagner E & Buschle M (1994). Lipopolysaccharide is a frequent contaminant of plasmid DNA preparations and can be toxic to primary human cells in the presence of adenovirus. *Gene Ther.* 1:239-246.

Dewey RA, Morrissey G, Cowsill CM, Stone D, Bolognani F, Dodd NJ, Southgate TD, Klatzmann D, Lassmann H, Castro MG, Lowenstein PR. et al. 1999. Chronic brain inflammation and persistent herpes simplex virus 1 thymidine kinase expression in survivors of syngeneic glioma treated by adenovirus-mediated gene therapy: implications for clinical trials. *Nat Med.* 5:1256-63.

DiSanto JP, Bonnefoy JY, Gauchat JF, Fischer A, de Saint Basile G (1993). CD40 ligand mutations in x-linked immunodeficiency with hyper-IgM. *Nature* 361:541-3.

Douglas JT, Miller CR, Kim M, Dimtriev I, Mikheeva G, Krasnykh V & Curiel DT (1999). A system for the propagation of adenoviral vectors with genetically modified receptor specificities. *Nat. Biotech.* 17: 470-475.

Duan D, Sharma P, Yang J, Yue Y, Dudus L, Zhang Y, Fisher KJ, Engelhardt JF (1999). Circular intermediates of recombinant adeno-associated virus have defined structural characteristics reponsible for long-term episomal persistence in muscle tissue. *J Virol.* 73:8568–8577.

Eck SL and Wilson JM (1996) Gene based therapy. The pharmacological basis of therapeutics. Goodman and Gilman 9th edition, Mc Graw-Hill. Chapter 5, 77-101.

Fabry Z, Raine CS and Hart MN (1994). Nervous tissue as an immune compartment :the dialect of the immune response in the CNS. *Immunol Today* 15:218-224.

Fischer HG, Reichmann G (2001). Brain dendritic cells and macrophages/microglia in central nervous system inflammation. *J Immunol* 166:2717-2726.

Flint ST, Enquist LW , Krug RM, Racaniello VR and Skalka AM (2000). Principles of Virology: Molecular Biology Pathogenesis and Control. American Society for Microbiology, Washington DC pp 82 and 772.

Gerdes CA, Castro MG and Lowenstein PR (2001). Innate vs. Adaptive immune responses against Recombinant Adenoviral Vectors (paper in preparation)

Gerdes CA, Castro MG and Lowenstein PR (2000). Strong promoters are the key to highly efficient, non-inflammatory and non-cytotoxic adenoviral-mediated transgene delivery into the brain. *Mol Ther.* **2** (4): 330-337.

Gerritse K, Laman JD, Noelle RJ, Aruffo A, Ledbetter JA, Boersma WJA, Claasen E (1996) CD40-CD40L interactions in Experimental alergic encephalomyelitis and Multiple-sclerosis. *Proc Natl Acad Sci U S A* 93:2499-2504.

Gorziglia MI, Kadan MJ, Yei S, Lim J, Lee GM, Luthra R & Trapnell BC (1996). Elimination of both E1 and E2a from adenovirus vectors further improves prospects for in vivo human gene therapy. *J Virol.* 70: 4173-4178.

Graham.F.L, Smiley.J, Russell.W.C & Nairn.R (1977) Characteristics of a human cell line transformed by DNA from human adenovirus type 5. *J Gen Virol.* 36: 59-72.

Grewal IS, and Flavell RA (1996). A central role of CD40 ligand in the regulation of T cell responses. *Immunol today* 17:410-414.

Grewal IS, Xu j, and Flavell RA (1995). Impairment of antigen specific T cell priming in mice lacking CD40L. *Nature* 378:617-619.

Hardy, S., Kitamura, M., Harris-Stansil, T., Dai, Y. and Philips, M.L. (1997). Construction of adenovirus vectors through Cre-lox recombination. *J Virol.* 71:1842-1849.

Heufler C, Koch K, Stanzl U, Topar G, Wysocka M, Trinchieri G, Enk A, Steinman RM, Romani N, and Shuler G (1996). Interleukin-12 is produced by dendritic cells and mediates TH1 development as well as interferon γ production by TH1 cells. *Eur J immunol.* 26:659-668.

Hewson R (2000). RNA viruses: emerging vectors for vaccination and gene therapy. *Mol Med Today* 6:28–35.

Hirsh RL (1982). The complement system: its importance in the host response to viral infection. *Microb Review*, 44:71-85.

Inaba K et al (1994). The tissue distribution of B7-2 costimulator in mice abundant expression on dendritic cells *in situ* and during maturation *in vivo. J exp med.*180:1849-1860.

Janeway CA Jr, Travers P (1997) in Immuno Biology, the immune system in health and disease. Thirth edition. Part IV: The adaptive immune response.

Kajiwara K, Byrnes AP, Ohomoto Y, Charlton HM, Wood MJA, Wood KJ (2000). Humoral immune responses to adenovirus vectors in the brain. *J Neuroimmunol.* 103:8-15.

Kass-Eisler A, Leinwand L, Gall J, Bloom B and Falck-Pedersen E (1996). Circumventing the immune response to adenovirrus mediated gene therapy. *Gene ther* 3:154-162.

Kay MA, Glorioso JC, Naldini L. (2001) Viral vectors for gene therapy: the art of turning infectious agents into vehicles of therapeutics. *Nat Med.* 7:33-40.

Kay MA, Dexi L, and Hoogerbrugge PM. (1997a) Gene therapy. *Proc.Natl.Acad.Sci.USA* 94:12744-12746.

Kay MA, Meuse L, Grow AM, Linsley P, Hollenbaugh D, Aruffo A, Ochs HD and Wilson CB (1997b). Transient immunomodulation wiyh anti-CD40L antibody and CTLA4Ig enhances percistance and secondary adenovirus mediated gene transfer into mouse liver. *Proc.Natl.Acad.Sci.USA*, 94:4688-4691.

Koch F, Stanzl U, Jennewein P, Janke K, Heufler C, Kampgen E, Romani N, and Schuler G (1996). High level IL-12 by murine dendritic cells: upregulation via MHC

class II and CD40 molecules and downregulation by IL-4 and IL-10. *J Exp Med.* 84:741-746.

Kochanek S, Clemens P, Mitani K, Chen HH, Chan S, and Caskey T (1996). A new adenoviral vector: replacement of all viral coding sequences with 28 Kb of DNA independently expressing both full length dystrophin and β galactosidase. *Proc. Natl. Acad. Sci. USA*, 93:5731-5736.

Kruisbbek AM, and Amsen D (1996) Mechanisms underlying T cell tolerance. *Curr Opin immunol.* 8:233-244.

Kuo CJ, Farnebo F, Yu EY, Christofferson R, Swearingen RA, Carter R, von Recum HA, Yuan J, Kamihara J, Flynn E, D'Amato R, Folkman J, Mulligan RC (2001). Comparative evaluation of the antitumor activity of antiangiogenic proteins delivered by gene transfer. *Proc. Natl. Acad. Sci. USA* 98: 4605-4610.

Lane P, Gerhard W, Hubele S, Lanzavecchia A, and McConnell F (1993). Expression and functional properties of mouse B7/BB1 using a fusion protein between mouse CTLA4 and human γ 1. *Immunology*, 80:56-61.

Liu F, Yang JP, Huang L and Liu D (1997). New cationic lipid formulations for gene transfer. *Pharm.Res.* 13, 1856-1860.

Lowenstein PR (2001). The immunology of gene transfer into the immune-privileged brain using viral vectors: an evolutionary and developmental perspective. (paper in preparation)

Lu LN, Li W, Fu FM, Chambers FG, Qian SG, Fung JI, Thomson AW (1997). Blockade of CD40-CD40L pathway potentiates the capacity donor-derived DC progenitors to induce long term cardiac allograft survival. *Transplantation*, 64:1808-1815.

Luria, S.E., Darnell, J.E Jr., Baltimore D. & Campbell, A. (1978) Eds. In: *General Virology* (John Wiley & Sons, New York), pp. 21-32.

Ma J, Xu JC, Peng QS, Wen L, Zhang J, Grewal I, Flavell R, Craft J (1995). Impared germinal center and memory cell formation in MRL/LPR mice deficient in CD40 ligand. *Arthritis and reumatism* 38:880-886.

Macatonia SE, Hosken M, Litton M, Vieira P, Culpepper JA, Wysocka M, Trinchieri G, Murphy KM, and O'Garra A.(1995). Dendritic cells produce IL-12 and direct the development of Th1 cells from naïve CD4 T cells. *J Immunol.* 154:5071-5079.

Maione D, Wiznerowicz M, Delmastro P, Cortese R, Ciliberto G, La Monica N, Savino R (2000). Prolonged expression and effective readministration of erythropoietin delivered with a fully deleted adenoviral vector. *Hum Gene Ther.* 11:859-868.

Marr RA, Hitt M, Muller WJ, Gauldie J & Graham FL (1998). Tumour therapy in mice using adenovirus vectors expressing human TNFα. *Int. J. Oncol.* 12:509-515.

Mathieu P, Guillot C, Bouchet D, **Gerdes CA,** Buzelin F, Lowenstein PR , Castro MG, Soulillou JP and Anegon I (2001a). Adenovirus-mediated expression of CD40 Ig attenuates graft arteriosclerosis (Under submision).

Mathieu P, Guillot C, **Gerdes CA,** Buzelin F, Lowenstein PR , Castro MG, Soulillou JP and Anegon I (2001b). Adenovirus-mediated CD40Ig expression attenuates chronic vascular rejection lesions. *Transplantation Proceedings* (in press).

Matsushita T, Elliger S, Elliger C, Podsakoff G, Villarreal L, Kurtzman GJ, Iwaki Y, Colosi P (1998). Adeno-associated virus vectors can be efficiently produced without helper virus. *Gene Ther.* 5, 938–945.

Miao CH, Snyder RO, Schowalter DB, Patijn GA, Donahue B, Winther B, Kay MA (1998). The kinetics of rAAV integration in the liver. *Nature Genet.* 19:13–15.

Miller DG, Adam MA & Miller AD (1990). Gene Transfer by retrovirus vectors occurs only in cells that are actively replicating at the time of infection. *Mol. Cell Biol.* 10:4239–4242.

Miller, A.D. in *Retroviruses*. (eds. Coffin, J., Hughes, S.H. & Varmus, H.E.) (ColdSpring Harbor Laboratory Press, Planview, 2000).

Mitani K, Graham FL, Caskey CT and Kochanek S (1995). Rescue, propagation and partial purification of a helper virus-dependent adenovirus vector. *Proc.Natl.Acad.Sci.USA* 92:3854-3858.

Mittereder N, March KL & Trapnell BC (1996). Evaluation of the concentration and bioactivity of adenovirus vectors for gene therapy. *J Virol.* 70:7498-7509.

Mosmann TR, Coffman RL (1989). Heterogeneity of cytokine secretion patterns and functions of helper T cells. *Adv. Immunol.* 46:111-147.

Morsy, M.A. et al. 1998. An adenoviral vector deleted for all viral coding sequences results in enhanced safety and extended expression of a leptin transgene. *Proc. Natl. Acad. Sci. USA* 95:7866-7871.

Morral N, Parks RJ, Zhou H, Langston C, Schiedner G, Quinones J, Graham FL, Kochanek S, Beaudet AL. (1998). High doses of a helper-dependent adenoviral vector yield supraphysiological levels of α1-antitrypsin with negligible toxicity. *Human Gene Ther.* 9: 2709-2716.

Morral N, O'Neal W, Rice K, Leland M, Kaplan J, Piedra PA, Zhou H, Parks RJ, Velji R, Aguilar-Cordova E, Wadsworth S, Graham FL, Kochanek S, Carey KD, Beaudet AL. (1999). Administration of helper-dependent adenoviral vectors and sequential delivery of different vector serotype for long-term liver-directed gene transfer in baboons. *Proc. Natl. Acad. Sci. USA* 96:12816-12821.

Nyberg-Hoffman C, Shabram P, Li W, Giroux D & Aguilar-Cordova E (1999). Sensitivity and reproducibility in adenoviral infectious titer determination. *Nat Med.* 3:808-811.

Palese P, Zheng H, Engelhardt OG, Pleschka S & Garcia-Sastre A (1996). Negative-strand RNA viruses: genetic engineering and applications. *Proc. Natl. Acad. Sci. USA* 93:11354–11358.

Parks RJ, Chen L, Anton M, Sankar U, Rudnicki MA and Graham FL (1996). A helper dependent adenovirus vector syistem: removal of helper virus by cre-mediated excision of the viral packaging signal. *Proc. Natl. Acad. Sci. USA* 94:4686-4691.

Podack ER, Lowrey DM, Lichtenheld M, Hameed A (1988). Functions of granule perforine and esterases in T cell mediated reactions. Ann. NY Acad. Sci. 532:292-302.

Ringrose L, Lounnas V, Ehrlich L, Buchholz F, Wade R, Stewart AF (1998). Comparative kinetic analysis of FLP and Cre recombinases: mathematical models for DNA binding and recombination. *J. Mol. Biol.* 284:363-384.

Roe T, Reynolds TC, Yu G & Brown PO (1993). Integration of murine leukemia virus DNA depends on mitosis. *EMBO J.* 12, 2099–2108.

Roelvink PW, Lizonova A, Lee JGM, Li Y, Bergelson JM, Finberg RW, Brough DE, Kovesdi I, and Wickham TJ (1998). The coxsackievirus-adenovirus receptor protein can function as a cellular attachment protein for adenovirus serotypes from subgroups A, C, D, E, and F. *J Virol.* 72 : 7909-7915.

Roelvink PW, Mi Lee G, Einfeld DA, Kovesdi I and Wickham TJ (1999). Identification of a conserved receptor-binding site on the fiber proteins of CAR-recognizing adenoviridae. *Science* 286:1568-1571.

Ross G, Erickson R, Knorr R, Motulsky AG, Parkman R, Samulski J, Straus SE, and Smith BR (1996). Gene therapy in the United States: a five-year status report. *Hum Gene Ther.* 7:1781-1790.

Sallovane JM, Xing Z, Simpson AJ, Graham FL, Gauldic J (1998). Adenovirus mediated expression of an elastase specific inhibitor (elafin): a comparison of different promoters. *Gene ther.* 5:352-360.

Samoilova EB, Horten JL, Zhang HD, Chen YH (1997). CD40L blockade prevents autoimmune encephalomyelitis and hampers TH1 but not TH2 pathway of T cell differentietion. *J Mol Med.* 75:603-608.

Samulski J, (2001). AAV vectors, pros and cons. Keystone symposia, Gene therapy 2001: A Gene Odyssey.

Sandig V, Youil R, Bett AJ, Franlin LL, Oshima M, Maione D, Wang F, Metzker ML, Savino R, Caskey CT. (2000). Optimization of the helper-dependent adenovirus system for production and potency in vivo. *Proc. Natl. Acad. Sci. USA* 97, 1002-1007.

Scaria A, St George JA, Gregory RJ, Noelle RJ, Wadsworth SC, Smith AE, Kaplan JM (1997). Antibody to CD40 ligand inhibits both humoral and cellular immune responses to adenoviral vectors and facilitates repeated administration to mouse airway. *Gene ther.* 4:611-617.

Schaack J, Guo XL & Langer SJ (1996). Characterisation of a replication-incompetent adenovirus type 5 mutant deleted for the preterminal protein gene. *Proc. Natl. Acad. Sci. USA* 93: 14686-14691.

Schiedner G, Morral N, Parks RJ, Wu J, Koopmans SC, Langston C, Graham FL, Beaudet AL & Kochanek S (1998). Genomic DNA transfer with a high-capacity adenovirus vector results in improved in vivo gene expression and decreased toxicity. *Nature Gen.* 18:180-183.

Schowalter DB, Meuse L, Wilson CB, Linsley PS and Kay MA (1997), Constitutive expression of murine CTLA4Ig from a recombinant adenovirus vector results in prolonged transgene expression. *Gene ther.* 4, 853-860.

Sclimenti CR & Calos MP (1998). Epstein-Barr virus vectors for gene expression and transfer. *Curr. Opin. Biotechnol.* 9:476–479.

Seth P, Fitzgerald D, Willingham M, and Pastan I (1984). Pathway of adenovirus entry into cells. *Mol Cell Biol.* 4:1528-1533.

Shent T (1996) Adenoviridae: The viruses and their replication. In Fundamental Viroogy. Third edition. Edited by Fields BN, Knipe DM, Howley PM, et al. Raven publishers, Philadelphia, USA. 30, 979-1016.

Shering AF, Bain D, Stewart K, Epstein AL, Castro MG, Wilkinson GWG & Lowenstein PR (1997). Cell type-specific expression in brain cell cultures from a short human cytomegalovirus major immediate early promoter depends on whether it is inserted into herpesvirus or adenovirus vectors. *J Gen Virol.* 78:445-459.

Smith-Arica J, Morelli AE, Larregina AT, Smith J, Lowenstein PR & Castro MG (2001). Cell-Type-Specific and Regulatable Transgenesis in the Adult Brain: Adenovirus-Encoded Combined Transcriptional Targeting and Inducible Transgene Expression. *Mol Ther.* 2:579-587.

Song Y, Chu SY and Liu D (1997). Characterisation of cationic liposome-mediated gene transfer *in vivo* by intravenous administration. *Hum Gene Ther.* 4, 517-523.

Soong L, Xu JC, Grewal IS, Kima P, Sun J, Longley, BJ, Ruddle NH, McMahon-Pratt D and Flavell RA (1996). Disruption of CD40-CD40 ligand interactions results in an enhanced susceptibility to Leishmania amazonensis infection. *Immunity* 4:263-273.

Southern E (1975) Detection of specific sequences among DNA fragmnets separated by gel electrophoresis. *J Mol Biol.* 98:503-517.

Southgate TD, Windeatt S, Smith-Arica J, **Gerdes CA**, Perone MJ, Davis JRE, Klatzmann D, Lowenstein PR & Castro MG (2000). Transcriptional targeting to anterior pituitary lactotrophic cells using recombinant adenovirus vectors *in vitro* and *in vivo. Endocrinology* 141:3493-505.

Stewart PL, Burnett RM (1995). Adenovirus structure by X-ray crystallography and electron microscopy. *Curr top Microbiol Immunol.* 199:25-38.

Strayer DS (1999). Gene therapy using SV-40 derived vectors: what does the future hold. *J Cell Physiol.* 181:375–384.

Tang AM, Judge TA, Turka LA (1997). Blockade of CD40-CD40L pathway induces tolerance in murine contact hypersensitivity. *Eur J immunol.* 27:3143-3150.

Thomas CE, Schiedner G, Kochankek S, Castro MG and Lowenstein PR (2000). Peripheral infection with adenovirus causes unexpected long-term brain inflammation in animals injected intracranially with first-generation, but not with high-capacity, adenovirus vectors: toward realistic long-term neurological gene therapy for chronic diseases. *Proc. Natl. Acad. Sci. USA* 97, 7482-7487.

Thomas CE, Birkett D, Castro MG & Lowenstein PR (2001). The role of vector toxicity versus inflammatory and immune responses in eliminating adenoviruse vector-mediated transgene expression from the rat brain. In press *Mol Ther.*

Thomas CE, Abordo-Adesida E, Maleniak TC, Stone D, **Gerdes CA** & Lowenstein, P.R. in: *Current Protocols in Neuroscience*, J.N. Crawley, C.R. Gerfen, R. McKay, M.A. Rogawski, D.R. Sibley, P. Skolnick, (2001b) Eds. (John Wiley and Sons, New York) In press.

Toogood CIA, Crompton J, and Hay RT (1992). Antipeptide antisera define neutralizing epitopes on the adenovirus hexon. *J Virol.* 73:1429-1435.

Umana P, **Gerdes CA**, Stone D, Davis JRE, Castro MG and Lowenstein PR (2001). An efficient, *in vitro*-evolved FLPe enables scalable production of helper-dependent adenoviral vectors with negligible helper contamination. *Nat Biotechnol.* 19:582-585.

Wekerle H, Linington C, Lassmann H and Meyermann R (1986). Cellular immune reactivity within the CNS. *Trend Neurosci.* 9:271-276.

Wickham TJ, Mathias P, Cheresh DA, and Nemerow GR (1993). Integrins $\alpha_v\beta_3$ and $\alpha_v\beta_5$ promote adenovirus internalization but not virus attachment. *Cell* 73 : 309-319.

Wisnivesky JP, Leopold PL and Crystal RG (1999). Specific binding of the adenovirus capsid to the nuclear envelope. *Hum Gene Ther.* 10 : 2187-2195.

Wohlleben G, Gray D and Schimpl A (1996). In vitro immunisation of naïve mouse B cells: establishment of IM secreting hybridomas specific for soluble protein or hapten from B cells cultured on CD40 ligand transfected mouse fibroblasts. *Int Immunol.* 8:343-349.

Wood MJ, Charlton HM, Wood KJ, Kajiwara K & Byrnes AP (1996). Immune responses to adenovirus vectors in the nervous system. *Trend Neurosci.* 19:497-501.

Xiao X., Li J & Samulski RJ (1998). Production of high-titer recombinant adeno-associated virus vectors in the absence of helper adenovirus. *J Virol.* 72:2224–2232.

Yang JP, Huang L (1997) Overcoming the inhibitory effect of serum on lipofection by increasing the charge ratio of cationic liposome to DNA. *Gene Ther.* 4, 950-60.

Yang Y, Nunes FA, Berencsi K, Furth EE, Gonczol E and Wilson JM (1994). Cellular immunity to viral antigens limits E1-deleted adenoviruses for gene therapy. *Proc. Natl. Acad. Sci. USA* 91, 4407-4411.

Yang Y, Li Q, Hildegrund CJE, Wilson JM (1995). Cellular and humoral immune responses to viral antigens create barriers to lung directed gene therapy with recombinant adenoviruses. *J Virol.* 69:2004-2015.

Yang Y, and Wilson JM (1996). CD40 ligand-dependent T cell activation: requirement of B7-CD28 signaling through CD40. *Science* 273:1862-1864

Zychlinsky A, Zheng LM, Liu CC, Young JD (1991). Cytolitic limphocytes induce both apoptosis and necrosis in target cells. *J immunol.* 146:393-400.

Chapter 8: Curriculum Vitae

Christian A. Gerdes

Molecular Medicine and Gene Therapy Unit
Room 1302 Stopford Buliding
University of Manchester
Oxford Road
Manchester M13 9PT, UK
Email: cagerdes@hotmail.com

Profile

Research scientist with experience in molecular biology, cytogenetics (clinic experience), microbiology, cell biology and virology techniques. These includes from plasmid and viral vector construction for gene therapy, tissue culture work, to animal work for *in vivo* models. Currently finishing my PhD at the University of Manchester under the supervision of professors P.R. Lowenstein and M.G. Castro, improving adenoviral vectors for gene therapy.

Technical skills

Microbiology: Bacterial culture, preparation of competent bacteria, bacterial transformation, and plasmid DNA cloning.

Molecular biology: all DNA basic techniques (restriction endonucleases digestions, agarose gel electrophoresis, cloning and subcloning, isolation and purification, labelling of DNA probes for colorimetric detection of nucleic acids, Southern blot, PCR, etc.). RNA isolation and purification.

Gene therapy: Generation of recombinant adenovirus by homologous recombination in 293 cells. Isolation, scale up, purification using CsCl gradients and titration of adenoviral vectors.

Cell culture: standard cell culture techniques with experience growing a wide variety of cell lines. DNA Transfections and transgene expression detection in cell cultures.

Cytogenetics: Peripheral blood lymphocytes culture and analysis with standard G, C, Nor and DAPI banding techniques. Fragile X chromosome analysis. High-resolution cytogenetic analysis. Amniotic cell culture and analysis for prenatal diagnosis. Chorionic Villi processing and analysis for prenatal diagnosis.

Protein analysis: Immunocytochemestry, indirect immunofluorescence of cell cultures and tissue sections. β-galactosidase and X-gal assays.

Animal work: standard rodent injections. Stereotactic Intracraneal injections. Cardiac perfusions and tissue fixation. Recovery, vibratome and microtome sectioning of tissues.

Miscellaneous: Photography skills for picture recording of results. Standard and Immunofluorescence microscopy. Broad software knowledge including all standard Microsoft software, image processing and graphs generation.

Education and Research experience.

1997-present. PhD student at the Molecular Medicine and Gene Therapy Unit, school of Medicine, University of Manchester, UK. Under the supervision of professors P.R.Lowenstein and M.G. Castro, "improving Adenoviral vectors for gene therapy in the brain". Including different project carried alone or in collaboration:

1. Characterisation of the mCMV promoter included in a Recombinant Adenoviral vector for its use in gene therapy.

2. Characterisation of the immune response generated against Adenoviral vectors.

3. Testing a new developed helper dependent adenoviral vector system.

4. Adenoviral immune tolerance blocking the CD40-CD40L interaction by infection of a generated Recombinant Adenoviral vector carrying a soluble CD40 Ig.

5. Anti-angiogenic gene therapy for gliomas using Recombinant Adenoviruses carrying Endostatin and Angiostatin.

1997-present. Personal licence to carry out regulated procedures on living animals (personal licence identification: 40/5370), granted by the Home Office, UK by the Secretary of State.

1997. Training programme approved by the Universities Accreditation Scheme, for Animals (scientific procedures) act 1986. Universities Training Group, University of Manchester.

1992-1993. Research Assistant, Microbiology Division, Institute of Pharmacology and Botany, Buenos Aires, Argentina, researching for a 37 C thermosensible Salmonella Typhimurium strain to be used as a live antigen-presenting cell in a bovine vaccine. I produced two different candidate strains, which resulted in the related publications mentioned.

1991-1992. Research Assistant at the Institute of Molecular Genetics and Biotechnology, Buenos Aires, Argentina, researching the efficiency of nitrogen

fixation and nodulation of different commercial and native populations of Rhyzobium Meliloti (Nif and Nod genes) for improving alfalfa production and soil enrichment for agriculture purposes. Project and idea entirely self developed.

1991-1992. M.Sc Molecular Biology and Biotechnology, School of Biological Sciences, University of Buenos Aires, Argentina.

1986-1990. B.Sc (honours first class) Biological sciences (molecular biology), School of Biological Sciences, University of Buenos Aires, Argentina.

Publications

Papers

1. Christian A. Gerdes, Maria G. Castro and Pedro R. Lowenstein (2001). Innate vs. Adaptive immune responses against Recombinant Adenoviral Vectors (paper in preparation).

2. P. Mathieu, C Guillot, D. Bouchet, **C.A. Gerdes,** M.G. Castro, P.R. Lowenstein J.P. Soulillou and I. Anegon (2001). Adenovirus-mediated expression of CD40 Ig attenuates graft arteriosclerosis. Under submision.

3. P. Mathieu, C Guillot, **C.A. Gerdes,** F. Buzelin, P.R. Lowenstein , M.G. Castro, J.P. Soulillou and I. Anegon (2001). Adenovirus-mediated CD40Ig expression attenuates chronic vascular rejection lesions. *Transplantation Proceedings* (in press).

4. Pablo Umana, **Christian A. Gerdes**, Daniel Stone, Julian R.E. Davis, Maria G. Castro and Pedro R. Lowenstein (2001). An efficient, *in vitro*-evolved FLPe enables scalable production of helper-dependent adenoviral vectors with negligible helper contamination. *Nature Biotechnology* 19 (6):582-585.

5. Christian A. Gerdes, Maria G. Castro & Pedro R. Lowenstein, (2000). Strong promoters are the key to highly efficient, noninflammatory and noncytotoxic adenoviral-mediated transgene delivery into the brain. *Molecular Therapy* 2 (4): 330-337.

6. Thomas, C.E., Abordo-Adesida, E., Maleniak, T.C., Stone, D., **Gerdes C.A.** & Lowenstein, P.R. in: *Current Protocols in Neuroscience*, J.N. Crawley, C.R. Gerfen, R. McKay, M.A. Rogawski, D.R. Sibley, P. Skolnick, Eds. (John Wiley and Sons, New York, 2000) 4.24.1-4.24.37.

7. Southgate TD, Windeatt S, Smith-Arica J, **Gerdes CA**, Perone MJ, Morris I, Davis JR, Klatzmann D, Lowenstein PR, Castro MG, (2000). Transcriptional targeting to anterior pituitary lactotrophic cells using recombinant adenovirus vectors *in vitro* and *in vivo* in normal and estrogen/sulpiride-induced hyperplastic anterior pituitaries. *Endocrinology.* **141** (9):3493-505.

8. Cerquetti MC, Brawer R, **Gerdes CA**, Gherardi MM, Sordelli DO, (1995). Fts insertional mutant of Salmonella typhimurium. *FEMS Microbiol Lett.* 132(1-2):73-8.

Abstracts

1. Christian A. Gerdes, Maria G. Castro and Pedro R. Lowenstein (2001). Innate vs. Adaptive immune responses to first generation adenoviral vectors. *Molecular Therapy, ASGT edition* (in press).

2. Pablo Umana, **Christian A. Gerdes**, Daniel Stone, Julian R.E. Davis, Maria G. Castro and Pedro R. Lowenstein (2001). *in vitro* and *in vivo* characterization of a helper-dependent adenovirus produced with a scalable Flpe-based system. *Molecular Therapy, ASGT edition* (in press).

3. P.A. Kingston, **C.A. Gerdes**, A.M. Heagerty, M.G. Castro, P.R. Lowenstein, (2000). The Murine Cytomegalovirus Immediate-Early Enhancer/Promoter Is a More Potent Regulator of Transgene Expression Than the Human Promoter in Vascular Smooth Muscle Cells *In Vitro. J Am Coll Cardiol.* 2001; (in press).

4. Christian A. Gerdes, Maria G. Castro and Pedro R. Lowenstein, (2001). The adaptive immune system recognises and eliminates transgene expression from as little as 1000 infectious adenoviral particles in the brain implications for neurological gene therapy. *Keystone symposia, Gene therapy 2001: A Gene Odyssey,* abstract 106.

5. Pablo Umana, **Christian A. Gerdes**, Julian R.E. Davis, Maria G. Castro and Pedro R. Lowenstein (2001). An efficient, *in vitro*-evolved FLPe enables scalable production of helper-dependent adenoviral vectors with negligible helper contamination. *Keystone symposia, Gene therapy 2001: A Gene Odyssey,* abstract 135.

6. Christian A. Gerdes, Maria G. Castro & Pedro R. Lowenstein, (2000). Highly efficient and non-inflammatory transgene delivery into the CNS using a first generation adenoviral vector. *British Neuroendocrine group annual meeting*, P55.

7. Christian A.Gerdes, Maria G. Castro & Pedro R. Lowenstein, (2000). One adenoviral particle is enough to efficiently transduce brain cells *in vivo. Molecular Therapy*, **1**, S66.

8. Christian A.Gerdes, Maria G. Castro & Pedro R. Lowenstein, (2000). Highly efficient, non-inflammatory transgene delivery and expression in the brain, with a first generation adenoviral vector. *European Journal of Neuroscience*, **12,** 361.

9. Pedro R.Lowenstein, Clare E.Thomas, **Christian A.Gerdes**, Maria G.Castro, (2000). Experimental gene therapy of brain tumors: increasing the efficiency of gene therapy by reducing the side effects of adenoviral mediated gene transfer into the brain. *European Journal of Neuroscience*, **12,** 522.

10. Christian A.Gerdes, Maria G. Castro & Pedro R. Lowenstein, (2000). Stronger and sustained transgene expression from a recombinant adenoviral vector under the control of the mCMV promoter *in vivo. Journal of Endocrinology,* **164,** P165.

11. Tom Southgate, Simon Windeatt, Joe Smith-Arica, **Christian A.Gerdes**, M.Perone, D. Klatzmann, J.R.E.Davis, P.R.Lowenstein & M.G.Castro, (2000). Transcriptional Targeting to anterior pituitary lactotrophic cells using recombinant adenovirus vectors: *in vitro* and *in vivo* studies. *Journal of Endocrinology,* **164,** OC28.

12. P.R.Lowenstein, C.E.Thomas, G.Morrisey, C.Cowsill, F.Bolognani, G Schidner, S.Kochanek, **C.A.Gerdes**, M.G.Castro, (2000). Towards realistic gene therapy for neurological diseases. *Journal of Endocrinology,* **164,** S10.

13. Christian A. Gerdes, Pedro R. Lowenstein & Maria G. Castro, (1999). Generation of recombinant adenoviral vectors expressing soluble CD40-Ig under the control of different promoter strength to suppress the acquired immune response. *Graduate student symposium, Medical school, University of Manchester.*

14. Christian A. Gerdes, Pedro R. Lowenstein & Maria G. Castro, (1998). Generation of recombinant adenoviral vectors expressing soluble CD40-Ig to suppress the humoral immune response. *Graduate student symposium, Medical school, University of Manchester.*

15. Valeria Gonzales Nicolini, Enrique Millan, Marcelo Perone, Adriana Larregina, **Christian A. Gerdes**, Pedro R. Lowenstein and Maria G. Castro, (1997). Genetically modified cells-mediated gene therapy. *The join Centre on Aging Research Away-Day Poster Session, Penrith, Uk.*

16. Cerquetti MC, **Gerdes CA**, Gherardi MM, Sordelli DO, (1994). Fts insertional mutant of Salmonella typhimurium. *Abstract of the 94th General meeting of the American Society of Microbiology, Las Vegas*, 225.

Clinical Experience

1996-1997. Head Biologist and manager of the Cytogenetic laboratory at the human Genetic Foundation, Buenos Aires, Argentina. *During this period I was responsible for 17 technicians, which processed 400-500 cytogenetic studies per month.*

1995-1996. Head Biologist of the Peripheral Blood Diagnostic area, Human Genetic Foundation, Buenos Aires, Argentina. *During this period 48% of the costs per patient were cut, with an increment in efficiency, which resulted in the shortened of the delay of the analysis results from 3 month to 2-3 weeks.*

1994-1995. Cytogeneticist of the peripheral blood diagnostic area, Human Genetic foundation, Buenos Aires, Argentina.

Awards

Overseas research scheme Award: three years PhD studentship, University of Manchester.

Sir Halley Stewart Trust: three years economical support for the PhD, plus 6-month extension, University of Manchester.

Personal Details

Date of Birth: 19/06/67; Place of Birth: Buenos Aires, Argentina; Marital status: married; Languages: Spanish, English, Italian and Portuguese.

ARTICLE

doi:10.1006/mthe.2000.0140, available online at http://www.idealibrary.com on IDEAL

Strong Promoters Are the Key to Highly Efficient, Noninflammatory and Noncytotoxic Adenoviral-Mediated Transgene Delivery into the Brain *in Vivo*

Christian A. Gerdes, Maria G. Castro, and Pedro R. Löwenstein[1]

Molecular Medicine and Gene Therapy Unit, School of Medicine, University of Manchester, Room 1.302 Stopford Building, Oxford Road, Manchester M13 9PT, England

Received for publication August 7, 2000, and accepted in revised form August 29, 2000

Using the major immediate early murine cytomegalovirus (MIEmCMV) promoter to drive expression of β-galactosidase, we have demonstrated that, following adenoviral-mediated transduction of brain cells *in vivo*, a single viral infectious unit is capable of producing detectable levels of transgene expression and that gene transfer into the brain is close to 100% efficient. By reducing 100-fold the amount of virus needed to detect large numbers of transduced brain cells, we were able to completely eliminate the cellular inflammation and viral cytotoxicity associated with the delivery of adenoviral vectors into the brain compared to saline-injected controls. These results demonstrate that a strong promoter is necessary to allow the use of low concentrations of adenoviral vectors for gene transfer into the brain, thereby eliminating deleterious side effects and increasing the potential efficacy of gene therapy.

INTRODUCTION

Gene therapy using viral vectors is currently being developed to replace a missing protein product in inherited diseases, to deliver therapeutically active proteins to diseased tissues, or to eliminate tumor cells (1). In spite of their importance to the potential clinical success of gene therapy, neither the efficiency of viral vector-mediated gene transfer *in vivo* nor the number of viral infectious particles (iu) needed to transduce a single cell *in vivo* has been previously determined. Although viral vector-mediated gene transfer *in vitro* is believed to be very efficient, *in vivo* gene transfer normally requires the use of high numbers of viral infectious units to achieve anatomically detectable and physiologically relevant levels of transgene expression. Similar data have been reported with all different types of viral vectors utilized to date (2).

In addition to the low efficiency of transgene expression *in vivo*, we and others have recently demonstrated important side effects of first-generation adenovirus vector used to transfer genes to the CNS. Direct cytotoxicity and strong persistent brain inflammation were seen following injection of functionally effective doses of first-generation adenoviral vector into the brain (3–5). Acute inflammation (macrophage/microglial and CD8+ lymphocyte/NK cell infiltration) follows injection of 10^7 iu, and direct cytotoxicity (astrocyte and neuronal cell death) occurs when doses above 10^8 iu are injected into the adult rat brain (4). Using an adenoviral vector expressing β-galactosidase from the very strong MIEmCMV promoter (6–8), we now demonstrate close to 100% gene transfer efficiency and expression in the adult rat brain. At very low doses of this vector (10^1–10^3 infectious units per injection site), the number of detectable transduced brain cells is equal or very close to the number of viral infectious units injected. This vector allows transgene expression throughout relatively large areas of the brain at high levels, in the complete absence of any cellular inflammation or cytotoxicity compared to saline-injected controls.

MATERIALS AND METHODS

Gene transfer in vitro. Rat CNS-1 cells, mouse Neuro2A cells, hamster Chinese hamster ovary (CHO) cells, nonhuman primate COS7 cells, and human HeLa cells were grown using the cell growth medium described previously (9). Cell lines were plated in 24-well plates at a density of 2×10^4 cells/well 1 day prior to infection. On the day of infection, 2 wells were counted, and plates were infected at appropriate m.o.i. values for each virus (m.o.i. values used: 10, 30, 100, and 300). Forty-eight hours later cells were stained for β-galactosidase histochemistry, or β-galactosidase enzyme assays were carried out on cell lysates as described previously (10). Expression of the *lacZ* gene under transcriptional control of the 1.4-kb MIEmCMV promoter (−1336 to +36) was compared to the expression of β-galactosidase from RAd 35, which uses a short 0.4-kb MIEhCMV promoter (−299 to +72), in cell lines from different species. In all cell lines used the levels of β-galactosidase activity, driven by the MIEmCMV promoter, were significantly higher, in agreement with Refs. 6–8 and 11. The

[1]To whom correspondence and reprint requests should be addressed. Fax: 44-(0)-161-275-5672. E-mail: lowenstein@man.ac.uk.

1525-0016/00 $35.00

difference of expression varied from ~9-fold in human HeLa cells to ~500-fold in rat CNS-1 cells, at m.o.i. = 10. The glioblastoma cell line (CNS-1) was kindly provided by Dr. William F. Hickey (Pathology Department, Dartmouth Medical School, NH). The murine neuroblastoma cell line (Neuro2A), the SV40 transformed African green monkey kidney cell line (COS7), the human cervical epitheloid carcinoma cell line (Hela), and the chinese hamster ovary (CHO) cell line were purchased from the European Collection of Animal Cell Cultures (Porton Down, Salisbury, UK).

Generation of recombinant adenoviruses RAd 36 and RAd 35. A *Hin*dIII fragment was excised from the pMCMV 3 plasmid (kindly provided by Dr. Martin Messerle, Max von Pettenkofer Institute, Munich, Germany), containing 1.4 kb from the major immediately early murine cytomegalovirus promoter (MIEmCMV) and a 0.15-kbp SV40 polyadenylation signal was subcloned into *Hin*dIII-digested pAL119 (pMV35 in Ref. 12) from which the sMIEhCMV promoter and SV40 polyadenylation signal were deleted. The resulting plasmid was called pAL120. The shuttle vector pAL120-*lacZ* was constructed by blunt-end ligation of a 3.4-kb *Eco*RV–*Sal*I *lacZ* fragment with blunt-ended *Sal*I-linearized pAL120. Plasmid pAL120 was used to generate RAd36. RAd 35 (an adenovirus encoding *lacZ* under the control of the MIEhCMV promoter) was originally described by Wilkinson and Akrigg (13) and has been used previously (3, 4, 9, 14). The methods for adenoviral generation, production, characterization, scale up, and viral vector purification have been previously described (10, 14). Titrations were carried out in triplicate and in parallel for all viruses by end-point dilution, cytopathic effect (cpe) assay, with or without centrifugation of infected 96-well plates as described in detail by Nyberg-Hoffman *et al.* (15). Titers obtained using the standard accepted calculations, from plates with or without centrifugation, were identical. The only difference we found following centrifugation of infected plates was that titers could already be read 3 days after infection (and did not change even when examined at 10 days postinfection), while in the absence of centrifugation titers could only reliably be read 8 days after infection. The titer, determined by standard calculations routinely utilized in our laboratory and elsewhere, was 8.2×10^{10} iu/ml for RAd36, with a particle:pfu ratio of 17. The titer of RAd35 was 6.55×10^{11} iu/ml, and the particle:pfu ratio was 27. If, in addition to centrifugation of infected plates, we applied the mathematical correction described by Nyberg-Hoffman *et al.* (15), the infectious titer obtained for RAd36 becomes 2.3×10^{11}, and for RAd35 it becomes 1.8×10^{12}. [The mathematical correction used was Eq. [6] described in Ref. 15: $V = -\ln (1 - P_W/n)\ 1/\varphi C_T(d + lt)$, where $l = 2.38 \times 10^{-4}$ cm/s$^{1/2}$, φ (average cell area for 293 cells) = 6.3×10^{-6} cm^2, C_T is total number of cells per well, t is duration of the assay, P_W is positive wells, n is total wells, V is virus concentration, and d is displacement (by centrifugation) or depth of the well, whichever is less. Calculations are in centimeters for distances and seconds for time; adjusted titers must be multiplied by the dilution factors to obtain the titers of the preparation.] Throughout the description of our experiments we refer to vector titers as calculated from the standard method of titration, because this is the accepted international standard used in the estimation of adenoviral titers, and this allows comparisons to be made across all previously published reports. The human embryonic kidney 293 cell line (293) used to produce recombinant adenoviral vectors was obtained from Microbix Biosystems Inc. (Toronto, Canada). All viral preparations were tested for the presence of replication-competent adenovirus (16) and for LPS content (17), and preparations used were negative for both. All relevant adenoviral methods and quality control procedures are described in detail in Ref. (10).

Stereotactic surgery and immunohistochemistry. Male Sprague–Dawley rats (200–250 g) were anesthetized with a combination of halothane (1.5–4%) using an O_2 flow of 1l/min and nitrous oxide (0.6l/min) and then placed in a stereotactic frame. Different infectious units of each virus were injected directly into the striatum in a total volume of 3 µl [coordinates from bregma: anterior 0.6 mm, lateral 3.4 mm (for RAd 36) or –3.4 mm (for RAd 35), ventral –5 mm] using a 10-µl Hamilton syringe as described previously (3, 5). At doses of 10^4–10^8, both vectors were injected into the same animal, one vector into each hemisphere, to improve the comparison between both vectors, while in other experiments (i.e., RAd36 10^1–10^3) only one virus vector was injected per animal. A different Hamilton syringe was used for each vector. Five days after virus inoculation, animals were perfusion-fixed. After removing the brain from the skull, one hemisphere was marked with a small cut throughout the neocortex to differentiate the right from the left hemisphere and thus identify which virus had been injected into either side of the brain. All practical aspects of gene delivery into the brain using adenoviruses are described in detail in Ref. (18). The following number of injection sites (n) were analyzed for each dose of virus: RAd36, 1×10^1–1×10^3 iu, $n = 4$; 1×10^4–1×10^5 iu, $n = 3$; 1×10^6–1×10^8 iu, $n = 6$; RAd35, 1×10^4–1×10^5 iu, $n = 3$; 1×10^6–1×10^8 iu, $n = 6$; saline injection, $n = 6$. Five days after surgery, the rats were perfusion-fixed with 300 ml of Tyrode's buffer, followed by 300 ml of 4% paraformaldehyde in 0.1 M phosphate-buffered saline. Immediately following perfusion, the brains were removed and postfixed for 6 h. Fifty-micrometer-thick sections were cut using a vibratome (3, 4). Immunohistochemistry was performed on these sections as described in detail elsewhere (3, 4, 18). The primary antibodies used were mouse anti-rat CD8, Serotec Ltd. (1:500); mouse anti-rat ED1, MCA341, Serotec Ltd. (1:800); and mouse anti-β-galactosidase, Z3781, Promega (1:1000). A biotinylated rabbit anti-mouse, E0464, DAKO (1:200), was used as secondary antibody. To detect specific antibody binding, we used the Vectastain ABC detection kit from Vector Laboratories following the manufacturer's instructions. In brains injected with 10^1–10^3 infectious units of RAd36, the viral injection site was cut in serial vibratome sections, and immunoreactive cells were counted throughout each site in one of each of three sections. The diameter of β-galactosidase-positive cells was estimated, and total immunoreactive cell counts were corrected using Abercrombie's correction (19), according to the formula $(\Sigma x)\ f\ st/(st + cd)$, where Σx is the total number of cells counted, f is the frequency of sections sampled, st is the section thickness, and cd is the cell body diameter. Cell body diameter was estimated experimentally and was found to be 12 µm. Sites injected with doses of 10^4 infectious units and above were cut serially, and one of six sections was stained for the immunocytochemical detection of β-galactosidase, ED1, or CD8.

Transduced area quantification. The analysis to determine the area of striatum occupied by cells immunoreactive with antibodies against β-galactosidase was performed using a Leica Quantimet 600 image analysis system (Leica Cambridge Ltd., UK) controlled by QWin software using a Leica RMDB microscope. The equipment was calibrated using standard micrometer slides for each lens and then used to measure the area of transduced cells.

RESULTS

Transgene expression and acute inflammation were compared between vectors expressing β-galactosidase under the control of the major immediate early human cytomegalovirus (MIEhCMV) promoter (RAd35) or of the major immediate early murine cytomegalovirus (MIEmCMV) promoter (RAd36). Prior to their use *in vivo,* both viruses were tested *in vitro;* in all cell lines tested, including nonhuman primate and human cell lines, expression from RAd36 was consistently and substantially higher than expression from RAd35.

Highly Efficient Transgene Expression in the Brain in Vivo

In vivo, viral doses from 10^4 to 10^8 infectious units of RAd 35 and RAd 36 were injected into adult rat striata. Five days later, the brains were sectioned and the presence of immunoreactive β-galactosidase enzyme was assessed by immunohistochemistry. At all doses used, the levels of immunoreactive β-galactosidase expressed from RAd36 were higher than those detected following injec-

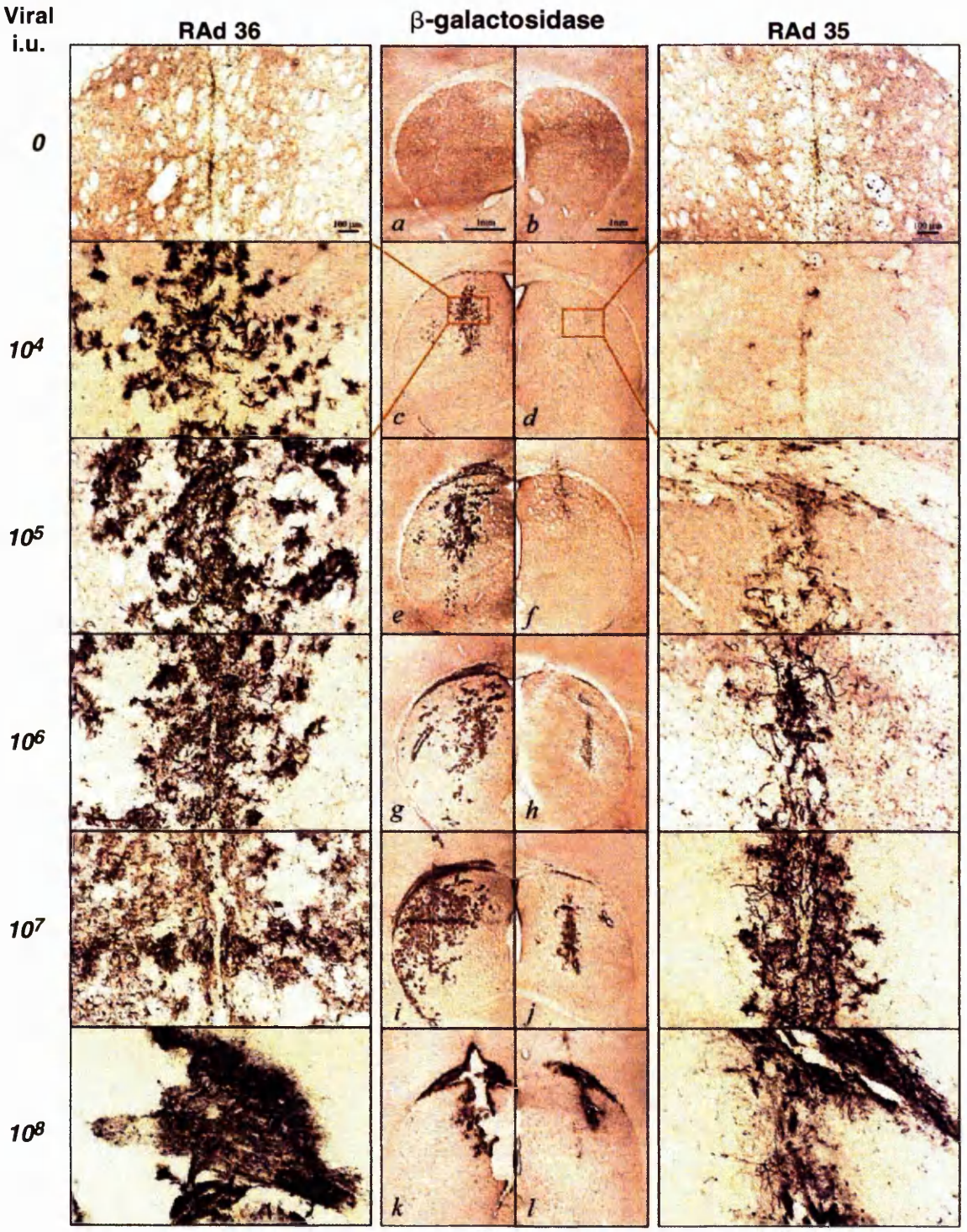

FIG. 1. Increasing doses of vectors were injected into the striatum of adult rats. Three microliters containing the appropriate dose of either RAd36 or RAd35 was injected into the brain, and animals were perfusion-fixed 5 days later. Brains were processed as described in Ref. (18). Note that already at 10^4 iu substantial transduction can be seen with RAd36, while expression is barely detectable in the site injected with RAd35. The area of striatum encompassing transduced cells is always larger in those sites injected with RAd36, compared with those injected with RAd35. The central panels show low-magnification views of the centers of each injection site; the lateral panels at either side of the central panels show higher magnification of boxes, as indicated in c and d. Scale bars for the central panels are shown in a and b, while scale bars for the lateral panels are shown in the top left and top right images. Viral iu = 0 represents injection of saline.

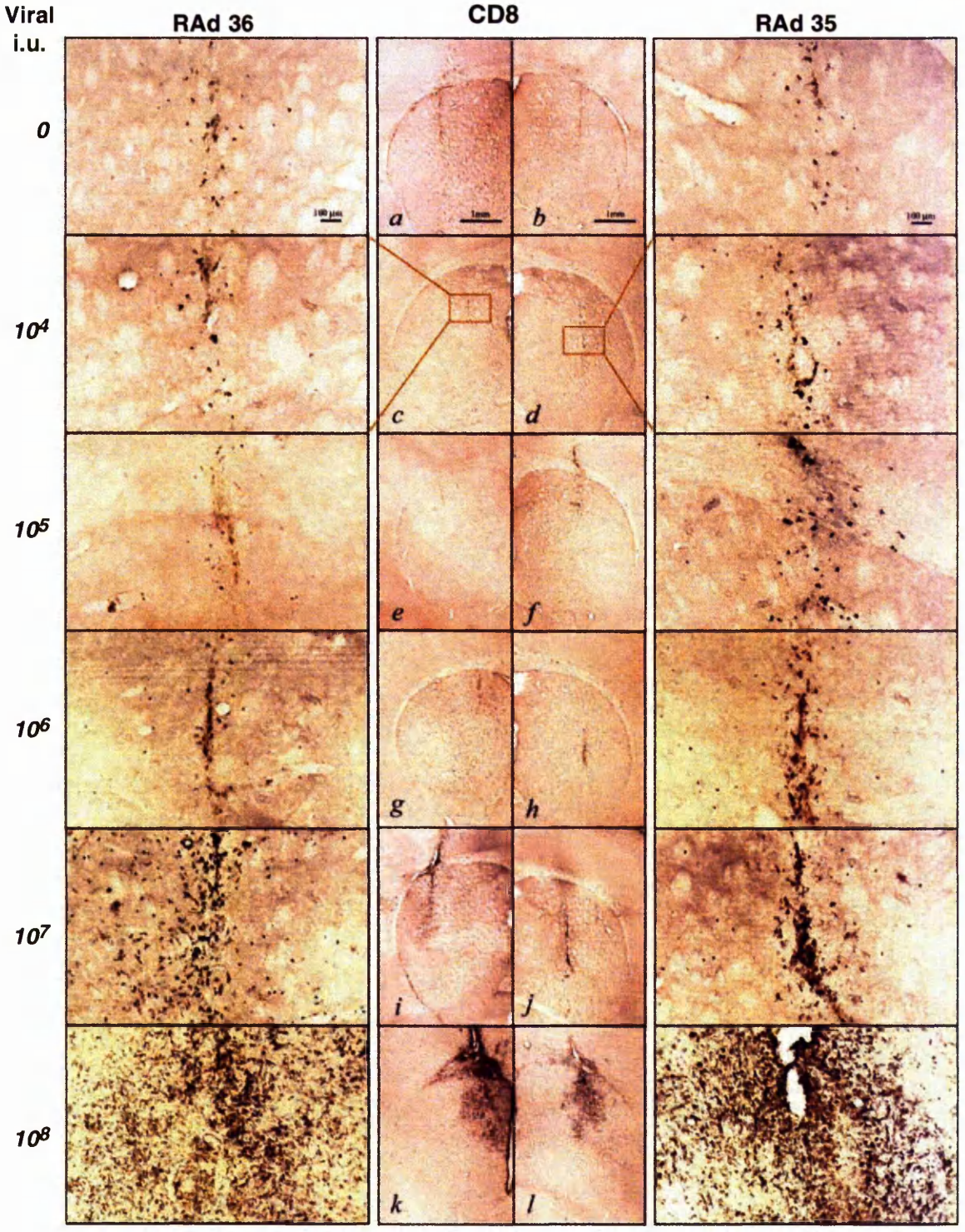

FIG. 3. Increasing doses of vectors were injected into the striatum of adult rats, and serial sections to those illustrated in Fig. 1 were analyzed for the presence of CD8+ inflammatory NK and T cells and are shown. Increased influx of CD8+ cells is only seen at 10^7 and 10^8 iu of RAd36 and 10^8 iu of RAd35. The central panels show low-magnification views of the centers of each injection site; the lateral panels at either side of the central panels show higher magnification of boxes, as indicated in c and d. Scale bars for the central panels are shown in a and b, while scale bars for the lateral panels are shown in the top left and top right images. Viral iu = 0 represents injection of saline.

tion of RAd35 (Fig. 1). A low dose of 10^4 infectious units of RAd 36 allowed transduction of a relatively large area of the rat striatum (Fig. 1c), comparable to the area transduced by 10^7 iu of RAd 35 (Fig. 1j; Fig. 2). A dose of 10^4 iu of RAd35, however, produced only very few immunoreactive cells (Fig. 1d).

A quantitative analysis of the total area of β-galactosidase immunoreactivity in the center of the injection sites demonstrated that the area transduced by RAd36 is significantly larger than that transduced by RAd35 following injection of vector doses of 10^4–10^7 (Fig. 2; see Figs. 1c–1j). At 10^8, the difference in transduction between both vectors was not significant due to the neurotoxicity associated with the high dose of vector and high levels of transgene expression. Maximal transduction for RAd36 and RAd35 was achieved at 10^7 iu. At 10^8 iu there was significant toxicity associated with both vectors (Figs. 1k and 1l; Fig. 2; Figs. 3k and 3l; Figs. 4k and 4l). Following infection with 10^8 iu of RAd35, β-galactosidase expression appeared to be higher than at 10^7 iu, but not statistically different due to a high variability in β-galactosidase levels in animals injected with 10^8 iu. This was possibly a result of direct vector cytotoxicity observed following the injection of high vector dose (Figs. 1j and 1l; Fig. 2) (4). Further, when comparing the efficiency of expression, statistical analysis demonstrated that a dose of 10^4 infectious units of RAd36 expresses β-galactosidase throughout an area equivalent to that achieved by 10^7 infectious units of RAd35 (Fig. 2). This indicates that RAd36 is approximately 1000 times more effective than RAd35 in expressing β-galactosidase in the brain *in vivo*.

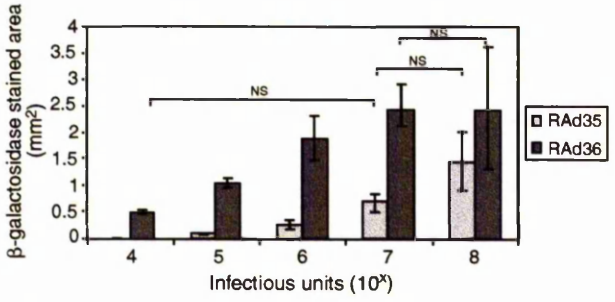

FIG. 2. Quantification of the area of the brain encompassing β-galactosidase immunoreactive cells using a semiautomatic Quantimet imaging system. Expression of β-galactosidase following injection of RAd36 (green bars) was always significantly higher than expression from RAd35 (blue bars) at all doses ($P < 0.001$), except at 10^8 iu, at which the difference was not statistically significant. The area of β-galactosidase immunoreactivity after injecting 10^4 iu of RAd36 was not statistically different from that obtained following infection of RAd35 at 10^7 iu. This shows the expression from RAd36 to be approximately 1000-fold more effective than expression from RAd35. The difference in expression from RAd36 did not differ between 10^7 and 10^8 iu, demonstrating that with RAd36 maximal transgene expression is achieved at 10^7 iu. The difference in expression between 10^7 and 10^8 iu of RAd35 was not statistically significant, probably due to the increased toxicity at 10^8 iu, which can eliminate transduced cells.

Absence of Virus-Induced Brain Cytotoxicity and Inflammation at Viral Doses Achieving High-Level Transgene Expression

Inflammatory cell infiltration in response to viral vector injection was studied in serial brain sections from animals injected with either RAd35 or RAd36 and stained for the presence of CD8+ NK and T-cells (Fig. 3) or ED1+ macrophages/microglia (Fig. 4) by immunohistochemistry. The inflammatory response to injection of either viral vector was greater than that observed following the injection of saline, only at doses of 10^7 iu and above. At these doses (10^7 iu and above), inflammation was higher in animals injected with RAd36 (Figs. 3i and 3k; Figs. 4i and 4k) compared to animals injected with RAd35 (Figs. 3j and 3l; Figs. 4j and 4l). This is probably due to inflammatory effects caused by higher levels of β-galactosidase expression from RAd36 (Figs. 1i and 1j).

One Infectious Event Is Enough to Allow Transgene Detection in the Brain in Vivo

To determine the lower limit of detection of transgene expression from RAd36 in the brain *in vivo* and to assess whether transduction *in vivo* was linear with respect to viral vector dose, we injected into the brain viral doses ranging from 10 to 1000 total infectious units. Serial brain sections taken throughout the injection sites were immunohistochemically stained for β-galactosidase and positive cells were counted throughout the injection sites. In animals injected with 10 infectious units ($n = 4$), we detected 7 ± 2 β-galactosidase immunoreactive cells; in animals injected with 100 infectious units ($n = 4$), we detected 102 ± 9 β-galactosidase immunoreactive cells; and in animals injected with 1000 infectious units ($n = 4$), we detected 1046 ± 23 immunostained cells (Fig. 5). Thus, gene transfer into the brain appears to be 100% efficient following injection of low doses of RAd36. The correlated linear increase in the number of positive cells with increasing dose of RAd36 (in the 10^1–10^3 iu range) shows that *in vivo* infection by a single infectious unit of RAd36 is sufficient to express enough β-galactosidase to detect transgene expression in an infected cell by immunohistochemistry. Such a linear relationship is predicted by Poisson's distribution if, and only if, a single infectious viral unit directs the expression of sufficient transgene to be reliably detected (20, 21). This linearity is lost at doses of 10^4 iu and above. It is only at these doses that transduction becomes detectable in brains injected with RAd35, an effect we attribute to the occurrence of multiple infectious events.

Method of Titer Determination Does Not Affect the High Transduction Efficiency

The calculated efficiency of transgene expression obtained in our experiments depends on the infectious titer assigned to the virus stock used. The worldwide

accepted standard method, for determining adenovirus titers, gives a titer which is calculated from the highest dilution of virus which results in productive infection of cells and complete cytopathic effect within infected wells. Recently, Nyberg-Hoffman *et al.* (15) have proposed that titers obtained by this method may be an underestimate of the actual number of infectious units present in any individual vector batch. Using the standard method of titration, we obtained a titer for RAd36 of 8.2×10^{10} iu/ml (with a particle:pfu ratio of 17) and an efficiency of gene transfer of 100% (Fig. 5). Applying the theoretical corrections to the titer, according to Eq. [6] of Nyberg-Hoffman *et al.* (15), we obtained a titer of 2.3×10^{11} iu/ml (with a particle:iu ratio of 6) and a corresponding efficiency of 33%. Regardless of whether the standard titer or the corrected titer is used for the calculations, the efficiency of RAd36-mediated gene transfer to the brain remains very high. In this work, we refer to vector titers as calculated from the standard method of titration. With either titer, the linear increase in the number of β-galactosidase-expressing cells obtained at increasing viral doses from 10^1–10^3 proves that each stained cell is infected by a single viral particle, demonstrating that one infecting physical particle is enough to produce detectable levels of β-galactosidase in a cell *in vivo* (20, 21).

Discussion

Efficiency of gene delivery and expression is likely to depend on a number of factors: possessing the appropriate viral receptors at high density, the processes of viral internalization and delivery of the vector genome from endosomes to the nucleus of infected cells, and transcription–translation efficiency of the transgene will all play a role. *In vivo,* one must further consider the role played by the diffusion of virus throughout brain tissue and the effects of inflammatory and immune cells. Single viral particles are very efficient in infecting their preferred target cells *in vitro* during the determination of viral titers. However, *in vivo* gene transfer, as assessed by the number of detectable transduced cells, appears to be inefficient. This has led to the use of high titers of vectors to transduce the brain *in vivo* and to obtain either anatomically detectable cells or a therapeutic effect in animal models of disease.

When using adenoviral vectors encoding marker transgenes under the transcriptional control of very powerful promoters (i.e., an adenovirus vector encoding β-galactosidase under the transcriptional control of a powerful short MIEhCMV promoter), no transgene expression is seen if fewer than 10^4 infectious units is injected into the target brain area. Similar data have been reported by many other laboratories, but the reasons for the apparently inefficient gene transfer and expression *in vivo* have never been properly explored. In most papers doses of 10^4–10^{10} total infectious units have been injected into the brain of rodents. All studies available so far report that at least 10^6–10^8 or higher total infectious units need to be injected into the brain to detect anatomically or physiologically relevant transgene expression. Significantly, similar titers (10^6–10^8 infectious units) have been used when transducing the brain with AAV, lentiviral, or herpes simplex virus type 1 vectors (2).

The reasons underlying the apparently inefficient gene transfer *in vivo* could be attributed to any of the factors listed above. In a previous paper (14), we demonstrated that, while RAd35 was able to infect neocortical neurons in primary cultures, transgene expression was not seen until cells were superinfected with other viruses, an experimental paradigm which was found to activate the sMIEhCMV promoter sequence in RAd35. This was taken to indicate that although neurons in primary culture were infected with RAd35, the MIEhCMV promoter remained silent. Our current work demonstrates that *in vivo* gene expression from viral vectors depends on the promoter element employed. Using very low doses of a viral vector expressing a transgene from a very strong promoter, we have demonstrated for the first time that a single viral infectious unit is sufficient to transduce a single brain cell *in vivo.* This in turn allowed us to determine that the efficiency of Ad-mediated gene transfer into the rat brain *in vivo,* under our experimental conditions, is 100%. The reason for the generally low efficiency of gene transfer and expression hitherto observed *in vivo* appears thus to be due to the low activity of promoters used previously.

Viral vector diffusion throughout brain tissue has so far been regarded as very poor, but has not been evaluated experimentally. Our data show that RAd36 at each viral vector dose transduces an area of the striatum which is much larger than the area transduced by the same dose of RAd35. We suggest that this is due to the fact that a single viral particle of RAd36 leads to detectable β-galactosidase expression, while coinfection with a high number of particles of RAd35 is necessary to achieve detectable levels of transgene expression in the brain. RAd35 transgene expression can only be detected at 10^4 iu. Since experiments with RAd36 show that virus does indeed enter brain cells after delivery of lower doses, multiple hits must be necessary for detectable transgene expression following infection with RAd35. Results with RAd36 demonstrate that adenoviral vectors can diffuse relatively large distances in the brain, even in the absence of special physical delivery methods such as high-pressure injections into the brain (22).

Much work has been devoted to the development of cell-type-specific promoters, inducible promoter elements, or even combined cell-type-specific and inducible transcriptional regulatory systems. Such cell-type-specific promoters are at least 10^3- to 10^4-fold weaker than the MIEmCMV promoter we used in our experiments (unpublished data from our laboratory; Refs. 11 and 23), and thus at least 10^3- to 10^4-fold more virus would be required to detect equivalent numbers of transduced cells

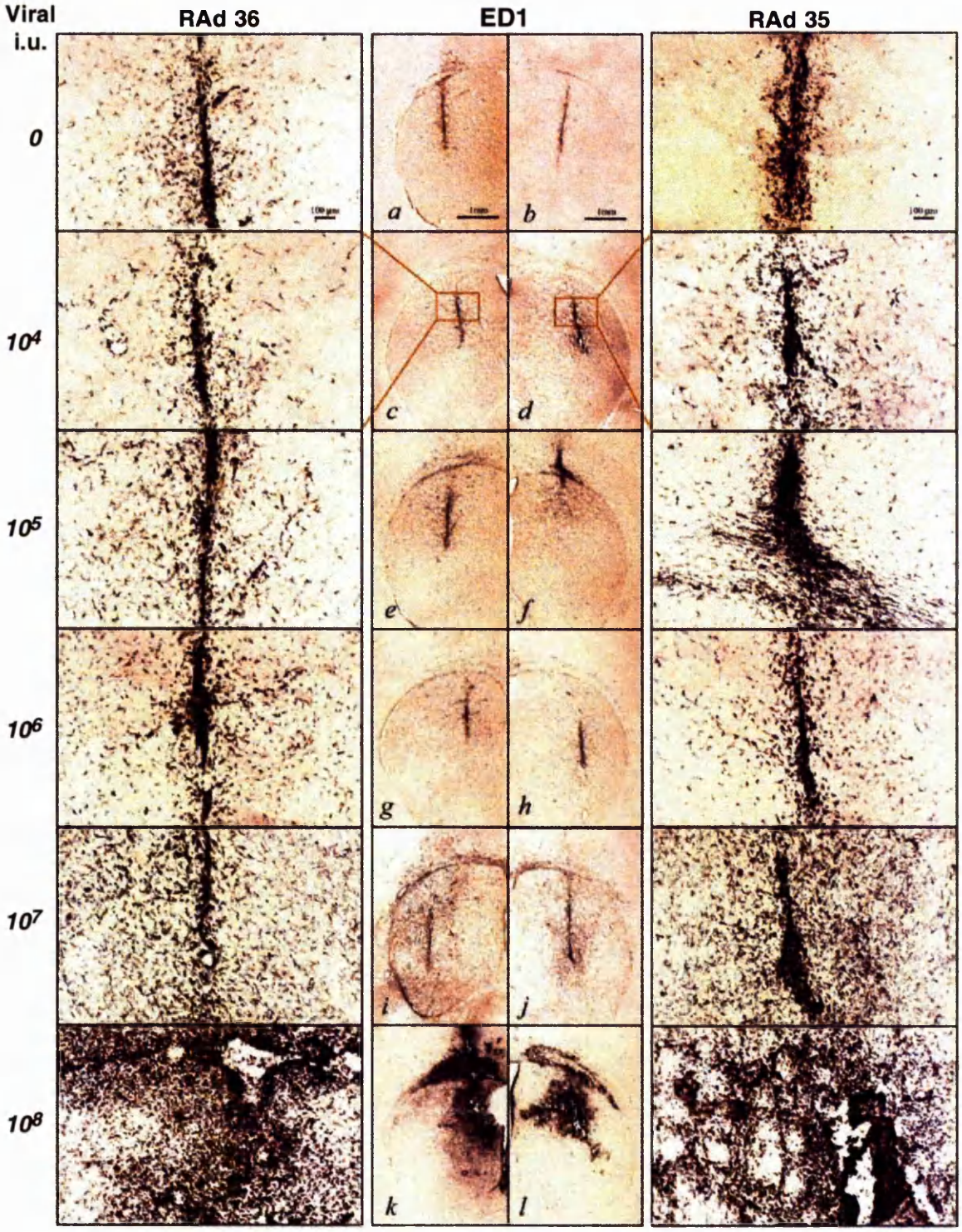

FIG. 4. Increasing doses of vectors were injected into the striatum of adult rats, and serial sections of those illustrated in Fig. 1 were analyzed for the presence of ED1+ activated macrophages/microglial cells and are shown. Increased influx of ED1+ cells is only seen at 10^7 and 10^8 iu of both RAd36 and RAd35. The central panels show low-magnification views of the centers of each injection site; the lateral panels at either side of the central panels show higher magnification of boxes, as indicated in c and d. Scale bars for the central panels are shown in a and b, while scale bars for the lateral panels are shown in the top left and top right images. Viral iu = 0 represents injection of saline.

MOLECULAR THERAPY Vol. 2, No. 4, October 2000

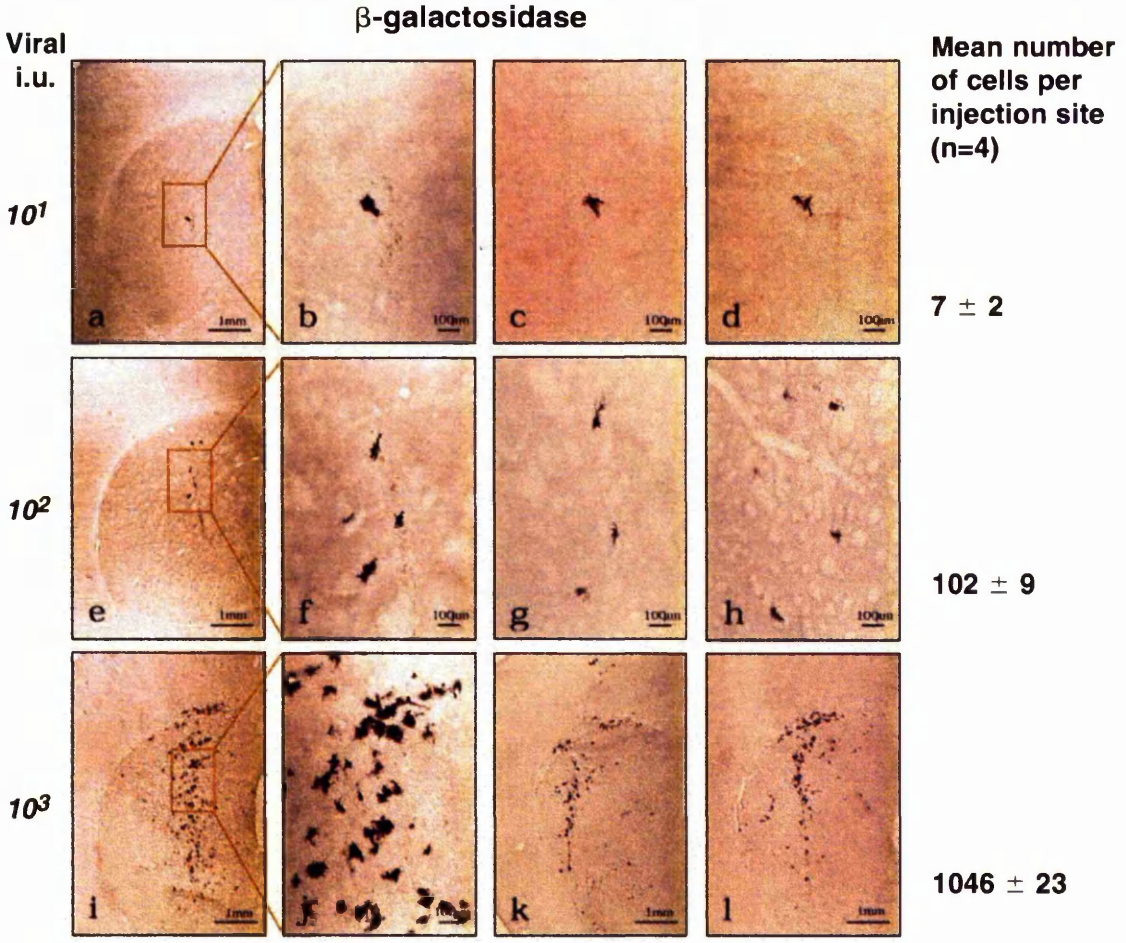

FIG. 5. Low doses of RAd36 were injected into the adult rat striatum: 10^1, 10^2, and 10^3 iu. a, e, and i show low-power views through the middle of an injection site at one of the doses. b, f, and j show enlarged views of the injection site, as outlined in the boxes in a, e, and i. c, d, g, h, k, and l each show further examples of different injection sites. In c, d, g, and h, higher power views are shown to illustrate the morphology of transduced cells, while k and l are shown at lower power to demonstrate the full extent of distribution of RAd36 transduced cells at this viral vector dose. Scale bars and magnifications are shown for each panel. The mean numbers of cells per injection site ($n = 4$) are shown to the right of the figure. All transduced cells detected at these low doses displayed a characteristic astrocyte-like morphology.

in the brain. Investigators have so far been forced to choose between accepting a high degree of inflammation and cytotoxicity accompanying administration of higher doses of vector, which will in turn curtail the duration of transgene expression, or using lower doses and achieving a more limited transduction (4, 17, 24). We now demonstrate for the first time that high-level expression in the brain can be obtained in the complete absence of cellular inflammation and using very low doses of adenoviral vectors. The activity of cell-type-specific or inducible promoters will have to be improved substantially in order to achieve efficient and safe gene therapy approaches for the treatment of human neurological diseases.

We suggest that, concomitantly with further optimization of viral vectors (25), including the basic knowledge necessary for successful retargeting of viral vectors (26, 27) and engineering of appropriate transcriptional regulation it will be possible to maximize transgene expression and eliminate direct cytotoxicity and inflammation. In conclusion, our data demonstrate that gene delivery using adenoviruses *in vivo* can be extremely efficient and devoid of any direct cytotoxicity or acute brain inflammation.

ACKNOWLEDGMENTS

We acknowledge the support our lab receives through European Union grants, Biomed II, BIO4-CT98-0297; Biomed II, BMH4-CT98-3277; and Biomed V, QLK3-CT-1999-00364. Also, we acknowledge the support received from The Parkinson's Disease Society (UK), Grants 3087 and MAP 96/28, as well as Grant 051248 from The Wellcome Trust (UK). Work in our laboratory is further funded by grants from the Biotechnology and Biological Sciences Research

Council (UK) (34/T08236), Medical Research Council (UK) (G9713347) and a grant from The Royal Society (17900). We thank T. Maleniak, P. Stanley, and E. Jones for excellent technical assistance, R. Poulton for excellent secretarial assistance, and Professor A. M. Heagerty and Professor D. Gordon for their continued support. We thank Pablo Umana, Daniel Stone, Clare Thomas, and Paul Kingston for discussions regarding the implications of the work presented and useful comments on the manuscript. We also thank Stephen Dunnett for his advice on cell counting in the brain and John Denton for his help with the quantitative analysis of β-galactosidase expression. P.R.L. is a Research Fellow of The Lister Institute of Preventive Medicine. C.A.G. was funded by The Sir Halley Stuart Trust (UK) and EU Grant BMH4-CT98-3277.

REFERENCES

[1]Anderson, W. F. (1998). Human gene therapy. *Nature* **392:** 25–30.

[2]Blomer, U., Naldini, L., Kafri, T., Trono, D., Verma, V., and Gage, F. H. (1997). Highly efficient and sustained gene transfer in adult neurons with a lentivirus vector. *J. Virol.* **71:** 6641–6649.

[3]Dewey, R. A., *et al.* (1999). Chronic brain inflammation and persistent herpes simplex virus 1 thymidine kinase expression in survivors of syngeneic glioma treated by adenovirus-mediated gene therapy: Implications for clinical trials. *Nat. Med.* **5:** 1256–1263.

[4]Thomas, C. E., Birkett, D., Castro M. G., and Lowenstein, P. R. (2000). The role of vector toxicity versus inflammatory and immune responses in eliminating adenovirus vector-mediated transgene expression from the rat brain. Submitted.

[5]Wood, M. J., Charlton, H. M., Wood, K. J., Kajiwara, K., and Byrnes, A. P. (1996). Immune responses to adenovirus vectors in the nervous system. *Trends Neurosci.* **19:** 497–501.

[6]Addison, C. L., Hitt, M., Kunsen, D., and Graham, F. L. (1997). Comparison of the human versus murine cytomegalovirus immediate early gene promoters for transgene expression by adenoviral vectors. *J. Gen. Virol.* **78:** 1653–1661.

[7]Sallanave, J. M., Xing, Z., Simpson, A. J., Graham, F. L., and Gauldie, J. (1998). Adenovirus-mediated expression of an elastase-specific inhibitor (elafin): A comparison of different promoters. *Gene Ther.* **5:** 352–360.

[8]Marr, R. A., Hitt, M., Muller, W. J., Gauldie, J., and Graham, F. L. (1998). Tumour therapy in mice using adenovirus vectors expressing human TNFα. *Int. J. Oncol.* **12:** 509–515.

[9]Morelli, A. E., *et al.* (1999). Evaluation of the concentration and bioactivity of adenovirus vectors for gene therapy. *J. Gen. Virol.* **80:** 571–583.

[10]Southgate, T. D., Kingston, P. A., and Castro, M. G. (2000). In *Current Protocols in Neuroscience* (J. N. Crawley, C. R. Gerfen, R. McKay, M. A. Rogawski, D. R. Sibley, and P. Skolnick, Eds.). Wiley, New York.

[11]Southgate, T., *et al.* (2000). Transcriptional targeting to anterior pituitary lactotrophic cells using recombinant adenovirus vectors *in vitro* and *in vivo*. *Endocrinology,* **141:** 3493–3505.

[12]Byrnes, A. P., Wood, M. J. A., and Charlton, H. M. (1996). Role of T cells in inflammation caused by adenovirus vectors in the brain. *Gene Ther.* **3:** 644–651.

[13]Wilkinson, G. W., and Akrigg, A. (1992). Constitutive and enhanced expression from the CMV major IE promoter in a defective adenovirus vector. *Nucleic Acids Res.* **20:** 2233–2239.

[14]Shering, A. F., *et al.* (1997). Cell type-specific expression in brain cell cultures from a short human cytomegalovirus major immediate early promoter depends on whether it is inserted into herpesvirus or adenovirus vectors. *J. Gen. Virol.* **78:** 445–459.

[15]Nyberg-Hoffman, C., Shabram, P., Li, W., Giroux, D., and Aguilar-Cordova, E. (1999). Sensitivity and reproducibility in adenoviral infectious titer determination. *Nat. Med.* **3:** 808–811.

[16]Dion, D. L., Fang, J., and Garver, R. I., Jr. (1996). Supernatant rescue assay vs polymerase chain reaction for detection of wild type adenovirus-contaminating recombinant adenovirus stocks. *J. Virol. Methods* **56:** 99–107.

[17]Cotten, M., Baker, A., Saltik, M., Wagner, E., and Buschle, M. (1994). Lipopolysaccharide is a frequent contaminant of plasmid DNA preparations and can be toxic to primary human cells in the presence of adenovirus. *Gene Ther.* **1:** 239–246.

[18]Thomas, C. E., Abordo-Adesida, E., Maleniak, T. C., Stone, D., Gerdes, C. A., and Lowenstein, P. R. (2000). In *Current Protocols in Neuroscience* (J. N. Crawley, C. R. Gerfen, R. McKay, M. A. Rogawski, D. R. Sibley, and P. Skolnick, Eds.). Wiley, New York.

[19]Abercrombie, M. (1946). Estimation of nuclear populations from microtome sections. *Anat. Rec.* **94:** 239–247.

[20]Mittereder, N., March, K. L., and Trapnell, B. C. (1996). Evaluation of the concentration and bioactivity of adenovirus vectors for gene therapy. *J. Virol.* **70:** 7498–7509.

[21]Luria, S. E., Darnell, J. E., Jr., Baltimore, D., and Campbell, A. (Eds.) (1978). In *General Virology,* pp. 21–32. Wiley, New York.

[22]Bobo, R. H., Laske, D. W., Akbasak, A., Morrison, P. F., Dedrick, R. L., and Oldfield, E. H. (1994). Convection-enhanced delivery of macromolecules in the brain. *Proc. Natl. Acad. Sci. USA* **91:** 2076–2080.

[23]Smith-Arica, J., Morelli, A. E., Larregina, A. T., Smith, J., Lowenstein, P. R., and Castro, M. (2000). Cell-type-specific and regulatable transgenesis in the adult brain: Adenovirus-encoded combined transcriptional targeting and inducible transgene expression. Submitted.

[24]Cartmell, T., Southgate, T., Rees, G. S., Castro, M. G., Lowenstein, P. R., and Luheshi, G. N. (1999). Interleukin-1 mediates a rapid inflammatory response after injection of adenoviral vectors into the brain. *J. Neurosci.* **19:** 1517–1523.

[25]Thomas, C. E., Schiedner, G., Kochanek, S., Castro, M. G., and Lowenstein, P. R. (2000). Peripheral infection with adenovirus causes unexpected long term brain inflammation in animals injected intracranially with first generation, but not with high capacity adenovirus vectors: Toward realistic long term neurological gene therapy for chronic diseases. *Proc. Natl. Acad. Sci. USA* **97:** 7482–7487.

[26]Roelvnik, P. W., Mi Lee, G., Einfeld, D. A., Kovesdi, I., and Wickham, T. J. (1999). Identification of a conserved receptor-binding site on the fiber proteins of CAR-recogniz-ing adenoviridae. *Science* **286:** 1568–1571.

[27]Douglas, J. T., *et al.* (1999). A system for the propagation of adenoviral vectors with genetically modified receptor specificities. *Nat. Biotech.* **17:** 470–475.

tive analysis of GFNR expression, average red fluorescence was subtracted from average green fluorescence to obtain an estimate of specific GFNR fluorescence.

Identification of trapped genes and northern blot. Total RNA was prepared from cell cultures using the Trizol reagent (Gibco BRL), according to the manufacturer's protocol. To recover and identify trapped genes, we did a 5′ RACE on total RNA by using the Smart RACE cDNA amplification kit (Clontech), according to the manufacturer's protocol, using two EGFP primers (5′-CTTGTGGC-CGTTTACGTCGCCG-3′, 5′-CGGTGAACAGCTCCTCGCC-3′) in the first round and nested PCR, respectively. Inverse PCR was performed as described[21], using a SupF primer (5′-GGAGCAGGCCAGTAAAAGCATTACCCGTG-3′) and a NTR primer (5′-AGTAGCGTTTTGATCTGCTCGGCCTGTTCC-3′), followed by PCR with two nested primers (5′-CTTCCCCCACCACCATCACTTT-3′, 5′-TAGTGGAATGACGCTTTAAGGC-3′). PCR products were cloned using the Invitrogen (Carlsbad, CA) TOPO TA cloning kit and sequenced using fluorescent dye terminators on a Perkin-Elmer (Foster City, CA) 310 sequence analyzer, according to the manufacturer's protocols. For quantitative northern blot analysis, bound radioactivity was detected and quantified using a STORM 840 phosphorimager apparatus (Molecular Dynamics, Sunnyvale, CA).

Acknowledgments

We gratefully acknowledge Richard Palmiter (University of Washington–Seattle) for providing NTR cDNA. Thanks to Giuseppe Basso, Massimo Geuna, and the Fred Hutchinson Cancer Research Center (FHCRC) flow cytometry resource staff for their help with flow cytometry and cell sorting. We thank Weisheng Chen, Jon Cooper, Guy Hamilton, Jeff Hildebrand, and Masayuki Komada for critical comments on the manuscript. During his stay at FHCRC, E.M. was supported by a short-term fellowship from Fondazione Italiana per la Ricerca sul Cancro (FIRC). This research was supported by grants HD24875 and HD25326 from NIH to P.S., and by grants from the Armenise-Harvard Foundation for Advanced Scientific Research and Associazione Italiana per la Ricerca sul Cancro (AIRC) to P.M.C.

Received 16 January 2001; accepted 5 April 2001

1. Li, X. *et al.* Generation of destabilized green fluorescent protein as a transcription reporter. *J. Biol. Chem.* **273**, 34970–34975 (1998).
2. Bridgewater, J.A. *et al.* Expression of the bacterial nitroreductase enzyme in mammalian cells renders them selectively sensitive to killing by the prodrug CB1954. *Eur. J. Cancer* **31**, 2362–2370 (1995).
3. Medico, E. *et al.* The tyrosine kinase receptors Ron and Sea control "scattering" and morphogenesis of liver progenitor cells in vitro. *Mol. Biol. Cell* **7**, 495–504 (1996).
4. Brown, S.D. & Nolan, P.M. Mouse mutagenesis-systematic studies of mammalian gene function. *Hum. Mol. Genet.* **7**, 1627–1633 (1998).
5. Forrester, L.M. *et al.* An induction gene trap screen in embryonic stem cells: identification of genes that respond to retinoic acid in vitro. *Proc. Natl. Acad. Sci. USA* **93**, 1677–1682 (1996).
6. Gogos, J.A., Lowry, W. & Karayiorgou, M. Selection for retroviral insertions into regulated genes. *J. Virol.* **71**, 1644–1650 (1997).
7. Whitney, M. *et al.* A genome-wide functional assay of signal transduction in living mammalian cells. *Nat. Biotechnol.* **16**, 1329–1333 (1998).
8. Akiyama, N., Matsuo, Y., Sai, H., Noda, M. & Kizaka-Kondoh, S. Identification of a series of transforming growth factor beta-responsive genes by retrovirus-mediated gene trap screening. *Mol. Cell. Biol.* **20**, 3266–3273 (2000).
9. Komada, M., McLean, D.J., Griswold, M.D., Russell, L.D. & Soriano, P. E-MAP-115, encoding a microtubule-associated protein, is a retinoic acid-inducible gene required for spermatogenesis. *Genes Dev.* **14**, 1332–1342 (2000).
10. Baker, R.K. *et al.* In vitro preselection of gene-trapped embryonic stem cell clones for characterizing novel developmentally regulated genes in the mouse. *Dev. Biol.* **185**, 201–214 (1997).
11. Bonaldo, P., Chowdhury, K., Stoykova, A., Torres, M. & Gruss, P. Efficient gene trap screening for novel developmental genes using IRES beta geo vector and in vitro preselection. *Exp. Cell Res.* **244**, 125–136 (1998).
12. Iyer, V.R. *et al.* The transcriptional program in the response of human fibroblasts to serum. *Science* **283**, 83–87 (1999).
13. Velculescu, V.E., Zhang, L., Vogelstein, B. & Kinzler, K.W. Serial analysis of gene expression. *Science* **270**, 484–487 (1995).
14. Bridgewater, J.A., Knox, R.J., Pitts, J.D., Collins, M.K. & Springer, C.J. The bystander effect of the ntroreductase/CB1954 enzyme/prodrug system is due to a cell-permeable metabolite. *Hum. Gene Ther.* **8**, 709–717 (1997).
15. Markowitz, D., Goff, S. & Bank, A. A safe packaging line for gene transfer: separating viral genes on two different plasmids. *J. Virol.* **62**, 1120–1124 (1988).
16. Coller, H.A. *et al.* Expression analysis with oligonucleotide microarrays reveals that MYC regulates genes involved in growth, cell cycle, signaling, and adhesion. *Proc. Natl. Acad. Sci. USA* **28**, 3260–3265 (2000).
17. Ishida, Y. & Leder, P. RET: a poly A-trap retrovirus vector for reversible disruption and expression monitoring of genes in living cells. *Nucleic Acids Res.* **27**, e35 (1999).
18. Ben-Porath, I., Yanuka, O. & Benvenisty, N. The tmp gene, encoding a membrane protein, is a c-Myc target with a tumorigenic activity. *Mol. Cell. Biol.* **19**, 3529–3539 (1999).
19. Song, H.J. *et al.* Mouse Sprr2 genes: a clustered family of genes showing differential expression in epithelial tissues. *Genomics* **55**, 28–42 (1999).
20. Desiderio, M.A., Pogliaghi, G. & Dansi, P. Hepatocyte growth factor-induced expression of ornithine decarboxylase, c-met, and c-myc is differently affected by protein kinase inhibitors in human hepatoma cells HepG2. *Exp. Cell Res.* **242**, 401–409 (1998).
21. Ochman, H., Gerber, A.S. & Hartl, D.L. Genetic applications of an inverse polymerase chain reaction. *Genetics* **120**, 621–623 (1988).
22. Friedrich, G. & Soriano, P. Promoter traps in embryonic stem cells: a genetic screen to identify and mutate developmental genes in mice. *Genes Dev.* **5**, 1513–1523 (1991).
23. Soriano, P., Friedrich, G. & Lawinger, P. Promoter interactions in retrovirus vectors introduced into fibroblasts and embryonic stem cells. *J. Virol.* **65**, 2314–2319 (1991).
24. Naldini, L. *et al.* Biological activation of pro-HGF (hepatocyte growth factor) by urokinase is controlled by a stoichiometric reaction. *J. Biol. Chem.* **270**, 603–611 (1995).

Efficient FLPe recombinase enables scalable production of helper-dependent adenoviral vectors with negligible helper-virus contamination

Pablo Umaña[1,4], Christian A. Gerdes[1], Daniel Stone[1], Julian R.E. Davis[2], Daniel Ward[3], Maria G. Castro[1,5], and Pedro R. Lowenstein[1,5*]

Helper-dependent (HD), high-capacity adenoviruses are one of the most efficient and safe gene therapy vectors, capable of mediating long-term expression[1–12]. Currently, the most widely used system for HD vector production avoids significant contamination with helper virus by using producer cells stably expressing a nuclear-targeted Cre recombinase and an engineered first-generation helper virus with parallel *loxP* sites flanking its packaging signal[1,3–12]. The system requires a final, density-based separation of HD and residual helper viruses by ultracentrifugation to reduce contaminating helper virus to low levels. This separation step hinders large-scale production of clinical-grade HD virus[13]. By using a very efficient recombinase, *in vitro*–evolved FLPe (ref. 14), to excise the helper virus packaging signal in the producer cells, we have developed a scalable HD vector production method. FLP has previously been shown to mediate maximum levels of excision close to 100% compared to 80% for Cre (ref. 15). Utilizing a common HD plasmid backbone[1,7,8,10–12], the FLPe-based system reproducibly yielded HD virus with the same low levels of helper virus contamination before any density-based separation by ultracentrifugation. This should allow large-scale production of HD vectors using column chromatography–based virus purification[13].

[1]*Molecular Medicine and Gene Therapy Unit, Room 1.302 Stopford Building, School of Medicine, University of Manchester, Oxford Road, Manchester M13 9PT, United Kingdom.* [2]*Endocrine Sciences Research Group and* [3]*ARC Epidemiology Unit, University of Manchester, Stopford Building, Oxford Road, Manchester M13 9PT, United Kingdom.* [4]*Current address: GlycArt Biotechnology AG, Einsteinstrasse, 8093 Zurich, Switzerland (pablo.umana@glycart.com).* [5]*Address from 1 July 1 2001: Board of Governors Gene Therapeutics Research Institute, 5th Floor Room R-5089, Research Pavilion, Cedars-Sinai Medical Center, 8700 Beverly Boulevard, Los Angeles, CA 90048-1860, USA.* **Corresponding author (lowenstein@man.ac.uk or PRLowenstein@cs.com).*

A helper virus, a first-generation adenovirus with a packaging signal flanked by FLPe-recombination target (FRT) sites and excisable by FLPe-mediated recombination, was constructed as illustrated in Figure 1A. The genome of this helper virus (designated FL helper) is similar to that of the helper widely used in the Cre-based system, namely the AdLC8luc virus[1,4,6–12]. The packaging signal of the FL helper is flanked by parallel FRT sites, instead of the *loxP* sites of AdLC8luc. Both viruses encode a luciferase expression cassette driven by the human cytomegalovirus (hCMV) promoter (in the same orientation in both genomes) and a stuffer of similar size, inserted into the E3-deleted region. FL helper virus has the essential core packaging-signal (domains A1–A5), shown not to have deleterious effects on replication and packaging of adenoviral genomes[16,17].

Human embryonic kidney (HEK) 293 cells were transfected with a vector for strong, constitutive expression of a nuclear-targeted FLPe recombinase gene operatively linked by an internal ribosome entry site (IRES) to a puromycin resistance gene. Cells with stable expression of this cassette were selected for growth in the presence of puromycin, and characterized as described in the Experimental Protocol section. Clone 293-FLPe6 was chosen for further work. Efficient excision of the packaging signal was shown functionally (data not shown), and confirmed at the DNA level (Fig. 1B).

To rescue a β-galactosidase–expressing HD virus from HD plasmid (pGS46), 293-FLPe6 cells were transfected with linearized pGS46 (refs 10,12) using a high-efficiency variant of the calcium phosphate transfection method[18] (Fig. 2A). Plasmid pGS46 consists of the adenoviral inverted terminal repeats (ITRs), the wild-type packaging signal, noncoding human stuffer DNA sequences, and a β-galactosidase expression cassette[10,12] (Fig. 2B). The transfected cells were subsequently infected with FL helper virus using a multiplicity of infection (MOI) of 5, and virus was harvested after full cytopathic effect (CPE). Titers of GS46-FLPe HD virus generated after the initial rescue step were 5×10^4 to 2×10^5 blue-forming units (BFU)/ml (i.e., 1.3 to 5.3×10^4 BFU/μg of transfected DNA) (Fig. 2A).

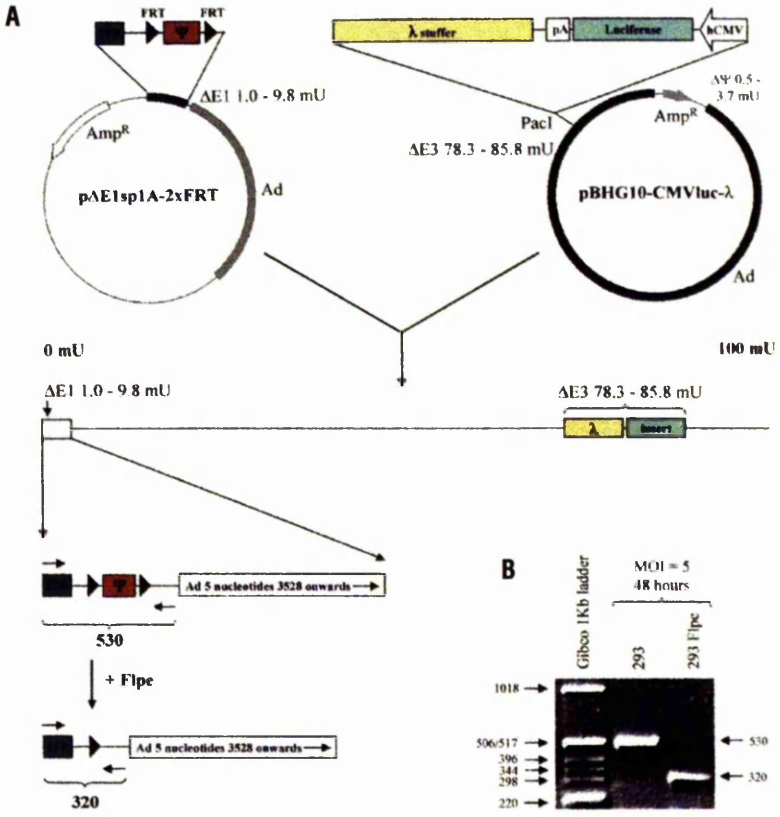

Figure 1. An E1-, E3-deleted helper adenovirus (FL helper) with a packaging signal sensitive to FLPe-mediated excision. (A) FL helper was generated by homologous recombination in 293 cells after co-transfection with plasmids pDE1sp1A-2xFRT and pBHG10-CMVluc-I. The bottom half of the figure indicates the the left-end region of the helper virus genome, before and after FLPe-mediated recombination; the figure also indicates the location of the PCR primers used to determine excision of the packaging signal (black arrows). (B) The result of PCR amplification of the the left-end region of the helper genome 48 h after infection of either 293 cells, or 293-FLPe6 cells with an MOI of 5. Notice that growth in 293-FLPe6 cells leads to the excision of the packaging signal, visible as a band of ~320 bp. No higher molecular weight band is detected in this lane. Helper viral genomes were extracted from 293 or from 293-FLPe6 cells using a modified Hirt procedure[19]. mμ, Map units.

GS46-FLPe HD virus was scaled up through three to four amplification steps, by co-infecting 293-FLPe cells with FL helper virus plus lysate from the previous step. The titers of GS46 HD and FL helper vectors for each step are shown in Figure 2A. In two independent vector preparations, the final HD vector yield in the crude lysate was 5×10^{10} BFU from 9×10^7 cells, and 1.8×10^{11} BFU from 3.6×10^8 cells, respectively (i.e., ~500 BFU/cell in the final step for both preparations), similar to that reported for HD vectors produced with the same HD plasmid backbone using the AdLC8luc helper/293-Cre system[1,7,10,12].

The level of helper virus in the final steps of both preparations was 0.05% and 0.04% (IU/BFU), before any density-based separation by ultracentrifugation. This is an improvement over previous results obtained for HD vector production using the same HD plasmid backbone and the 293-Cre system[1,7,8,10–12], which at best reached these low levels of contamination only after one or two ultracentrifugation steps. The use of GS46-FLPe HD virus *in vivo* indicated a qualitative level of transduction comparable with a first-generation virus containing a similar transgenic cassette (Fig. 3) and to a HD vector tested by us previously[10,12].

If the level of helper vector contamination is assessed by a quantitative TaqMan real-time PCR method, contamination levels are at most 1.4% before, and 0.22% after CsCl gradient centrifugations (Table 1). Compared with data reported in a previous study using quantitative PCR (ref. 11), and the same plasmid vector backbone, our levels of helper virus contamination before CsCl gradient centrifugation are as good as those obtained with a Cre-based system after gradient centrifugation. For both recombination systems, helper virus contamination calculated by quantitative TaqMan real-time PCR differs by a factor of 1–1.5 logs to that calculated by biological titration (Table 1). The reasons for these differences remain to be determined. The level of contamination of replication-competent E1a$^+$ genomes in our preparation, determined by quantitative PCR, was below $1{:}10^9$ copies of HD genomes.

It is well known that CsCl density gradient purification limits large-scale production of HD vectors for clinical use. In contrast, FLPe-based excision of the helper packaging signal should enable purification of HD vectors directly from the final crude lysates or

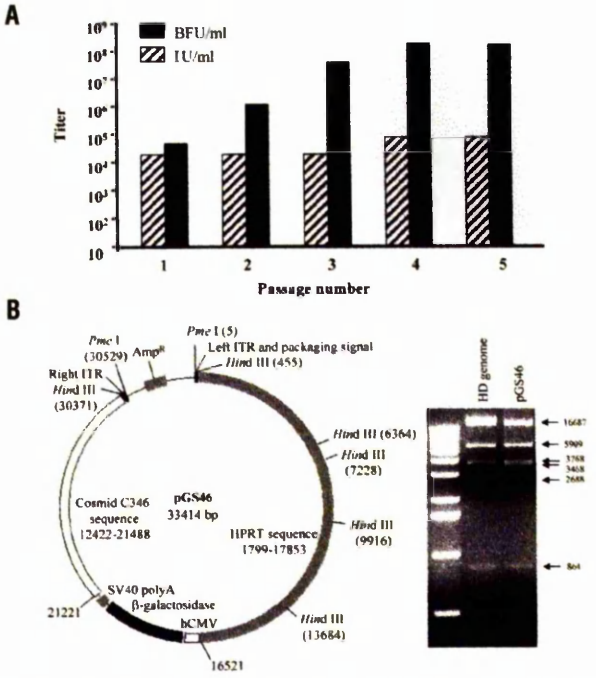

Figure 2. Rescue and amplification of a β-galactosidase–expressing HD virus using 293-FLPe cells and FL helper virus. (A) 293-FLPe cells were transfected with *Pme*I-digested HD plasmid pGS46, and HD virus was rescued by infection with FL helper virus (passage number 1). HD virus was amplified in a series of four further passages by co-infecting 293-FLPe6 cells with lysate from the previous passage plus FL helper virus. GS46-FLP HD virus titer was measured as blue-forming-units (BFU)/ml, whereas contaminating FL helper virus titer was measured as infectious-units (IU)/ml. (B) Map of plasmid GS46, which was rescued as a HD vector. Viral genome rescued from CsCl gradient-purified HD vector, or pGS46, were digested with *Hin*dIII and separated on a 1% agarose gel. The identical banding pattern indicates the absence of major rearrangements of the HD vector produced after five passages in 293-FLPe6 cells; the extra band visible in *Hin*dIII-digested pGS46 (i.e., 3,468 bp), but absent from the HD genome, represents the fragment containing the ampicillin resistance gene removed upon *Pme*I digestion.

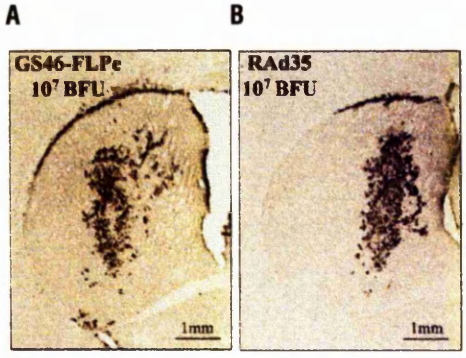

Figure 3. *In vivo* β-galactosidase expression in rat brain infected with either GS46-FLPe HD vector or first-generation adenovirus (RAd35). (A) GS46-FLPe HD virus (7×10^7 BFU) or (B) 7×10^7 BFU of RAd35, a first-generation, replication-deficient adenovirus also expressing β-galactosidase from the hCMV promoter[20], were injected into male Sprague–Dawley rat brains[20]. Six days later animals were perfusion-fixed and 50-μm-thick sections were cut using a vibratome, and β-galactosidase, under the control of the hCMV promoter in both viruses, was detected using immunohistochemistry[21].

Table 1. Helper virus contamination (for pSTK120-derived vectors).

Recombination system	Production stage	Infectious units ratio (biological assay, %)[a]	Genome copies ratio (%)[b]
FLPe	Crude	0.04–0.05 (this study)	1.4 (this study)
	CsCl gradient	0.004–0.01 (this study)	0.22 (this study)
Cre	Crude	Not available	Not available
	CsCl gradient	0.08–0.15 (refs 1,7,8,10,12)	1.0 (ref. 11)

[a]Infectious units ratio, calculated as the ratio between the titer of helper virus (determined as infectious units) to the HD vector titer (e.g., determined as blue-forming units in the case of vectors expressing β-galactosidase); for a double CsCl gradient–purified material, 1×10^6 IU/ 2.4×10^{10} BFU = 0.004.
[b]Genome copies ratio, determined by quantitative Taq Man real-time PCR.

extracts using a column chromatography step, a process that easily lends itself to large-scale production methods[13]. Important modifications introduced recently by others to the HD plasmid backbones and helper virus for this system[11] may be combined with the FLPe-mediated recombination described here and lead to widespread use of HD adenoviral vectors for gene therapy.

Experimental protocol

Introduction of FLP-recombinase target (FRT) sites flanking the adenoviral packaging signal. Minimal (34 bp) FRT sites (5′-gaagttcctattctctagaaagtataggaacttc) were introduced in parallel orientation flanking the adenoviral packaging signal by PCR and reassembling the left end adenoviral sequences in plasmid pΔE1sp1A (Microbix, Toronto, ON, Canada). The resulting plasmid was designated pΔE1sp1A-2xFRT. Further details of the cloning are available from the authors upon request.

Subcloning of a luciferase expression cassette and stuffer DNA in the adenoviral ΔE3 region. A luciferase expression cassette under the control of the hCMV promoter and including a simian virus 40 (SV40) polyadenylation sequence was subcloned into pABS.4 (Microbix), a plasmid designed to facilitate the introduction of DNA into the adenoviral ΔE3 region[17]. A 2.9 kbp, *Pst*I restriction fragment of bacteriophage λ-DNA was subsequently introduced as a stuffer into the modified pABS.4. The luciferase mammalian expression cassette, the stuffer DNA fragment, and a bacterial kanamycin resistance cassette were then subcloned into the *Pac*I site of adenoviral-backbone plasmid pBHG10 (Microbix). The resulting plasmid was designated pBHG10-CMVluc-λ.

Generation of a helper virus with a packaging signal sensitive to FLPe-mediated excision. pΔE1sp1A-2xFRT and pBHG10-CMVluc-λ DNA were co-transfected by a calcium phosphate method[18] into low-passage 293 cells (Microbix). A first-generation, replication-defective, E1- and E3-deleted helper adenovirus, with its packaging signal flanked by FRT sites and with a luciferase expression cassette plus stuffer DNA subcloned into the ΔE3 region (total DNA size of 35.7 kbp), was generated by homologous recombination in co-transfected 293 cells as described[19,20]. The resulting virus (FL helper virus) was isolated and amplified by standard methods and titrated by an end-point dilution, CPE assay (see below)[19,20]. To determine the excision of the packaging signal, PCR primers were designed that corresponded to Ad 5 base pairs 1–35 (5′-catcatcaataatatacctattttggattgaagc-3′) and the reverse complement of pΔE1sp1a base pairs 418–450 (5′-ccccaccttatatattctttcccacccttaacc-3′). Two nanograms of viral DNA extracted from either 293 or 293-FLPe6 cells were subjected to 20 cycles of PCR with an annealing temperature of 63°C.

Calcium phosphate transfections. 293 cells were transfected using a version of the calcium phosphate transfection method[18] using 10% fetal calf serum.

Establishment of a 293-FLPe cell line. Low-passage 293 cells were transfected with linearized plasmid pCAGGSFLPeIRESpuro (a gift of Francis Stewart, EMBL, Heidelberg, Germany)[18]. pCAGGSFLPe-IRESpuro carries a strong, constitutive expression cassette for an *in vitro*–evolved FLP recombinase (FLPe)[14] under the control of the chicken β-actin promoter and a hCMV immediate early

enhancer. The FLPe recombinase carries a minimal, nuclear localization signal from the SV40 large T antigen and is operatively linked by an IRES to a puromycin resistance gene. Additional elements of the expression cassette are an intron with splice donor and acceptor sites upstream of the FLPe gene and a bovine growth hormone polyadenylation signal downstream of the puromycin resistance gene. Transfected cells were selected for stable expression of transgenes by culturing in the presence of 1.5 μg/ml of puromycin. Individual cell clones were isolated, amplified, and compared by a functional assay.

HD virus rescue and amplification. To rescue HD virus from HD plasmid, 293-FLPe6 cells were first transfected with *Pme*I-linearized, β-galactosidase–expressing HD plasmid pGS46 (ref. 16) (a gift of S. Kochanek and G. Schiedner)[18]. Following 16 h of incubation, cells were infected with FL helper virus using an MOI of 5. Upon full CPE, virus was harvested lysing the cells by three freeze–thaw cycles. The lysate from this initial rescue was used to amplify the HD virus in three to four serial steps, co-infecting 293-FLPe cells (at ~80% confluency) with FL helper virus plus lysate from the previous step. First, three wells of a six-well plate with 293-FLPe cells were co-infected with all of the lysate from the rescue step plus FL helper virus at an MOI of 5 (for passages 1 and 2, and MOI of 3.5 for subsequent passages). Plates were centrifuged at 1000 *g* for 90 min at room temperature and incubated at 37°C for 3 h. The medium was replaced by fresh culture medium and cells were incubated until complete CPE. The same procedure was repeated for the third step, but infecting six instead of three wells of the six-well plate, and using an MOI of FL helper of 3.5. All of the lysate from the third step was used to infect nine large T182 culture flasks (182 cm^2 of culture area each) adding FL helper at an MOI of 3.5. A volume of 0.5 ml of culture medium per cm^2 of culture area was used in all steps. Alternatively, for a larger preparation, all the lysate from the third step was used to infect 3 T75 flasks adding FL helper at an MOI of 3.5. All of the lysate from this step was used to infect 30 T182 culture flasks, again adding FL helper at an MOI of 3.5.

Titration of HD and helper virus. HD virus was titrated by quantifying the BFU (ref. 4). Cell lysates or purified viruses were serially diluted (10^{-2}–10^{-10}), and 0.5 ml of each dilution was used to infect in triplicate 293 cells cultured at ~90% confluency in 24-well plates. The plates were centrifuged as described above and incubated at 37°C for 20 h. Cells were fixed in 0.5% glutaraldehyde in PBS and stained using the X-gal method[4]; BFUs were calculated by counting blue cells per well under an inverted microscope, taking the average of blue cell counts within at least two different dilutions within the linear range of the assay, and dividing the values obtained by the volume tested (0.5 ml) and by the dilution factor. FL helper virus was titrated by quantifying the infectious-units (IU) in 96-well plates by end-point CPE as described[19], using 5×10^3 293 cells per well, assaying each dilution in quadruplicate, incubating the plates for 14 days, and inspecting the plates visually for CPE every 24 h. Titers expressed as IU/ml were calculated by multiplying the number of wells with CPE at the highest dilution and dividing by the total volume tested and the dilution factor.

Molecular quantification of relative levels of vector and helper virus genomes. The amount of helper genomes was measured relative to HD vector genomes by quantitative TaqMan real-time PCR (Perkin-Elmer, Boston, MA). DNA was extracted from either crude freeze–thaw lysates (subjected to DNase digestion, followed by pelleting by centrifugation through a 20% sucrose cushion, and heat inactivation) or CsCl gradient–purified vectors, using the QIAamp DNA Kit (Qiagen, Basel, Switzerland). Specific sets of primers and probes labeled with 6-carboxyfluorescein and 6-carboxyltetramethylrhodamine were designed for both helper and HD vector genomes using the program Primer Express (Perkin-Elmer). A plasmid containing the target sequences for both the vector and helper virus was constructed and used as a standard. pJM17 (Microbix) was used as a standard when quantifying the relative concentration of replication-competent virus and helper virus genomes. DNA copy numbers were calculated by using the 7700 software (Perkin-Elmer). Primers were as follows: HD vector forward: 5′-ATGCCAGGACCACCAGGAA-3′ (bases 2,554–2,572 from the C346 stuffer in pGS46); HD vector reverse: 5′-TGCAGGGCTGTCATAGGGA-3′ (bases 2,602–2,620); HD TaqMan probe: 5′-AAGCCTCAGTCCTCTTCT-CAATGTCCT-3′ (bases 2,574–2,600); helper forward: 5′-GTTGGCACCCC-TATTCGACA-3′ (bases 14,322–14,351 in the adenovirus type 5 genome); helper reverse: 5′-GGATGCCACATCCGTTGACT-3′ (bases 14,379–14,398); helper TaqMan probe: 5′-ACCCGTGTGTACCTGGTGGACAAC-3′ (bases 14,354–14,377); E1a forward: 5′-CCAGTGACGACGAGGATGAA-3′ (bases 951–970 in the adenovirus type 5 genome); E1a reverse: 5′-CCGTATTCCTC-CGGTGATAATG-3′ (bases 1,031–1,052); E1a TaqMan probe: 5′-CAAGAC-CTGCAACCGTGCCC-3′ (bases 1,010–1,029).

Acknowledgments

This work was supported by grants from the Medical Research Council (MRC, UK), Biotechnology and Biological Sciences Research Council (BBSRC, UK), The Parkinson's Disease Society, The Royal Society, and European Union-Biomed program grants Contract No. BMH4-CT98-3277 and BMH4-CT98-0297. P.R.L. was a research fellow of The Lister Institute of Preventive Medicine, and D.S. was funded through a BBSRC studentship. We kindly thank A. Francis Stewart for providing us with the pCAGGSFLPe-IRESpuro plasmid, and Stefan Kochanek and Gudrun Schiedner for providing us with the pGS46 plasmid.

Received 21 December 2000; accepted 30 March 2001

1. Maione, D. *et al.* Prolonged expression and effective readministration of erythropoietin delivered with a fully deleted adenoviral vector. *Hum. Gene Ther.* **11**, 859–868 (2000).
2. Mitani, K., Graham, F.L., Caskey, C.T. & Kochanek, S. Rescue, propagation, and partial purification of a helper virus–dependent adenovirus vector. *Proc. Natl. Acad. Sci. USA* **92**, 3854–3858 (1995).
3. Kochanek, S. *et al.* A new adenoviral vector: replacement of all viral coding sequences with 28 kb of DNA independently expressing both full-length dystrophin and beta-galactosidase. *Proc. Natl. Acad. Sci. USA* **93**, 5731–5736 (1996).
4. Parks, R.J. *et al.* A helper-dependent adenovirus vector system: removal of helper virus by Cre-mediated excision of the viral packaging signal. *Proc. Natl. Acad. Sci. USA* **93**, 13565–13570 (1996).
5. Hardy, S., Kitamura, M., Harris-Stansil, T., Dai, Y. & Philips, M.L. Construction of adenovirus vectors through Cre-lox recombination. *J. Virol.* **71**, 1842–1849 (1997).
6. Chen, H.H. *et al.* Persistence in muscle of an adenoviral vector that lacks all viral genes. *Proc. Natl. Acad. Sci. USA* **94**, 1645–1650 (1997).
7. Schiedner, G. *et al.* Genomic DNA transfer with a high-capacity adenovirus vector results in improved in vivo gene expression and decreased toxicity. *Nat. Genet.* **18**, 180–183 (1998).
8. Morsy, M.A. *et al.* An adenoviral vector deleted for all viral coding sequences results in enhanced safety and extended expression of a leptin transgene. *Proc. Natl. Acad. Sci. USA* **95**, 7866–7871 (1998).
9. Morral, N. *et al.* Administration of helper-dependent adenoviral vectors and sequential delivery of different vector serotype for long-term liver-directed gene transfer in baboons. *Proc. Natl. Acad. Sci. USA* **96**, 12816–12821 (1999).
10. Thomas, C.E., Schiedner, G., Kochanek, S., Castro, M.G. & Lowenstein, P.R. Peripheral infection with adenovirus causes unexpected long-term brain inflammation in animals injected intracranially with first-generation, but not with high-capacity, adenovirus vectors: toward realistic long-term neurological gene therapy for chronic diseases. *Proc. Natl. Acad. Sci. USA* **97**, 7482–7487 (2000).
11. Sandig, V. *et al.* Optimization of the helper-dependent adenovirus system for production and potency in vivo. *Proc. Natl. Acad. Sci. USA* **97**, 1002–1007 (2000).
12. Thomas, C.E. *et al.* Pre-existing anti-adenoviral immunity is not a barrier to efficient and stable transduction of the brain, mediated by novel high-capacity adenovirus vectors. *Hum. Gene Ther.*, in press (2001).
13. Blanche, F. *et al.* An improved anion-exchange HPLC method for the detection and purification of adenoviral particles. *Gene Ther.* **7**, 1055–1062 (2000).
14. Buchholz, F., Angrand, P.O. & Stewart, A.F. Improved properties of FLP recombinase evolved by cycling mutagenesis. *Nat. Biotechnol.* **16**, 657–662 (1998).
15. Ringrose, L. *et al.* Comparative kinetic analysis of FLP and Cre recombinases: mathematical models for DNA binding and recombination. *J. Mol. Biol.* **284**, 363–384 (1998).
16. Grable, M. & Hearing, P. *cis* and *trans* requirements for the selective packaging of adenovirus type 5 DNA. *J. Virol.* **66**, 723–731 (1992).
17. Bett, A.J., Haddara, W., Prevec, L. & Graham, F.L. An efficient and flexible system for construction of adenovirus vectors with insertions or deletions in early regions 1 and 3. *Proc. Natl. Acad. Sci. USA* **91**, 8802–8806 (1994).
18. Umaña, P., Jean-Mairet, J. & Bailey, J.E. Tetracycline-regulated over-expression of glycosyltransferases in Chinese hamster ovary cells. *Biotechnol. Bioeng.* **65**, 542–549 (1999).
19. Southgate, T.D., Kingston, P.A. & Castro, M.G. Adenoviral vectors for gene transfer into neural cells in primary culture. In *Current protocols in neuroscience.* (eds Sibley, D.R. *et al.*) 4.23.1–4.23.40 (John Wiley and Sons, New York, NY; 2000).
20. Gerdes, C.A., Castro, M.G. & Lowenstein, P.R. Strong promoters are the key to highly efficient noninflammatory and noncytotoxic adenoviral-mediated trangene delivery into the brain in vivo. *Mol. Ther.* **2**, 330–338 (2000).